



October 16th-18th, 2014

HOSTS:
PENNSYLVANIA
GEOLOGICAL SURVEY &
DICKINSON COLLEGE



79TH ANNUAL
FIELD CONFERENCE
OF PENNSYLVANIA GEOLOGISTS



Pennsylvania's
Great Valley &
Bordering Mountains
near Carlisle

About the LiDAR Images in this Guidebook and Road Log

LiDAR (Light Detection and Ranging) is a remote sensing method that depicts precise, three-dimensional topographic and other surfaces, such as forest canopy, in detail. Computer processing produces a detailed image of measured surfaces.

Obtained from an airplane or helicopter using an instrument consisting of a laser, a scanner, and a specialized GPS receiver, airborne LiDAR scans a swath of the earth's surface, measuring the time delay of reflected pulses. Location is obtained from GPS and inertial measurements in the plane. In forested terrain, especially if flown in the spring when leaves are off, some pulses make it through branches to the ground and return. Multiple pulses from objects at different heights can be distinguished. Processed using only those pulses that go the greatest distance produces a "bare earth" digital elevation model (DEM), a boon for all who map the earth's surface (engineers, field geologists and geomorphologists)

We are fortunate that Pennsylvania is one of the few states with LiDAR and various derived products, including DEM's for the entire state through the stalwart efforts of Dr. Jay Parrish, State Geologist (Retired). PAMAP data is freely available to all users through downloading for use in GIS software at Pennsylvania Spatial Data Access site (www.pasda.psu.edu). Numerous software products produce images or perform analysis using LiDAR data.

Vertical accuracy of PAMAP LiDAR data is 18.5 cm (7 inches) in open areas and 37 cm (14 inches) in tree cover. PAMAP DEM's are gridded with a 3.2-foot (1 m) pixel size. Also available are files of 2-foot contours—much better than standard USGS topographic maps.

LiDAR derived images in this guidebook are Shaded Slope Maps—where each pixel's value reflects steepness of slope, and the darker the color the steeper the slope. Shaded slope images provide precise three-dimensional data that is extremely useful in bedrock and surficial material mapping.

Another useful visualization tool for LiDAR is a hillshade image, where calculated brightness represents effects of a false sun angle in the modeled landscape. A statewide hillshade image may be viewed at www.pamap.dcnr.state.pa.us Higher resolution hillshades, or ones with other sun angles, may be made with GIS software from the LiDAR DEM files.

Terrestrial LiDAR is obtained on the ground by tripod- or vehicle-mounted instruments, often of buildings, engineering works (e.g., bridges, road cuts, etc), or even large outcrops.

Helen L. Delano, Pennsylvania Geological Survey

Guidebook for the
79th ANNUAL FIELD CONFERENCE OF PENNSYLVANIA GEOLOGISTS
October 16 — 18, 2014

**PENNSYLVANIA'S GREAT VALLEY & BORDERING MOUNTAINS
NEAR CARLISLE**

Editor

Robin Anthony, Pennsylvania Geological Survey, Pittsburgh, PA

Field Trip Organizers

Don Hoskins, Pennsylvania Geological Survey, retired

Noel Potter, Dickinson College, retired

Field Trip Leaders and Guidebook Contributors

Don Hoskins, Pennsylvania Geological Survey, retired

Noel Potter, Dickinson College, retired

Marcus M. Key, Jr., Dickinson College

Frank J. Pazzaglia, Lehigh University

Todd Hurd, Shippensburg University

Tom Feeney, Shippensburg University

Dorothy Merritts, Franklin & Marshall College

Hosts

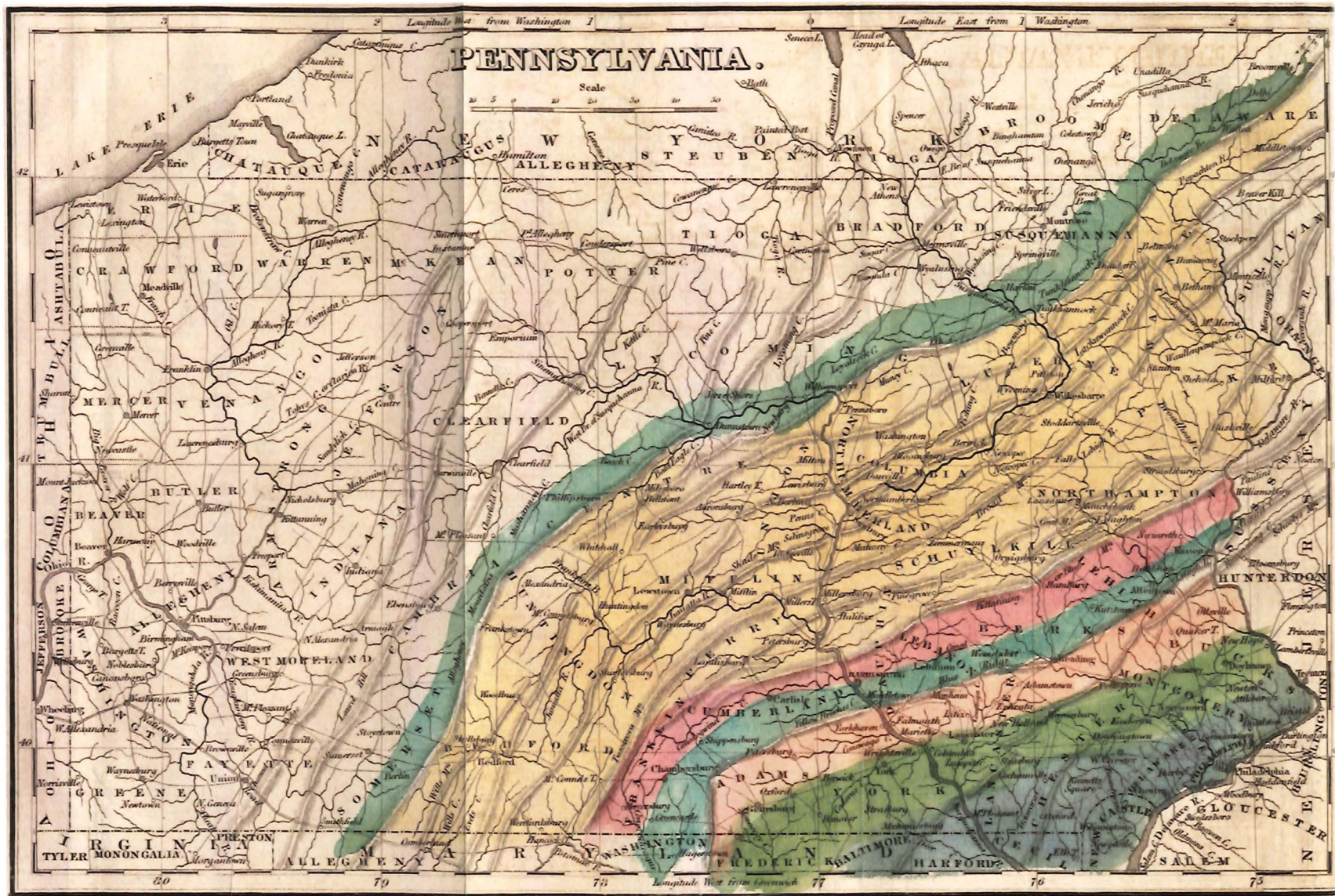
Dickinson College

Pennsylvania Geological Survey

Headquarters: Comfort Suites, Carlisle, PA

Cartoons: Dr. John A. Harper, PhD.

Cover: LiDAR slope compilation image of the Great Valley near Carlisle, PA and scenic photographs of the Great Valley viewed from Waggoner's Gap courtesy of Thomas Whitfield (PaGS)



First geological map of Pennsylvania by William Darby, 1824

THE EARLIEST GEOLOGICAL MAP OF PENNSYLVANIA'S GREAT VALLEY

William Darby, a self-taught geographer, surveyor, writer and life-long traveler published a hand-colored geological map of Pennsylvania in 1824 depicting, with some accuracy, the principal rocks types of the Great Valley, the focus of the 2014 Field Conference of Pennsylvania Geologists. Depicted using separate colors on a base map of counties, streams and transportation routes with shaded mountains and ridges, the geology follows the then recognized topographic trends of Pennsylvania.

Based in part on Maclure's 1809 map of the United States, Darby adopted the accepted terminology of that era for classifying rocks. *Primitive* rocks were without organic remains and consisted largely of granite and gneiss, which occurred in patches in southeasternmost Pennsylvania. *Transition* rocks had organic remains and were largely 1. Greywacke (German Grau Wacke using Darby's term) which occurred in valley bottoms; 2. "Quartzzy aggregates" which formed the ridges; and, 3. Limestone, which underlay valleys. *Secondary* or floetz (flat) rocks covered the most of Pennsylvania to the north and west, our Appalachian Plateau Province. On his map, Darby defined our Piedmont with blue and green with pink used for the "Old Red Sandstone", an erroneous use of the English name for Devonian age rocks, but which are our Triassic sediments. The carbonates of the Great Valley are again green with the clay/slate, our "Martinsburg", in red. Light yellow colors Pennsylvania's Appalachian Mountains Section.

A narrow ridge sketched along the north side of the "Old Red Sandstone", which Darby considered an extension of the southern state's Blue Ridge, is our South Mountain. Kittatinny Mountain, our Blue Mountain, borders the clay/slate of the Kittatinny Valley, our Great Valley. Darby describes the contact of the carbonates and clay/slate at several sites to support his refutation of the valley as the "great limestone valley of Pennsylvania" noting that only half of the valley is limestone.

Darby's publications include the self-published "Geographical, Historical, and Statistical Repository" issued in two parts in 1824, which includes the figured map. To prepare his gazetteer he visited all of the counties of Pennsylvania collecting data, including local names, many still used, for the many ridges that he depicts on the base map he prepared. Impressed by the linear nature of many of these ridges, he projected them uncritically into neighboring states. An original hand-colored copy of this map and explanatory text are now available in the library archives of the Pennsylvania Bureau of Topographic and Geologic Survey.

Additional publications were "Map and Statistical account of Louisiana" "Emigrant's Guide" "Tour from New York to Detroit"; and "Universal Geographical Dictionary". Designed for the layperson all provided a view of the surface of the earth and its opportunities for settlement, as well as location of usable minerals, and suggestions for canal routes.

Donald M. Hoskins

ACKNOWLEDGMENTS

We extend special thanks to FCOPG officers, guidebook contributors, volunteers, Robin Anthony (PaGS), Editor and cover designer of the Roadlog and Guidebook and to Tom Whitfield (PaGS) for the many digitally combined images herein and at each field stop.

And to:

- * Superintendent Scott Hackenberg, DCNR, for arranging Stop 1 bus parking at Kings Gap Environmental Education Center.
- * Randy Van Scyoc, Vice President, Valley Quarries, Inc. and Quarry Superintendents for access and safety concerns to their quarries at Stops 3, 4 and 5.
- * Dickinson College for access to their quarry at Stop 7.
- * Kimberly Rhoades, President, N. L. Minich & Sons, Inc. for access to their quarry at Stop 8.
- * Mr. Frank Herr and family for access to their property at Stop 9.
- * Audubon Pennsylvania for access to their property at Stop 10.
- * David Grove, Leader of the Hawk Watchers at Stop 10.
- * Gildef Family Farms for access to bus parking at Stop 10.
- * Walt Leis for Steve Jakatt's memorial.
- * Andre Weltman, Banquet Speaker, President of the Friends of Pine Grove Furnace State Park.

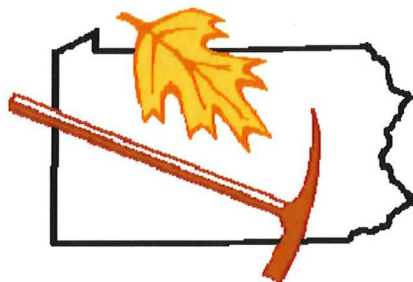


TABLE OF CONTENTS

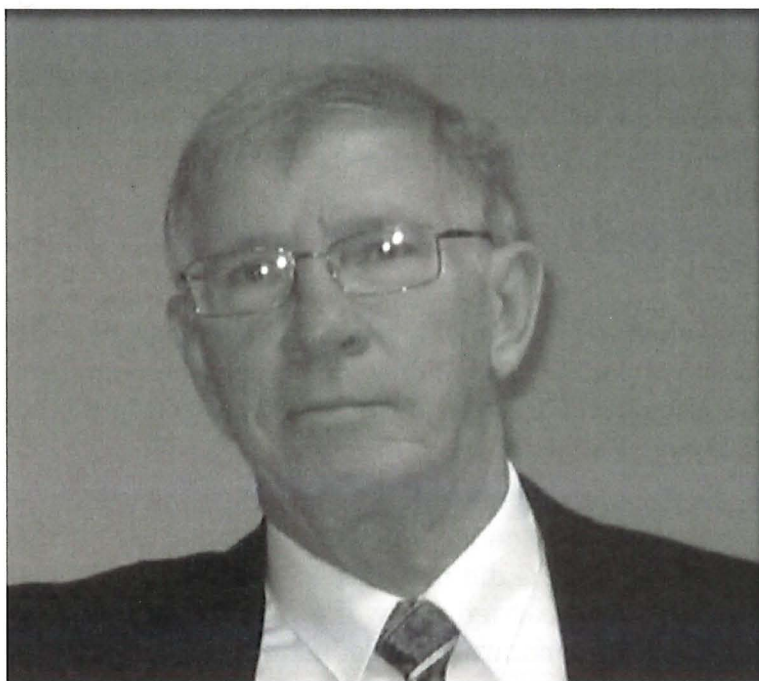
"*Skolithos* in the Lower Cambrian Antietam Formation at South Mountain, Pennsylvania" was omitted in a printing error at the time of guidebook publication.

The article has been appended to this guidebook on page 235 of this PDF.

Page

About LiDAR images.....	inside front cover
The Earliest Geologic Map of Pennsylvania's Great Valley	ii
Acknowledgements	iv
In Memoriam: Steve E. Jakatt, P.G.	vii
Introduction	1
Pine Grove Furnace – A Brief Introduction and History	5
Determination of Preferential Groundwater Flow Patterns to Cumberland County Springs with Fluorescent Dye Tracing	13
Brief Thoughts on Long-Term Landscape Evolution in The Mid-Atlantic Region with a Focus on The Pond Bank Lignite	23
LiDAR Analysis of Periglacial Landforms and Their Paleoclimatic Significance, Unglaci- ated Pennsylvania	35
Day 1 Field Trip	
MAP	60
Stop 1 – Kings Gap Pond sediment core indicates Late Wisconsinan tundra was present here; LiDAR defines nearby solifluction lobe	63
Stop 2 – Hammonds Rock tor includes deformed pebbles in Weverton sandstone and conglomerate; effects of frost and solifluction.....	79
Stop 3 – Valley Quarries Mount Cydonia #3 exposes Antietam and Montalto Formations with <i>Skolithos</i>	93
Stop 4 – Valley Quarries Mainsville Pit – a deep pit into colluvium / alluvium provides history of denudation of South Mountain.....	101
Stop 5 – Valley Quarries Shippensburg Limestone Quarry provides view of the overturned Ordovician Stonehenge and Rockdale Run Formations.....	113
Day 2 Field Trip	
MAP	117
Stop 6 – Big Spring dye tracing experiments reveal long travel distances of groundwater in carbonate rocks; highly cleaved Shady Grove Formation.....	121

Stop 7 – Dickinson College Quarry, producer of Chambersburg Formation dimension Stone.....	129
Stop 8 – Minich Shale Pit contains autochthonous Ordovician Martinsburg Formation shales and graptolite fossils.....	137
Stop 9 – Enola Allochthon exposes folded exotic limestones and shale emplaced within autochthonous Martinsburg Formation.....	145
Stop 10 – Waggoners Gap exposes beach and braided river sandstones of the Silurian Tuscarora and Ordovician Juniata Formations; Late Pleistocene Tuscarora Formation colluvium.....	151
Appendix A – Reprint of Edward Cotter’s “Waggoner’s Gap in Blue Mountain” from SEPM-ES Guidebook, May 1982.....	160
Appendix B – Arthropycus burrows, mud lumps and relief features	167
Pre-Conference Field Trips	
Hydrogeology of Boiling Springs, Cumberland County, Pennsylvania	169
Geology Guide to the Yellow Breeches Creek from Messiah College to McCormick Road	177
Structural Complexities of the Marcellus Formation in Central Pennsylvania A Field Trip	193
Conodoguinet Cave Pre-Conference Field Trip	203
Military Geology of the Battle of South Mountain	217
Donors.....	inside back cover
Group Conferee photo of the 2013 Field Conference of Pennsylvania Geologists at Williamsport.....	back cover



IN MEMORIAM: STEVE E. JAKATT P. G.

In February of 2014 we lost a friend and colleague. Those of us who worked or spent any time with Steve remember him as the tall, bass-voiced one who was a stickler for data that had to be correct to the 4th decimal, knew the correct score and whose turn it was at bat.

Steve came to the practice of geology by a circuitous route. He started as an engineering student who, disenchanted with the program, was drafted by the US Army, graduated from OCS, and was sent to Vietnam during the opening choruses of the Tet Offensive.

"I spent most of my days surveying the various brands of beer and ducking mortar rounds," was his terse response when asked about his Vietnam days.

While in "Nam", the attrition of officers was fairly high, so Steve rose to platoon commander and communication officer of 4 artillery platoons (for which he was awarded a Bronze Star for meritorious service).

After an honorable discharge, Steve married his college sweetheart, Maria, and they promptly went about starting and raising a family of 2 daughters and a son.

"Don't ever ask me for a favorite because they're all unique kids," Steve often said when we were able to ratchet out any information about him.

Overall Steve was very private about some of the scars left by his time in-country. "If anyone spends lots of time talkin' about his time in Nam, he probably wasn't there at all," he would say.

This experience in combat did lead Steve to take part in many versions of "Operation Welcome Home". I remember one time when we were in a bar near Tyrone, PA, Steve greeted a local patron who, from his speech patterns, carried some of his own painful scars. Steve, like he just found a small drowning kitten, spent the next few hours with this vet. Steve just sat with the guy and bought him some rounds while winking to me that he'd be busy for a time, and then later said to us, "Hey, I had to do this; this guy still hasn't come home."

Steve had a heart as big as you can imagine and wasn't ashamed to show this tender side.

At the time of Steve's death, he and his wife were even part of a national program to keep and care for pets owned by US military personnel who would soon be sent to the Middle East. They thought of small things like that to gusset up the hopes and cares of our soldiers who'd been stationed abroad.

Steve's geology education involved a BS and MS in his fields of interest, which included Applied Sedimentology and Flow-in-Porous-Media. He finished his MS in 1978 from Adelphi University where he did his Thesis on the statistical analyses of bedform features of recent beaches. He carried this work into his career where he was hired as an "Exploration geologist" for a natural gas production company.

We met Steve in the mid 1980's, as the oil and gas boom was quieting down, and he was attending field training in horizontal well drilling to assist DoE in site cleanup.

He was hired as a team leader by Weston Engineering Company in 1986 and spent the next 15 years at that company working as a team leader for investigations and cleanup of oil and gas pipelines as well as nuclear waste (where everyone had to keep quiet about what they were about). Steve then moved on to begin an applied geophysics company and a small ground-water services company in Chester County, where he became active in several professional organizations and his local government.

Steve had a "dog's breakfast" of a professional life, and he earned the respect and admiration of all who ever met or worked with him. If we can "take away" anything from a life like Steve's, I'd like to suggest the following:

HONESTY – Steve spent late hours fact checking and having calculations done again and again just to make sure everything was correct. If a project had developed an error, he would call clients and inform them and tell them how the whole thing would be corrected.

HUMOR – In Vietnam, he was celebrated for orderly dispensing his platoon's R&R fund to meet an expected influx of new "zero-based resources" for calendar 1974. To Steve, this meant "Free Beer as long as we can afford it!"

HONOR – What can you say about a guy who lived his life according to his oath of service?

He is sadly missed and will be remembered with a smile.

Your friends

INTRODUCTION

Donald Hoskins, State Geologist, Pennsylvania Geological Survey (Retired) and Noel Potter, Jr., Dept. of Earth Sciences (Retired), Dickinson College, Carlisle, PA

With a focus on South Mountain, its minerals, and its adjacent carbonate producing areas of the Great Valley Section, detailed standard scale geologic mapping began by U.S. Geological Survey staff soon after the start of the 20th century. The Carlisle quadrangle (Stose, 1953), headquarters site of our 2014 Conference, initiated in 1903 (but not published until 1953) is an example of this early quadrangle mapping.

It has been over two decades since the geology of Pennsylvania's Great Valley and embracing mountains was examined by Conferees. Visited in 1966, the field focus was the carbonates of Cumberland valley. A decade+ later, in 1982, we examined the shales and coarser rocks of the Martinsburg Formation. In 1991, we met to consider the details of South Mountain's geology.

LiDAR now provides very detailed views of formerly hidden topographic features allowing accurate interpretation of local geomorphology and of the structural and sedimentological grain of bedrock. Modern mapping, greatly aided by LiDAR technology, reveals so much new information about these land surfaces and underlying bedrock such that Conferee reconsideration of the Great Valley is merited.

Rocks and their resulting topography

Topography in the trip area delicately relates to rock type. Resistant sandstones underlie mountains and valleys reflect the underlying shale and limestone. Even within the shale and limestones, slight composition differences result in minor ridges clearly defined in LiDAR images.

South Mountain (SM) is an anticlinorium and represents the southeasternmost subdivision of the Ridge and Valley Province (Faill, 1998, p. 148). Underlain predominantly by resistant Cambrian Chilhowee Group sandstones, SM was long considered as the northern extension of the Blue Ridge of Virginia and Maryland into Pennsylvania, but at least structurally, this concept is now discounted (MacLachlan, 1991 and Faill, 1998).

To the north and west of SM is the Great Valley Section, known locally as the Cumberland Valley. The valley is bounded on the north and west by Blue (locally North) Mountain. An approximately 3 km thick sequence of Cambro-Ordovician carbonates underlies the southern $\frac{2}{3}$ of the Cumberland Valley. The Ordovician Martinsburg shale underlies the northern $\frac{1}{3}$. Very resistant sandstones of the Ordovician Juniata and Silurian Tuscarora Formations support Blue Mountain.

Structure

Most structures are of Late Paleozoic Alleghanian origin. Cleavage consistently strikes NE parallel to the "grain" of the mountains and dips SE. Folds are typically asymmetrical to overturned with axial surfaces dipping SE. Some SE-dipping thrust faults occur. The easternmost part of the trip area was subject to deformation during the Ordovician, resulting in allochthonous blocks of rocks becoming enveloped in the

Ordovician Martinsburg shale (Root and MacLachlan, 1978; Ganis, et al., 2001). Most folds in the field trip area plunge gently E or NE. Discussions of the structure of SM can be found in Root (1970) and Root and Smith (1991).

Geomorphology

The quartz-rich sandstones of South and Blue Mountain are the most resistant rocks in the area. Chemically resistant to acidic rain they weather to large pieces not easily moved by fluvial processes. The shale in the northern part of the Cumberland Valley is also chemically resistant, but the shale weathers to small pieces easily removed by fluvial processes. The carbonates in the southern part of the Cumberland Valley dissolve easily in acid rain and its resulting groundwater, which removes substantial parts. What remains is an insoluble residue of fine silt and clay and some chert, which make up the soils on these rocks. Carbonate areas underlie some of the lowest terrain in the valley.

On the carbonates, over the long term, an approximate equilibrium between new soil formed at the soil-rock interface and older soil removed by subaerial processes exists. However, an exception to this occurs at the NW base of South Mountain where 30-100 m thick mantle of coarse sandstone-rich colluvium and alluvium overlies the carbonate rocks. There, a 2-5 km wide belt of this mantle prevents removal of the residuum left from weathering of the carbonates, now trapped beneath the alluvium. In places, the clay-rich residuum is as much as 40-50 m thick.

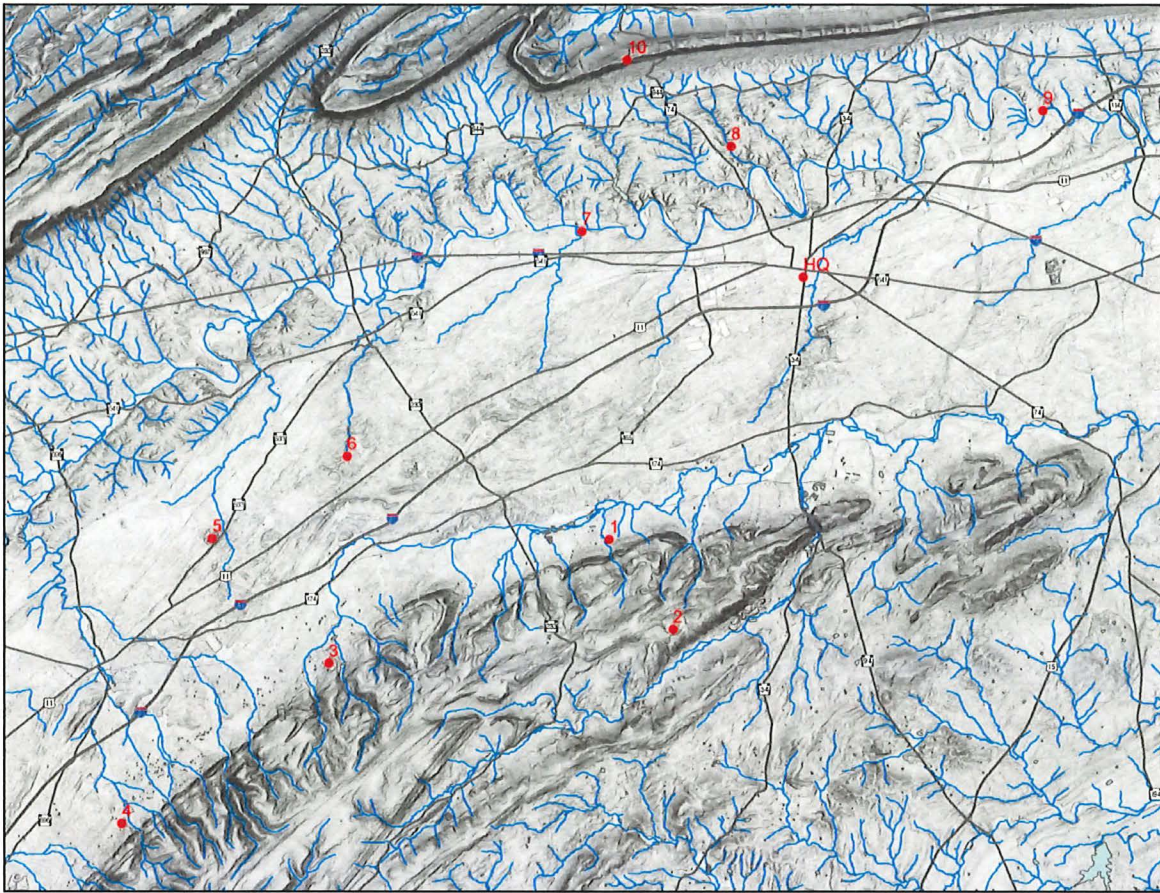
Hydrogeology

Average annual precipitation of the Cumberland Valley is about 42 inches (107 cm)/year, of which slightly more than half runs off and the rest returns to the atmosphere through evaporation and transpiration (Becher and Root, 1981).

Major drainage of the Conference area is to the Susquehanna River (Cover LiDAR map) via Conodoguinet Creek in the northern part of the valley and Yellow Breeches Creek in the southern part. The drainage divide between the Susquehanna and Potomac Rivers is west of Shippensburg where the Conococheague Creek flows southwestward. Ground water in the valley generally flows eastward. A Jurassic diabase dike east of Carlisle runs N-S across the valley that dams the groundwater. There the water table is about 50 feet higher on the west side of the dike than on the east side.

Water that falls on South Mountain follows small drainages northward toward the Cumberland Valley. Reaching the colluvium/alluvium over the carbonate rocks at the base of the mountain, some water seeps deep underground where it flows to large springs farther north in the valley. Some of these springs drain to Yellow Breeches Creek, but several others flow northward to Conodoguinet Creek. The Cover LiDAR map nicely illustrates through the paucity of streams on the carbonates how much water must drain in the subsurface. Karst is common on the carbonates, and the presence of numerous dolines containing vernal ponds on the colluvium/alluvium at the NW base of South Mountain attest to the solution of the carbonates.

Precipitation that falls on Blue Mountain and the shale in the northern part of the valley produces a network of many gullies carved into the shale and drains to Conodoguinet Creek.



**LiDAR slope compilation image of the Great Valley and bordering mountains near Carlisle, PA
(red numbered dots are stop locations for this field trip)**

References

- Becher, A. E. and Root, S. I., 1981, Groundwater and Geology of Cumberland Valley, Cumberland County, Pennsylvania: Pennsylvania Geological Survey, 4th Series, Water Resource Report W-50, 95 p.
- Faill, R. T., 1998, A geologic history of the north-central Appalachians; Part 3, The Alleghany Orogeny: American Journal of Science, v. 298, no. 2, p. 131-179.
- Ganis, G. R., Williams, S. H., and Repetski, J. E., 2001, New biostratigraphic information from the western part of the Hamburg Klippe, Pennsylvania, and its significance for interpreting the depositional and tectonic history of the klippe: Geological Society of America Bulletin, v. 113, no. 1, p. 109-128.
- MacLachlan, D. B., 1991, A tale of two mountains—both South: in Sevon, W. D. and Potter, N., Jr., eds., Geology in the South Mountain area, 56th Annual Field Conference of Pennsylvania Geologists, p. 47-53.
- Root, S. I., 1970, Structure of the northern terminus of the Blue Ridge in Pennsylvania: Geological Society of America Bulletin, v. 81, no. 3, p. 815-830.
- Root, S. I., 1978, Geology and Mineral Resources of the Carlisle and Mechanicsburg Quadrangles, Cumberland County, Pennsylvania: Pennsylvania Geological Survey, 4th Series, Atlas A 138ab.



Figure 1. LiDAR Shade Slope Map of Pine Grove Furnace area. White dots near Pole Steeple and elsewhere are the platforms where charcoal was made.

PINE GROVE FURNACE—A BRIEF INTRODUCTION AND HISTORY

Noel Potter, Jr., Department of Earth Sciences (retired), Dickinson College, Carlisle, PA 17013, pottern@dickinson.edu and Helen L. Delano, Pennsylvania Geological Survey, 3240 Schoolhouse Road, Middletown, PA 17057, hdelano@pa.gov

Introduction and Location

Pine Grove Furnace (PGF) (40°01'54.65" N, 77°18'54.65" W) On the south side of South Mountain in the valley of Mountain Creek operated as an iron furnace from colonial times until the 1890's (Fig. 1). PGF State Park preserves some remnants of the substantial village and industry. Of particular interest may be the restored furnace stack (Fig. 2) just SW of the park office, the former Ironmaster's Mansion (Fig. 3) now restored and managed by the Central Pennsylvania Conservancy as a hostel, and Fuller Lake, which occupies the former ore pit (Figs. 1 and 4). The state park is along the valley of Mountain Creek near the junction of Pine Grove Road and Pennsylvania Route 233.



Figure 2. The restored stack at Pine Grove Furnace today. Compare Fig. 12-5, taken in 1875 when the iron works was in operation.



Figure 3. The Ironmaster's Mansion at Pine Grove Furnace has been restored and is now a Youth Hostel.

PGF is the result of the presence of all the resources needed for iron making near one another here. These resources are: 1) iron ore, albeit low grade, that occurs in clays over the Tomstown Dolomite, 2) carbonate rock, the Tomstown Dolomite here, for flux, 3) metarhyolite for ganister to build and line the stack, 4) sand for making molds, and 5) abundant trees in the adjacent forest for charcoal making to heat the furnace. See Figure 1 for the sources of each of these. Iron making continued to the 1890's, when the whole operation ceased as high grade iron ore was discovered in the Precambrian of Michigan, Wisconsin, and Minnesota. In its heyday, PGF was a thriving community (Fig. 5).

The geology of the PGF area is shown in Figure 7. PGF and the valley of Mountain Creek SW of PGF are underlain by the Cambrian Tomstown dolomite, the first carbonate unit above the Cambrian Chilhowee Group. Precambrian metarhyolite is faulted against the Tomstown just to the N of PGF. The iron ore here was lumps and nodules of limonite and related iron oxides, which occur within the clay residuum formed from chemical weathering of the Tomstown.

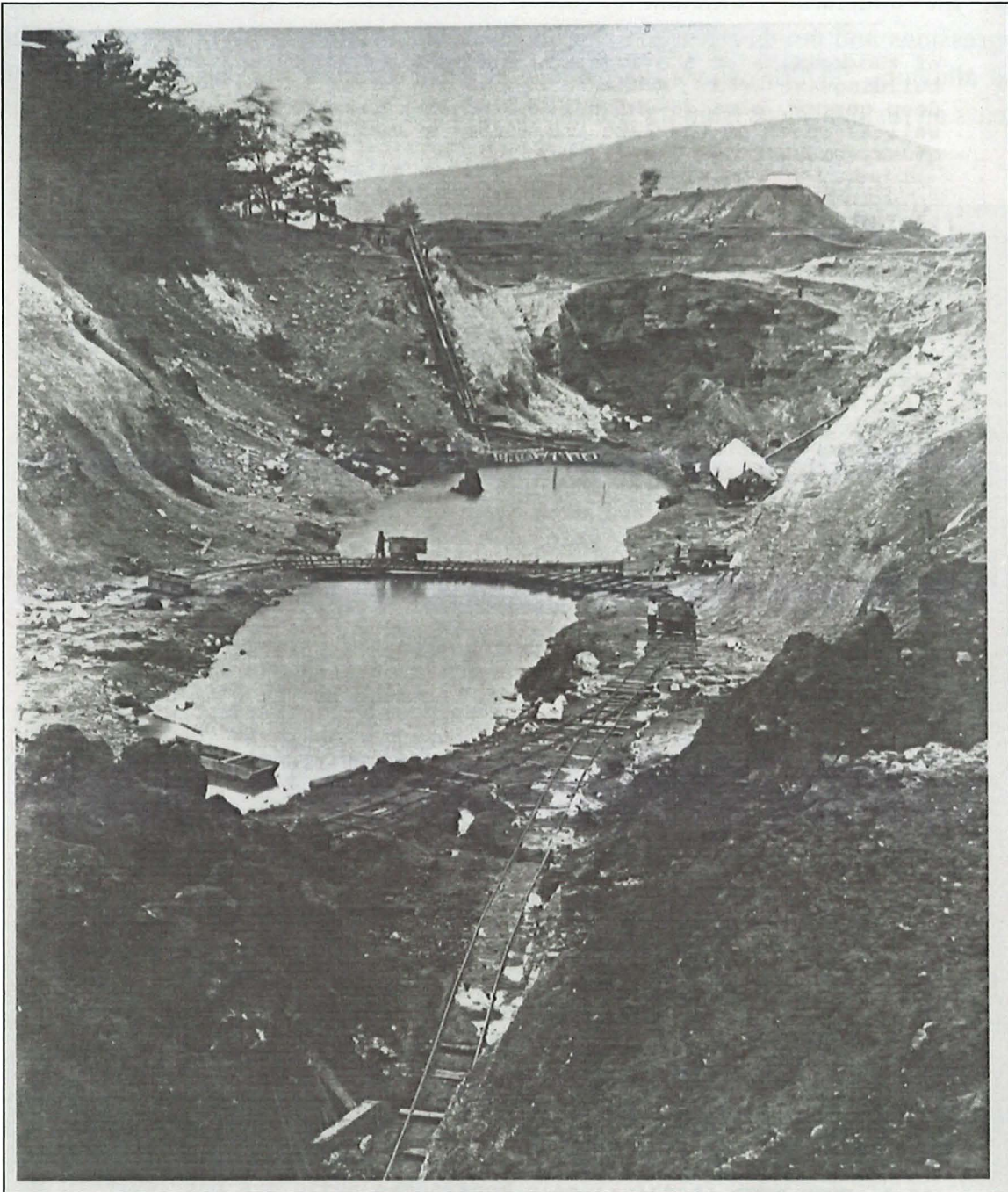


Figure 4. The iron ore pit at Pine Grove Furnace in about 1875. The pit is now Fuller Lake. Photo courtesy of Cumberland County Historical Society.

Origin of the Iron Ore

The iron ore mined at PGF and many places at the base of the NW flank of South Mountain all the way down into the Shenandoah Valley in Virginia occurs in a distinct setting. Most of the limonite iron ores occur as nodules, pods, and stringers associated with the residual clays on the Cambrian Tomstown Dolomite. The favored location is

next the underlying Antietam or other sandstones. In the Great Valley karst depressions and ponds attest to solution of the dolomite beneath quartzite colluvium and alluvium. At PGF where the geology is more complex (Fig. 6), the iron ore still occurs on residual clays from the Tomstown, but against the Montalto sandstone.

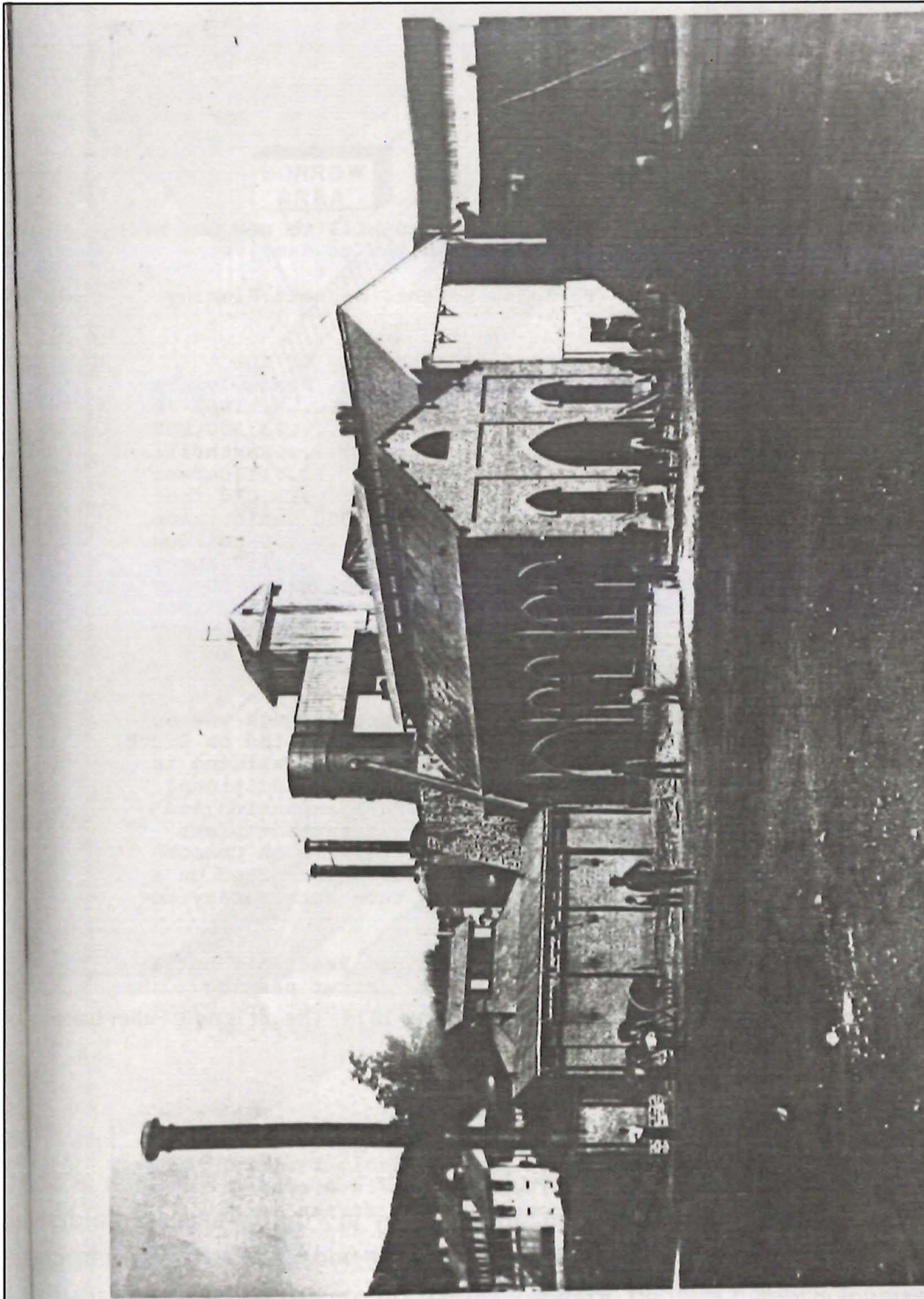


Figure 5. Pine Grove Furnace in 1875. The stone furnace stack, which still stands today, is in center behind first building. Ironmaster's Mansion is in distance at far left. Photo courtesy of the Cumberland County Historical Society.

A good review of the origin of both iron and manganese oxide ores is in Hack (1965) on the ores in the Shenandoah Valley. According to Hack the Tomstown Dolomite contains small amounts of both iron and manganese carbonates, but sufficient to concentrate as oxides over a long period of weathering and time. Rain that falls and runs off from sandstones remains acidic (low pH). When it reaches the carbonate rock it dissolves the carbonate and becomes neutral or alkaline (high pH), and yields ions of Ca^{+2} , Mg^{+2} , and HCO_3^- that are carried away in solution. Meanwhile the now low acidity of the water causes Fe and Mn to precipitate as oxides. Of course when the carbonates dissolve, insoluble residue, mostly clays, are left behind. It is these clays over the Tomstown Dolomite in which much of the iron ore is found.

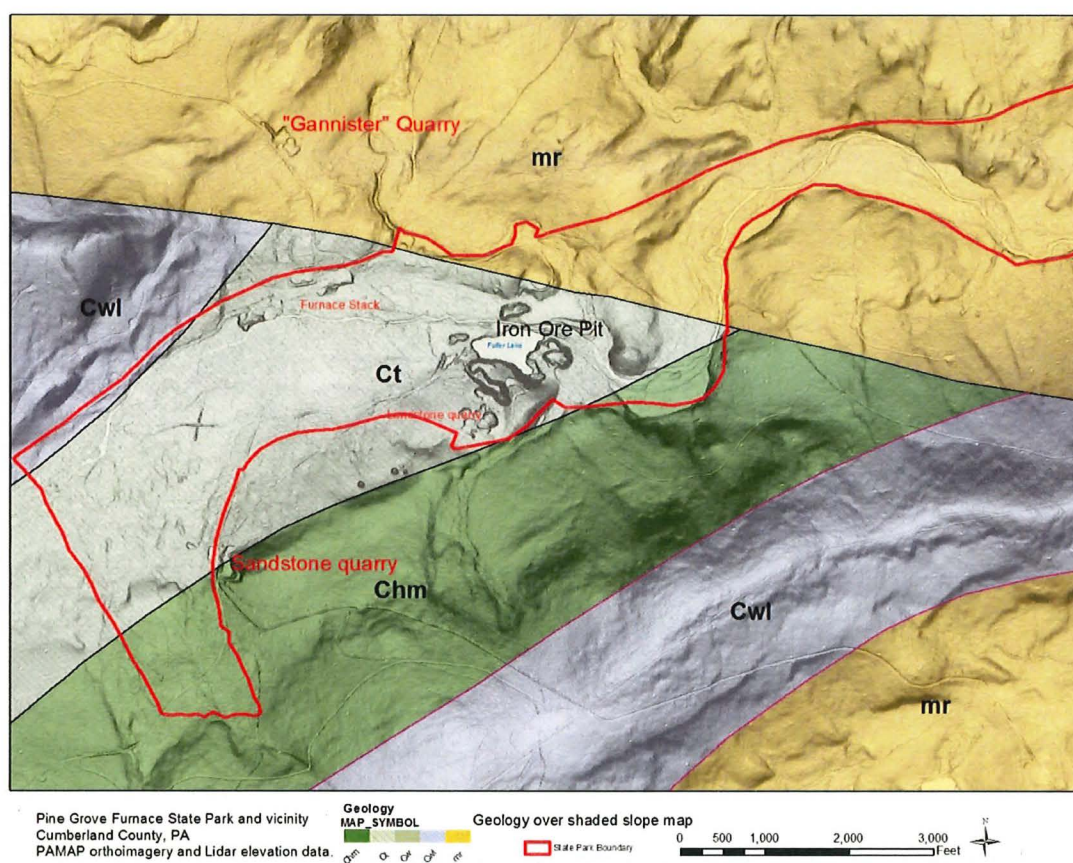
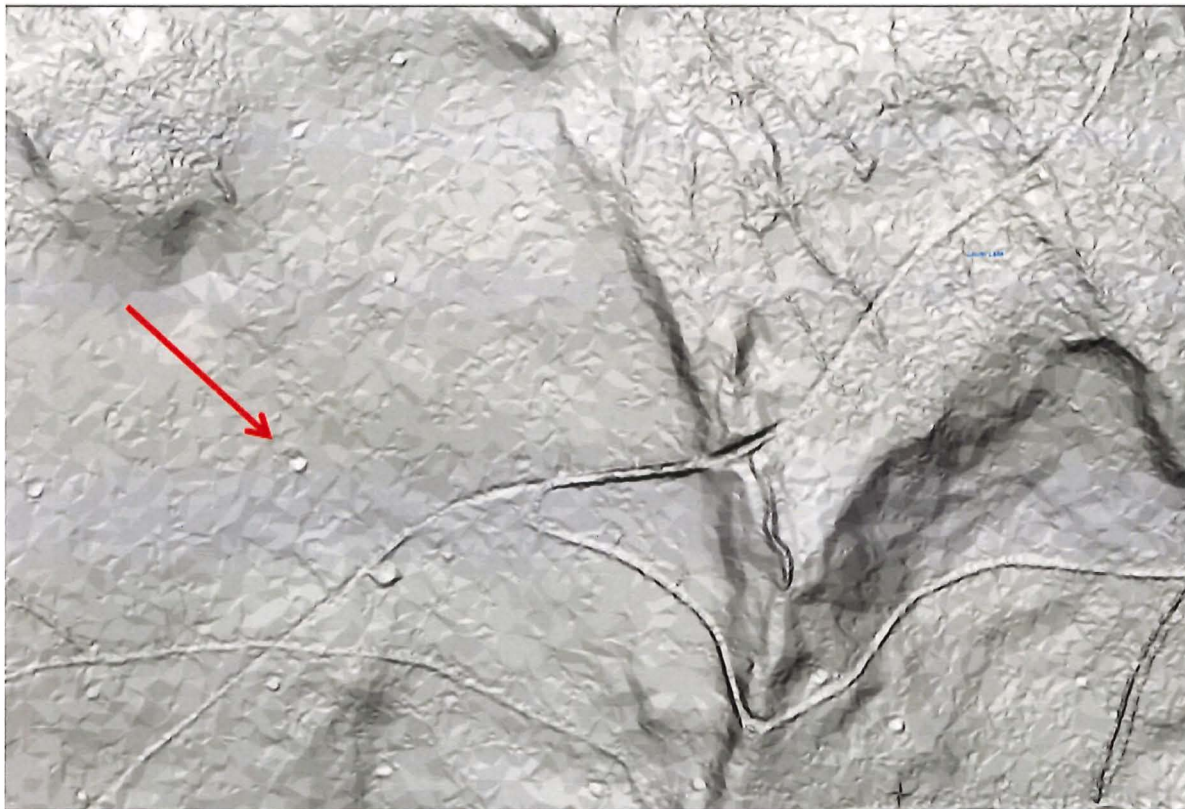


Figure 6. Geology superimposed on Lidar slope shade at Pine Grove Furnace, showing where rocks used came from. mr = Precambrian metarhyolite, Cwl = Cambrian Loudon and Weverton sandstones, Chm = Cambrian Harpers and Montalto formations, and Ct = Cambrian Tomstown Dolomite.

Charcoal was made by cutting trees on South Mountain, stacking the wood, covering it with leaves and soil, and letting the mass smolder for a week or so. This required a large crew to cut the wood, a collier to oversee the charcoal making, and a crew of teamsters to haul the charcoal to the furnace. It took about an acre of forest a day to keep the furnace running 24/7. By the late 1800's, South Mountain was nearly denuded of trees to make the charcoal. Today one can find the ubiquitous charcoal hearths on Lidar slope shade images as small circles (Fig. 7 and 8). We have mapped these on South Mountain (Potter, et al., 2013).



Pine Grove Furnace State Park and vicinity
Cumberland County, PA
PAMAP orthoimagery and Lidar elevation data

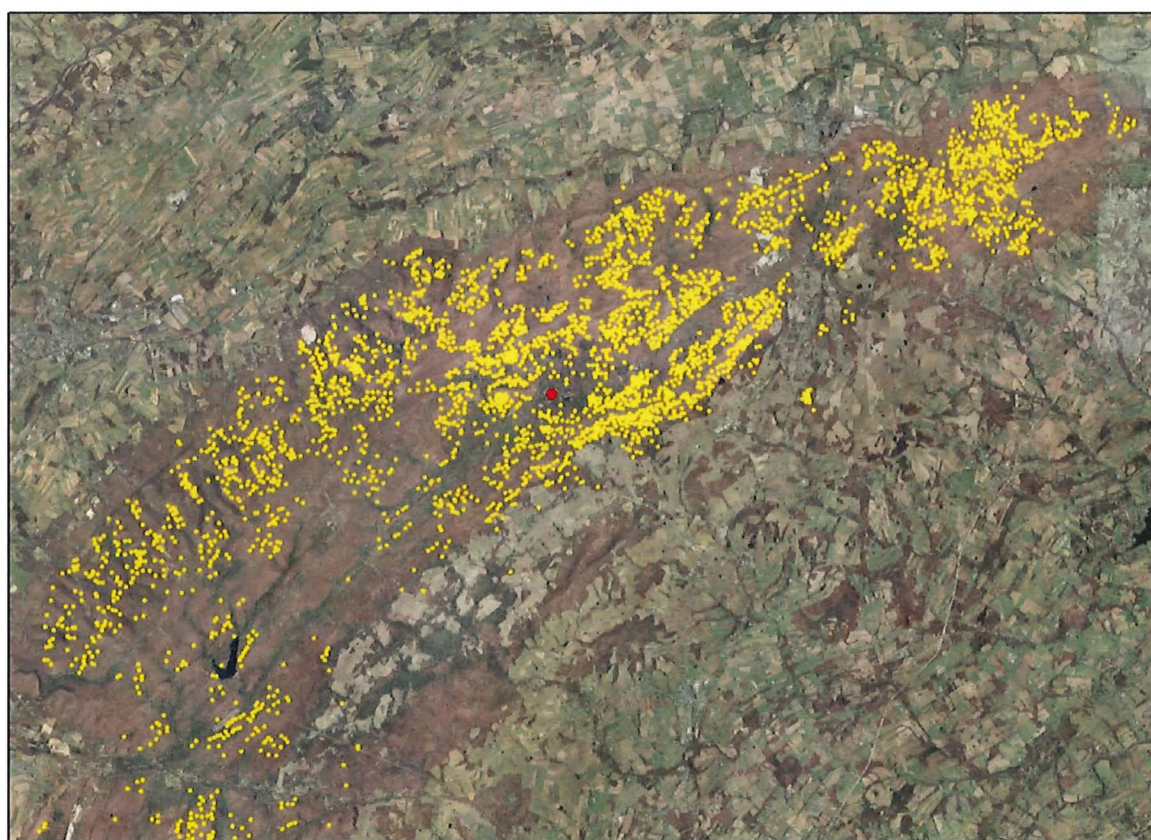
0 50 100 200 300 Feet

Figure 7. Lidar slope shade image showing charcoal hearths SW of Pine Grove Furnace. Arrow indicates hearth shown in Figure 9.

In the ~40 km stretch of South Mountain between Dillsburg and Caledonia Gap there we have counted over 3000 charcoal hearths, many of which were used more than once (Fig. 9). The iron making process and features that can be seen today are described in Way, (1986, 1991) and Wilshusen (1982, 1983).



Figure 8. Panorama of a charcoal hearth near Pine Grove Furnace. Cut bank on up slope side is to left of person. Soil excavated there was piled to right and toward person on downhill side. Diameter is about 13-15 m.



0 1 2 4 6 8 Miles

Charcoal Hearths on South Mountain



Figure 9. Charcoal Hearths on South Mountain. Each yellow dot is one hearth. There are over 3,000 in the image. Base is a color orthophoto. Dillisburg is near the east end of the image, and Caledonia Gap is near the west end. Red dot is Pine Grove Furnace.

There is a USGS Stream Gage on Mountain Creek at the bridge just S of the Ironmaster's Mansion. Real-time stage and discharge, plus historic data is available. USGS Stream Gage URL: <http://waterdata.usgs.gov/nwis/uv?01571184> Flooding on Mountain Creek every few years is severe enough to break the small berm between Mountain Creek and the bathing beach at Fuller Lake. The swimming site is so popular that it is usually repaired within a month or so. The USGS also has a ground water observation well near PGF just N of the mansion, which is in metarhyolite. Real-time stage plus historic data is available. USGS Ground Water Observation Well URL: <http://groundwaterwatch.usgs.gov/CRNSites.asp?S=400209077183301>

References

- Potter, N., Jr., Brubaker, K., and Delano, H. L., 2013, Lidar Reveals Thousands of 18th and 19th Century Charcoal Hearths on South Mountain, South-central Pennsylvania: Geological Society of America, Abstracts with Programs, v. 45, no. 1, p. 99.
- Way, J. H., 1986, Your guide to the geology of the Kings Gap area, Cumberland County, Pennsylvania: Pennsylvania Geological Survey, 4th Series, 31 p. (See p. 11-14 re PGF). Way, J. H., 1991, Pine Grove Iron Furnace and Early American Iron Making: *in* Sevon, W. D. and Potter, N., Jr., eds., *Geology in the South Mountain Area, Pennsylvania: Guidebook*, 56th Annual Field Conference of Pennsylvania Geologists, p. 133-142.
- Way, J. H., 1991, Stop 10, Guide to the Pine Grove Furnace area: *in* Sevon, W. D. and Potter, N., Jr., eds., *Geology in the South Mountain Area, Pennsylvania: Guidebook*, 56th Annual Field Conference of Pennsylvania Geologists, p. 217-219.
- Wilshusen, J. P., 1982, Stop 4, Pine Grove Furnace: *in* Potter, N., Jr., ed., *Geology in the South Mountain Area, Pennsylvania, Field Trip Guide*, Harrisburg Area Geological Society, p. 19-21.
- Wilshusen, J. P., 1983, *Geology of the Appalachian Trail in Pennsylvania*: Pennsylvania Geological Survey, 4th series, General Geology Report 74, 121 p. (See p. 88-90 re Pine Grove Furnace)

DETERMINATION OF PREFERENTIAL GROUNDWATER FLOW PATTERNS TO CUMBERLAND COUNTY SPRINGS WITH FLUORESCENT DYE TRACING

Todd M. Hurd, Department of Biology, Shippensburg University, Shippensburg, PA 17257
reprinted from *Pennsylvania Geology*, v.42 no.3, fall 2012, p. 3-11.



The two Big Spring source springs in Cumberland County, Pa., responded differently to a large rain event of July 2004

The larger west spring (foreground) became turbid with sediment. The east spring (background) remained clear

photo by Todd Hurd

Introduction

Carbonate springs of southern Pennsylvania are important as water resources for productive wild fisheries, trout hatcheries, and municipal supplies (Kochanov, 2010), yet karst groundwater basins are vulnerable to surface contaminants (Kacaroglu, 1999). Water and contaminants may pulse rapidly through karst flow systems to springs (Vesper and others 2003). In the Great Valley section of the Ridge and Valley physiographic province (locally known as the Cumberland Valley), agricultural nutrients and pesticides and runoff from impervious surfaces of developed areas rapidly enter the karst drainage system through sink collapses or sinking streams (Figure 1) and are carried rapidly to springs. Walderon and Hurd (2009) estimated that Letort Spring Run in Carlisle carries more than 170,000 kilo- grams per year (374,786 pounds per year) of nitrate-N, much of which resurges directly at springs. This much loading from the springhead of a single tributary in the lower Susquehanna basin means that there is a need for better management of runoff to our karst basins. Such management focus must occur above the point of spring resurgence, and along identified flow paths, for the protection of local water quality and for decreased nutrient loading to the Susquehanna and Potomac Rivers and to the Chesapeake Bay. As karst areas of

Pennsylvania are developed, there will be similar vulnerability of karst groundwater to associated industrial contaminants. For example, industrial activity at Letterkenny Army Depot in the Great Valley resulted in groundwater contaminated with volatile organics that flowed rapidly along pathways traced with fluorescent dyes to area springs (Aley and others, 2004).



Figure 1. Karst features in Cumberland County.

A. A sink collapse in the Zullinger Formation within a detention basin on a quarry property on the southeastern boundary of Big Spring's surface watershed.



B. A swallow in a surface stream fed by quarry pump water in the surface watershed of Green Spring/Bullshead Branch.

In order to better manage land and water resources in these areas, it is necessary to first delineate the contributing areas of karst springs with fluorescent dye tracing (Käss, 1998). In karst environments, regional groundwater flow may cross topographic divides, and rapid flow through karst solution channels makes it necessary

to utilize fluorescent dye tracing with, or in place of, hydrological models. Without an understanding of pathways and travel times to springs, there is little that can be done to identify and mitigate pollutants associated with a particular spring or to plan for a safe water supply in instances where carbonate springs are utilized for this purpose.

Fluorescent Dye Traces

In early 2003, I became interested in identifying source areas for Big Spring, one of the largest karst spring systems in Cumberland County (Figures 2 and 3) and Pennsylvania's fifth largest spring (Kochanov, 2010). In 2003, Big Spring was rapidly recovering from eutrophication (an increase in dissolved nutrients and plant growth, and a decrease in dissolved oxygen) caused by aquaculture discharge (Hurd and others, 2008), and a limestone quarry just a little over a mile south and east of the two primary source springs was undergoing the permitting process. Big Spring received much scrutiny because of these and other potential impacts on water quality or quantity, due to both its historical value as a wild-brook-trout fishery and its use as a municipal water supply. A contributing spring in Newville serves the borough and adjacent township, and the channel is permitted as a secondary supply. The source springs together contribute a mean discharge of $0.79 \text{ m}^3/\text{s}$ (cubic meters per second) or 28 cfs (cubic feet per second) (U.S. Geological Survey, 2009). The estimated contributing area for the springs is 76 km^2 (square kilometers) (29.3 mi^2 [square miles]), whereas the surface basin area is only about 9 km^2 (3.4 mi^2) (Hurd and others, 2010). These calculations clearly point to regional flow patterns from source areas beyond the topographic basin.

Through Donald Seigel, Department of Geology at Syracuse University, I met Martin H. Otz, who has extensive global experience conducting fluorescent dye tracing projects, along with his wife Ines and father Heinz. The Otz family conducted field reconnaissance in Cumberland County and helped me plan a fluorescent dye trace of Big Spring's source areas. In addition to determining general source areas, we wanted to determine if there was a hydrological connection from a recently permitted quarry east of Big Spring or to surrounding springs, in order to address stakeholder concerns over potential changes in flow and turbidity. Our plan was to delineate the contributing areas of Big Spring and surrounding springs using tracer release points to the south and west, and eventually from the south and east boundary of Big Spring's surface basin where the recently permitted quarry was being constructed (Figure 3, eastern asterisk). The Department of Environmental Protection, Bureau of Mining, did not require a fluorescent dye trace in order to approve the quarry permit, citing adequacy of a flow model that indicated slow (meters per day) localized northward groundwater flow (Continental Placer, 2003) and concerns about coloration of water that might result from the dye.

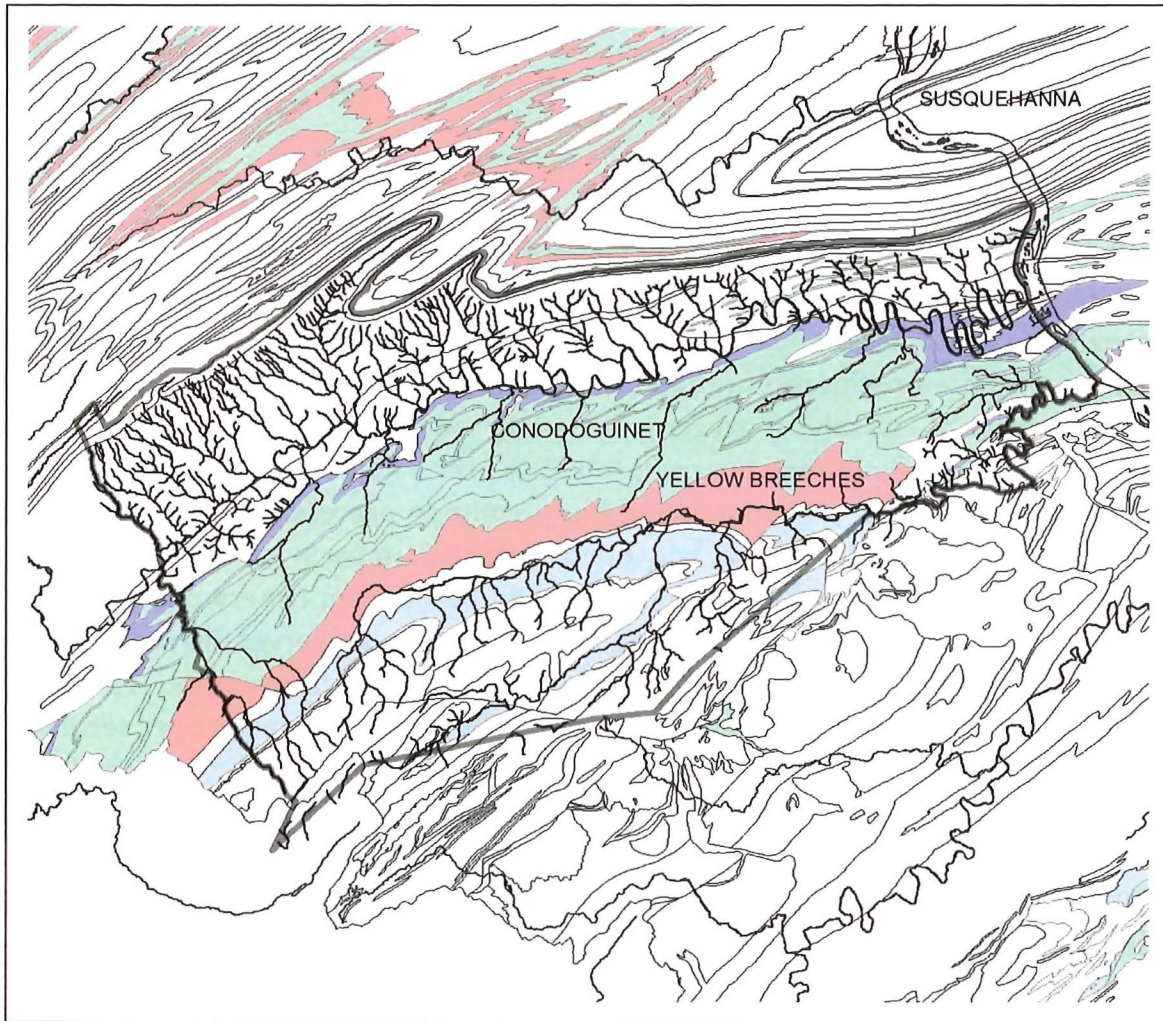
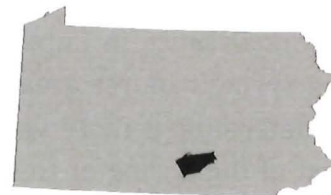


Figure 2. Streams of Cumberland County, Pa., showing the influence of karst geology in the Great Valley.

Surface drainage to the Susquehanna River occurs from the Yellow Breeches Creek along the flank of South Mountain and from the Conodoguinet Creek along the flank of North Mountain.



Nutrient-rich springs with largely undefined source areas surface at the valley center and flow north to Conodoguinet Creek. Blue, Cambrian Tomstown Formation; pink, Cambrian Elbrook Formation; blue-green, Cambrian and Ordovician limestones (Cambrian Zullinger and Shadygrove Formations, Ordovician Stonehenge [including the Stoufferstown Member], Rockdale Run, and Pinesburg Station Formations; Ordovician St. Paul Group, and Ordovician Myerstown Formation); purple, Ordovician Chambersburg Formation. Map data (major rivers, streams, bedrock, and counties) from PASDA (Pennsylvania Spatial Data Access, 2012).

Consultants did note, however, that some of the Cambrian Zullinger Formation that underlies most of the property is fractured. Moreover, the newly constructed detention pond never filled, due to rapid drainage into an associated sink (Figure 1A), indicating rapid groundwater flow to unknown receptors.

Fluorescent tracers were chosen based on their known effectiveness and low levels of human or ecotoxicity (Field and others, 1995; Käss, 1998). For initial traces (Hurd and others, 2010), water and charcoal receptor samples were analyzed by Nano Trace Technologies™ (Martin and Ines Otz) and by the Crawford Hydrology Lab (University of Western Kentucky), respectively, using synchronous scanning spectrofluorometers. For subsequent studies, analyses were completed with Perkin Elmer LS series fluorescence spectrometers.

We conducted fluorescent dye traces from sinking reaches of the Yellow Breeches Creek to the south and a sink collapse in western Cumberland County close to Shippensburg in the Zullinger Formation (Figure 3). Chichester (1996) noted that the Yellow Breeches loses water to the Conodoguinet Creek via springs in the valley center. Nevertheless, Becher and Root (1981) mapped a groundwater divide between the Yellow Breeches and the springs of western Cumberland County. This mapped divide suggested continuity between groundwater in the upper Middle Spring watershed near Shippensburg and the springs in the valley center, although well levels in the region generally indicate more northward groundwater flow.

Rapid Regional Flow Patterns

Hurd and others (2010) described rapid flow to Big Spring (about 2 km or 1.2 mi per day) closely parallel to geologic strike from 9 km (5.6 mi) away (Figure 3). This rapid flow path is highly susceptible to surface contaminants. The sinkhole where sulforhodamine-B dye was released receives runoff from a large impervious area into the Zullinger Formation from Interstate Route 81 and a developed area near the State Route 174 interchange outside of Shippensburg. An open ditch between the impervious area and the sink collapse crosses under Interstate Route 81 and could easily conduct highway spills to the sink. Also in that study, loss of water was traced from the Yellow Breeches Creek in Walnut Bottom to carbonate springs at Huntsdale State Fish Culture Station with uranine (sodium fluoresceine) fluorescent dye. This flow was slower, likely due to the influence of the colluvial mantle between the release point and these springs in the southern portion of the Great Valley. Nevertheless, groundwater traveled relatively fast (about 9.5 km/month, or 6 mi/month) and followed the general trend of geologic strike, in this case remaining within the Yellow Breeches drainage (Figure 3). There was no sign of this tracer in Big Spring or any of the north-flowing spring creeks around Big Spring. These results pointed to a source area for Big Spring to the west, and the sinking tributaries of Middle Spring Creek appeared to be potential candidates.

The Burd Run subbasin of Middle Spring Creek is unique in that its channel is continuous across the Great Valley. The tributaries sink strongly where the South Mountain colluvium thins, and the surface channels serve as overflow for the complex karst system beneath. In Shippensburg, Burd Run receives steadier flow from carbonate springs and joins another branch of Middle Spring Creek to become the largest tributary of the Conodoguinet Creek on the Great Valley's north side. All tributaries of Middle Spring Creek commonly sink completely up-gradient from Shippensburg, especially the eastern (Thompson Creek) branch of Burd Run. This is an interesting area in terms of karst surface features and caves, and it includes Cleversburg Sink and other caves (Smeltzer, 1958).

During the spring of 2009, Shippensburg undergraduate David Miller, Jr., and I traced a 10 km (6.2 mi) interbasin flow path from Thompson Creek to Big Spring (Figures 3 and 4). Effective linear velocity was determined to be 0.6 km/day (0.4 mi/day), using uranine released at a railroad bridge near Airport Road at the boundary between the Elbrook and Zullinger Formations.

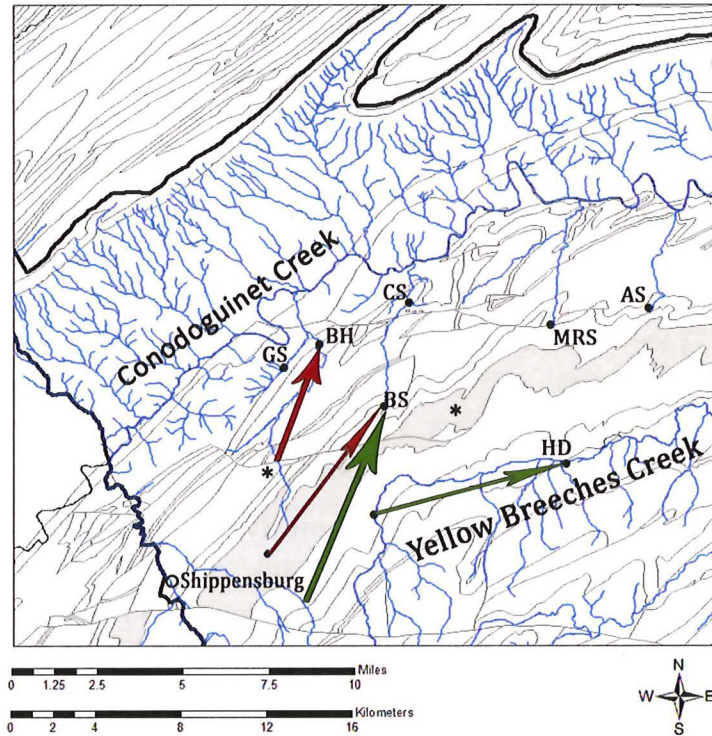


Figure 3. Groundwater flow in western Cumberland County as determined by fluorescent dye tracing. Thin arrows show groundwater flow determined by Hurd and others (2010); bold arrows show groundwater flow direction determined in 2009. Uranine (URA) was used to trace interbasin flow from upper Burd Run/Middle Spring to Big Spring and flow from the upper Yellow Breeches to Huntsdale Springs. Sulforhodamine B (SRB) was used along with sodium naphthionate to trace flow in the Bullshead Branch system and from a sinkhole in the Zullinger Formation near the Interstate Route 81 and State Route 174 interchange. The Zullinger Formation is shown in light gray, and the asterisks show locations of limestone quarries in the region. Springs sampled were Big Spring (BS), Green Spring (GS), Bullshead Branch (BH), Cool Spring, Newville's municipal supply (CS), Mount Rock Spring (MRS), Alexander Spring (AS), and Huntsdale Springs (HD). Burd Run of Middle Spring was also sampled but there was no definitive detection of uranine, suggesting a different source water than that sinking higher in the watershed.

Interestingly, dominant dye breakthrough occurred first in the smaller east source spring, the opposite result of the 2005 trace into the failed detention basin further out in the Zullinger (Hurd and others, 2010). Both traces showed flow to the source springs from the same general vicinity, yet with specific flow to particular springs and some crossover that likely depends on precipitation and water level (Figure 4). It is interesting to note that discharge was increasing between $0.71 \text{ m}^3/\text{s}$ (25 cfs) and $0.85 \text{ m}^3/\text{s}$ (30 cfs) in the first trace, when breakthrough occurred first and most strongly in the west source spring. Discharge was decreasing between these same values in 2009 when there was first and strongest breakthrough in the east source spring (Figure 4).

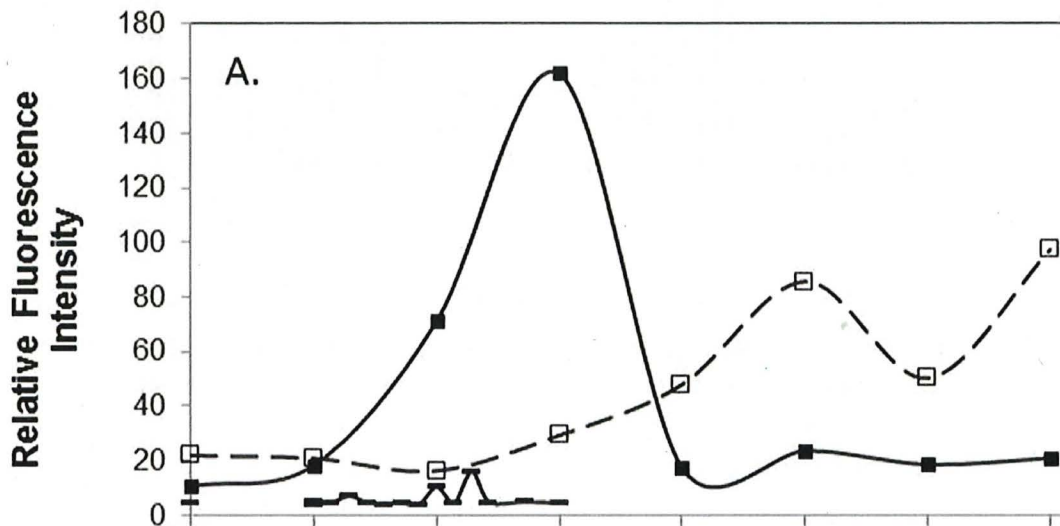


Figure 4. A. Breakthrough (dye detection) of uranine in Big Spring source springs released from upper Burd Run/Middle Spring 10 km (6.2 mi) away. Relative Fluorescence Intensity (RFI) of uranine (sodium fluoresceine) showing breakthrough at Big Spring East (solid squares) and Big Spring West (open squares), detected in charcoal eluate after February 26, 2009, release, and under 1 ppb (part per billion) in water from Big Spring East two weeks following release (flat line symbols). Charcoal receptors were changed weekly and so indicate a slight lag in breakthrough. 160 RFI = 10.3 ppb uranine in eluate.

The east source spring does not show turbidity response to large rain events, whereas the west spring shows turbulent flow and discharge of sediment from associated conduits (see cover). The east source spring also exhibits higher electrical conductivity (574 vs. $537 \mu\text{S}/\text{cm}$ [microsiemens per centimeter] in a recent measurement). These patterns demonstrate unique contributing flow paths from different surface inputs in the upper Burd Run/Middle Spring watershed. Big Spring is an Exceptional Value (EV) stream in its upper reaches. An EV stream receives Pennsylvania's highest water use

designation based primarily on water quality. It is also a secondary water supply for Newville and Centerville and is susceptible to contaminant spills from the distant highway interchange or railroad line where the tracers were released. Different travel times of the tracers indicate the approximate response time needed to protect the stream and water supply if highway or railway spills were to occur, in addition to

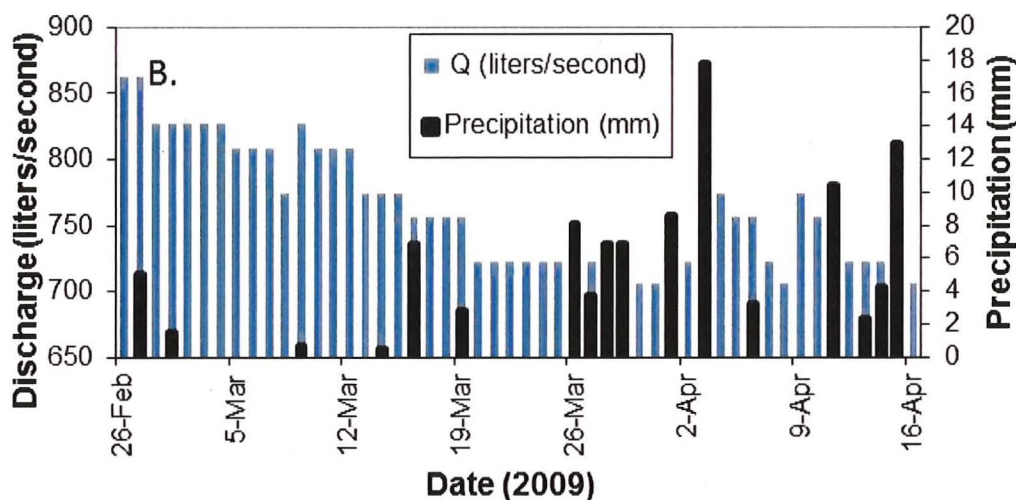


Figure 4. B. Big Spring discharge (Q, shown in light blue) (Bruce Lindsey, U.S. Geological Survey, personal communication) and precipitation at Shippensburg University.

specific hydrogeological flow paths.

Other recent fluorescent dye traces showed flow from a sinking stream of the Bullshead Branch subbasin of Green Spring Creek (Figures 1B and 3) to a major spring of Bullshead Branch (Figure 3). One connected spring is utilized as a residential water supply. This flow is also rapid (2 km/day or 1.2 mi/day) and generally parallel to strike, although the area is also heavily faulted (Becher and Root, 1981). This faulting appears to influence sinking of surface waters and flow direction in the area (Figure 3). This system has proven more complex to trace, due to more sediment, the structural complexity, and variable pumping of pit water in another limestone quarry (Figure 3, western asterisk) that influences the surface flow and also possibly groundwater flow patterns. After being pumped, the surface flow is exposed directly to pastured livestock, eroding pastures, fields, and roadsides, then sinks rapidly (Figure 1B) into the Ordovician Rockdale Run Formation near the Pinesburg Station Formation and St. Paul Group (Becher and Root, 1981). The swallet where loss of surface flow occurs is plugged intermittently with sediment. Sodium naphthionate released at this site was detected intermittently at greater than 10 times the background, but sulforhodamine B did not break through at more than 5 times the background from this release point (Figure 5), perhaps due to adsorption on sediment or dilution into separate receiving waters. Results from both dyes suggested that lower Big Spring as well as Bullshead

Branch of Green Spring Creek rapidly received water from this site, but more work is needed to confirm these and other karst flow patterns and their potential to carry sediments and surface pollutants to springs. Also of note is that all positive traces were detected in water at the parts per trillion level, far below visible detection, or at parts per billion level after being concentrated on activated carbon. Modern fluorescent dye tracing techniques utilize smaller quantities of non-toxic fluorescent tracers that typically result in subvisible concentrations in receptor springs in rivers. These techniques can therefore safely demonstrate actual groundwater flow patterns in karst geology for improved understanding and protection of our water resources.

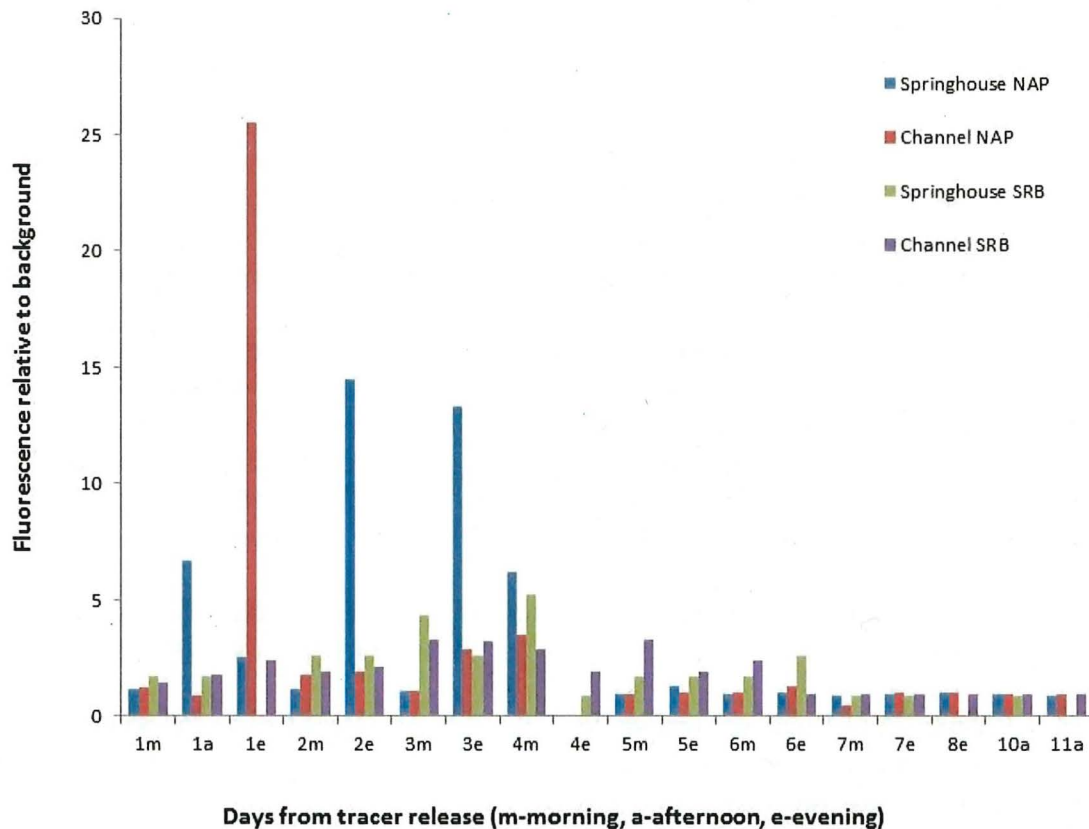


Figure 5. Sodium naphthionate (NAP) broke through intermittently between days 1 and 4 in major springs of Bullshead Spring Branch following release into the strongly faulted Rockdale Run Formation of the valley center, about 5 km (3.1 mi) away. The trace was repeated with a small quantity of sulforhodamine B dye (SRB), which likely adsorbed onto sediments, or possibly went to other receptor springs. Both tracers returned to background levels within one week, indicating strongly preferential flow patterns in the karst.

Acknowledgments

The Big Spring Watershed Association, Alexander Stewart Foundation, Pennsylvania State System of Higher Education, Shippensburg University Undergraduate and Graduate Research Programs, and Shippensburg University Center

for Land Use all provided funding for these studies. In addition to assistance from the Otz family, Ashley Brookhart-Rebert was the Shippensburg University graduate student on the initial project, and Nick Crawford of the University of Western Kentucky (Crawford Hydrology Lab and Center for Cave and Karst Studies) and Tom Feeney of Shippensburg University also provided planning assistance. I thank Martin and Ines Otz of Nano Trace Technologies™ and Tom Feeney for ongoing assistance and collaboration, Shippensburg undergraduates David Miller, Jr., and Renae Saum, and former Shippensburg student Kaja Spaseff for field assistance, Robert Schott of DEP Water Quality for consideration of best fluorescent dyes to use, and two anonymous reviewers for improvements to the manuscript.

References

- Aley, Thomas, Tucker, Mark, and Stone, P. R., III, 2004, Letterkenny Army Depot Southeastern Area National Priorities List site, Operable Unit Six off-post groundwater, Appendix A-4, Groundwater Tracing Study, Off-Post Trace 3, prepared by Ozark Underground Laboratory, Protom, Missouri, in Shaw Environmental, Inc., compiler, SEOU6 Southeastern Area Off-Post Groundwater Remedial Investigation Report LEADSEOU6RI1104: Cherry Hill, N.J., Shaw Environmental, Inc., 141 p.
- Becher, A. E., and Root, S. I., 1981, Groundwater and geology of the Cumberland Valley, Cumberland County, Pennsylvania: Pennsylvania Geological Survey, 4th ser., Water Resource Report 50, 95 p. (also online at www.dcnr.state.pa.us/topogeo/pub/water/w050.aspx) (accessed December 17, 2012).
- Chichester, D. C., 1996, Hydrogeology of, and simulation of ground-water flow in, a mantled carbonate-rock system, Cumberland Valley, Pennsylvania: U.S. Geological Survey, Water-Resources Investigation 94-4090, 39 p.
- Continental Placer, 2003, Quarry dewatering impact evaluation: West Albany, N.Y., Continental Placer, Inc., produced for Pennsy Supply, Inc., Penn Township Operation, December 2003, 7 p.
- Field, M. S., Wilhelm, R. G., Quinlan, J. F., and Aley, T. J., 1995, An assessment of the potential adverse properties of fluorescent tracer dyes used for groundwater tracing: *Environmental Monitoring and Assessment*, v. 38, no. 1, p. 75-96.
- Hurd, T. M., Brookhart-Rebert, Ashley, Feeney, T. P., and others, 2010, Fast, regional conduit flow to an exceptional-value spring-fed creek—Implications for source water protection in mantled karst of south central Pennsylvania: *Journal of Cave and Karst Studies*, v. 72, p. 129-136.
- Hurd, T. M., Jesic, Slaven, Jerin, J. L., and others, 2008, Stable isotope tracing of trout hatchery carbon to sediments and foodwebs of limestone spring creeks: *Science of the Total Environment*, v. 405, p. 161-172.
- Kacaroglu, Fikret, 1999, Review of groundwater pollution and protection in karst areas: *Water, Air and Soil Pollution*, v. 113, nos. 1-4, p. 337-356.
- Käss, Werner, 1998, Tracing technique in geohydrology: Rotterdam, A. A. Balkema, 581 p.
- Kochanov, W. E., 2010, Pennsylvania's top ten springs: *Pennsylvania Geology*, v. 40, no. 1, p. 15., www.dcnr.state.pa.us/topogeo/pub/pageolmag/pdfs/v40n1.pdf (accessed December 17, 2012).

BRIEF THOUGHTS ON LONG-TERM LANDSCAPE EVOLUTION IN THE MID-ATLANTIC REGION WITH A FOCUS ON THE POND BANK LIGNITE

(updated from SE Friends of the Pleistocene South Mountain Trip, Spring, 2013)

*Frank J. Pazzaglia, Department of Earth and Environmental Sciences
Lehigh University, 1 West Packer Ave., Bethlehem, PA 18015, fjp3@lehigh.edu*

Introduction

The 2014 Pennsylvania field conference focuses on the South Mountain region that preserves, among other deposits, a Pleistocene and locally pre-Pleistocene record of colluvial, fluvial, and debris-flow deposition in the Cumberland Valley. This short contribution aims to frame what we know about the Cenozoic history of South Mountain in the broader context of long-term landscape evolution of the mid-Atlantic region. Field trip participants are likely familiar with the venerable arguments of the cycle of erosion (Davis, 1899) and dynamic equilibrium (Hack, 1960) so this summary will steer clear of trying to support or falsify either model. Rather, the summary briefly reviews what we know and identifies how particular observations and data compel or constrain our thinking on this subject. The interested reader is directed to Pazzaglia and Brandon (1996), Pazzaglia et al. (2010), Portenga et al. (2013) and McKeon et al., (2013) for more thorough recent reviews of the basic long-term landscape evolution arguments.

Landscape evolution is best quantified as changes in the mean elevation, mean relief, rate of erosion, and unsteadiness of that erosion, the latter being a good measure of the degree of disequilibrium and transient processes operating on the landscape. Here, data and observations for long-term (million to tens of millions of years) and intermediate (hundreds of thousands to million year) scale erosion and landscape change are presented. The reader interested in studies addressing short-term rates of erosion for the mid-Atlantic region are directed to Sevon (1989), Langland and Haney (1997), Conrad and Saunderson (1999), and Walter and Merritts (2008). Excellent examples of how paleorelief could be inferred from geomorphic data are found in McKeon et al. (2014), Gallen et al. (2013), and Miller et al. (2013).

Thermochronology

Thermochronology, or the study of how certain mineral phases cool as they are exhumed from deep in the crust to the surface of the Earth, provides a robust method for determining erosion rates over very long periods of time. Although the method can typically only give long-term averages, recent understanding of how cooling rate and mineral composition influence results has allowed for more sophisticated modeling and the inference of erosional (cooling) unsteadiness using these data. One common

mineral used in thermochronology is apatite because of its inclusion of radioactive U and Th in the crustal lattice. Through both spontaneous fission (Apatite Fission Track – AFT) and alpha decay (U-Th/He – AHe), apatite provides at least two ways to reconstruct mineral cooling by erosional exhumation. Apatite retains lattice damage generated by fission tracks when the mineral cools below $\sim 100^{\circ}\text{C}$. In contrast, the U-Th/He parent-daughter system becomes closed to rapid diffusion and escape of He when the mineral cools below $\sim 60\text{--}70^{\circ}\text{C}$. Given the gentle geothermal gradient of $15\text{--}20^{\circ}\text{C/km}$ for the central Appalachians, these temperatures correspond to depths of $\sim 4\text{--}5$ and $3\text{--}4$ km respectively.

U-Th/He cooling ages for Pennsylvania ($n=31$) range from $\sim 60\text{--}240$ Ma and show different pooled ages for the Ridge and Valley (~ 198 Ma), Blue Ridge (~ 98 Ma) and Piedmont (~ 172 Ma) provinces (Fig. 1). The Blue Ridge cooling ages are more tightly clustered and do not have any overlap with the Piedmont or Ridge and Valley samples that exhibit considerable overlap in their ages. Ridge and Valley and Piedmont AHe mean cooling ages are younger than corresponding AFT (Roden and Miller, 1989) and ZFT (Kohn et al., 1993) cooling ages respectively; however, there is overlap in the cooling age ranges for these different thermochronometers.

Assuming a uniform geothermal gradient of $\sim 20^{\circ}\text{C/km}$ for all of Pennsylvania and New Jersey over the cooling history of these samples, it appears that the Ridge and Valley and Piedmont provinces cooled through 70°C in the Early to Middle Jurassic and the erosion rate since that time has averaged ~ 16 m/m.y. (3000 m in 185 m.y.). For a similar geothermal gradient, the Blue Ridge, including presumably South Mountain has been eroded more rapidly at ~ 31 m/m.y. (3000 m in 98 m.y.).

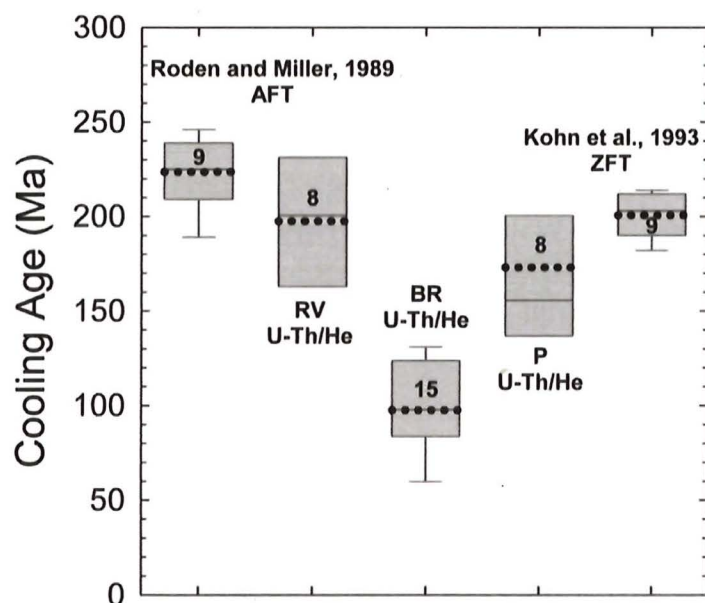


Figure 1. AHe bedrock cooling ages for PA and NJ.
 RV = Ridge and Valley
 BR = Blue Ridge
 P = Piedmont
 AFT = Apatite fission track
 ZFT = Zircon fission track
 Numbers in boxes are the number of samples. Dash lines are means, solid lines are modes, gray box incorporates the 10th and 90th percentile, and whiskers are the 5th and 95th percentile (shown where statistically valid).

A somewhat more sophisticated treatment of these data, including samples spanning the entire Appalachians is presented in McKeon et al. (2014). Modeling of the cooling history of samples collected from ridge tops and valley bottoms in the southern Appalachians, they find that between 160 and 60 Ma, the ridge tops have eroded at a rate of ~ 20 m/m.y. whereas the valley bottoms eroded more rapidly at a rate of ~ 35 m/m.y. The implication is that relief grew in the Appalachian landscape through the Cretaceous and into the early Cenozoic. Since ~ 60 Ma, relief has been slowly decreasing and the mean rate of erosion for both the ridge tops and valleys has been ~ 20 m/m.y. It is not yet known if the McKeon et al. (2014) results could be extended into the South Mountain landscape in describing its long-term erosion history.

Pond Bank

The well-known Cretaceous lignite at Pond Bank (*Pierce, 1965; Fig. 2*) places some constraints on how much relief, erosion, and chemical dissolution is possible at South Mountain over tens of millions of years. The lignite contains upper Cretaceous (early Campanian, ~ 80 Ma) terrestrial pollen, distinctly lacking any marine palynomorphs, encased in part by residuum derived from the host carbonate bedrock.

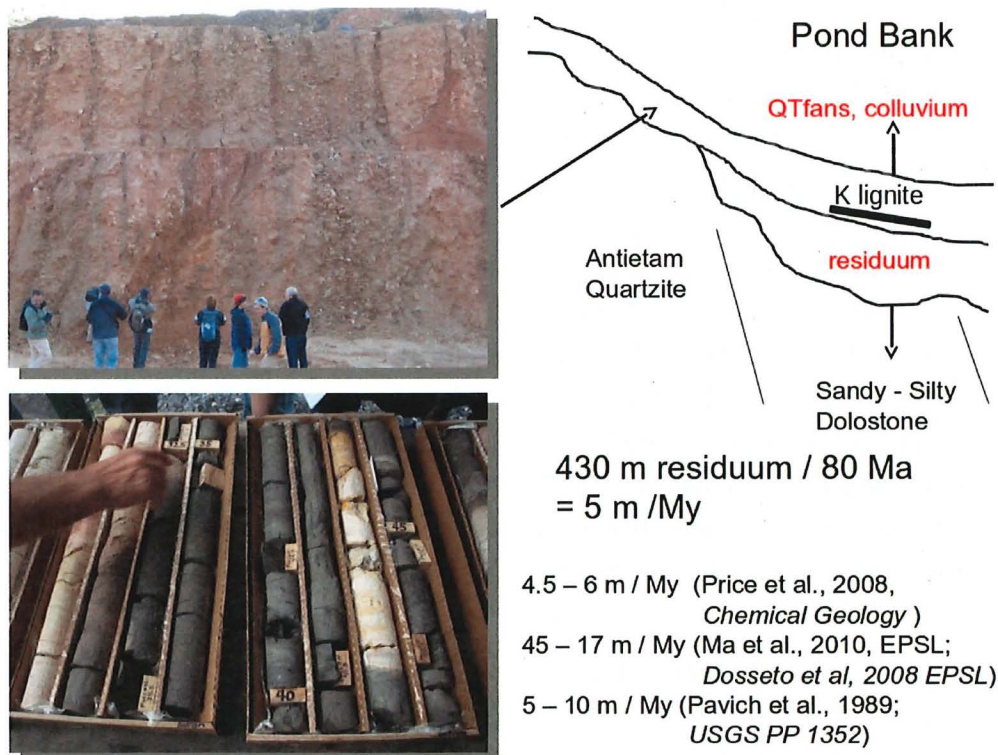


Figure 2. Photographs of thick accumulations of unconsolidated Cenozoic alluvium and colluvium preserved along the western flank of South Mountain (upper left, Mainsville Pit) and part of the Pond Bank core recovered by the USGS that shows the lignitic horizons (lower left). The sketch on the right shows the general depositional setting of the Pond Bank lignite along with several recent estimates for the source of the subsidence and sediment accommodation space that is driven by dissolution of the bedrock. Note the peculiar way that the stratigraphy here youngs both upward and downward from the Cretaceous horizon.

This biostratigraphic age overlaps with the upper part of the Potomac Group lithostratigraphy represented by the Raritan and Magothy formations in New Jersey and eastern Maryland and Patapsco Formation in western Maryland and is at least in part consistent with the lignite common in the Magothy Formation. The highest sea levels in the Cretaceous are Cenomanian in age (~91-92 Ma; Sahagian et al., 1996), coincident with Raritan-Patapsco Fm deposition, thus it is possible that the Pond Bank lignite represents the fluvial, upstream equivalent of these Coastal Plain deposits. The Pond Bank deposit is unique for the Great Valley and it is probably no coincidence that it was preserved in a carbonate sink hole given that the thermochronology argues for ~3 km of average erosion since its deposition. As long as the rate of carbonate dissolution matches the long-term rate of unroofing fixed by the thermochronology, then the Pond Bank deposit could have been lowered vertically through carbonate dissolution, escaping removal by mechanical erosion.

Preservation of the Pond Bank lignite illustrates a peculiar way in which Cenozoic sediments are preserved in the South Mountain – Cumberland Valley landscape. The juxtaposition of a forested quartzite ridge against immature, sandy carbonates drives dissolution of those carbonates, production of an insoluble residue (Price et al., 2008), and accommodation space due to karst subsidence. Sediment washed off of the western flank of South Mountain is trapped by that subsidence, and a stratigraphy of Cenozoic erosion is preserved. The Pond Bank deposit is preserved at depth near the base of a thick colluvial and alluvial fan stratigraphic package. That package thickens upwards reflecting the relative contributions of sediment supply and subsidence. At the same time, dissolution of the carbonate to produce a residual deposit including saprolite proceeds beneath the lignite. Measurements of carbonate dissolution in Pennsylvania (White et al., 1984, 2000; Price et al., 2008) range from ~8-30 m/m.y., values consistent with the long term average determined by the thermochronology. Using an insoluble residue content of 10% for the carbonates at Pond Bank, Pierce (1965) inferred that at least 430 m of carbonates have weathered beneath the gravel to produce the residuum below the lignite-bearing beds. Thus, the stratigraphic column in this setting is oldest in the middle, at the horizon that preserves the Late Cretaceous lignite. That stratigraphy youngs both upward towards the surface, and downward towards the bedrock-saprolite interface (*Fig. 2*).

Two recent cores were obtained at the Pond Bank site by the U.S. Geological Survey. A photograph of the core is seen in *Fig. 2*. Core #1 was drilled to a depth of 330 feet. The upper ~170 feet is mostly sandy clay whereas the lower half of the core is much coarser grained with several horizons of coarse, weathered Antietam clasts and rounded vein quartz pebbles. The second core only penetrated 100 feet, encountering dark, silty lignitic clay between approximately 30 -50 feet. The plan is to have the core available for inspection during the lunch stop of Day 1 of the field trip. Look for

evidence of dark, lignitic layers and the tell-tale purple and maroon colors of the Cretaceous sandy sediments.

Tertiary ages for residual deposits associated with the alluvial fans trapped in the Cumberland Valley karst-generated basin stratigraphically above the Pond Bank lignite are supported by K-Ar geochronology of K-bearing Mn-oxide (cryptomelane) ores (Bikerman et al., 1999) that are common in the Cumberland and Shenandoah valleys (Hack, 1965). Five samples from these ores from the western flank of South Mountain are dated between 6 and 58 Ma. The precise stratigraphic relationship of any of these samples to the alluvial fans has yet to be determined, but they are consistent with the growth and preservation of the thick and ancient residuum that underlies the western flank of South Mountain.

River Incision

River channels in the Appalachian landscape of Pennsylvania including South Mountain are segmented, containing concave-up graded reaches with intervening steep, convex reaches containing one or more knickpoints (*Fig. 3, 4*). Where these knickpoints are not fixed by some particularly resistant bedrock, they are presumed to have been caused by unsteady, rapid base level fall at the mouth of the Susquehanna River, and have been since migrating upstream (Miller et al., 2013). The lower Susquehanna River is particularly steep, having seen a base level fall of ~100 m in the past 10 Ma (Pazzaglia and Gardner, 1993, 1994). Correspondingly, river incision in the Pennsylvania Piedmont since the late Miocene is ~10 m/m.y. as a long term average, but can be as rapid as ~250 m/m.y. (Reusser et al., 2005) in the late Pleistocene (*Fig. 3*). At Marietta PA and within the zone evidently impacted by the post-Miocene base level fall outside of the Piedmont, an excellent suite of Pleistocene terraces (Engle et al., 1996) indicates a river incision rate of ~20 m/m.y.

The post-late Miocene base level fall and its knickpoints have not yet propagated upstream into the Great Valley and South Mountain landscape, given that the elevation of the strike-valley streams draining South Mountain are at elevations above ~152 m. Stream long profile convexities attributable to base level falls and the transient upstream migration of knickpoints in the South Mountain landscape would therefore have to be > 10 Ma. The fact that such knickpoints would be preserved at all attest to the overall slow pace of landscape change as well as the operation of an omnipresent, but not necessarily uniform background rate of erosion that is lowering all parts of the river channel and the intervening hillslopes such that memory of past higher base levels and landscapes of lower-than present relief can be preserved.

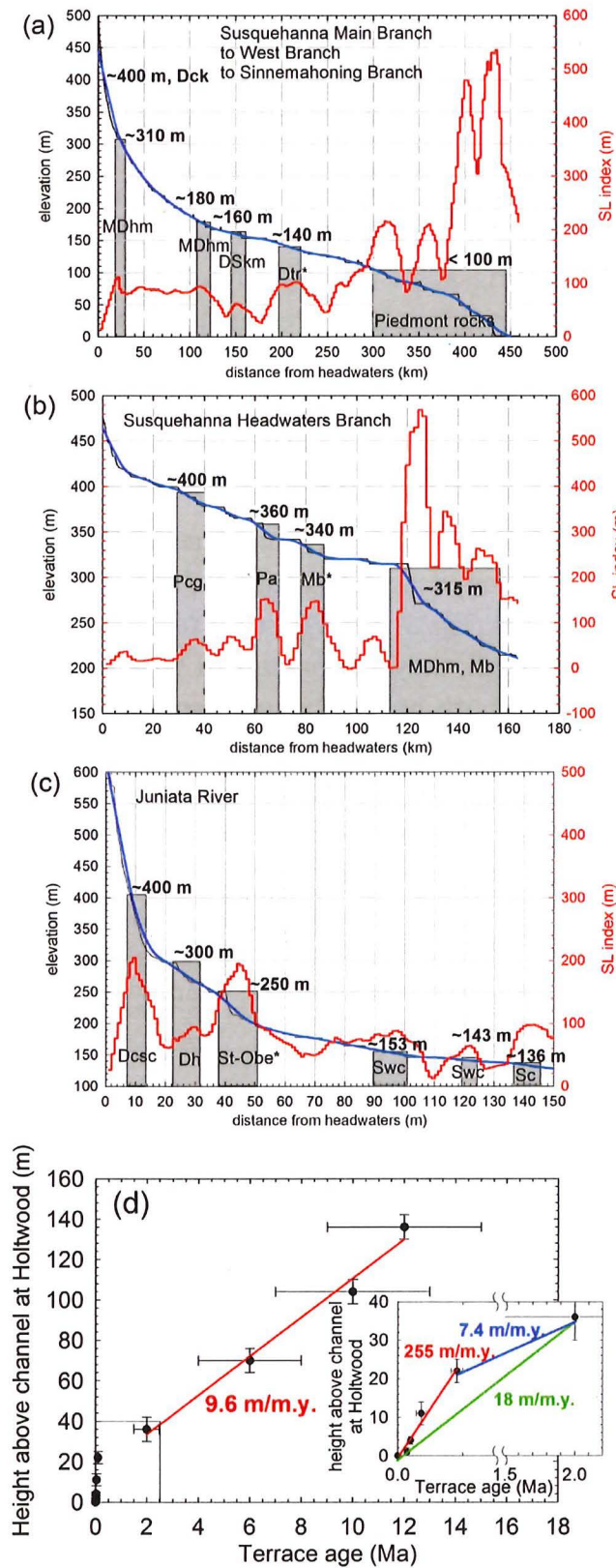


Figure 3.
Long profiles of the
(a) Susquehanna River and its major tributaries,
(b) the Main Branch above Westport, and
(c) the Juniata River.
 The black profile are the raw data extracted from a 90-m DEM, the blue line is a lowess filtered profile to remove high frequency noise, the red line is the Hack SL-index (Hack, 1973). The shaded rectangles indicate knickpoints.
Rock-types:
 MDhm=Huntley Mountain Fm,
 DSk = Keyser through Mifflintown Fm undivided,
 Dtr = Trimmers Rock Fm,
 Pcg = Conemaugh Group,
 Pa = Allegheny Fm,
 Mb = Burgoon Fm,
 Dcsc = Sherman Creek Mbr, Catskill Fm,
 Dh = Hamilton Group,
 St-Obe = Tuscarora through Bald Eagle Fms,
 Swc = Wills Creek Fm,
 Sc = Clinton Group.
 An asterisk indicates possible rock type control on the knickpoint. (d) Susquehanna River incision rates at the Holtwood gorge. Inset graph shows detail in the incision rates for the past 2.5 m.y.

Cosmogenic and chemical dissolution-determined rates of erosion and landscape change

The recent work of Price et al (2008), Hancock and Kirwan (2007), and Portenga et al (2013) offer excellent summaries of what we know about these background rates of erosion of bedrock exposures in the central Appalachians, including South Mountain. Coupled with cosmogenic radio nuclide (CRN) determination of basin-wide erosion rates determined from river alluvium (Matmon et al., 2003; Reuter, 2005) these data allow for a landscape view of denudation over 10^5 – 10^6 yr time scales (*Fig. 4*). Portenga et al (2013) report an average ridge-line erosion rate of exposed bedrock of ~ 9 m/my and landscape-scale averages of all bedrock outcrops of 6 m/m.y. which compares favorably to those reported by Hancock and Kirwan (2007). Similarly, geochemical mass balances for watersheds in the Pennsylvania Piedmont of Lancaster County determine that the rate of chemical dissolution of non-carbonate bedrock accompanying its conversion to saprolite is occurring between ~ 4.5 and 6 m/m.y. (Price et al., 2008).

These rates account for one-third to one-half of the long-term, watershed-averaged CRN-determined rates of ~ 10 – 20 m/m.y. obtained by sampling channel alluvium (Reuter, 2005). The degree of landscape change as measured by the increase or decrease in relief hinges on what is done with the chemically-weathered bedrock once it is produced. If saprolite or other chemically altered bedrock remains on the landscape and weathering profiles thicken through time because of no surface erosion, relief should increase because the rates of river incision are clearly faster than these hillslope and ridgeline chemical weathering rates. Conversely, it is well known that conversion of bedrock to saprolite slows as the thickness of saprolite grows (Heimsath et al., 1997), favoring the establishment of a steady state thickness for the weathering profile. Under these circumstances, the landscape can attain a near steady-state relief where the combination of chemical dissolution of rock and the gravity-driven mechanical erosion of creep/colluvial processes combine to match the fluvial incision rate. Even under these conditions, transients in the fluvial system like knickpoints will act to grow the relief because channels can respond to base level changes much more readily in the Appalachian landscape in comparison to the hillslopes.

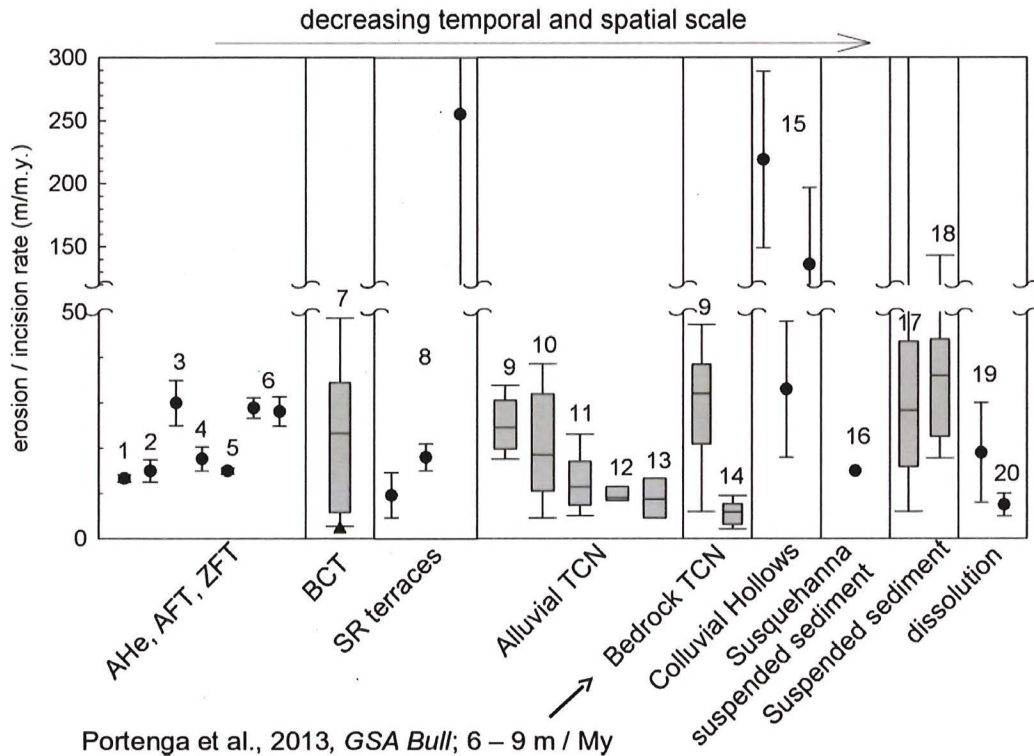


Figure 4. Comparison of erosion and incision rates over a range of time and space scales. 1 = AFT Ridge and Valley (Roden and Miller, 1989), 2 = AHe Ridge and Valley (this report), 3 = AHe PA-NJ Blue Ridge (this report), 4 = AHe PA Piedmont (this report), 5 = ZFT PA Piedmont (Kohn et al., 1993), 6 = Alluvial AHe New England (this report), 7 = Pazzaglia and Brandon (1996), 8 = Pazzaglia and Gardner (1993) and Reusser et al. (2006), 9 = Smokies (Matmon et al., 2003), 10 = PA Allegheny Plateau (Reuter, 2005), 11 = PA Ridge and Valley (Reuter, 2005), 12 = PA Piedmont (Reuter, 2005), 13 = Shenandoah N.P. (Duxbury et al., in press), 14 = Dolly Sods, WV (Hancock and Kirwan, 2007), 15 = PA Ridge and Valley (Braun, 1989), 16 = Ott et al., 1991, 17 = Conrad and Saunderson (1999), 18 = Sevon (1989), 19 = Carbonates (White, 1984, 2000), 20 = Piedmont schist (Cleaves et al., 1970, 1974; Pavich et al., 1989).

A more direct comparison of hillslope weathering rates for South Mountain is offered by other recent work that has emerged from the Shale Hills Critical Zone Observatory in central Pennsylvania (Ma et al., 2010). Here, the relief and sedimentary rock substrate compare reasonably well to South Mountain. Soil production has been calculated using a novel U-series technique (Dosseto et al., 2008) along a ridge to valley bottom catena. The rates of soil production vary from ~45 m/m.y. at the ridge top to ~17 m/m.y. for the toeslope. These rates are not in conflict with the CRN data reported above because they are calculated for soil-mantled, rather than exposed bedrock parts of the landscape. In fact, the faster ridge-line rates compare well to those calculated by Braun (1989) estimated from the volume of fill in colluvial hollows along the periglacial fringe of Pennsylvania. Particularly for those parts of the landscape that are in the latitude or elevation-defined zone impacted by Pleistocene periglacial processes, ridge

lines may be lowering faster than the rest of the landscape, resulting in a reduction of relief for these regions.

Colluvial stratigraphy in Pennsylvania

Colluvium is ubiquitous on Pennsylvania hillslopes and a goal of the 2014 Field Conference is to observe and discuss its origin and stratigraphy (see papers by Merritts et al., Pazzaglia et al., this guidebook). Along the NW flank of South Mountain, colluvial fans have accumulated an impressive thickness of these deposits and intervening soils (Sevon, 2001; Grote, 2006). A general observation here and elsewhere in Pennsylvania is that the colluvial stratigraphy is characterized by a generally coarsening-up texture and unsteady deposition. The colluvium is differentially weathered, where buried allostratigraphic packages are bound by red, deeply-weathered paleosols, with surficial units being characterized by weakly-developed, brown soils. One way to interpret these observations is to suggest that Pleistocene climates, particularly in the periglacial fringe, have driven an unroofing of ridge tops and redistributed weathered materials from the tops to the bottoms of the hillslopes. This process has been going on, episodically, for 1-2 million years. The ridge tops have been lowered and now expose mostly bedrock, the slow weathering of which is recorded by the CRN data. Colluvial fans and colluvial hollows contain the material moved off of those ridgetops and preserve a better record of Pleistocene erosion, which tends to equal or surpass the long-term river incision and thermochronologically-determined rates.

In summary, all available data point to erosion and landscape change in the mid-Atlantic region including Pennsylvania and South Mountain to be generally slow, on the order of ~5 – 30 m/m.y. Embedded in those slow long-term rates are a non-uniformities linked to rock type, the distinction between fluvial and hillslope environments, and the distinction between ridge tops and toeslopes. Furthermore, erosion and landscape change is unsteady and driven by unsteady changes in climate and base level. There are spatial and temporal transients in the landscape, namely in the form of river channel knickpoints, and these take millions if not tens of millions of years to propagate through Pennsylvania's watersheds, imparting their base level signal to the hillslopes. The result is a largely transient landscape that still reflects basic differences in rock type and proximity to base level change, but which also is slowly and dynamically adjusting to changes in climate and base level.

References

- Braun, D.D., 1989, Glacial and periglacial erosion of the Appalachians, *in* Gardner T. W. and Sevon, W. D., eds., *Appalachian Geomorphology: Geomorphology*, v. 2, p. 233-256.

- Bikerman, M., Myers, T., Prout, A.A., and Smith, R.C., 1999. Testing the feasibility of KAR Dating of Pennsylvania cryptomelanes [potassium manganese oxides]: *Journal of the Pennsylvania Academy of Science*, v. 72, pp. 109-114.
- Conrad, C. T. and Saunderson, H. C., 1999, Temporal and spatial variation in suspended sediment yields from eastern North America, in Smith, B. J., Whalley, W. B., and Warke, P. A., eds., *Uplift, Erosion, and Stability: Perspectives on Long-term Landscape Development: Geological Society Special Publication 162*, London, p. 219-228.
- Cleaves, E. T., Godfrey, A. E., and Bricker, O. P., 1970, Geochemical balance of a small watershed and its geomorphic implications: *Geological Society of America Bulletin*, v. 81, p. 3015-3032.
- Cleaves, Emery T, Fisher, Donald W, and Bricker, Owen P , 1974, Chemical Weathering of Serpentinite in the Eastern Piedmont of Maryland: *Geological Society of America Bulletin*, vol.85, p.437-444.
- Davis, W. M., 1899, The geographical cycle: *Geography Journal*, v. 14, p. 481-504.
- Dosseto, A., Turner, S P., and Chappell, 2008, The evolution of weathering profiles through time: New insight from uranium-series: *Earth and Planetary Science Letters*: 274, 359-371.
- Duxbury, J., Bierman, P., Larsen, J., Pavich, M.J., Southworth, S., Miguéns-Rodríguez, M., and Freeman, S., in press, Erosion rates in and around Shenandoah National Park, VA, determined using analysis of cosmogenic ¹⁰Be: *American Journal of Science*.
- Engel, S. A., Gardner, T. W., and Ciolkosz, E. J., 1996, Quaternary soil chronosequences on terraces of the Susquehanna River, Pennsylvania: *Geomorphology*, v. 17, p. 273-294.
- Gallen, S. F., Wegmann, K. W., and Bohenstiehl, D. R., 2013, Miocene rejuvenation of topographic relief in the southern Appalachians: *GSA Today*, 23, doi:10.1130/GSATG163A.1.
- Grote, T. D., 2006 Late Cenozoic Stratigraphy and Landscape Dynamics in the Unglaciated Central Appalachians - a Case Study from the Northern Blue Ridge, South-Central Pennsylvania, USA (Ph.D. Dissertation): Morgantown, West Virginia University, 117 p., URL: <https://eidr.wvu.edu/eidr/documentdata.eIDR?documentid=4954>
- Hack, J.T., 1960, Interpretation of erosional topography in humid temperate regions: *American Journal of Science*. v. 258-A. p. 80-97.
- Hack, J.T., 1965, Geomorphology of the Shenandoah Valley, Virginia and West Virginia and the origin of the residual ore deposits: *U.S. Geological Survey Professional Paper 484*, 84 p.
- Hack, J. T., 1973, Stream-profile analysis and stream-gradient index: *Journal of Research of the U. S. Geological Survey*, v. 1, p.421-429.

- Hancock, G. and Kirwan, M., 2007, Summit erosion rates deduced from ^{10}Be ; implications for relief production in the Central Appalachians, *Geology* v. 35, p. 89-92.
- Heimsath, A.M., Dietrich, W.E., Nishiizumi, K., and Finkel, R.C., 1997. The soil production function and landscape equilibrium. *Nature*, 388: 358-361
- Kohn, B. P., Wagner, M. E., Lutz, T. M., and Organist, G., 1993, Anomalous thermal regime, central Appalachian Piedmont: evidence from sphene and zircon fission track dating: *Journal of Geology*, v. 101, p. 779-794.
- Langland, M. J. and Haney, R. A., 1997, Changes in bottom-surface elevations in three reservoirs on the lower Susquehanna River, Pennsylvania and Maryland, following the January 1996 flood – implications for nutrient and sediment loads to Chesapeake Bay: U.S. Geological Survey Water Resources Investigations Report 97-4138, 34 p.
- Ma, L., Chabaux, F., Pelt, E., Blaes, E., Jin, L., and Brantley, S., 2010, Regolith production rates calculated with uranium-series isotopes at Susquehanna/Shale Hills Critical Zone Observatory: *Earth and Planetary Science Letters*, 297, 211-225.
- Matmon, A., Bierman, P. R., Larsen, J., Southworth, S., Pavich, M. J., Caffee, M. W., 2003, Temporally and spatially uniform rates of erosion in the southern Appalachian Great Smoky Mountains: *Geology*, v. 31, p. 155-158.
- McKeon, R., Zeitler, P. K., Pazzaglia, F. J., Idelman, B., and Enkelmann, E., 2014, Decay of an old orogen: inferences about Appalachian landscape evolution from low-temperature thermochronology: *Geological Society of America Bulletin*, 126, 31-46.
- Miller, S.R., Sak, R.B., Kirby, E., and Bierman, P.R. (2013): Neogene rejuvenation of central Appalachian topography: Evidence for differential rock uplift from stream profiles and erosion rates. *Earth and Planetary Science Letters* 369-370:1-12. DOI: [10.1016/j.epsl.2013.04.007](https://doi.org/10.1016/j.epsl.2013.04.007)
- Ott, A. N., Takita, C. S., Edwards, R. E., and Bollinger, S. W., 1991, Loads and yields of nutrients and suspended sediment transported in the Susquehanna River basin, 1985-89: Susquehanna River Basin Commission Report, Publication 136, 253 p.
- Pavich, M. J., Leo, G. W., Obermeier, S. F., and Estabrook, J. R., 1989, Investigations of the characteristics, origin, and residence time of the upland residual mantle of the Piedmont of Fairfax County, VA: U. S. Geological Survey Professional Paper 1352, 114 p.
- Pazzaglia, F. J. and Brandon, M. T., 1996, Macrogeomorphic evolution of the post-Triassic Appalachian mountains determined by deconvolution of the offshore basin sedimentary record: *Basin Research*, v. 8, 255-278.
- Pazzaglia, F. J. and Gardner, T. W., 1993, Fluvial terraces of the lower Susquehanna River: *Geomorphology*, v.8, p.83-113.
- Pazzaglia, F. J. and Gardner, T. W., 1994, Late Cenozoic flexural deformation of the middle U.S. Atlantic passive margin: *Journal of Geophysical Research*, v. 99, n. B6, p. 12,143-12,157.

- Pazzaglia, F. J., Zeitler, P. K., Idleman, B. D., McKeon, R., Berti, C., Enkelmann, E., Laucks, J., Ault, A., Elasmir, M., and Becker, T., 2010, Tectonics and topography of the Cenozoic Appalachians: Field Conference of Pennsylvania Geologists, 75th Field Conference, Lancaster, PA, 111-126.
- Pierce, K. L., 1965, Geomorphic significance of a Cretaceous deposit in the Great Valley of southern Pennsylvania: US Geological Survey Professional Paper 525C, p. C152-C156.
- Portenga, E. W., Bierman, P. R., Rizzo, D. M., and Rood, D. H., 2013, Low rates of bedrock erosion in the central Appalachian Mountains inferred from in-situ ¹⁰Be: Geological Society of America Bulletin, 125, 201-215.
- Price, J. R., Heitmann, N., Hull, J., and Szymanski, D., 2008, Long-term average mineral weathering rates from watershed geochemical mass balance methods: using mineral modal abundance to solve more equations in more unknowns: Chemical Geology, 254, 36-51.
- Reusser, L., Bierman, P., Pavich, M., Larsen, J., and Finkel, R., 2006, An episode of rapid bedrock channel incision during the last glacial cycle, measured with ¹⁰Be: American Journal of Science, v. 306, p. 69-102.
- Reuter, J. M., 2005, Erosion rates and patterns inferred from cosmogenic ¹⁰Be in the Susquehanna River basin: M.S. Thesis, Burlington, University of Vermont, 160 p.
- Roden, M. K. and Miller, D. S., 1989, Apatite fission-track thermochronology of the Pennsylvania Appalachian basin: Geomorphology, v. 2, p. 39-51.
- Sahagian, D., Pinous, O., Olferiev A., and Zakharov, V., 1996, Eustatic curve for the Middle Jurassic-Cretaceous based on Russian Platform and Siberian stratigraphy: Zonal Resolution: AAPG Bulletin, 80, 1435-1458.
- Sevon, W. D., 1989, Erosion in the Juniata River drainage basin, Pennsylvania: Geomorphology, v. 2, p. 303-318.
- Sevon, W. D., 2001, Landscape evolution in the Cumberland Valley, southeastern Pennsylvania: in Potter, N., Jr., editor, The geomorphic evolution of the Great Valley near Carlisle, Pennsylvania: Guidebook for Southeast Friends of the Pleistocene 2001 Annual Meeting, Carlisle, PA, 159 p.
- Walter, R. C. and Merritts, D. J., 2008, Natural streams and the legacy of water-powered mills: Science, 319, 299-304.
- White, W. B., 1984, Rates and Processes: chemical kinetics and karst landform development, in LaFleur, R. G., ed., Groundwater as a geomorphic agent: Boston, Allen and Unwin, p. 227-248.
- White, W. B., 2000, Dissolution of limestone from field observations: in Speleogenesis evolution of karst aquifers, in Klimchouk, A. B., Ford, D. C., Palmer, A. N., Dreybrodt, W., eds., National Speleological Society, Huntsville, AL, United States, p. 149-155.

LIDAR ANALYSIS OF PERIGLACIAL LANDFORMS AND THEIR PALEOCLIMATIC SIGNIFICANCE, UNGLACIATED PENNSYLVANIA

Authors: Dorothy Merritts, Kayla Schulte, Aaron Blair, Noel Potter, Robert Walter, Erin Markey, Ben Weiserbs, Sam Alter, Sally Guillorn, Evan Lewis, Larissa Kehne, and Yunan Xie (all of Department of Earth and Environment, Franklin and Marshall College, Lancaster, PA, except Noel Potter, Department of Earth Sciences, (retired) of Dickinson College, Carlisle, PA)

Introduction

Key questions regarding the impact of climate change on landscapes are how periglacial landforms can be used as paleoclimatic indicators, and which landforms are diagnostic of the former existence and degradation of permafrost (c.f., Péwé, 1983; Matsuoka, 2011; French and Millar, 2014). As used by Washburn (1980), the term “periglacial” refers to cold climate environments both with and without permafrost. Permafrost is ground that remains at or below the freezing point of water (0°C) for two or more consecutive years (ACGR, 1988), with an uppermost active layer (typically $\leq 0.5\text{ m}$ thick) that thaws seasonally. Continuous permafrost exists today in regions with mean annual air temperatures (MAAT) less than approximately -6° to -8°C , and discontinuous permafrost occurs in regions with MAAT less than approximately -0.5°C to -2°C (Brown and Péwé, 1973; Gruber, 2012). If particular landforms, or suites of landforms, are associated with continuous or discontinuous permafrost, their relicts could be used as indicators of paleotemperature and perhaps even paleoprecipitation (c.f., Washburn, 1980; Ballantyne and Harris, 1994; Matsuoka, 2001; Matsuoka, 2011; French and Millar, 2014).

Evidence of past ice, vegetation, and landforms can be used as proxies for climate change, but the first two have received more attention than geomorphic features as paleoclimate indicators. With recent work in polar regions to identify geomorphic features that are diagnostic of permafrost thaw (e.g., Gooseff et al, 2009), it is timely to examine paleo-landforms at lower latitudes that might have formed under conditions of permafrost and its degradation, and to evaluate their potential as analogs of future landscape conditions in polar regions. The boundaries of continuous and discontinuous permafrost have shifted north and south with multiple cold glacial to warm interglacial climate cycles during the Quaternary Period (~ 2.6 million years to present), with the last glacial maximum (LGM) from 26.5 to 19 to 20 ka.

Times of transitions from glacial to interglacial conditions, referred to as terminations and deglaciation, occurred rapidly relative to the prolonged periods of cooling that ensued during each glacial cycle (Denton et al, 2010). Permafrost thawing might also have occurred relatively rapidly during terminations. The last glacial termination began in the Northern Hemisphere at 19 to 20 ka, when increased northern

summer insolation led to widespread changes in amounts and locations of glacial ice and permafrost, shifts in vegetation, and the downslope movement of sediment that shapes the landscape at Earth's surface.

In our ongoing work, which is focused on central, south-central, and southeastern Pennsylvania and parts of Maryland and Virginia to the south, we use LiDAR, field mapping, coring, trenching, and analysis of sediments and organic matter to characterize periglacial landforms and assess their potential as indicators of past permafrost and its degradation. Whereas much previous work has evaluated periglacial landforms, here we also emphasize those that are associated with permafrost thaw, or degradation. Pennsylvania offers an unusually rich record of climate change, as its northern half ($\sim 41^\circ$ northward) was glaciated repeatedly while the southern half remained ice free, presumably with permafrost and land surface processes similar to those found today in cold regions at high latitudes (*Fig. 1*).

We begin with a hypothesis for the periglacial origin of valley bottoms, and then a synopsis of previous mapping of periglacial features in the eastern US, particularly in the mid-Atlantic region just south of the borders of full glacial ice sheets. Next we review recent work on modern landforms in regions with permafrost. In a preliminary summary of our work on identifying relict landforms with LiDAR, we give examples of the sediments contained within those landforms. One field site, comprising the south- and north-facing slopes of Blue Mountain along Waggoner's Gap Road north of Carlisle, Pennsylvania, is used as a general case study for this field guide report. Several other field sites in central Pennsylvania provide supporting evidence. Finally, we conclude with a discussion of diffusion-dominated slopes as a way to bring together the on-the-ground mapping of previous workers, our LiDAR mapping, and what is known about landforms associated with modern permafrost.

Motivation for this Work: The Hypothesis of Periglacial Valley Bottoms

New technologies for studying and dating Earth surface processes and features, particularly the advent of high-resolution topographic datasets acquired with LiDAR, offer opportunities to map landforms at high resolution over broad areas. Airborne LiDAR datasets are available for all of the state of Pennsylvania, so that ridge tops, hill slopes, and valley bottoms can be examined for evidence of glacial-periglacial and deglacial landforms. As shown below, post-glacial modification of the landscape during the Holocene interglacial warm period ($\sim 11,500$ yrs BP to present) appears to be relatively insignificant in most places within our study region, with exception of areas impacted by mill damming and historic valley-bottom reservoir sedimentation (see Walter and Merritts, 2008).

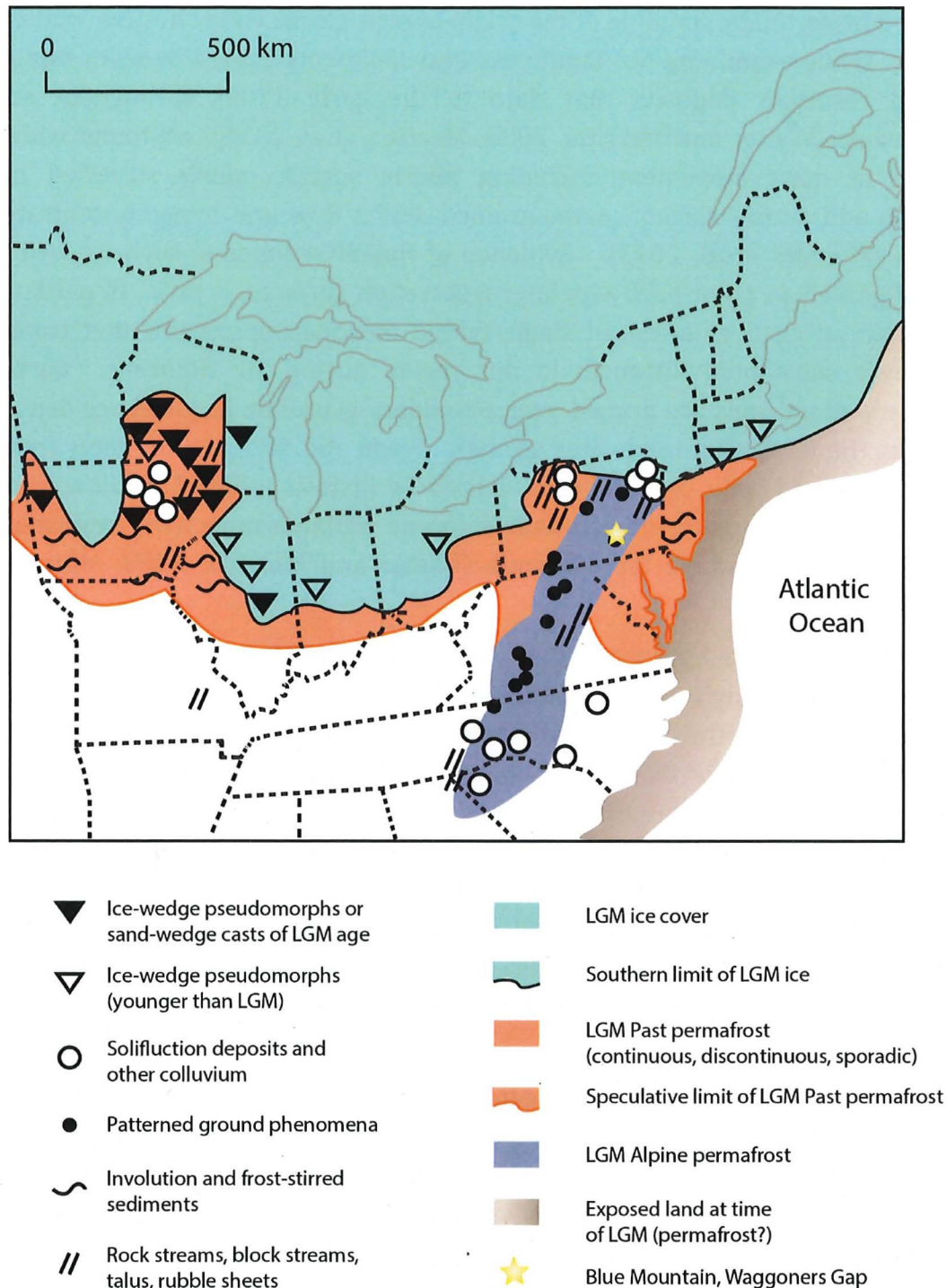


Figure 1. Extent of past permafrost south of the limit of maximum LGM ice for the eastern US, based on a variety of periglacial features. Map is modified from French and Millar (2014), in which the original map shows North America. French and Millar (2014) derived their map from Péwé (1983: fig. 9.11), adding more recent data (see French and Millar, 2014, Fig. 1, for multiple sources). Note the location of Waggoner's Gap, one of the sites referred to in this work. Most of the sites in our work are in Pennsylvania and Maryland.

In addition to its paleoclimate potential, this regional project was motivated by the need for a better understanding of the origin of post-glacial valley bottom wetlands and streams. While examining the landforms and sediments buried beneath fine-grained millpond reservoir deposits that date to the early 1700s throughout southern Pennsylvania (Walter and Merritts, 2008; Merritts et al, 2011), we found widespread evidence of mass movement, including poorly sorted, poorly stratified hillslope colluvium and poorly sorted, coarse-grained debris flow and hyperconcentrated flow deposits (Merritts et al, 2013). Evidence of fluvial sediments, such as well sorted, rounded gravels in point bars with lateral accretion surfaces, is rare. In particular, we have found no clear evidence of single-thread meandering streams that transported gravel over substantial distances in this region during the Holocene. Carbon-rich Holocene wetland soils are draped over a bouldery glacial to deglacial age depositional surface at the level of groundwater springs. Seeds and radiocarbon dates from these Holocene wetland soils, many of them buried by historic millpond sediment in valley bottoms, and our mapping indicate that Holocene wetlands once were extensive across valley bottoms and stable for millennia (Walter and Merritts, 2008; Merritts et al, 2011).

We developed the hypothesis that valley bottom infilling by mass movement was dominant in the unglaciated region just south of the LGM ice margin during deglaciation, and that the coarse size of much of the mass movement-derived sediment led to the inevitability of stable valley bottom surfaces. These low-amplitude surfaces have high roughness values that limit bed load sediment transport. In other words, many Holocene valley bottoms in the periglacial landscape are actually formed on glacial to deglacial age deposits at toe-of-slope, the generally concave up depositional parts of hillslopes. When at the level of groundwater, a common condition in this humid, temperate region, such valley bottoms are ideal locations for spring-fed wetlands and trapping of fine sediment and nutrients (e.g., carbon) during the Holocene.

This hypothesis of stable valley bottoms with a periglacial origin is consistent with previous field mapping of soils and deposits on hillslopes in the region (c.f., Fig. 19 in Pazzaglia and Cleaves, 1998). It is an extension of the proposition by Ciolkoscz et al (1986) that colluvial slopes in Pennsylvania are in a “super-stable” condition because their form is inherited from periglacial climatic conditions. Here, we explore the possibility that many of southern Pennsylvania’s valley bottoms began as toe-of-slope deposits inherited from periglacial climates and, as a result, are super-stable with respect to modern fluvial conditions.

Previous Work

Relict Periglacial Features in the Eastern US

Many workers in the eastern US have noted the evidence of periglacial features south of Pleistocene full glacial ice borders (*see Fig. 1*). Relict periglacial features mapped throughout Pennsylvania, Maryland, New Jersey, and other mid-Atlantic states include fossil ice wedge casts, pingos (at one location), patterned ground, block fields, block streams, nivation hollows, cryoplanation terraces, and various types of colluvial deposits that include grézes litées (c.f., Washburn, 1973; 1980; French, 2007; Walters, 1978; Carter and Ciolkosz, 1986; Ciolkosz et al, 1986, 1990; Marsh, 1987; Clark and Ciolkosz, 1988; Clark and Schmidlin, 1992; Braun, 1989; Pazzaglia and Cleaves, 1998; Cleaves, 2000; French et al 2003, 2007; Newell and DeJong, 2011; and French and Millar, 2014). With exceptions of some patterned ground and ice wedge casts on the Coastal Plain, and the one example of pingos in Pennsylvania, these features were identified on hillslopes.

Ice wedge casts have been identified in sediments exposed in quarries in the Coastal Plain of New Jersey, Maryland, and Delaware (French et al, 2007, 2009) and in shale quarries in Pennsylvania (c.f., Gardner et al, 1991). They have been used to map the approximate southern limit of Pleistocene permafrost in the mid-Atlantic Coastal Plain, but not to distinguish between continuous or discontinuous permafrost (*see Fig. 1*; French and Millar, 2014).

Possible relict pingos were identified in one headwater valley in eastern Pennsylvania (Marsh, 1987). Using LiDAR, we have found and field checked several other possible relict pingos in headwater valleys in central Pennsylvania. We interpret these to be open-system pingos associated with discontinuous (and/or degrading continuous) permafrost (Merritts et al, unpub. work).

The most commonly mapped periglacial feature in Pennsylvania, Maryland, and Virginia is colluvium on hillslopes (e.g., Denny, 1951; Hack, 1965; Ciolkosz et al, 1986; 1990; Braun, 1989; Pazzaglia and Cleaves, 1998, Eaton et al, 2003; Newell and DeJong, 2011). It occurs in the Piedmont, Blue Ridge, and Valley and Ridge physiographic provinces, but typically is thickest in more mountainous landscapes. Locally it is thickest in hollows, at least 20 m thick in places (e.g., Braun, 1989). The sediment in colluvial deposits has been described as a diamicton, typically poorly sorted and poorly stratified, with variable amounts of clasts that usually are matrix supported (e.g., Pazzaglia and Cleaves, 1998; Cleaves, 2000). The last of these attributes, matrix supported texture (rather than clast supported), is diagnostic of mass wasting, the downslope movement of sediment by gravity rather than as suspended or bed load within a column of flowing water or air.

Some workers have suggested that colluvial deposits in the Appalachian region might have formed as a result of solifluction (also gelifluction, as the words have been used differently with time). Lobate landforms atop colluvial deposits that resemble solifluction lobes and sheets in Arctic and other modern cold regions were identified at several sites just south of the last full glacial ice margin in Pennsylvania (Figure 2a; Potter and Moss, 1968; Hoover and Ciolkosz, 1988; Carter and Ciolkosz, 1986; and Craul, 2010; see Fig. 1).

Whereas colluvium has been noted as widespread in the unglaciated eastern US and its sedimentary and soil properties have been described at many sites (c.f., Pazzaglia and Cleaves, 1998; and Ciolkosz et al, 1990), lobate landforms have not been widely reported or described in detail because they are difficult to discern, especially under conditions of modern warm interglacial climate and vegetation.

Modern Landforms Indicative of Permafrost and its Degradation during Thaw

Although many of the relict features mapped in the eastern US are thought to be the result of colder conditions and greater rates of mass wasting than under present climatic conditions, not all of these features require permafrost to form. Work on modern landforms in cold regions indicates that ice wedges and pingos are conclusive evidence of permafrost, but only certain types of solifluction are associated with permafrost, as discussed below. Other features mapped in the Arctic today that are strongly associated with accelerated permafrost thaw include active layer detachments, thermokarst (i.e., thermal erosion) gullies, and retrogressive thaw slumps (Gooseff et al, 2009; Bowden, 2010; Jorgenson et al, 2013). To our knowledge, none of these has been recognized as a relict periglacial feature south of full glacial ice borders in the eastern US. As discussed below, we have identified thermokarst gullies and retrogressive thaw slumps with LiDAR topographic data.

Ice Wedges Ice wedges have been regarded as the best indicators of continuous (or cold) permafrost and of MAAT below about -3°C to -8°C (e.g., Péwé, 1966; Washburn, 1980). Ice wedges are part of polygonal structures with typical diameters of 15-30 m that are among the most common ground patterns in the Arctic today. During times of extreme cold, the soil contracts and cracks, and these cracks fill with meltwater during spring to summer thaw of the active layer. Subsequent freezing of meltwater and repeated cracking, thawing, and freezing lead to the formation of wedge-shaped masses of ice with downward pointing apices along borders of thermal contraction polygons. Wedges grow both deeper and wider with time. With warming, ice wedges thaw and the space that they occupied formerly can be filled with sediment, resulting in ice wedge casts.

A recent review by Matsuoka (2011) indicates that precise thermal resolution for ice wedges is complex due to factors such as differences between air and ground

temperatures, the thermal conditions at which contraction cracking occurs, the different types of ground material, and difficulties in distinguishing between ice wedges and frost wedges with different origins.

Pingos Mounds of ice-cored sediment up to 70 m high and up to 600 m in diameter called pingos occur in association with permafrost in Arctic and subarctic regions today. Closed-system pingos develop where advancing permafrost expels pore water from saturated sediment to near-surface permafrost, as in the area of a drained former lake, and the expelled water forms an ice core that deforms overlying frozen sediment. Open-system pingos form where unfrozen water within an aquifer, as beneath permafrost or within discontinuous permafrost, is under hydraulic pressure and rises to the surface and becomes frozen. Both open and closed-system types of pingos are found in areas with warm permafrost limits that range from -1° to -6° C. Lower temperatures and cold permafrost are associated more commonly with closed-system pingos (Matsuoka, 2011).

Solifluction Lobes and Sheets Solifluction comprises slow mass wasting processes resulting from freeze-thaw action and is common in frost-susceptible soils with a sandy and/or silty matrix (Ballantyne and Harris, 1994; Matsuoka, 2001). These include frost creep, needle ice creep, gelifluction, and plug-like flow and can result in lobate landforms (*Fig. 2a*). The first two processes occur close to the ground surface and have low displacement rates. The latter two can be associated with permafrost, affect greater depths of soil, and have downslope flow rates as high as several m/yr, but more typically less than one m/yr. We focus on these two here, as they produce mappable landforms and provide useful information about paleoclimate and landscape evolution.

Gelifluction, included within the broader category of solifluction, occurs when soil becomes saturated and weakened by seasonal thaw consolidation or the addition of water from snowmelt or rainfall (Matsuoka, 2001). The depth of freeze-thaw determines the amount of soil that flows. Gelifluction can occur in ground with deep seasonal freezing and thawing (i.e., no permafrost) or warm permafrost. Soil is desiccated as the freezing front moves downward from the surface (one-sided freezing) and ice lenses grow and segregate, limiting the potential depth and rate of flow. Where cold permafrost exists at depth, upward freezing can occur from the top of the permafrost (Mackay, 1981; Lewkowicz, 1988). This results in ice lens growth near the base of the frozen active layer. The whole active layer is affected by two-sided freezing (downward and upward) and can move downslope as a plug during thawing.

Profiles of soil velocity with depth for gelifluction and plug-like flow are distinctly different (see *Fig. 1*, Matsuoka, 2001). Downslope soil velocity increases asymptotically to the surface for gelifluction, but increases markedly at the base of the active layer for plug-like flow, then remains similar throughout the plug to the ground surface. In all

cases, the base of detectable movement rarely exceeds a depth of 0.7 m (Matsuoka, 2001). The surface velocity is at a maximum, often greater than 10 cm/yr, on slopes where MAAT is between -3°C and -5°C (see Matsuoka, 2001, Fig. 4). Below this optimum temperature range permafrost is generally cold and continuous, and surface soil velocity rarely exceeds 5 cm/yr (Matsuoka, 2001). High values of surface velocity also occur in mountains at mid- to low latitudes, in association with high frequency of diurnal freeze-thaw cycles.

Lobes, sheets, and stripes produced by solifluction exist today in regions with MAAT between 7°C and -20°C (Washburn, 1979; Harris, 1981; Matsuoka, 2001). In a global review of modern solifluction features, Matsuoka (2001) links their form and characteristics to permafrost conditions, noting that deeper freeze-thaw and solifluction result in thicker lobes. The frontal height of lobes is about the same or greater than the maximum depth of soil movement. Thin lobes and small-scale stripes are found in association with diurnal and seasonal frost with shallow frost creep and are not diagnostic of permafrost. However, medium-sized lobes and stripes are associated with diurnal and annual freeze-thaw and gelifluction in the upper active layer (shallower than 0.6 m) on slopes with seasonal frost to warm permafrost. Plug-like flow, thick lobes and large-scale stripes are associated with greater depths of soil movement (more than 0.6 m) on slopes with cold permafrost, two-sided freezing, and annual freeze-thaw action.

Rates of sediment movement by solifluction are documented for many parts of the world (see Fig. 10, Matsuoka, 2001), with maximum rates of about a meter per year. Downslope surface velocity (V_s in cm/yr) generally increases with hillslope gradient (θ , in degrees), with the maximum soil surface velocity corresponding roughly with the product of $100 \cdot \tan \theta$. For a slope of 35° , for example, $\tan \theta$ is 0.7 and maximum surface velocity by solifluction is about 70 cm/yr.

This Work: Using LiDAR to Map Landforms Associated with Permafrost and Thaw

Methods: LiDAR Analysis

LiDAR enables the distance to an object to be measured with signal return times of reflected light from a laser source. Airborne laser swath mapping (ALSM) for topographic LiDAR collects data aerially, providing high resolution, high accuracy elevation data. Point clouds of data are returned from land and objects (e.g., trees or buildings) on Earth's surface, but LiDAR data sets can be classified and filtered to generate a bare earth surface. Three-dimensional LiDAR point cloud data are provided as binary LAS (LASer) format files, a public file format for the interchange of 3-dimensional geospatial point cloud data.

Pennsylvania was one of the first states to collect and process high-resolution ALSM elevation data for the entire state, with data acquisition from 2006 to 2008, and processing and release of data up to several years later. Part of the PAMAP Program, this statewide effort was led by the PA Department of Conservation and Natural Resources, Bureau of Topographic and Geologic Survey. Each flight line had sidelap of about 30% with a nominal average LiDAR point spacing of 4.6 ft (1.4 m). Horizontal positional accuracy has a root-mean-square error (RMSE) of 1.5 m (5 ft) or better for 95% of the horizontal check points, and vertical positional accuracy has a RMSE of approximately ~0.2-0.4 m (0.6 to 1.2 ft) at the 95% confidence level.¹ The PAMAP Program provides a digital elevation model (DEM) of the LiDAR data as an ~3.2-foot pixel (1-meter equivalent) raster with an interpolated elevation value for each pixel in the raster.

Using LAS point cloud LiDAR elevation data, we make DEMs that are of higher resolution than the ~1-m DEM provided to the public by the PAMAP Program.

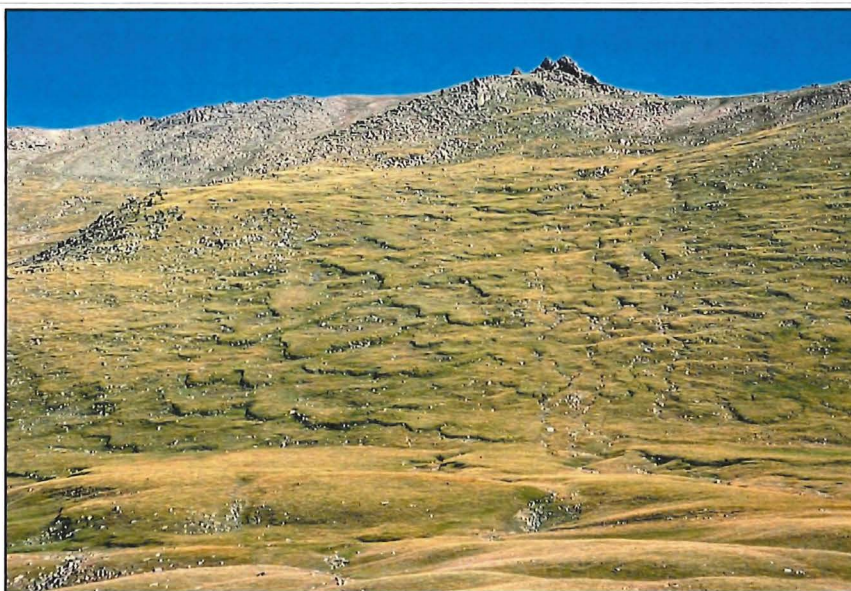
We use a cell size of about 0.6 m (2 ft), and from these DEMs we generate hillshade and slopeshade layers, with the latter of most value for assessing periglacial landforms.

Results: Mapping Periglacial Features with LiDAR

Solifluction Sheets and Lobes Based on our LiDAR mapping, two landforms in particular, solifluction lobes and sheets, are widespread and ubiquitous on nearly all slopes in south-central and southeastern Pennsylvania, especially those downslope of ridge crests consisting of sandstone, quartzite, or diabase (*Fig. 2b, 3, 4, and 5*). Our field mapping indicates that all bedrock near the surface in the region is highly fractured, and the spacing of bedding planes and fractures determines the initial (and maximum) size of clasts that are incorporated into solifluction lobes and sheets. It is possible that other rock types, such as shale, might produce solifluction lobes and sheets, but that they are not as easily discerned because the clasts of which they are composed, lobe size, and lobe thickness are smaller.

¹ See PAMAP Program LAS Files Metadata, at http://www.pasda.psu.edu/uci/FullMetadataDisplay.aspx?file=pamap_LiDAR_LAS.xml

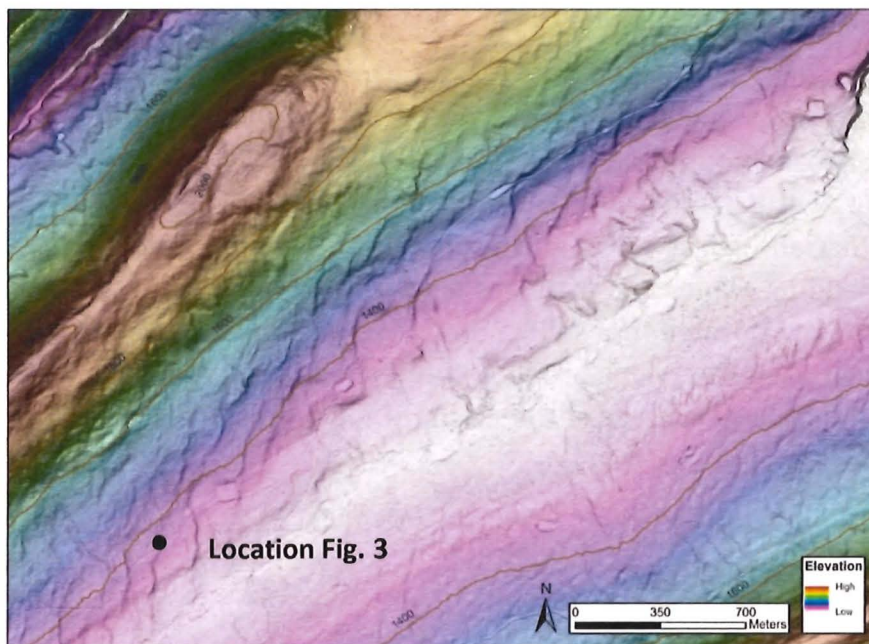
a



Solifluction lobes and sheets along the slopes of the Tien Shan Mountains, Kyrgyzstan

Figure 2. (a) Note that lobes widen downslope, becoming sheets, and in the valley bottom become much broader sheets with thermokarst features. *Photographer and copyright: Marli Miller, University of Oregon (<http://marlimillerphoto.com/>).*

b



LiDAR-derived (LAS files) slopesshade on color-shaded DEM showing solifluction lobes and sheets along the north- and south-facing slopes of Nittany Mountain, ~ 40 km south of the LGM maximum ice limit, near Madisonburg, central PA

Figure 2. (b) Lobes are better developed on the south-facing slope, and become longer and wider downslope. On the south-facing slope, lobes become sheets that trend become oriented obliquely with respect to slope. Note the presence of solifluction features at the toe-of-slope and along valley bottom areas both south (Roaring Run) and north (Rag Valley) of the northeast-trending ridge (Nittany Mountain) at upper left. At this location, Nittany Mountain is the northern limb of a syncline. Sandstone dipping south along the ridge crest is the Silurian Tuscarora Formation; mid-slopes and valley bottom are Silurian Clinton Group (sandstone and shale). Lobes along mid-slope contain Tuscarora sandstone from the ridge crest area.

The scale of modern solifluction lobes and sheets in cold regions is on the order of one to several m in height, several tens of m in width (across the slope), and up to several hundred m in length (downslope). Landforms of this size are difficult to distinguish readily by the human eye when standing on the ground among the features, but can be observed at a distance, as from a nearby hill or low altitude in a plane. Solifluction landforms are more easily discerned when the features are active and sparsely vegetated (*see Fig. 2a*). Relict (i.e., inactive) features, on the other hand, are likely to be covered with trees or other vegetation, as with those mapped in Pennsylvania, but can be distinguished on the ground during logging (*see Fig. 3*). Furthermore, because relict solifluction features are inactive, soil creep might have diminished the prominence of frontal risers of lobes and sheets since the time of their formation. For these two reasons—vegetation cover and diminished topography on relict forms—the use of enhanced topographic data from remote sensing, as with airborne LiDAR, is invaluable for discerning relict solifluction lobes and sheets.



Figure 3. Relict (i.e., inactive) solifluction features are topographically subtle (low-amplitude) and often covered with trees or other vegetation, but can be distinguished on the ground during logging (*see Fig. 2b* for location). View is to the southwest on the south-facing slope of Nittany Mountain. Bedrock is shale and sandstone (Silurian Clinton Group). Colluvium in lobe contains large clasts of sandstone. Sedimentology of lobes along slope is poorly sorted, matrix-supported diamicton with clay, silt, and sand in matrix. Note persons circled for scale. Lobe height is approximately 3 m.

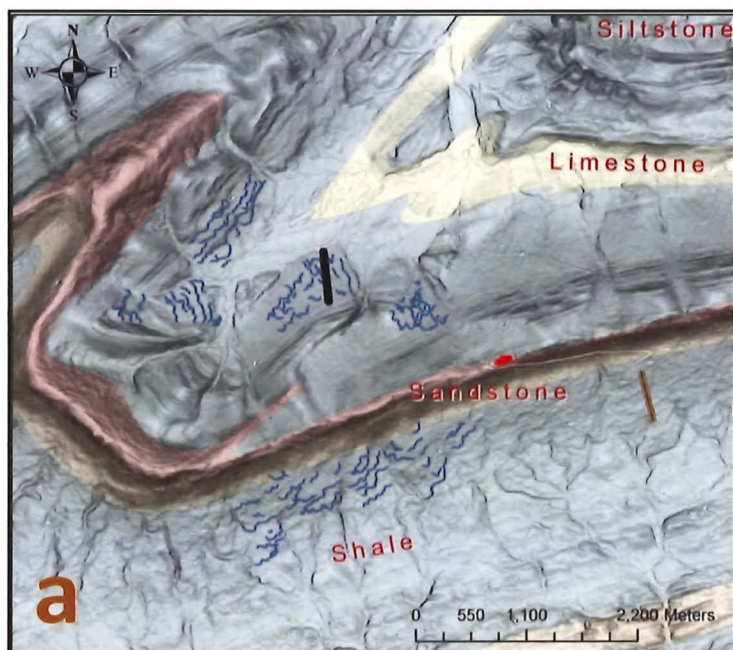
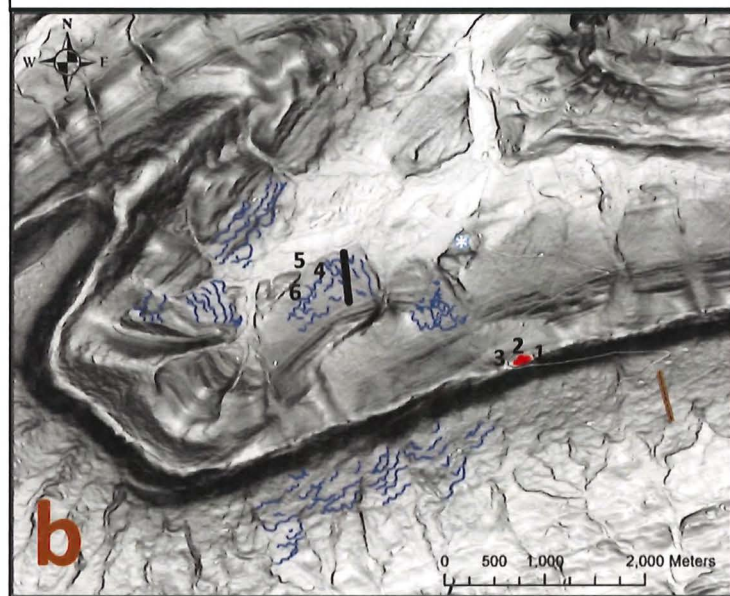


Figure 4. (a) Bedrock types on a slopesshade derived from LiDAR LAS files along Blue Mountain north of Carlisle, PA. Sandstone along the ridge crest is the Tuscarora Formation. Blue Mountain at this location is the southern limb of a syncline, with bedding dipping northward at the crest. Shale to the south of ridge crest occurs in the Ordovician Bald Eagle and Martinsburg Formations. Shale to the north of ridge crest occurs in the Silurian Clinton Group and Bloomsburg Formation. Limestone in Trout Run valley bottom at upper center and right is Silurian Tonoloway Formation. Some solifluction features are mapped (blue lines) as examples. Straight lines perpendicular to the slope are topographic profiles shown in Figure 5. Strike (254°) and dip (40-46°) symbol (red) at ridge crest represents average of multiple measurements. (b) Slopesshade derived from LiDAR LAS files along Blue Mountain, without bedrock types. Numbers represent photo sites referred to in text & Fig. 7.

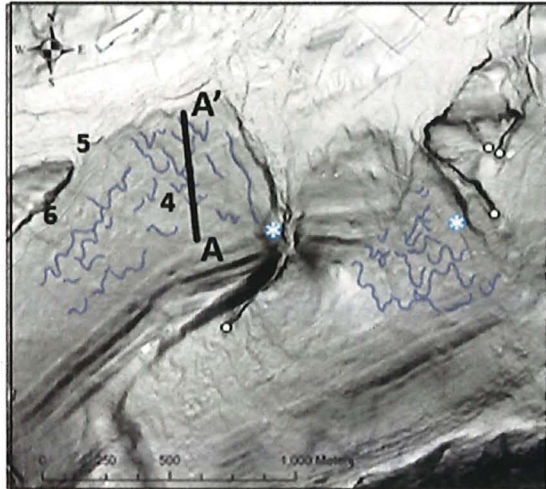


As shown in Figures 4 and 5, solifluction lobes and sheets are ubiquitous on nearly all of the upper and some lower slopes along Blue Mountain at the Waggoner's Gap location. Some lobes and sheets occur on fan-shaped deposits that emanate from gullies (see below), indicating that solifluction post-dates the fans' depositional surfaces.

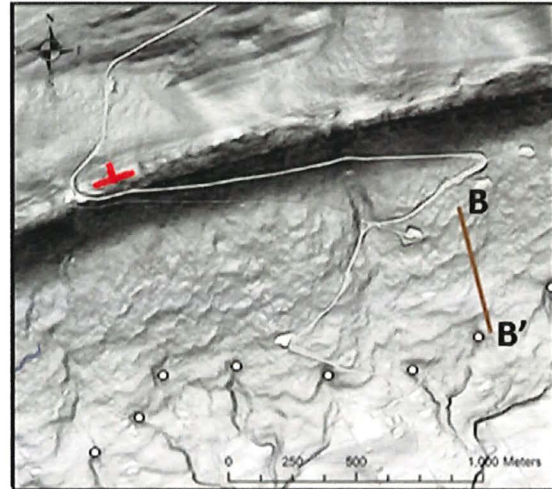
North-dipping Tuscarora sandstone along the ridge crest is highly fractured (see location "1", Fig. 4, and Fig. 6a) and broken into slabs of various sizes up to several meters in long-axis dimension (Fig. 6b). Finer particles, including sand-sized, can be found in crevices. Many slabs are dislodged from bedding planes and positioned randomly on the slope (see Fig. 6b). About 100 m downslope from the ridge crest, lobate landforms can be discerned, both in the field and on LiDAR slopesshades (Fig. 6c; see also location "2", Fig. 4).

Along Waggoner's Gap Road, a road cut at the ridge crest (location "3", Fig. 4) shows prominent ribs of more resistant beds within the Tuscarora sandstone that protrude from the slope and bracket low areas filled with colluvium (right side, Fig. 6d).

(a) N-facing dip slope



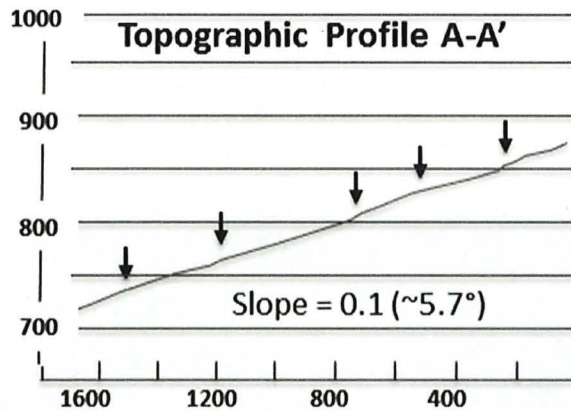
(b) S-facing anti-dip slope



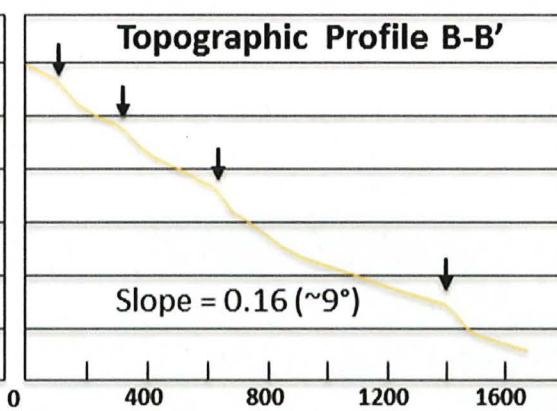
○ Thermokarst gully head

(c)

Elevation, ft



(d)



Distance, ft

Figure 5. Close-up views of LiDAR slopeshade from Figure 4 for north- and south-facing slopes, with topographic profiles. Small circles are heads of possible thermokarst gullies, and asterisks are possible examples of arcuate retrogressive thaw slumps along toe-of-slope at valley margins.

Several meters downslope, just north of the contact with the overlying Clinton Group, clasts of Tuscarora sandstone—some as large as boulders—are mixed with clasts from the former, primarily of shale, mudstone, and sandstone (*left side Fig. 6d*). Lobate forms become wider and longer downslope, possibly due to the greater distance of movement and incorporation of fine sediment from the Clinton Group. Even lower on the slope, the Clinton Group is overlain by the Bloomsburg Formation, which consists primarily of siltstone and shale. Solifluction lobes and sheets containing boulder-sized clasts of sandstone continue across this formation.

On the lower part of the north-facing slope, which has an overall gradient of about 5.9° , multiple lobes can be distinguished on LiDAR slopeshades as well as on the ground at the Florence Jones Rieneman Wildlife Sanctuary (*see location “4” Fig. 4 and 5a, Fig. 5c, and 7*). These lobes have a chevron appearance in plan view, and the sides of rectilinear chevrons are oriented in directions that parallel NE- and NW-trending bedrock fractures (*see Fig. 5a*). The chevrons might have been affected by water seeping from thawing ground along fractures at the time of permafrost thaw. Lobe fronts are up to a few meters in height.

The sedimentology of lobes can be examined in occasional erosional exposures along small streams at toe-of-slope (*e.g., location “5”, Fig. 4b; see Fig. 7b, d, and e*). Such exposures reveal poorly sorted, matrix-supported colluvial diamictons. Clasts from the lobe collapse into the streambed as the bank face retreats (*to the south at location “5”, Fig. 4b*), mantling the streambed with coarse sediment (*see Fig. 7c, d, and e*).

Figure 6. Views of frost-shattered bedrock and colluvium in solifluction lobes from ridgecrest to upper slope on north-facing slope of Blue Mountain. Orange lines represent long-axis orientation of bedrock slabs.



Fig 6. (a) Location 1 on Figure 4. View to northeast of north-dipping (to left) beds of highly fractured Silurian Tuscarora sandstone at crest of Blue Mountain northeast of Waggoner’s Gap Road. Red and yellow asterisks in (a) and (b) are the same locations.



Fig 6. (b) Location 1 on Fig 4. Approximately 40 m downslope, slabs become increasingly jumbled with respect to bedding.



Fig 6. (c) View downslope at location 2 on Figure 4. Farther downslope from (b), large clasts of Tuscarora sandstone occur at the surface of small solifluction lobes that can barely be discerned on the ground and from LiDAR slopeshades.



Fig 6. (d) Location 3 on Figure 4, looking northeast (approximately along bedding strike). Tuscarora sandstone at right is mostly in place, dipping northward (to left), but downslope to left slabs of sandstone become increasingly rotated to the north, with greater amounts of rotation near the ground surface at top. To left of the contact with the Clinton Group is colluvium with no discernible in-place bedrock, part of a solifluction lobe that can be traced across the road and downslope. Gray-black material to right of person (1.56 m high) is asphalt rubble.

At some locations, exposures of red shale in the Bloomsburg Formation can be seen beneath lobes from which fine sediment was winnowed, leaving a lag of coarse sandstone boulders on red shale (*see location "6", Fig. 4a, and Fig. 7c*). Near location "6" (*see Figs. 4b, 5a, and 7c*), several boulders contain *Skolithos* burrows, indicating that the boulders might have come from outcrops of Keefer sandstone (basal member of the Mifflintown Formation) which exists ~500 m upslope (pers. comm. Donald Hoskins, September 4, 2010). Given a maximum surface velocity of about 1 m/yr for solifluction flow (*see above, and Matsuoka, 2001*), downslope sediment movement via solifluction occurred for at least 500 years. Given a slope of 5.7° , the surface velocity during annual thaw probably was only ~0.1 m/yr (from $V_s = 100 \cdot \tan \theta$), yielding a possible duration for downslope sediment transport of approximately 5,000 years in order to move quartzite boulders 500 m.

Lobate forms also become more pronounced downslope on the south-facing slope of Blue Mountain at Waggoner's Gap (*see Fig. 4, 5b, and 5d*). Immediately south of the ridge crest, the north-dipping Juniata Formation (sandstone with interbedded siltstone and shale) underlies the Tuscarora Formation. Farther downslope to the south, the Martinsburg Formation (shale with some interbedded sandstone and siltstone) underlies the Juniata sandstone. Solifluction lobes containing boulders, some possibly of Tuscarora sandstone, occur in exposures of poorly sorted, matrix-supported colluvial diamicton at distances at least 750 m downslope, supporting 750 years or more of downslope movement (at typical maximum solifluction surface velocity of ~1 m/yr). The average slope at this location is about 9° (*see Fig. 5d*), so the surface velocity during thaw might have been about 0.1m/yr.

Retrogressive Thaw Slumps and Thermokarst Gullies In addition to solifluction landforms, we document two others in southern Pennsylvania—retrogressive thaw slumps and thermokarst gullies--that are common in regions of permafrost thaw today. To our knowledge, these have not been noted before as relict periglacial features in the unglaciated mid-Atlantic region.

Arcuate slumps along valley bottom margins are interpreted here as ***retrogressive thaw slumps***. Such slumps are common today along rivers, lakes, and coasts throughout northern to central Alaska (Gooseff et al, 2009) and northern Canada where permafrost thaw is occurring (*see summary in Jorgenson et al, 2013*). They form when erosion, for example by wave action, seepage, or stream migration results in a break in slope and exposes permafrost, which then thaws rapidly and initiates arcuate slumping. As slumped material is removed at the base of slope, the slump area expands with retrogressive thawing and more permafrost is exposed. Thaw slumps in permafrost regions typically form along erosional edges but stabilize within 30-50 years of expansion, leaving a series of arcuate scars that resemble a scalloped edge.

Figure 7. Views of solifluction lobes and colluvium at toe-of-slope on north-facing slope of Blue Mountain in the Florence Jones Rieneman Wildlife Sanctuary. Yellow lines indicate surface of lobes.



(a) Location 4 on Figure 4, view to northeast, on solifluction lobe on 6° dipping slope (see also Figure 5a and 5c).



(b) Location 5 on Figure 4, view to southwest. Exposure of colluvium in solifluction lobe along southern-bank of Trout Run reveals poorly sorted, matrix-supported diamicton (see close-up views of this outcrop in (d) and (e)). (c) Location 6 on Figure 4 shows view to southwest of quartzite boulders winnowed from solifluction lobe, resting on red shale of the Bloomsburg Formation. Hill to right is also Bloomsburg shale. Some of the quartzite boulders have *Skolithos* tubes (trace fossils), indicating a possible source of Tuscarora sandstone along the ridgecrest to the south.



(d) and (e) Close-up views of outcrop in (b), showing how large particles winnowed from solifluction colluvium drop to bed of Trout Run, mantling it with coarse sediment as the bank retreats.

Our LiDAR mapping and comparison with geologic maps shows that possible retrogressive thaw slumps occur locally along limestone or dolomite valley margins. One example occurs along the northern margin of Mountain Creek upstream of the town of Mount Holly Springs. Two possible retrogressive thaw slumps are indicated with asterisks on Fig. 5, although better and more numerous examples exist elsewhere in our regional study area. We interpret them as the result of retrogressive thaw slumping because of their location along slope breaks and their arcuate shape, shallow depth, and relatively small size in comparison to bedrock slumps.

Thermokarst gullies, also called thaw gullies, form during thaw as the active layer deepens, water is released from ice-rich soil, and surface water becomes channelized (see summaries in French, 2007, and Jorgenson et al, 2013). They are found in abundance in continuous permafrost regions where ice wedges are thawing, resulting in gullies up to 5 m deep. Commonly, they are associated with thaw settling of colluvium along gully margins.

In the unglaciated region of Pennsylvania, we observe gullies near the downslope margins of gelifluction-mantled slopes. Our preliminary findings indicate that they are more numerous to the north, toward full glacial ice margins, at higher altitudes, and on south-facing slopes. They occur along the mid-slope flanks of Blue Mountain at Waggoner's Gap, and we have mapped some of them on Figures 4 and 5.

Discussion: Diffusion and the Geomorphic Record of Solifluction

Our LiDAR mapping and analysis, combined with the field work of many others who have mapped and described periglacial features south of full glacial ice margins in the mid-Atlantic region, and reveals a landscape dominated by diffusive processes on most if not all hillslopes. Diffusion in the context of topography and hillslope processes is the downslope movement of sediment in which the rate of flux is proportional to slope and diffusivity constant, the latter of which is affected by climate, soil characteristics, and other factors. LiDAR slopeshades support the interpretation of solifluction as the specific process by which diffusion occurred within our study region. Recall from the work of Matsuoka (2001) discussed above that thick active layers are associated with higher fronts on solifluction lobes and sheets. The size of solifluction features mapped here with LiDAR, ranging from 1 to several meters in height and hundreds of meters in slope length, supports a thick active layer with repeated freeze-thaw and downslope sediment transport. Modern rates of soil surface velocity by solifluction are used here to determine that thousands of years of downslope flow occurred during times of permafrost, perhaps particularly during deglacial permafrost thaw.

LiDAR analysis indicates that solifluction lobes and sheets commonly are associated with gully heads on mid- to lower slope locations. We interpret these gullies as the result of dewatering of ice-rich ground that was saturated during permafrost thaw. The mid-slope location of thermokarst gullies, typically below a slope dominated by solifluction features, might be the result of an increase in sub-surface runoff with distance from the drainage divide. These gullies are etched into the diffusional slopes generated by solifluction, so we interpret them to be a deglacial feature associated with permafrost thaw and degradation during glacial terminations.

In a prescient paper based on diffusion modeling, Kirkby (1995) modeled variations in gelifluction flow rates with temperature and topography and concluded that the land between 40° and 65° N and S of the equator was shaped by intense gelifluction during warming and permafrost thaw at the end of full glacial periods. This zone would have fallen within the temperature ranges at which gelifluction flow rates were high during full glacial times, as discussed above. Kirkby's diffusion modeling (1995) of formerly periglacial landscapes at mid-latitudes assumed that downslope sediment transport was the result of gelifluction during thawing of the active layer in regions with permafrost. Highest rates of gelifluction occur during post-glacial warming, when mean annual temperature is rising and passes through the 0°C isotherm. This time period might persist for several thousand years, depending on the rate of warming, and is associated with rapid slope change. A wave of gelifluction-driven downslope sediment transport and slope change moves toward polar regions with deglacial warming. The more gradual the temperature change, the more prolonged the period of rapid gelifluction and, hence, the amount of sediment moved downslope by gelifluction.

Kirkby's landscape models demonstrate that the erosional profiles of hillslopes become smooth and broadly convex as a result of long-term erosion by gelifluction. Step-like gelifluction lobes mark these smooth convex slopes when gelifluction is active. Hollows do not enlarge with time but rather are filled by diffusive processes.

Our work indicates substantial impacts on valley bottoms, particularly those of 1st- and 2nd-order, by infilling of sediment derived from slopes (*see for example Figures 2b, 4, 5, and 7*). This finding is consistent with stratigraphic and geomorphic evidence of post-glacial valley filling in the eastern US and Europe (c.f., Braun, 1989; Ballantyne and Harris, 1994). Kirkby's (1995) modeling of formerly periglacial landscapes at mid-latitudes also showed that hollows, toe of slope areas, and valley bottoms adjacent to long steep slopes, as in mountainous areas, are filled with sediment by diffusive processes. Where sediment is deposited downslope from areas stripped by gelifluction, slopes are concave upward. Slopes with thick active layers, steep gradients, and abundant moisture for subsurface runoff have the highest rates of downslope sediment transport and valley bottom infilling.

Kirkby (1995) concluded that modern rates of diffusive sediment transport on hillslopes are an order of magnitude smaller than those during times of permafrost thaw and gelifluction. Nevertheless, diffusive processes blur microtopography with time, and Kirkby anticipated that relict landscapes at mid-latitudes are likely to have little geomorphic record of prior episodes of intense gelifluction-driven diffusion. A sedimentary record might exist in the sub-surface, as frost-stirred colluvium for example, but geomorphic expression of a solifluction lobe could be erased over a time span of >10 millennia. The duration of time during the Holocene would have been sufficient to smooth lobes by soil creep, even at low rates of diffusion. However, we find this not to be the case in Pennsylvania or Maryland, where LiDAR analysis reveals that solifluction lobes and sheets are pronounced and widespread. A possible explanation is that rates of creep since the early Holocene are even lower than thought by Kirkby (1995).

Conclusions

The goals of this work are to use LiDAR to evaluate the use of possible periglacial landforms as paleoclimatic indicators, and to determine which landforms—or suites of landforms—are diagnostic of the former existence and degradation of permafrost. Based on widespread and pronounced (i.e., thick and well developed) solifluction lobes and sheets, even at low elevations, throughout central, south-central, and southeastern Pennsylvania, we conclude that this region was affected by permafrost, and that mean annual temperatures during glacial maxima (and perhaps other times during glacial-deglacial cycles) must have been less than 0° C.

We continue to evaluate differences on north- and south-facing slopes, and note that solifluction lobes and sheets appear to vary with aspect. Other workers have found that south-facing slopes tend to have thinner regolith and lower gradients than north-facing slopes developed on shale in the central Appalachians (West et al 2014).

Our findings support previous work based on landform mapping, sedimentology of slope deposits, and paleoecology, although only the last of these has provided actual paleotemperature data. Paleoecological evidence from the central Appalachian region supports mean annual air temperatures at least 11° C lower than at present during the LGM (c.f., Woodcock and Wells, 1990). With modern MAAT ranging from 10-13° C in the study region, possible MAATs during LGM were -1 to 2° C or less. We posit that they were sufficiently cooler for permafrost, possibly continuous, to be widespread. Recent review of regional paleoclimate data by French and Millar (2014) yielded a map with a speculative southern limit of LGM permafrost (*see Fig. 1*). Our work supports a permafrost limit at least as far south as the Pennsylvania border.

Most paleoecological studies are based on sedimentary cores from a specific site, with pollen from the sediment derived regionally by wind transport. Such studies are complimented by topographic LiDAR analysis, for one provides a regional perspective on ecological processes whereas the other provides a regional perspective on landscape processes. With LiDAR, we are able to distinguish multiple landforms that are not easily identified in the sedimentary record, such as retrogressive thaw slumps and thermokarst gullies. We also are able to discern specific landforms, particularly those of solifluction lobes and sheets, which can be correlated to colluvial diamictons as a mechanism of colluvial sediment transport. The ubiquity of these features supports Kirkby's (1995) landscape modeling of a diffusion-dominated landscape during LGM, and our interpretation of valley bottom landscapes inherited from conditions of sediment infilling. As shown in Figure 7, for example, modern streams flowing on shale are unable to transport coarse material derived from upslope solifluction.

Acknowledgments

We are grateful to Lee Shull, Manager of the Florence Jones Reineman Wildlife Sanctuary for permission to work on the property along the northern slope of Blue Mountain near Waggoner's Gap, Pennsylvania. Funding for this work was provided by a generous alumnus of the Department of Geology (now Earth and Environment) at Franklin and Marshall College.

References

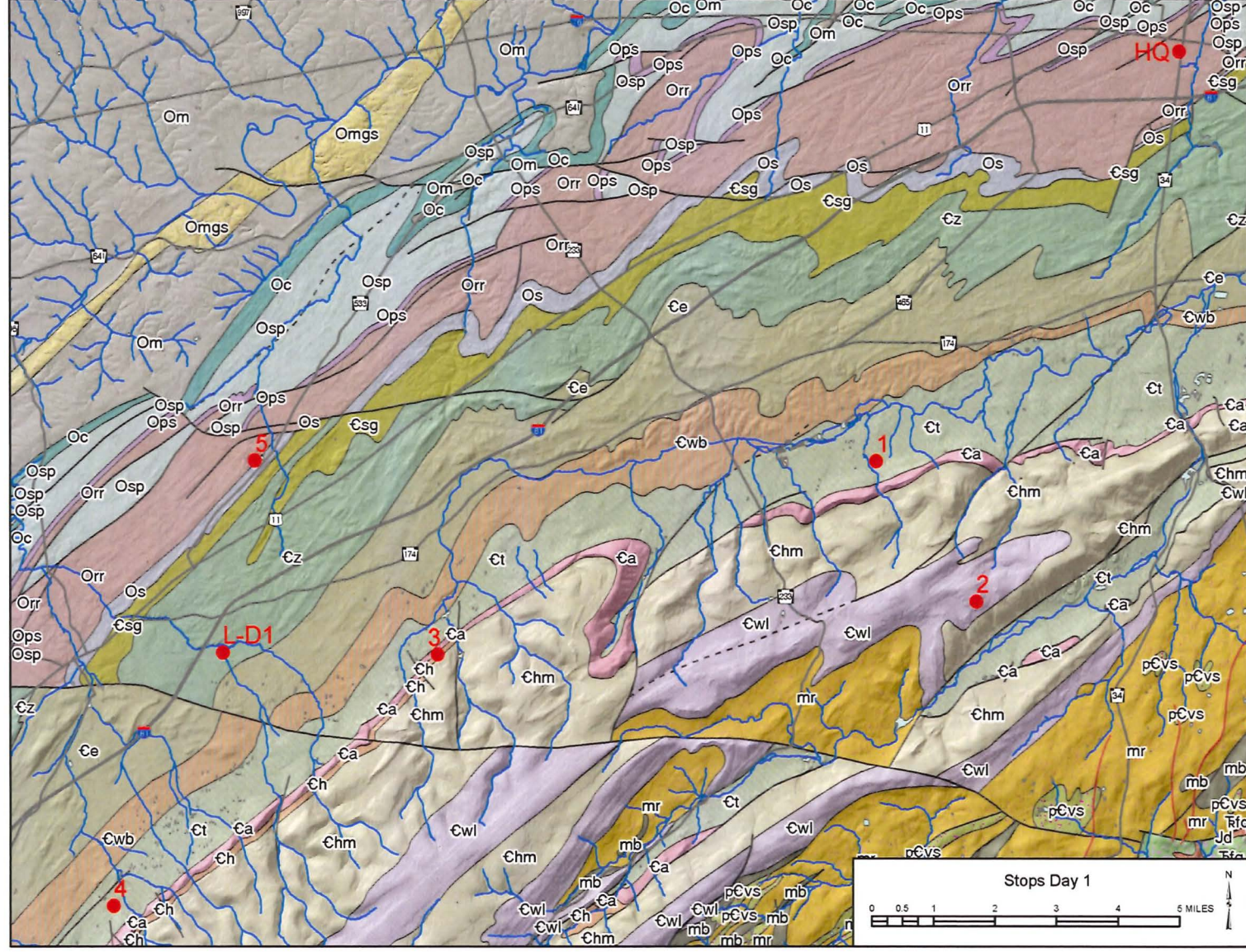
- ACGR. 1988. Glossary of permafrost and related ground ice terms, Associate Committee on Geotechnical Research (ACGR), National Research Council of Canada, Ottawa.
- Bowden, William B. 2010. "Climate Change in the Arctic – Permafrost, Thermokarst, and Why They Matter to the Non-Arctic World." *Geography Compass* 4 (10): 1553–66. doi:10.1111/j.1749-8198.2010.00390.x.
- Braun, Duane D. 1989. "Glacial and Periglacial Erosion of the Appalachians." *Geomorphology* 2 (1-3): 233–56. doi:10.1016/0169-555X(89)90014-7.
- Brown, R. J. E., and Péwé, T. L. 1973. Distribution of permafrost in North America and its relationship to the environment: A review, 1963-1973. In *Permafrost: North American Contribution [to The] Second International Conference* (Vol. 2, p. 71). National Academies.
- Carter, Brian J., and Edward J. Ciolkosz. 1986. "Sorting and Thickness of Waste Mantle Material on a Sandstone Spur in Central Pennsylvania." *CATENA* 13 (3): 241–56. doi:10.1016/0341-8162(86)90001-9.
- Ciolkosz, E.J., Cronce, R.C. and Sevon, W.D. 1986. Periglacial features in Pennsylvania. Pa. State Univ., Agron. Ser. 92, 15 pp.

- Ciolkosz, Edward J., Brian J. Carter, Michael T. Hoover, Richard C. Cronic, William J. Waltman, and Robert R. Dobos. 1990. "Genesis of Soils and Landscapes in the Ridge and Valley Province of Central Pennsylvania." *Geomorphology*, Proceedings of the 21st Annual Binghamton Symposium in Geomorphology, 3 (3-4): 245-61. doi:10.1016/0169-555X(90)90006-C.
- Clark, Michael G., and Edward J. Ciolkosz. 1988. "Periglacial Geomorphology of the Appalachian Highlands and Interior Highlands South of the Glacial Border — A Review." *Geomorphology* 1 (3): 191-220. doi:10.1016/0169-555X(88)90014-1.
- Clark, G. Michael, and Thomas W. Schmidlin. 1992. "Alpine Periglacial Landforms of Eastern North America: A Review." *Permafrost and Periglacial Processes* 3 (3): 225-30. doi:10.1002/ppp.3430030309.
- Cleaves, Emery T. 2000. "Regoliths of the Middle-Atlantic Piedmont and Evolution of a Polymorphic Landscape." Edited by G. Michael Clark, J. Steven Kite, and Hugh H. Mills. *Southeastern Geology*, Regolith in the Central and Southern Appalachians, 39 (3-4): 199-222.
- Craul, Timothy. 2010. "Solifluction expression on mountain footslopes of the Ridge and Valley [Pennsylvania]". Northeast Regional National Cooperative Soil Survey Conference, Elizabethtown, PA (oral presentation).
- Denny, C. S. 1951. "Pleistocene frost action near the border of the Wisconsin drift in Pennsylvania." *Ohio Jour. Sci.*, v. 51, p. 116-125.
- Denton, G. H., R. F. Anderson, J. R. Toggweiler, R. L. Edwards, J. M. Schaefer, and A. E. Putnam. 2010. "The Last Glacial Termination." *Science* 328 (5986): 1652-56. doi:10.1126/science.1184119.
- Eaton, L. Scott, Benjamin A. Morgan, R. Craig Kochel, and Alan D. Howard. 2003. "Quaternary Deposits and Landscape Evolution of the Central Blue Ridge of Virginia." *Geomorphology* 56 (1-2): 139-54. doi:10.1016/S0169-555X(03)00075-8.
- French, Hugh M. 1999. "Past and Present Permafrost as an Indicator of Climate Change." *Polar Research* 18 (2): 269-74. doi:10.1111/j.1751-8369.1999.tb00303.x.
- . 2007. *The Periglacial Environment*. John Wiley & Sons.
- French, Hugh M., and Susan W. S. Millar. 2014. "Permafrost at the Time of the Last Glacial Maximum (LGM) in North America." *Boreas* 43 (3): 667-77. doi:10.1111/bor.12036.
- French, Hugh M., Mark Demitroff, and Steve L. Forman. 2003. "Evidence for Late-Pleistocene Permafrost in the New Jersey Pine Barrens (latitude 39°N), Eastern USA." *Permafrost and Periglacial Processes* 14 (3): 259-74. doi:10.1002/ppp.456.






- French, Hugh M., Mark Demitroff, Steven L. Forman, and Wayne L. Newell. 2007. "A Chronology of Late-Pleistocene Permafrost Events in Southern New Jersey, Eastern USA." *Permafrost and Periglacial Processes* 18 (1): 49–59. doi:10.1002/ppp.572.
- French, Hugh, Mark Demitroff, and Wayne L. Newell. 2009. "Past Permafrost on the Mid-Atlantic Coastal Plain, Eastern United States." *Permafrost and Periglacial Processes* 20 (3): 285–94. doi:10.1002/ppp.659.
- French, Hugh. 2008. "Recent Contributions to the Study of Past Permafrost." *Permafrost and Periglacial Processes* 19 (2): 179–94. doi:10.1002/ppp.614.
- Gardner, Thomas W., John B. Ritter, Christopher A. Shuman, James C. Bell, Kathryn C. Sasowsky, and Nicholas Pinter. 1991. "A Periglacial Stratified Slope Deposit in the Valley and Ridge Province of Central Pennsylvania, USA: Sedimentology, Stratigraphy, and Geomorphic Evolution." *Permafrost and Periglacial Processes* 2 (2): 141–62. doi:10.1002/ppp.3430020208.
- Gooseff, Michael N., Andrew Balser, William B. Bowden, and Jeremy B. Jones. 2009. "Effects of Hillslope Thermokarst in Northern Alaska." *Eos, Transactions American Geophysical Union* 90 (4): 29–30. doi:10.1029/2009E0040001.
- Gruber, S. 2012. "Derivation and Analysis of a High-Resolution Estimate of Global Permafrost Zonation." *The Cryosphere* 6 (1): 221–33. doi:10.5194/tc-6-221-2012
- Hack, J. T. 1965. "Geomorphology of the Shenandoah Valley, Virginia and West Virginia, and origin of the residual ore deposits." *U.S. Geol. Surv. Prof. Pap.*, 484, p. 84.
- Harris, C., 1981. Periglacial Mass-Wasting: A Review of Research. *BGRG Research Monograph*, vol. 4, Geo Abstracts, Norwich.
- Harris, Stuart A. 1994. "Climatic Zonality of Periglacial Landforms in Mountain Areas." *ARCTIC* 47 (2): 184–92. doi:10.14430/arctic1288.
- Hoover, M. T., and Ciolkosz, E. J. 1988. Colluvial Soil Parent Material Relationships in the Ridge and Valley Physiographic Province of Pennsylvania1. *Soil science*, 145(3), 163-172.
- Jorgenson, M. T. 2013. "8.20 Thermokarst Terrains." In *Treatise on Geomorphology*, edited by John F. Shroder, 313–24. San Diego: Academic Press. <http://www.sciencedirect.com/science/article/pii/B9780123747396002153>.
- Kirkby, M. J. 1995. "A Model for Variations in Gelifluction Rates with Temperature and Topography: Implications for Global Change." *Geografiska Annaler. Series A, Physical Geography* 77 (4): 269–78. doi:10.2307/521336.
- Lewkowicz, A.G., 1988. "Slope processes." In: Clark, M.J. (Ed.), *Advances in Periglacial Geomorphology*. Wiley, Chichester, pp. 325–368.

- Mackay, J. Ross. 1981. "Active Layer Slope Movement in a Continuous Permafrost Environment, Garry Island, Northwest Territories, Canada." *Canadian Journal of Earth Sciences* 18 (11): 1666–80. doi:10.1139/e81-154.
- Marsh, Ben. 1987. "Pleistocene Pingo Scars in Pennsylvania." *Geology* 15 (10): 945–947. doi:10.1130/0091-7613(1987)15<945:PPSIP>2.0.CO;2.
- Matsuoka, Norikazu. 2001. "Solifluction Rates, Processes and Landforms: A Global Review." *Earth-Science Reviews* 55 (1–2): 107–34. doi:10.1016/S0012-8252(01)00057-5.
- . 2011. "Climate and Material Controls on Periglacial Soil Processes: Toward Improving Periglacial Climate Indicators." *Quaternary Research* 75 (2): 356–65. doi:10.1016/j.yqres.2010.12.014.
- Merritts, Dorothy, Robert Walter, Michael Rahnis, Jeff Hartranft, Scott Cox, Allen Gellis, Noel Potter, et al. 2011. "Anthropocene Streams and Base-Level Controls from Historic Dams in the Unglaciaded Mid-Atlantic Region, USA." *Philosophical Transactions of the Royal Society A: Mathematical, Physical and Engineering Sciences* 369 (1938): 976–1009. doi:10.1098/rsta.2010.0335.
- Newell, W. L., and B. D. Dejong. 2011. "Cold-Climate Slope Deposits and Landscape Modifications of the Mid-Atlantic Coastal Plain, Eastern USA." *Geological Society, London, Special Publications* 354 (1): 259–76. doi:10.1144/SP354.17.
- Pazzaglia, Frank J., and Emery T. Cleaves. 1998. *Surficial Geology of the Delta Quadrangle, Harford County, Maryland and York County, Pennsylvania*. Report of Investigations 67. Baltimore, MD: Maryland Geological Survey. http://www.ees.lehigh.edu/ftp/retreat/outgoing/preprints_and_reprints/Pazzaglia_a_Cleaves_1998_Delta_quad_MD_Rpt67.pdf.
- Péwé, T. L. 1983. The periglacial environment in North America during Wisconsin time. *Late-quaternary environments of the United States*, 1, 157–189.
- Stanford, Scott D., Gail M. Ashley, Emily W.B. Russell, and Gilbert J. Brenner. 2002. "Rates and Patterns of Late Cenozoic Denudation in the Northernmost Atlantic Coastal Plain and Piedmont." *Geological Society of America Bulletin* 114 (11): 1422–37. doi:10.1130/0016-7606(2002)114<1422:RAPOLC>2.0.CO;2.
- Walter, R. C., and D. J. Merritts. 2008. "Natural Streams and the Legacy of Water-Powered Mills." *Science* 319 (5861): 299–304.
- Walters, James C. 1978. "Polygonal Patterned Ground in Central New Jersey." *Quaternary Research* 10 (1): 42–54. doi:10.1016/0033-5894(78)90012-1.
- Washburn, A.L. 1980. "Permafrost Features as Evidence of Climatic Change." *Earth-Science Reviews* 15 (4): 327–402. doi:10.1016/0012-8252(80)90114-2.
- Washburn, A.L., 1973. *Periglacial Processes and Environments*. Arnold, London, 320 pp.

- Washburn, A.L., 1979. *Geocryology: A Survey of Periglacial Processes and Environments*. Edward Arnold, London.
- West, Nicole, Eric Kirby, Paul Bierman, and Brian A. Clarke. 2014. "Aspect-Dependent Variations in Regolith Creep Revealed by Meteoric ^{10}Be ." *Geology* 42 (6): 507–10. doi:10.1130/G35357.1.
- Woodcock, D. W., and P. V. Wells. 1990. "Full-Glacial Summer Temperatures in Eastern North America as Inferred from Wisconsinan Vegetational Zonation." *Palaeogeography, Palaeoclimatology, Palaeoecology* 79 (3–4): 305–12. doi:10.1016/0031-0182(90)90024-2.



Day 1 Road Log. LIDAR image with Geologic Map showing Stops 1 – 5, Starting at Comfort Suites in Carlisle (HQ) & including Lunch Stop (L-D1)

Mileage Interval	Cumulative Mileage	 = Stop Sign;  = Traffic Light; "T" = T Intersection; TR = Township Route; "Y" = Y intersection
0.0	0.0	Start at the Comfort Suites in Carlisle. Proceed south on South Hanover Street, passing 6 streets, some with traffic lights, until reaching West Willow Street.
0.4	0.4	At the  turn right onto West Willow Street continuing straight until reaching the intersection of South West Street and the junction of Walnut Bottom Road.
0.3	0.7	At the  turn half left onto Walnut Bottom Road; continue on Walnut Bottom Road for next 7.0 miles <i>Note: At mileage 1.1 houses to right, in karst depressions, living rooms were flooded during Hurricane Agnes in 1972</i>
0.9	1.6	I-81 Exit 45 underpass; continue straight . Over the next several route miles there are good views of South Mountain on the left, and of Blue (locally called North) Mountain on the right. <i>Note: From this point to cumulative mileage 8.9, no streams cross the route due to region's pervasive karst topography. Infrequent exposures are present along route to mile 7.6, stratigraphically downward they include the Ordovician Rockdale Run and Stonehenge formations, then Cambrian Shady Grove, Zullinger, and Elbrook formations.</i>
1.7	3.3	PA Route 465 joins Walnut Bottom Road from right. Continue straight .
4.4	7.7	At the junction of Walnut Bottom Road (PA Route 465) and PA Route 174-E turn left onto PA Route 174-E and then turn immediately right onto Montsera Road
0.5	8.2	At "Y" with Encks Mill Road, continue left to stay on Montsera Road
0.6	8.8	Cross railroad
0.1	8.9	Cross Yellow Breeches Creek
0.1	9.0	 turn right onto Pine Road <i>(to the left is Kings Gap General Store with excellent cheese wheel and 100 year old map of PA railroad routes)</i>
200 feet	9.0+	Take first left onto Kings Gap Road. <i>Note: sign for Kings Gap Environmental Education Center to left</i>
0.6	9.6	ARRIVE at Kings Gap Hollow pathway entrance to Kings Gap Pond – STOP 1

STOP #1 – KINGS GAP POND

Stop Leader Noel Potter, Jr., Dickinson College, Retired



Entrance to path accessing Kings Gap Pond

KINGS GAP POND, A WINDOW ON THE LATE PLEISTOCENE

Noel Potter, Jr., Department of Earth Sciences (retired), Dickinson College, Carlisle, PA 17013, pottern@dickinson.edu; Helen L. Delano, Pennsylvania Geological Survey, 3240 Schoolhouse Road, Middletown, PA 17057, hdelano@pa.gov; W. D. Sevon, East Lawn Research Center, 30 Meadow Run Place, Harrisburg, PA 17112-3364, wsevon30@comcast.net; Norton Miller (deceased), New York State Museum, Albany, NY.

Introduction

Kings Gap Pond (KGP) (40°06'02.06" N, 77°18'46.79" W) (Fig 1 – LiDAR & Fig 2) is the largest of several vernal ponds at the northern base of South Mountain just east of the entrance road to Kings Gap Environmental Education Center. The pond is significant because of a sediment core obtained from it in 2001 with a basal date of 16,080 years BP. The portion of the core below a twig dated at approximately 14,000 BP contains fragments of tundra vegetation. Since the pond is at the base of South Mountain, the entire mountain must have been tundra in the Late Wisconsinan. In addition, just south of the pond, LiDAR (Fig 1) shows lobes that we interpret as solifluction lobes formed under cold conditions.

Access

Access the pond from opposite a log house along the paved Kings Gap road along a short (~100 m) walk along a dirt service road with a “No Parking” sign (Stop 1 entrance photo). Walk past the first spur to the right and keep going. At a second spur to the right, turn south at right angles to the road you’ve been walking on and follow an indistinct path up over a gentle rise to the pond (Fig 2).



Figure 2. Kings Gap Pond (January, 2008 photo) looking SE at moderate mid-winter depth. In a very wet spring the pond overflows an outlet behind the photographer. In a dry summer, the pond margin retreats well beyond the logs in water in the middle distance.

Geologic Setting

The steep north flank of South Mountain is about 0.5 km south of KGP (Figs. 3 and 4). This is underlain by the resistant Antietam sandstone of the Lower Cambrian Chilhowee Group. The gently sloping terrain northward from the base of the mountain to approximately Yellow Breeches Creek (top of Figs. 3 and 4) is underlain by the Cambrian Tomstown dolomite.



Figure 3. Orthophoto from PAMAP showing location of Kings Gap Pond (black triangle near left edge indicated by arrow). Compare to Fig. 4.

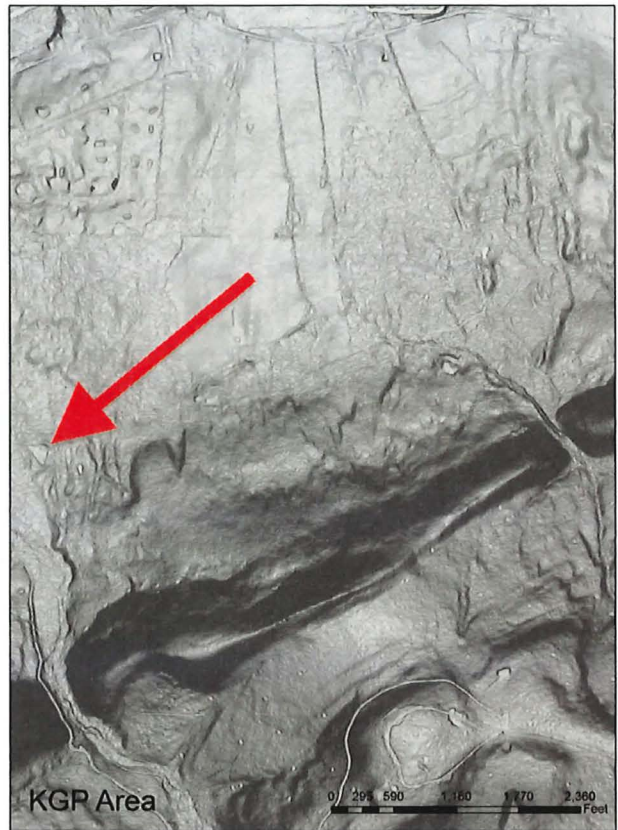


Figure 4. LiDAR Shaded Slope Map from PAMAP showing location of Kings Gap Pond (white triangle near left edge). Compare to Fig.3.

The Tomstown is rarely seen in outcrop because it is buried beneath a thick mantle of sandstone-rich colluvium and alluvium derived from South Mountain. This mantle is 1-4 km wide and extends the entire length of South Mountain in Pennsylvania and farther south into the Shenandoah Valley in Maryland and Virginia (Fig. 5). Depth to bedrock near KGP is >30 m, as obtained from records for nearby water wells. Elsewhere depths to bedrock are as much as 125 m.

Vernal Ponds

KGP is one of hundreds of vernal ponds on top of the colluvium/alluvium at the NW base of South Mountain. The water level in vernal ponds fluctuates significantly with the seasons. In late fall and winter KGP fills so that it is a meter or more deep, most years reaching maximum depth in spring. During summer water levels go down due to drainage and evaporation, and in some very dry years KGP becomes a small mud hole near its NE corner (Fig. 2). We have never seen KGP totally dry.

KGP and other vernal ponds at the base of South Mountain formed as karst depressions in the colluvium/alluvium due to long-term solution of the underlying Tomstown dolomite. The ponds are important habitat for several species of salamanders and toads, which migrate to the ponds to breed (Wingert, 2001).

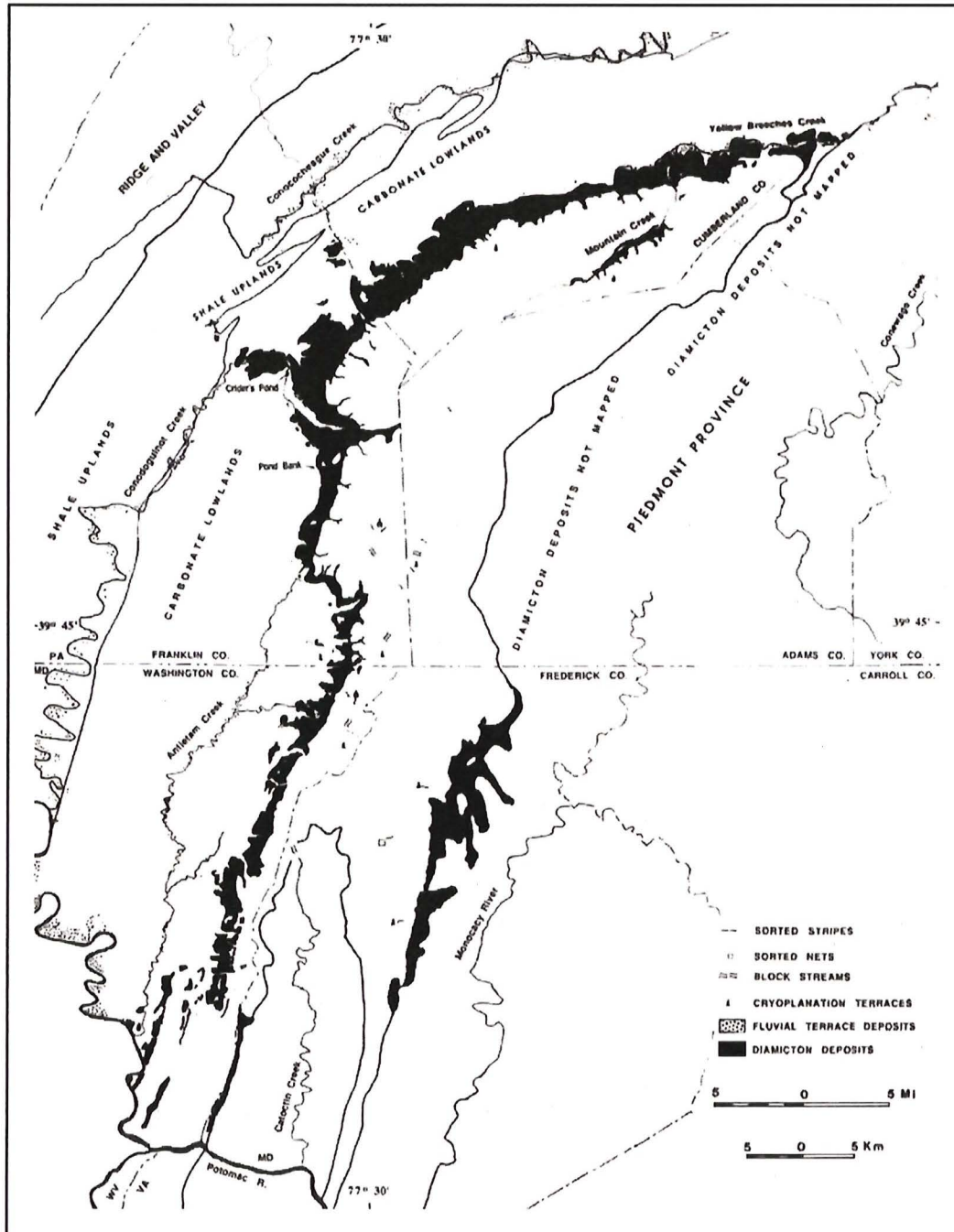


Figure 5. Black area shows distribution of colluvial apron along the west side of South Mountain (from Clark, 1991, Figure 13, p. 61).

KGP Sediment Core

In January, 2001 Noel Potter, Bill Sevon, Helen Delano, and a cast of helpers cored KGP through ice and obtained a core just short of 5 m long (Delano and Potter, 2001; Delano, et al., 2002). We obtained a basal radiocarbon date on the core of 16,080 years BP and a date about half-way up of 14,450 years BP (Fig. 6). The sediment was alternating layers of silty clay and sand, with sand less abundant in the top meter. Norton Miller, of the New York Biological Survey, studied the plant macrofossils (Fig. 6) from the KGP core and found the dominant vegetation from the base to a bit above the 14,450 year date to be tundra vegetation. The key indicator is *Dryas arctifolia*, a classic and distinctive tundra plant, along with dwarf birch, also common on tundra. A spruce zone, then post-spruce shrubs and other plants follow the tundra zone up the core to the present. Several people attempted to examine pollen from the core, but recoverable pollen grains were too sparse for useful analysis. Pine and hardwoods might have been identifiable by pollen, but were probably present based on the other plants that are identified in the upper zone. The uppermost 1 m of sediment is bioturbated. Think of the vegetation one would traverse traveling from northern Hudson's Bay to our hardwood forests here. As one moves south to warmer climates one would leave the tundra and go to spruce forests, then to pine forests, then to mixed pine and hardwood

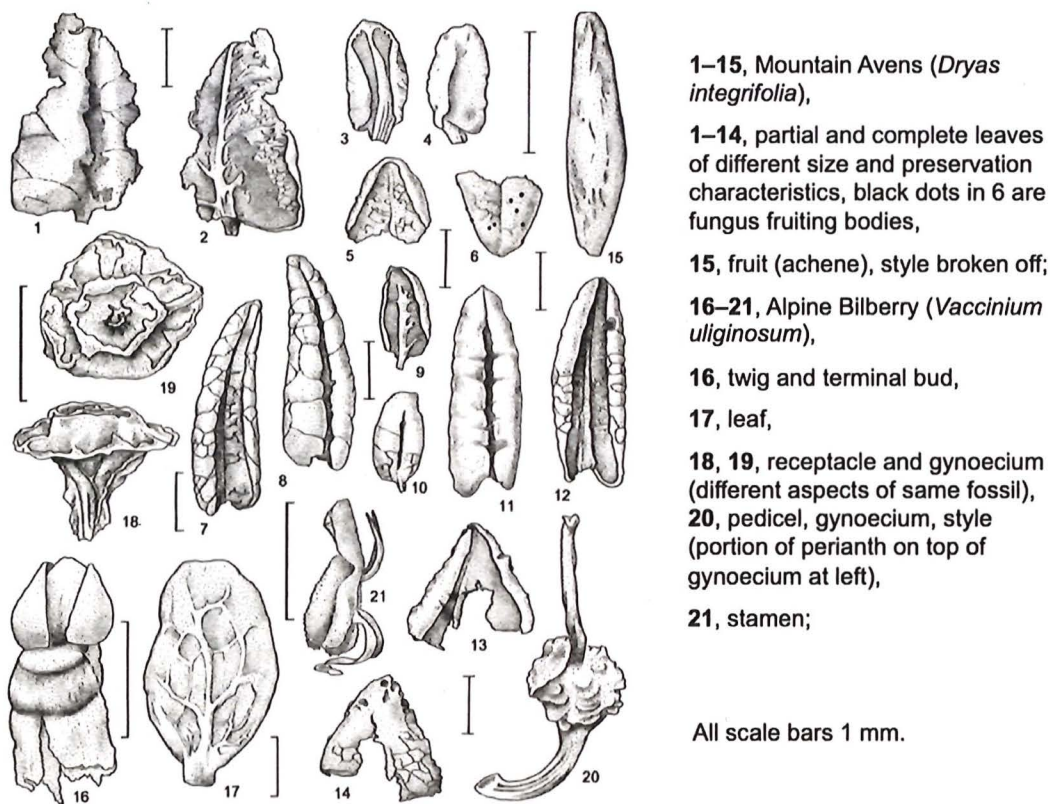


Figure 7A. Illustrations of plant macrofossils from the Kings Gap Pond core by Patricia Kernan, New York Biological Survey.

such as one would find in the Adirondacks and northern New England, and finally to the hardwoods we have in Pennsylvania. These vegetation changes are a measure of climate change here since the Late Wisconsin. Figures 7A and 7B are illustrations of some of the plant macrofossils from the KGP core.

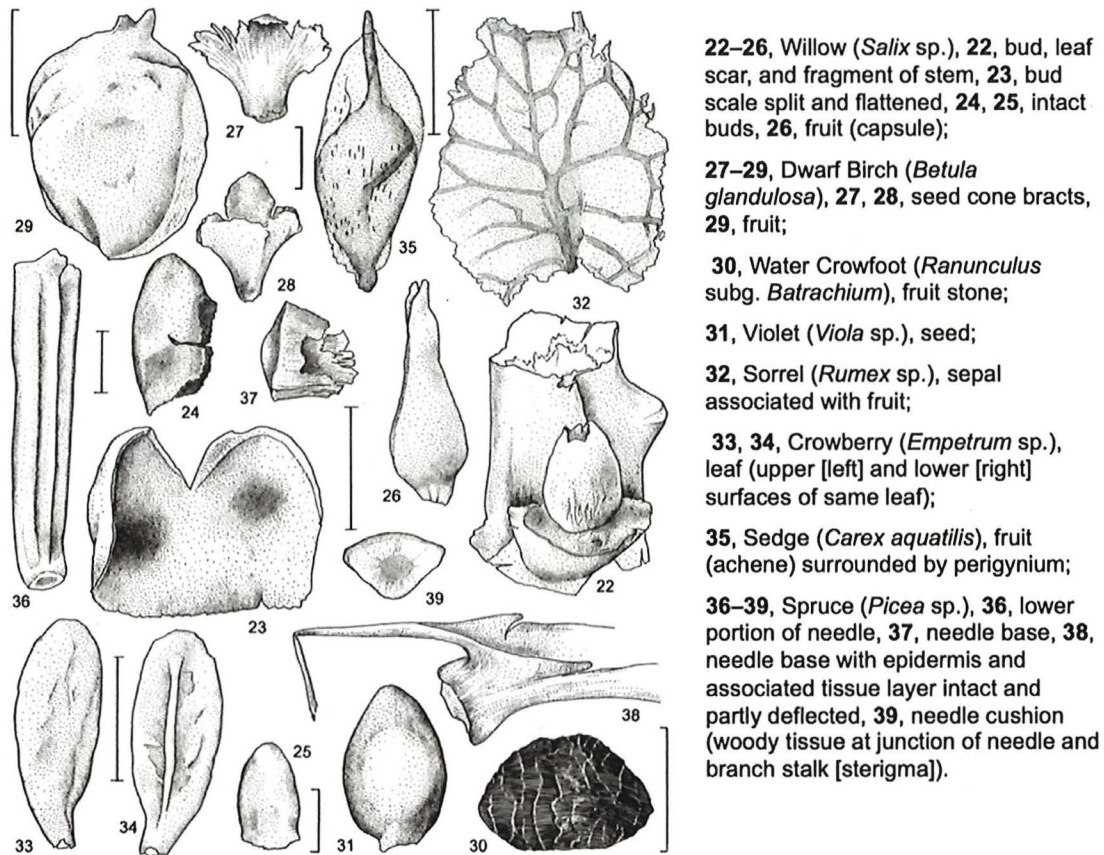


Figure 7B. Illustrations of plant macrofossils from the Kings Gap Pond core by Patricia Kernan, New York Biological Survey.

It is interesting to note that the lower half of the core represents only about 2,000 years, whereas the upper half covers roughly 14,000 years. This probably means that the whole Holocene is represented by less than the top meter of sediment. David Cruz, a Dickinson College student, recently performed loss on ignition (LOI) on the KGP core (Fig. 8) and shows that all but the topmost part of the core is low in organics. The fact that the sedimentation rate was considerably higher in the Late Wisconsin may be related to the presence of gelifluction lobes just to the south (see below). The significance of the tundra vegetation during the Late Glacial at this site at the base of South Mountain, means that locally the top of South Mountain would also have been tundra. This strengthens the case that bedrock knobs like Hammonds Rocks (Day 1, Stop 2) are tors.

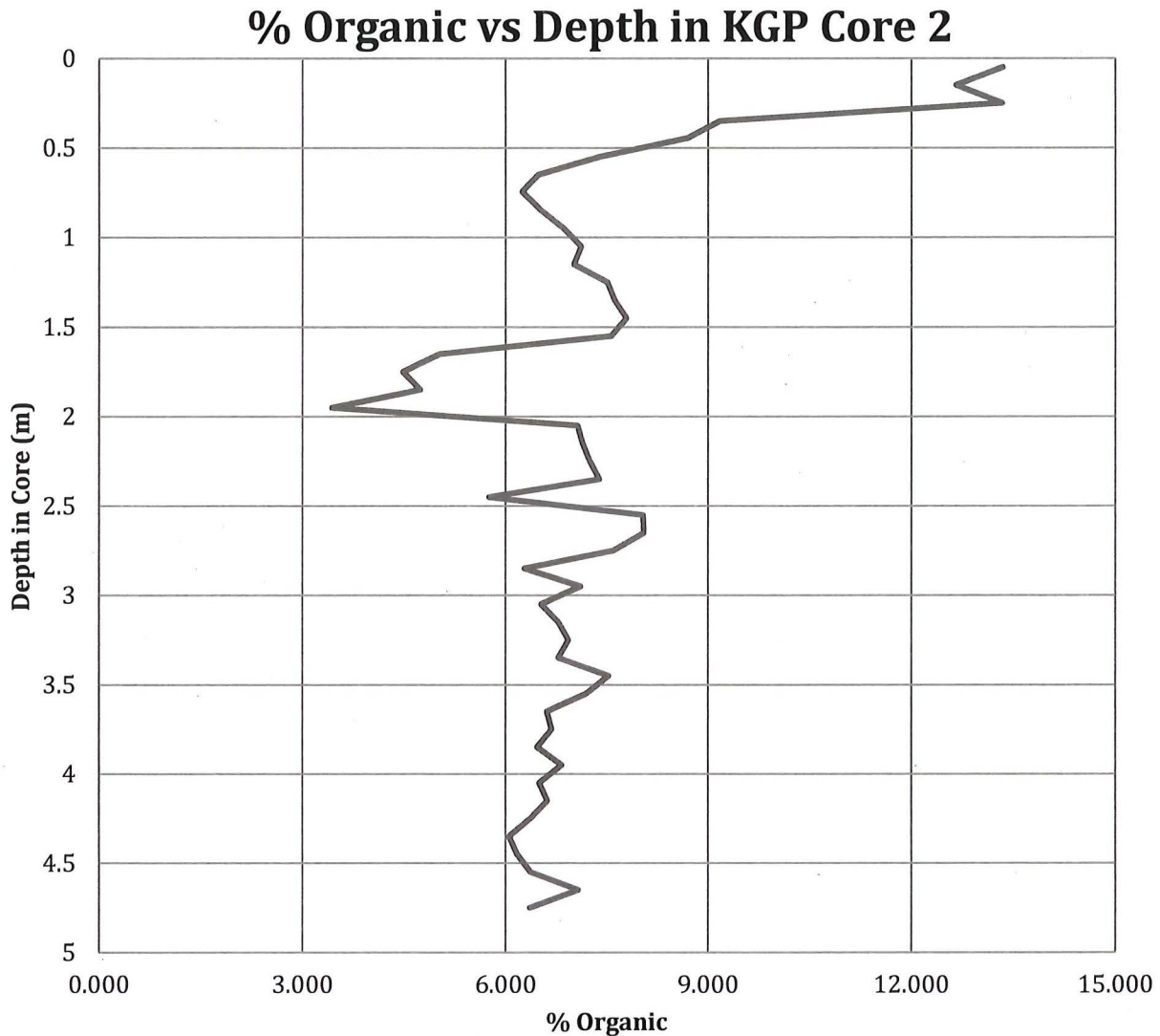


Figure 8. Loss on ignition in Kings Gap Pond Core. Analysis by David Cruz, Dickinson College.

Following page:

Figure 9. Kings Gap Core – Graphic Log

The length of total recovered core and of each section are shown graphically along the left side.

Sediment texture is shown by the width of the bar (scale above each column). Determinations were by visual inspection of the cut surfaces with the aid of a binocular microscope

Colors are approximately those shown.

Relative abundance of minute (<1mm) organic fragments is shown by letters along the left side of the bar. VS-Very sparse, S-sparse, C- Common, A- Abundant, VA- Very abundant. Range of abundance in banded or mottled units is shown with minimum and maximum as S/A (sparse to abundant).

Other features noted in the core are indicated by single letters in the bar. These include O-larger organic fragments, leaves and twigs, P – quartzite pebbles, most 1 to 2 cm diam., V – Vivianite blebs, most < 1mm, some to 1.5 cm.

Sample locations for two AMS radiocarbon dates are shown by red stars.

71

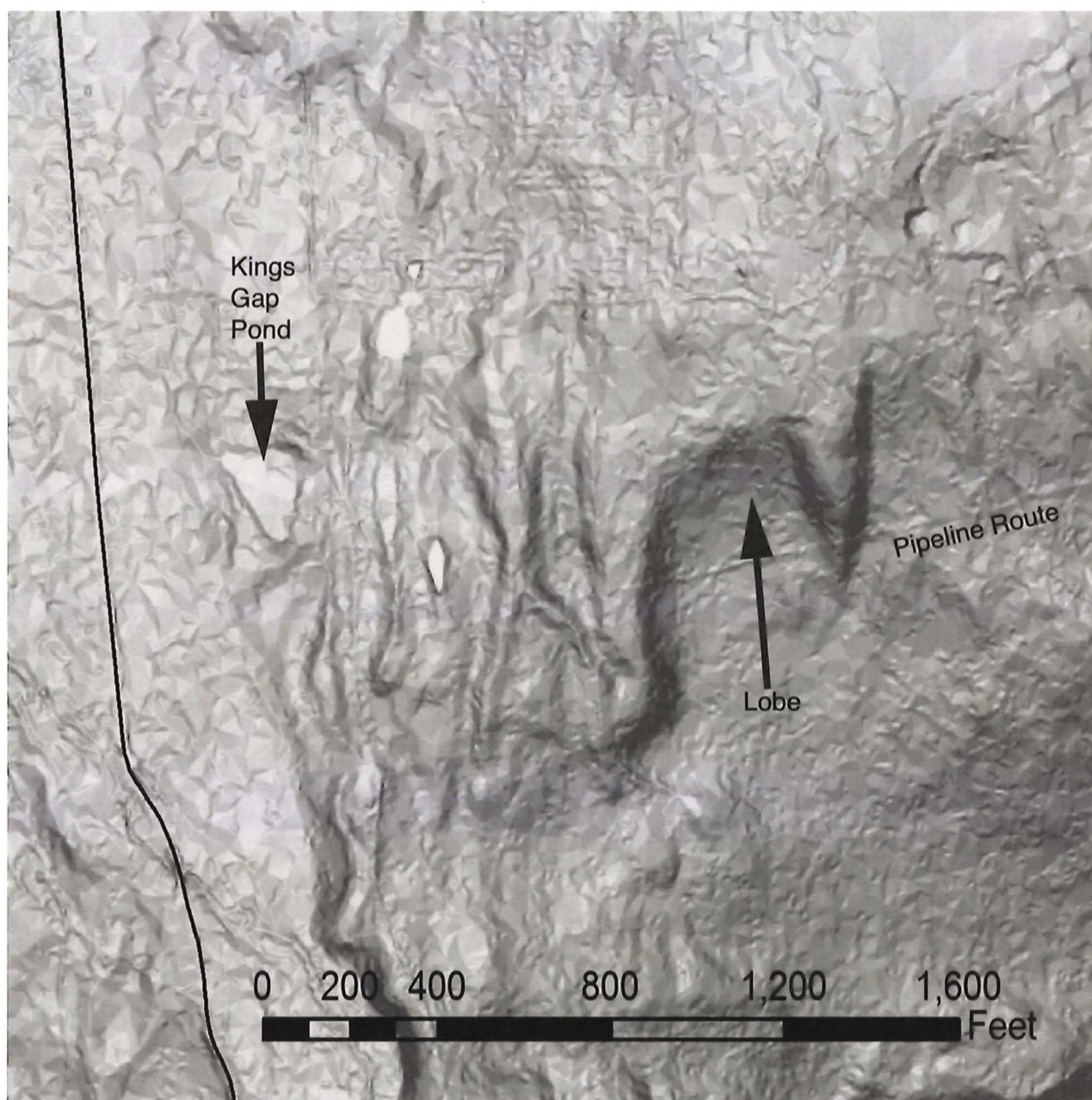


Figure 10. Detailed LIDAR Shaded Slope Map of Stop 1 area

Lobate Features South and East of KGP

A prominent lobe and steep front occurs about 250 m E of KGP (*Fig. 10*). The steep front is about 10 m high, and to the S of this front topography is subdued compared to N of it (*Fig. 10*). Similar lobes occur farther to the East (*Fig. 4*) and elsewhere on the North flank of South Mountain. The material in the lobe is bouldery colluvium with abundant clasts of sandstone derived from steep slopes on the near-vertical Antietam sandstone just to the south.

We interpret these lobes as solifluction or gelifluction lobes that moved northward from South Mountain under periglacial conditions during the Late Wisconsin. These features are not active in our present climate. The lobes are almost perfect replicas of periglacial gelifluction lobes and sheets, ubiquitous in arctic and alpine regions today. These features generally move a few centimeters a year.

Figure 11 shows classic lobes and sheets in Alaska. Discussions of similar features can be found in Benedict (1976), Matsuoka (2001), and French (2007, especially Chapter 9). These features generally move a few centimeters a year.

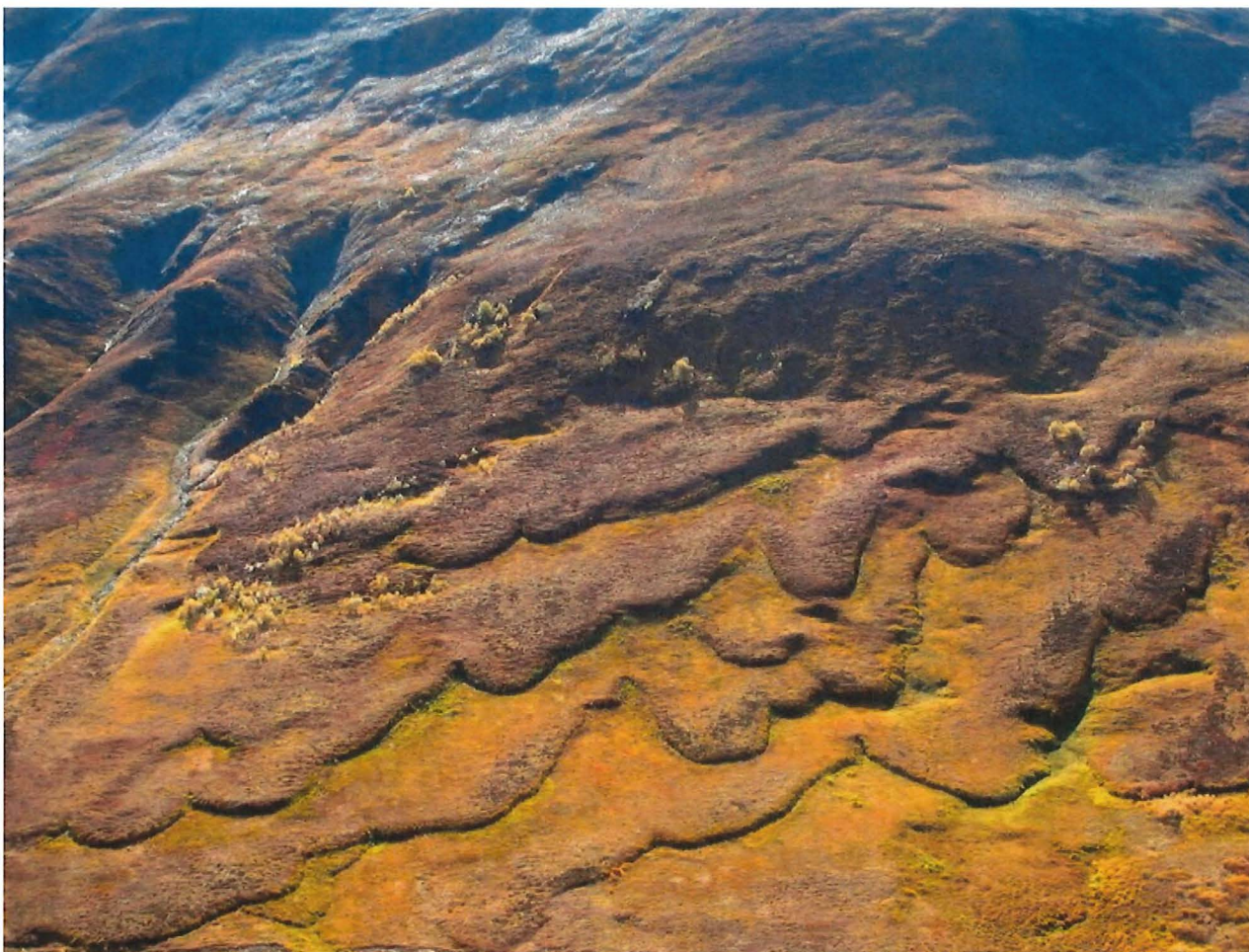


Figure 11. Gelifluction sheets and lobes in Alaska. Ed Plumb photo at: <http://edplumb.blogspot.com>.

Solifluction vs. Gelifluction?

Solifluction, "the slow viscous flow of waterlogged soil and other unsorted and saturated surficial material" (Neuendorf, et al., 2005) is the more generic term and may or may not involve frozen ground. Gelifluction occurs over frozen ground. The frozen ground may be deep annual frost or permanently frozen ground (permafrost). Clearly, frozen ground is highly conducive to downslope movement of overlying soil, for the thawed active layer in summer remains saturated because downward movement of water is impeded by ice.

Thus we ask—was there permafrost here on and near South Mountain? Clark (1991) and Ciolkosz, et al. (1986) catalog an abundance of periglacial features on South Mountain, including sorted stone stripes, small block fields, and tors, but none of these requires permafrost—merely cold periglacial conditions. Tundra vegetation from the KGP core could have existed on permafrost, but can also grow where there is only deep annual frost. The higher sedimentation rate in KGP during the Late Wisconsinan is not surprising given the cold conditions and intermittent surface thaw inferred from the lobes just to the south. Gelifluction can occur in deep annual frost. The best indicator of permafrost is ice-wedge casts, for the ground must be permanently frozen for ice-wedges to develop. Ice-wedge casts have been described from the Pine Barrens of southern New Jersey and in the northern Delmarva Peninsula (French, et al., 2003; French, 2007). A map by French (2007) showing reconstruction of the maximum extent of Late Pleistocene periglacial conditions in the USA south of maximum glaciation limits shows the southern limit of "continuous and discontinuous permafrost" crossing the northern part of Chesapeake Bay into Virginia and West Virginia. Marsh (1987) described pingo scars in Union County to the north, and pingos require permafrost to form. We cannot say from local evidence that there was permafrost on and near South Mountain, but the evidence from adjacent areas says it likely was here.

Karst from the Lobate Features Northward






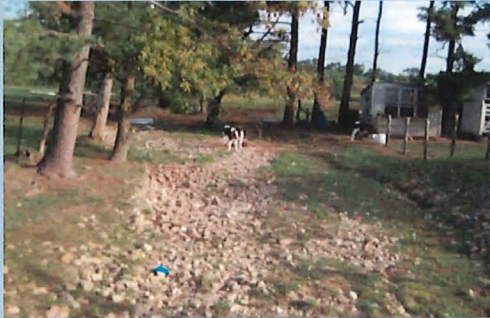
North of the lobate features, including KGP and the area we traversed to get to the lobe, topography is much more hummocky (*Fig. 1*), typical of karst. This topography persists, with abundant sandstone clasts at the surface, all the way north to the floodplain of Yellow Breeches Creek near Pine Road. We infer that this surface is much older than the lobes because it is modified by karst, and it is clear that at least in the case of KGP, the bottom has not sunk significantly in the last 16K years. Are these older colluvial deposits also of periglacial origin, but much older, or are they simply coarse sediment carried out of the streams that drain from South Mountain? We will re-visit this question at Stop 4, where we will see a deep pit into the colluvial material.

References

- Becher, A. E. and Root, S. I., 1981, Groundwater and Geology of Cumberland Valley, Cumberland County, Pennsylvania: Pennsylvania Geological Survey, 4th Series, Water Resource Report W-50, 95 p.
- Benedict, J. B., 1976, Frost creep and gelifluction features: a review: Quaternary Research, v. 6, p. 55-76.
- Ciolkosz, E. J., Cronce, R. C., and Sevon, W. D., 1986, Periglacial features in Pennsylvania: Pennsylvania State University, Agronomy Series, No. 92.
- Clark, G. M., 1991, South Mountain geomorphology: *in* Sevon, W. D. and Potter, N., Jr., eds., Geology in the South Mountain area, Pennsylvania: Guidebook for the 56th Annual Field Conference of Pennsylvania Geologists, p. 55-94.
- Delano, H. and Potter, N., 2001, Kings Gap Pond: *in* Potter, N., Jr., editor, The Geomorphic evolution of the Great Valley near Carlisle, Pennsylvania: Guidebook, Southeast Friends of the Pleistocene, 2001 Annual Meeting, Carlisle, PA, p. 111-119.
- Delano, H. L., Miller, N. G., Potter, N., Jr., 2002, Plant fossil evidence for late Pleistocene tundra conditions in south-central Pennsylvania: Geological Society of America, Northeastern Section, 37th Annual Meeting, Abstracts with Programs, v. 34, no. 1, p. 27.
- French, H. M., Demitroff, M., and Forman, S. L., 2003, Evidence for Late-Pleistocene permafrost in the New jersey Pine Barrens (latitude 39°N) eastern USA: Permafrost and Periglacial Processes, v. 14, p. 259-274.
- French, H. M., 2007, The periglacial environment, 3rd edition: John Wiley & Sons, Chichester, England, 458 p.
- Marsh, Ben, 1987, Pleistocene pingo scars in Pennsylvania: Geology, v. 15, no. 10, p. 945-947.
- Matsuoka, N., 2001, Solifluction rates, processes and landforms: a global review: Earth Science Reviews, v. 55, p. 107-134.
- Neuendorf, K. K. E., et al., 2005, Glossary of Geology, 5th edition: American Geological Institute, Alexandria, VA.
- Watts, W. A., 1979, Late Quaternary vegetation of central Appalachia and the New Jersey coastal plain: Ecological Monographs, v. 49, p. 427-469.
- Wingert, H. Eugene, 2001, Life in a Vernal Pond: Keystone Outdoors, March/April issue, p. 28-31.



LiDAR slopeshade image of two unique geologic features showing underlying structure and Holocene weathering effects.

Mileage Interval	Cumulative Mileage	 = Stop Sign;  = Traffic Light; "T" = T Intersection; TR = Township Route; "Y" = Y intersection
0.0	9.6	Return north to Pine Road
0.6	10.2	 Turn left on Pine Road (TR 3006)
1.3	11.5	Cross Lebo Road; PA Fish Commission Huntsdale hatchery to right
0.9	12.4	 Turn Left onto PA Route 233 (Centerville Road) <i>Note: the stream immediately prior to the intersection and diagonally crossing Centerville Road is ephemeral; during periods of low flow the stream's water infiltrates into stream bed colluvium derived from South Mountain (ahead) that mantles the underlying karstic carbonates.</i>
<p>Ephemeral stream at PA 233 and Pine Road, looking downstream</p> <div>   </div> <p>during minor flood on May 12, 2008 during dry period on September 19, 2008</p> <p><i>(Photos by Noel Potter)</i></p>		
1.0	13.4	At the south border of Mt. Ashbury Camp (right) is the mapped contact and topographic rise signifying the contact of sandstones of South Mountain with carbonates of the Great Valley.
2.4	15.8	Turn left onto Ridge Road; road is gravel and dirt
2.0	17.8	Cross Cold Springs Road; continue straight
0.7	18.5	ARRIVE at Hammonds Rocks – STOP 2

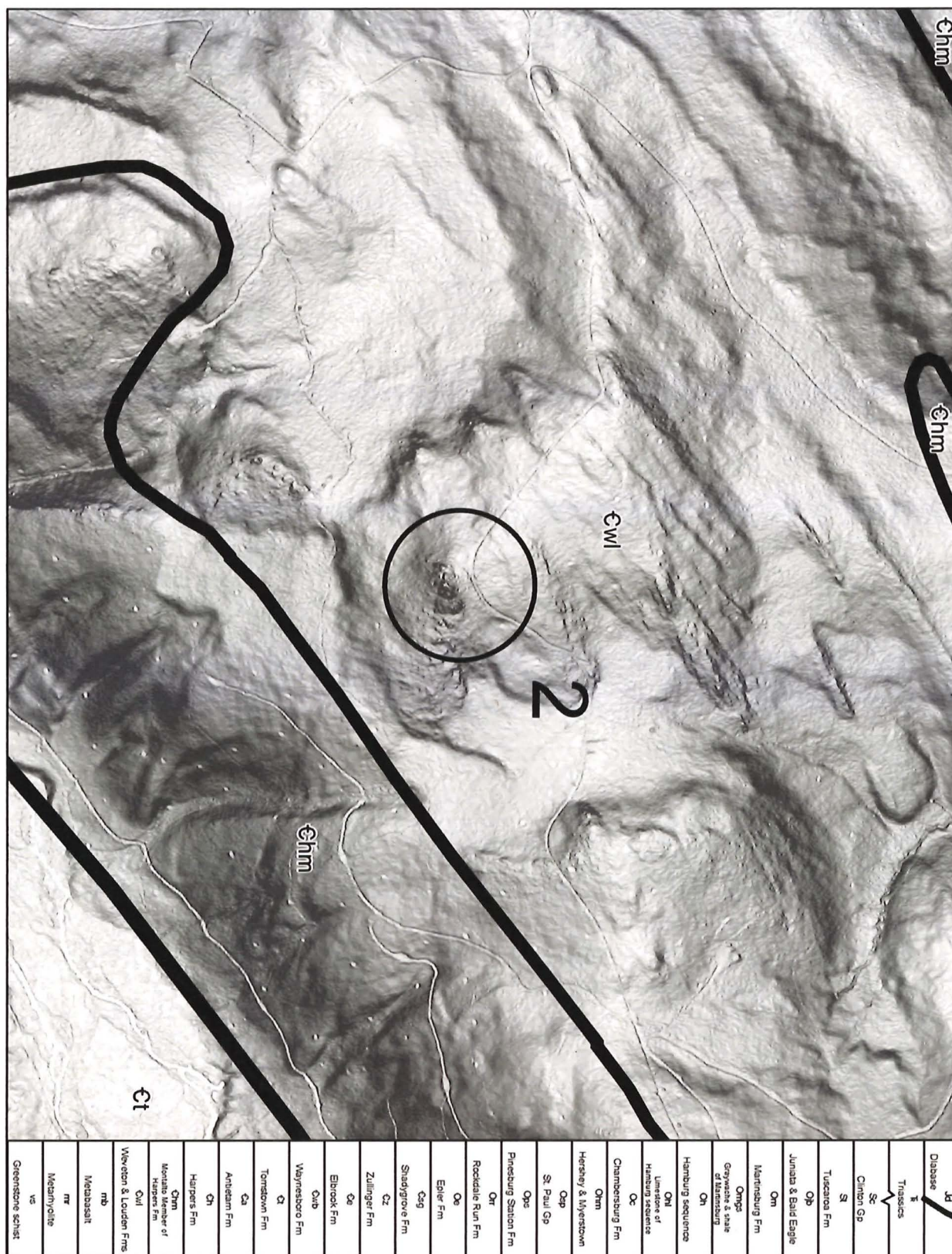


Figure 1. LiDAR image of Stop 2 – Hammonds Rocks area, with geologic contacts overlain

STOP # 2 – HAMMONDS ROCKS

Stop Leader – Noel Potter, Jr.



Entrance path to Hammonds Rocks, a Tor

HAMMONDS ROCKS, SOUTH MOUNTAIN, CUMBERLAND COUNTY, PENNSYLVANIA

*Noel Potter, Jr., Department of Earth Sciences (retired), Dickinson College,
Carlisle, PA 17013, pottern@dickinson.edu*

Introduction and Location

Hammonds Rocks (HR) (40°05'04.44" N, 77°14'56" W) is a prominent knob on the crest of South Mountain made of sandstone and conglomerate that protrudes above bouldery surfaces that gently slope away from it (Fig. 1 – LiDAR). The in-place core of HR nicely demonstrates how the pebbles in the conglomerate were deformed during the Alleghanian. Very large blocks that broke away from the core and lobate features (Fig. 1) that formed east of the rock knob attest to a periglacial climate during the Pleistocene. HR is on the crest of South Mountain (see Stop 2 entrance photo, above) on the south side of Ridge Road 0.7 mi east of Cold Spring Road. It is in the Mount Holly Springs 15' Quadrangle mapped by Freedman (1967).

Stratigraphy

HR (most detailed description is in Potter, et al., 1991) is composed of the Weverton formation, which is mostly sandstone, but some of the rocks here are conglomeratic. Typically pebbles are 2-5 cm long (Fig. 2), but at least one is 12 cm long.



Figure 2. Pebbles flattened in the plane of cleavage, which dips downward to the right (SE). View is looking NE. Divisions on scale are in decimeters.

The Weverton is the next to bottom-most formation of the Lower Cambrian Chilhowee group clastic rocks (which overlies the bottom-most Loudon formation, which in turn overlies Precambrian metavolcanics) (see Key, 1991). Source for the Weverton formation was from the West on the North American craton, as determined by Whitaker (1955), in contrast to younger Paleozoic clastic rocks north of the Cumberland Valley whose sources were from the East (Fig. 3).

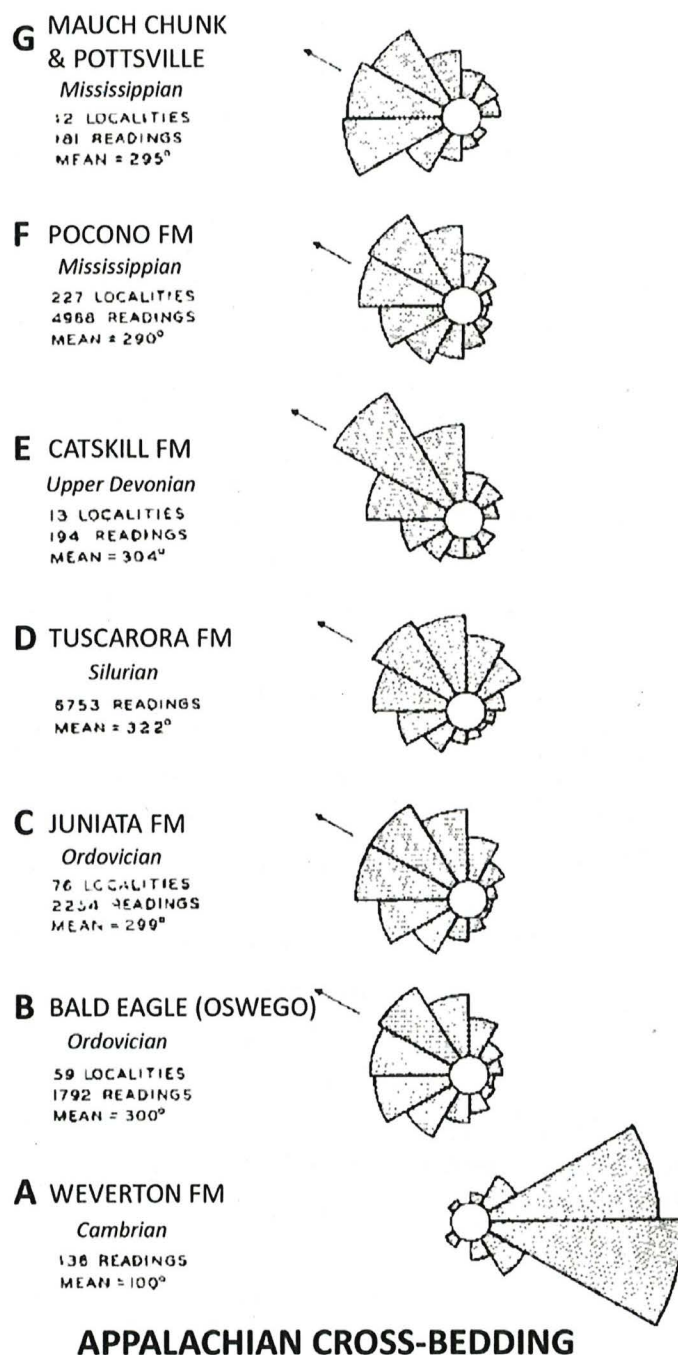


Figure 3.
Paleocurrent directions showing
how Cambrian Weverton
formation is derived from West,
whereas later Paleozoic
sediments are derived from East.
(after Pettijohn, 1962).

Structure

Discretion is needed in examining the structure. Many large (up to several m long) blocks have been tilted and moved away from the core outcrop by frost during the Pleistocene. In many places in the outcrop cleavage, which dips SE, is more prominent than bedding, so one has to be careful to find compositional differences, usually pebbly layers, to make sure one is seeing bedding. Bedding is near vertical to slightly overturned in most of the outcrop (Fig. 4, Net A), but in a few places beds dip gently

East, forming a girdle that shows a fold hinge that gently plunges $\sim N70^{\circ}E$. Cleavage consistently dips $\sim 60^{\circ}SE$ (Fig. 4, Net B). A plot of bedding/cleavage intersections (Fig. 4, Net C) shows that they trend $\sim N70^{\circ}E, 10^{\circ}NE$.

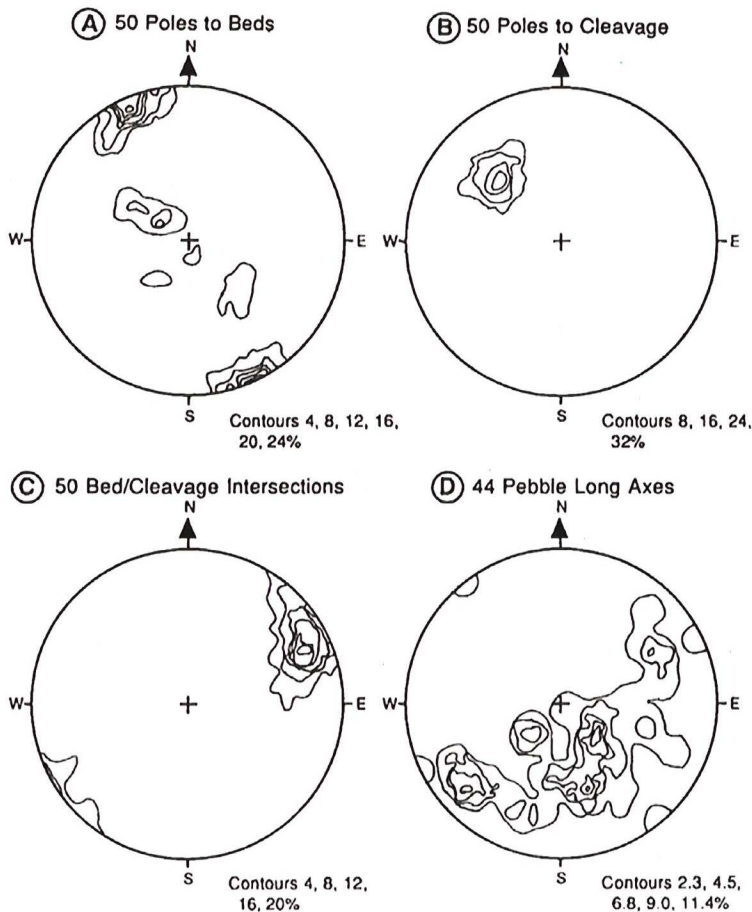


Figure 4. Equal-area nets showing orientation of: A) bedding, B) cleavage, C) bedding/cleavage intersections, and D) pebble long axes at Hammonds Rocks. (from Potter, et al., 1991, STOP 8)

weathered out of HR and measured their 3 axes and plotted their axial ratios on Flinn diagrams (Potter, et al., 1991, Fig. 64). By far, more were oblate spheroids (hamburgers) rather than prolate (hot dogs).

Deformed Pebbles

Pebbles in the conglomerate are flattened so that their shortest axes are nearly perpendicular to cleavage (Fig. 2). Long axes of these flattened pebbles form a diffuse girdle with the same orientation as cleavage (Fig. 4, Net D), showing that though the short axes of pebbles are nearly perpendicular to cleavage, long axes lie in any direction near parallel to the plane of cleavage. We collected 350+ loose pebbles that had

We applied the Rf/Phi technique (Lisle, 1985) in 5 in-situ exposures (A through E on Figure 6) to determine strain in a plane perpendicular to cleavage and fold axes—that is in a near-vertical plane trending about N20°W. At the five sites the strain ration varied between 1.9 and 2.5 (mean 2.1) (Potter, et al., 1991).

At another outcrop of the Weverton conglomerate at Whiskey Spring, 9 mi E of Hammonds Rocks we discovered striae on many of the pebbles (Potter, et al., 1995), and since then we have found them here at HR.. Surfaces on the pebbles that are parallel to cleavage often have very fine striae on them. These striae are always parallel

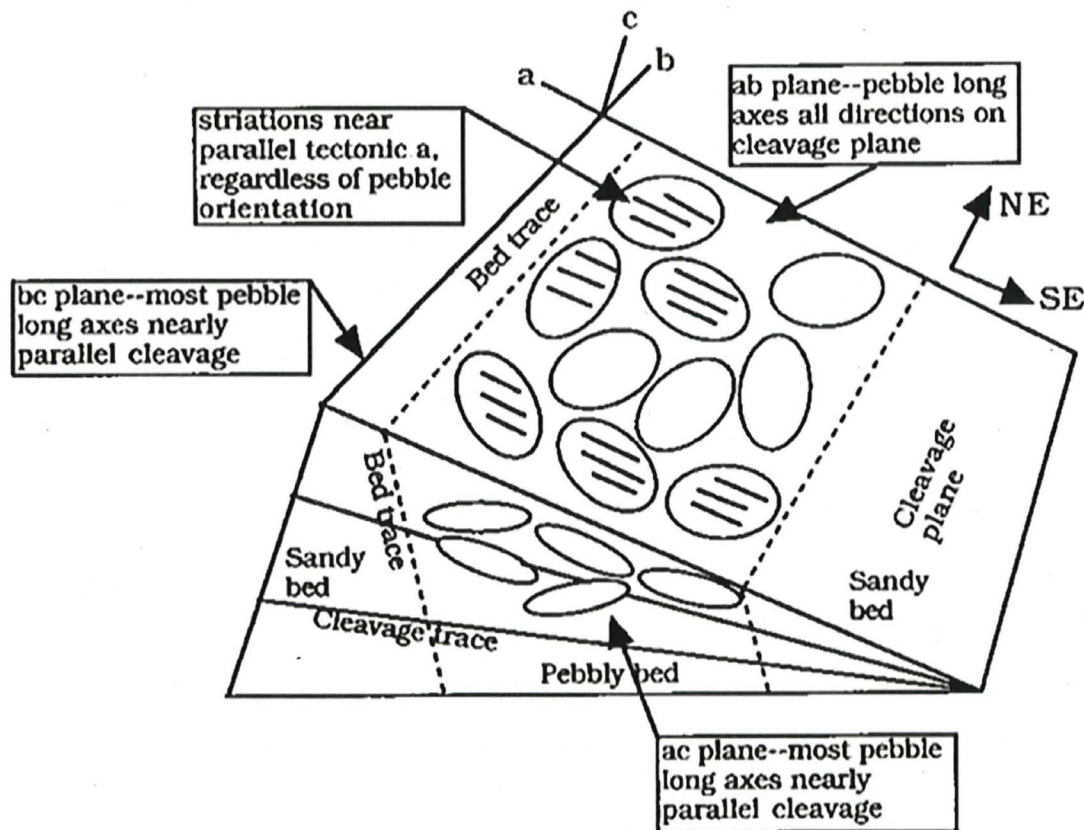


Figure 5. Relation of flattened pebbles and striae to bedding and cleavage at Hammonds Rocks. (Diagram from Potter, et al., 1995)

to tectonic a, the direction of tectonic transport, and perpendicular to bedding-cleavage intersections, despite random orientation of long axes of pebbles in or nearly parallel the plane of cleavage (Fig. 5). A hand lens and a strong flashlight (or mirror using the sun) to give low oblique illumination are best for seeing the striae. It is inferred that shear parallel to cleavage removed the "tops and bottoms" of the pebbles by pressure solution. Thin sections show fine quartz as "tails" to the pebbles.

We attempted to determine paleocurrent direction using cross-beds here, but in nearly all cases when we measured inferred topset and foreset beds and plotted them on a stereonet, the angle between the two was much greater than the angle of repose for sand—presumably the angle between the two has been changed during deformation.

At the Outcrop

A map and series of cross-sections of HR prepared in 1991 are reproduced as Figs. 6 and 7. The map of HR (Fig. 6) has a number of stations labeled with Roman numerals. A series of cross sections (Fig. 7) along lines labeled with Arabic numbers are also reproduced here. Highlights of some Roman Numeral stations from the map are:

- I) a prominent channel with lag gravel in it. This is one of the few places where beds are horizontal in the outcrops here. It is an interesting place to ask where one would go to find a similar environment of deposition today. Remember that there was no land vegetation in the Cambrian.
- II) good cross beds at the E end of the outcrop.
- III) a good view of pebbles flattened in cleavage.
- IV) If you crawl under the large (several m long and high) block here, you can find three irregularly spaced quartz veins in the block above and the rock below to see that the large block has moved about 1 m downslope. Note on cross-sections several large blocks with cleavage dipping the wrong way (N rather than SE).

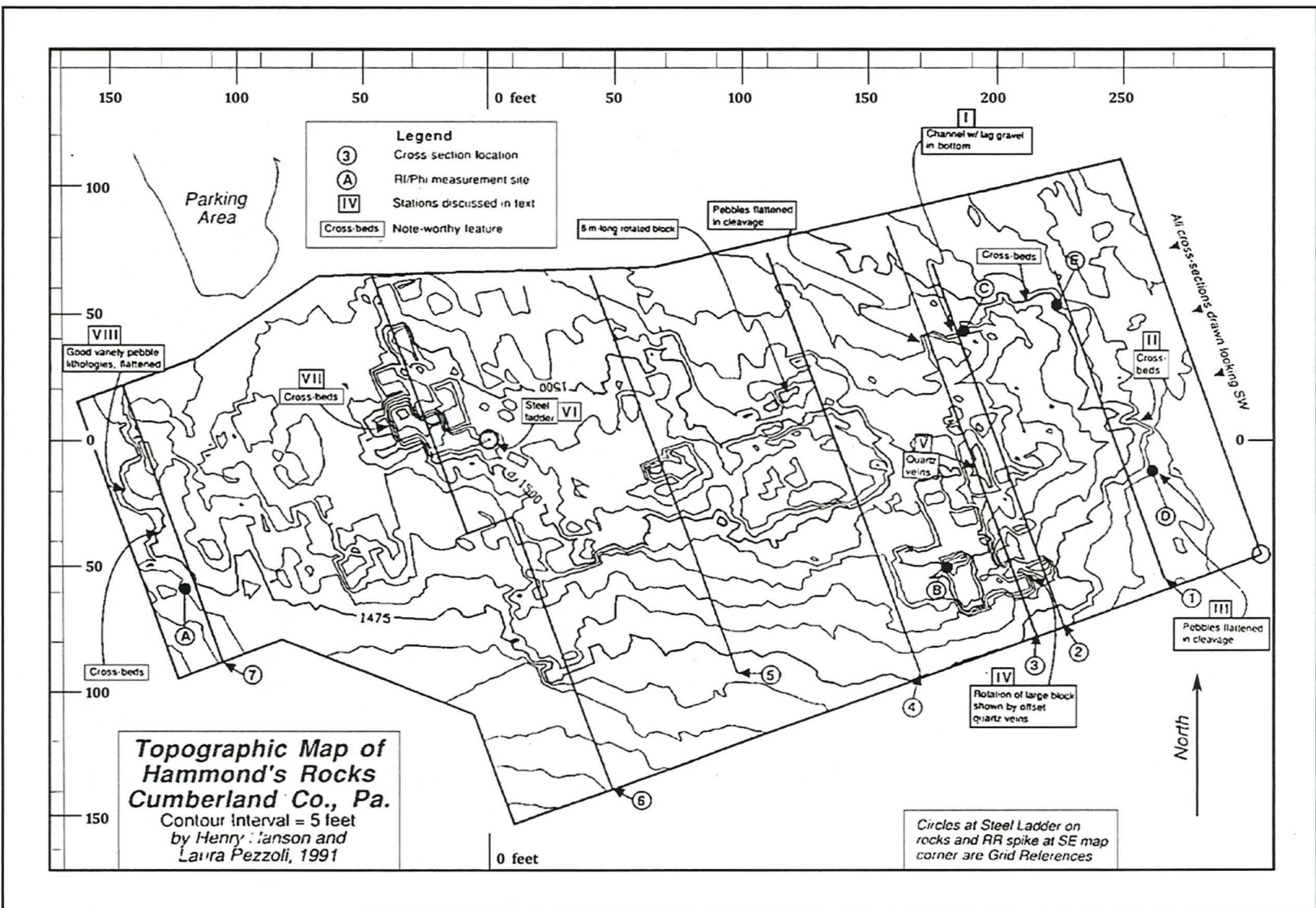


Figure 6. Topographic map of Hammonds Rocks showing locations of cross sections (Fig. 7) and features described in text. From Potter, et al., 1991, STOP 8.

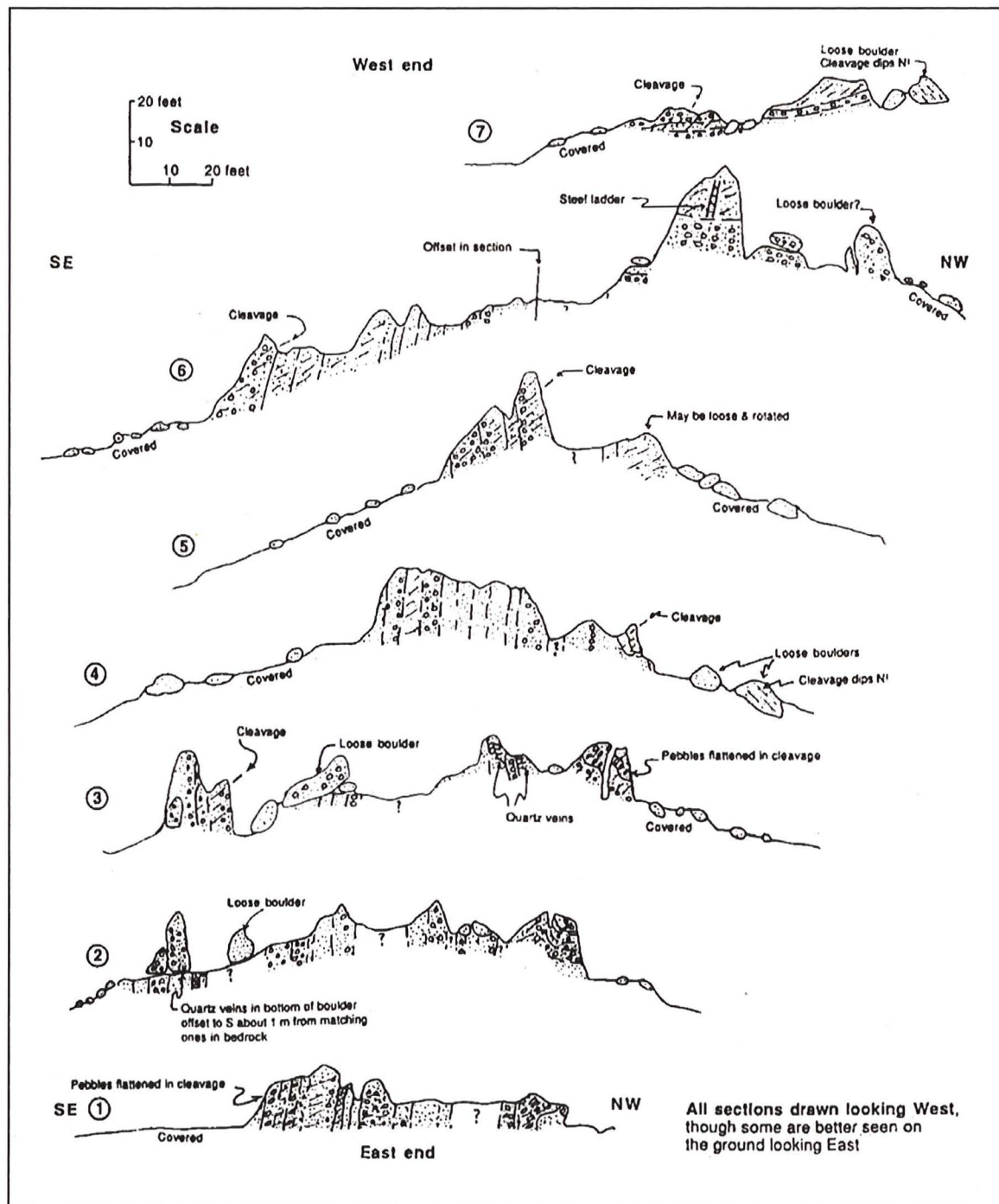


Figure 7. Cross sections of Hammonds Rocks. All sections are drawn looking WEST for ease of comparison, despite the fact that some are better seen at the outcrop looking in the opposite direction. Locations of sections are on Figure 6. From Potter, et al., 1991, STOP 8.

Periglacial Features

HR has been interpreted by Clark (1991) as a tor, a prominent erosional remnant that sticks up above an otherwise gently-sloping surface that is inferred to have formed in a periglacial climate during the colder parts of the Pleistocene. Other similar knobs occur to the south and north of HR (Fig. 1). A modern tor in Alaska is shown in Figure 8. We know that during the late Wisconsinan, from at least 16,000 to 14,000 years BP, there was tundra here (Delano, et al., 2002; see Stop 1—Kings Gap Pond this volume).



Figure 8. A modern tor in Alaska. Note gently sloping surface covered with boulders at base of bedrock knob.

We have already remarked on the large tilted blocks next to the core of HR. Since cleavage consistently dips SE in true bedrock, any blocks with cleavage dipping in other directions are “out of place.” It is clear that none of the large blocks are moving today, so we interpret the movement of the large blocks as the result of periglacial conditions during the Pleistocene.

To the East of HR are two prominent lobes (Fig. 9) that have moved downslope to the East. The large blocks in these lobes have cleavage dipping in random directions, clearly showing that they are not in place. We interpret these lobes to have formed by gelifluction during the cold phases of the Pleistocene.

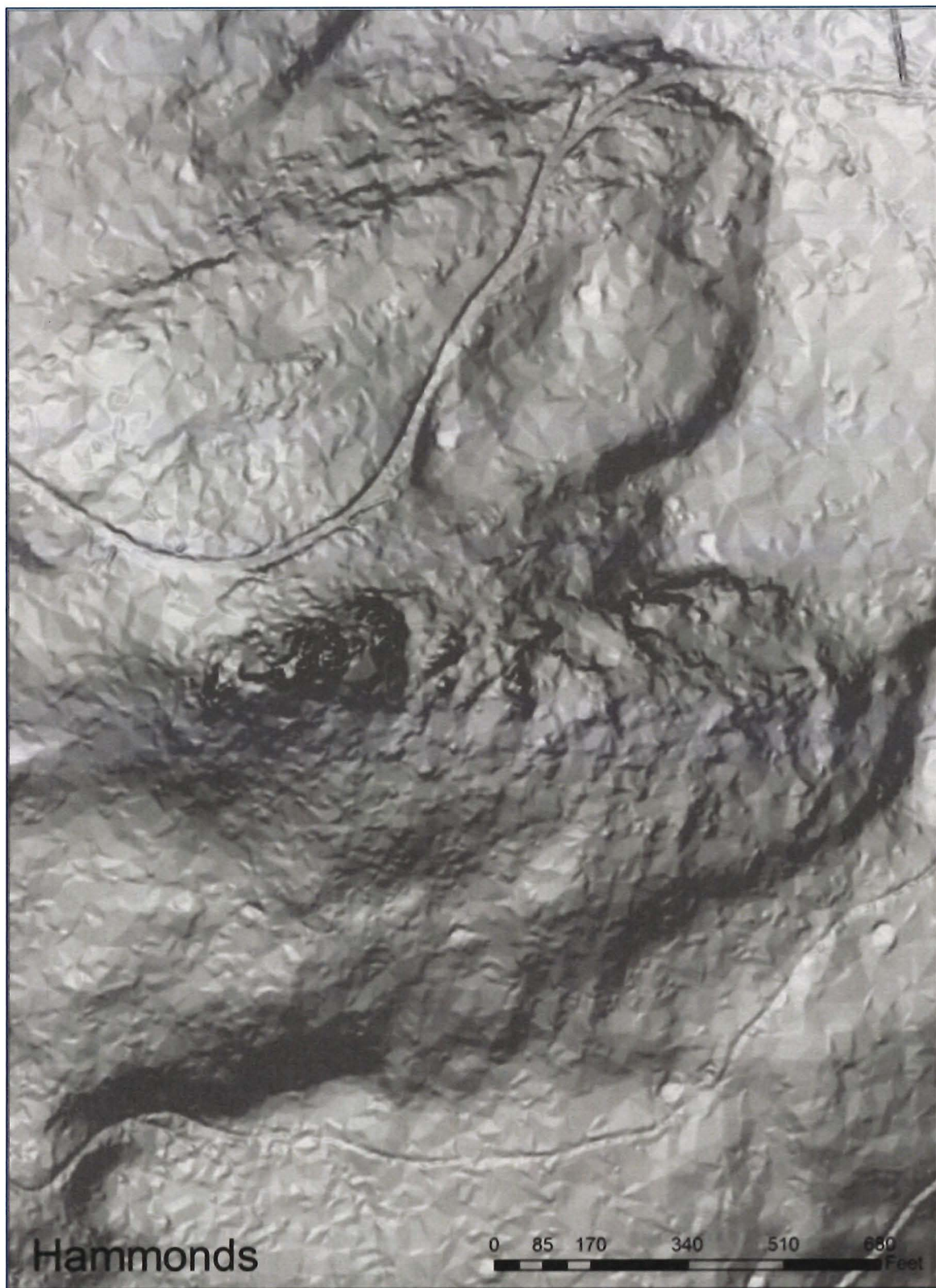
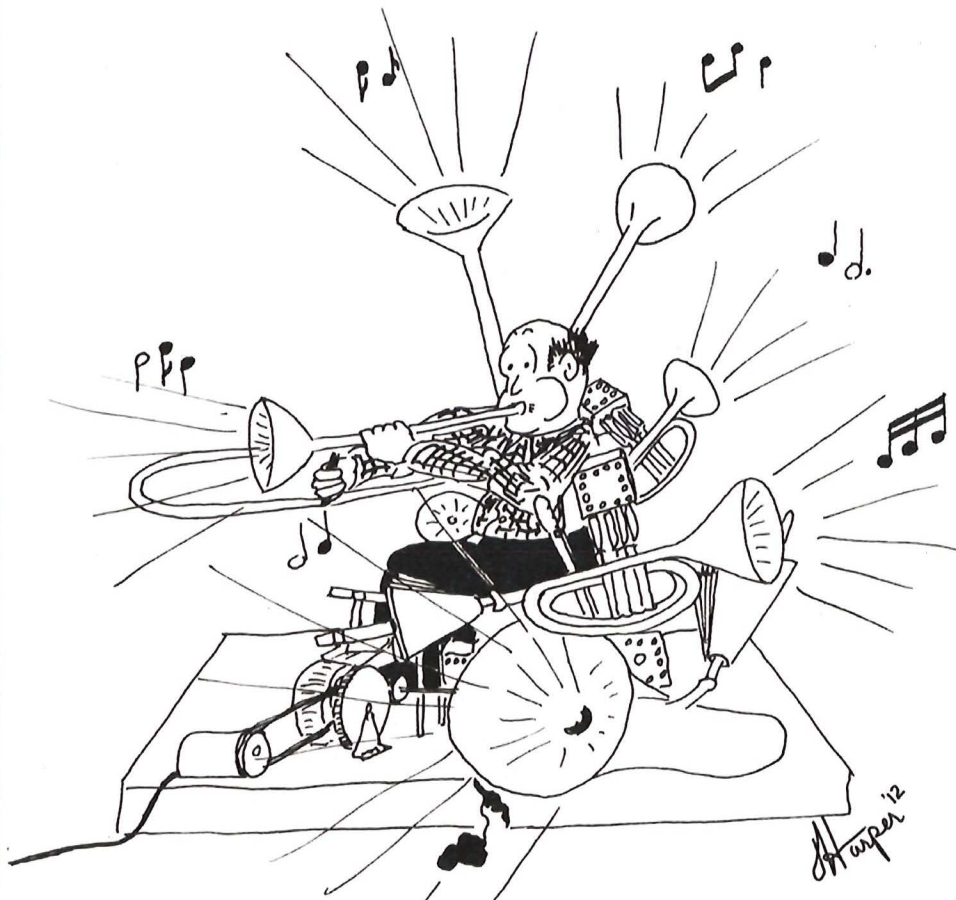


Figure 9. Enlarged LiDAR image of Hammonds Rocks (left center) and large lobes to the East.









References

- Clark, G. M., 1991, South Mountain Geomorphology: *in* Sevon, W. D. and Potter, N., Jr., eds., *Geology in the South Mountain area, Pennsylvania: Guidebook for the 56th Annual Field Conference of Pennsylvania Geologists*, p. 55-94.
- Delano, H. L., Miller, N. G., Potter, N., Jr., 2002, Plant fossil evidence for late Pleistocene tundra conditions in south-central Pennsylvania: Geological Society of America, Northeastern Section, 37th Annual Meeting, Abstracts with Programs, v. 34, no. 1, p. 27.
- Freedman, J., 1967, Geology of a Portion of the Mount Holly Springs Quadrangle, Adams and Cumberland Counties, Pennsylvania: Pennsylvania Geological Survey, 4th Series, Progress Report PR 169, 66 p.
- Key, M. M., Jr., 1991, The Lower Cambrian Clastics of South Mountain, Pennsylvania: *in* Sevon, W. D. and Potter, N., Jr., eds., *Geology in the South Mountain area, Pennsylvania: Guidebook for the 56th Annual Field Conference of Pennsylvania Geologists*, p. 21-28.
- Lisle, R. J., 1985, Geological strain analysis, a manual for the Rf/Phi technique: New York, Pergamon Press, 11 p.
- Pettijohn, F. J., 1962, Paleocurrents and paleogeography: *Bulletin American Association of Petroleum Geologists*, v. 46, no. 8, p. 1468-1493.
- Potter, N., Jr., et al, 1991, Stop 8, Hammonds Rocks: *in* Sevon, W. D. and Potter, N., Jr., eds., *Geology in the South Mountain area, Pennsylvania: Guidebook for the 56th Annual Field Conference of Pennsylvania Geologists*, p. 194-213.
- Potter, N., Jr., et al, 1995, Mechanism of strain as indicated by deformed pebbles and sand grains, Whisky Spring, South Mountain, Cumberland Co., Pennsylvania: Dickinson College, Studies in Geology, No. 5 (Structural Geology class project), 19 p. plus tables.
- Whitaker, J. C., 1955, Direction of current flow in some Lower Cambrian clastics in Maryland: *Geological Society of America Bulletin*, v. 66, no. 6, p. 763-766.

HARPER'S GEOLOGICAL DICTIONARY



HORNBLLENDE - A one-man brass band.

Mileage Interval	Cumulative Mileage	 = Stop Sign;  = Traffic Light; "T" = T Intersection; TR = Township Route; "Y" = Y intersection
0.0	18.5	Return on Ridge Road
2.7	21.2	 Turn right on PA 233, Centerville Road
3.4	24.6	 Turn left onto Pine Road
3.7	28.3	"T"; turn left on Mountain View Road; see photo. Note: use caution at this turn. Traffic arriving from right from the railroad underpass may suddenly appear. 
0.8	29.1	After sharp right turn (note farm buildings to left), quartzite cobbles mantle the local hill. These cobbles derive from South Mountain, seen to our left. How did they cross the large depression to get to this hill?
1.1	30.2	 Turn left on paved road (Furnace Hollow Road)
0.5	30.7	Continue past Foreman Hill Road
0.25	30.95	Steep side linear pit (sometimes water filled) to the left in forest was likely prospected as a bog iron ore source for nearby iron furnace. X-ray analysis of samples from this site show the material to be the mineral Goethite (personal communication, John Barnes, PA Geological Survey)
0.75	31.7	"Y" - Keep left on the unpaved road (still Furnace Hollow Road); do not follow paved road that curves 180 degrees to the right. Note: abandoned Big Pond Iron Furnace is immediately on left. Built in 1836, In 22 weeks in 1857 it produced 46.5 tons of iron from mines about 1 mile west (Lesley, 1859, p.??)
<div>  <div> <p>See "Pine Grove Furnace – A Brief Introduction & History" for reference on iron-making from colonial times through the 1800's</p> <p>Big Pond Iron Furnace at mile 31.7</p>  </div> </div>		
0.05	31.75	Cross small stream with graffiti on cement bridge
0.05	31.8	"Y" - Turn right on gravel road (Hudleber Lane)
0.6	32.4	Turn left onto paved Sand Bank Road
0.2	32.6	ARRIVE at plant entrance to Valley Quarries Mt. Cydonia III-STOP3

92

STOP #3. VALLEY QUARRIES, INC., MT. CYDONIA III QUARRY

(Entrance requires signed liability waiver)

Stop Leader: Marcus M. Key, Jr., Dickinson College



Entrance to Valley Quarries, Inc. Mt. Cydonia III Quarry

3.1 Processing Plant, Latitude = N40°03.238', Longitude = W77°24.926'

The quarry is located in the southwest corner of Cumberland County and is owned and operated by Valley Quarries. A small sand and clay mining interest existed at this location adjacent the Michaux State Forest for many years prior to its acquisition by Valley Quarries in 1999. Following this acquisition, the processing scheme was upgraded and a bench quarrying plan was implemented to allow for the blending of various areas of the deposit. The upper level of the pit is developed primarily in the Harpers Quartzite and the lower lifts transition into the Antietam. The quartzite throughout has been highly weathered to significant depths and as a result, large amounts of clay and silt must be processed out of the shot and quarried material in order to meet specifications. Since significant quantities of water are needed to scrub and wash the sand products, a fairly sophisticated treatment plant and fines recovery system has been employed to recycle all process water and allow for more efficient handling of the clay and silt by-products.

Valley Quarries sells stone, aggregate, blacktop, and ready-mix concrete in the Mid-Atlantic region. Mt. Cydonia Sand Plant III is their most recent commercial quarry in the Valley Quarries' family, and it produces four main aggregate products. 1) Washed concrete sand, also known as PennDOT Type A sand, which meets ASTM standard C33.

2) Washed masonry sand, which is a fine grade of sand also used as a bedding material in free stall dairy operations. 3) DEP sand that is certified for use in septic sand mounds. 4) A special "Ballfield Mix" of sand and clay with a rich red color. It is used in the infields of baseball and softball diamonds and also in the construction of horse racing tracks. This special mix is sold as far away as Staten Island, NY. As the main contributor to the price of aggregate is shipping costs, this product has a high value per unit weight than the more ubiquitous concrete and masonry sands which are only sold more locally.

3.2 Upper bench, Latitude = N40°03.016', Longitude = W77°24.688'

The upper bench is located on the south side of the Cumberland Valley on the northwest flank of the Blue Ridge Anticlinorium in the South Mountain Section of the Ridge and Valley Physiographic Province. The quarry is on the boundary between the Antietam and Harpers Formation (*Fig. 1-LiDAR*), the youngest formations of the Chilhowee Group. The Antietam is conformably overlain by the dolostones of the Tomstown Formation and the Harpers is conformably underlain by the meta-conglomerates of the Weverton Formation (Stose, 1909; Freedman, 1967; Fauth, 1968; Root, 1968; Key, 1991; Smoot and Southworth, 2014).

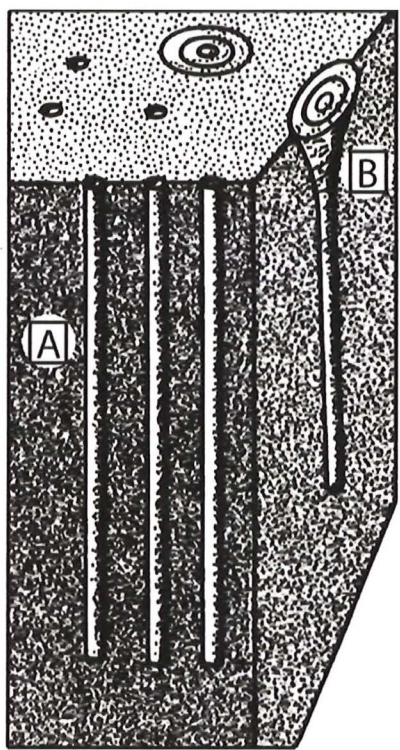


Figure 2. Schematic representation of (A) *Skolithos* and (B) *Monocraterion* trace fossils in plan and cross section view. Modified from Frey and Pemberton (1984, fig. 10).

The age of the Antietam and Harpers is constrained by a variety of paleontologic, radiometric, and stratigraphic evidence as 516.5-539 Ma in the Lower Cambrian (Smoot and Southworth, 2014). Following the Ediacaran to earliest Cambrian breakup of the supercontinent Rodinia and the opening of the Iapetus Ocean, they were deposited on the prograding shelf of the eastern-facing, passive, continental margin of Laurentia (Tull et al., 2010; Smoot and Southworth, 2014). Paleocurrent data indicate the primary terrestrial source was to the exposed Laurentian craton to the northwest (Dickinson et al., 1983; Tull et al., 2010). The Antietam Formation is a medium-to coarse-grained, white to grayish quartzite with *Skolithos* trace fossils present, whereas the Upper Harpers Member is a green to greenish-gray, quartzose phyllite, distinct from the underlying *Skolithos*-rich Montalto Quartzite Member (Fauth, 1968). *Skolithos* is a pipe-like cylindrical trace fossil (*Figure 2A*) (Key, 2014).

The eight numbered stops on this bench begin with 3.2.1 – 3.2.2 on the west side, 3.2.3 – 3.2.5 on the north side, and 3.2.6 – 3.2.8 on the south side (Figure 3). You are welcome to collect hand samples. Feel free to examine the outcrop behind the berm; just make sure you have your hard hat on in case any loose pieces fall off the highwall. I will also pass around six vials containing *Skolithos linearis* tubes that have weathered out of their surrounding matrix. You are welcome to take one of these tubes as well.

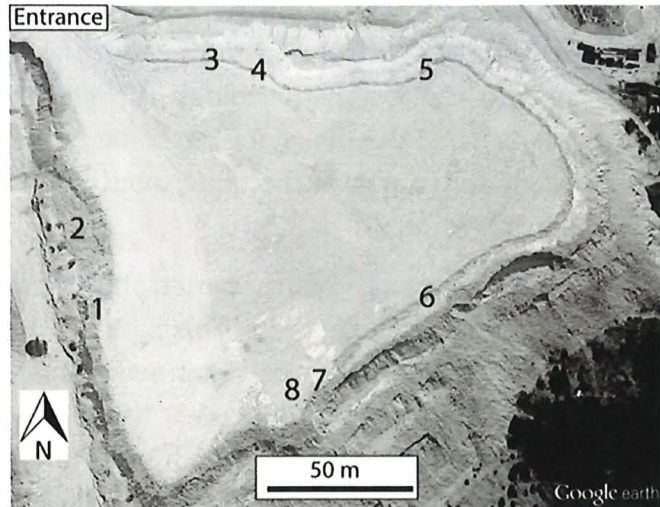


Figure 3. Google Earth image of Mt. Cydonia Sand Plant III's upper bench showing the 3.2.X stop numbers referenced in the text.

On a clear day, there is a good view across Cumberland Valley to Blue Mountain, 14 mi to the north through the entrance to this bench between stops 3.2.2 and 3.2.3. The finer-grained interbeds make it easy to see the bedding, especially at Stop 3.2.3. The *Skolithos* tubes are roughly perpendicular to bedding which also helps. Standing back from the highwall and looking around the bench, one can see that the beds strike parallel to the mountain and dip southeast toward the mountain indicating we're on the northwest limb of an overturned anticline. This is typical on the northwestern limb of the Blue Ridge anticlinorium, locally known as South Mountain, where the beds often dip to the southeast (Cloos, 1971).

The bedding exposed in this upper bench of the quarry strikes $\sim N51^{\circ}E$. But which way is stratigraphic up? Due to intense bioturbation by *Skolithos* and the overprinting of the Alleghanian subgreenschist metamorphism (Tull et al., 2010), it is hard to tell which way is up. The best evidence I found is concave up bedding at Stop 3.2.6 indicating stratigraphic up is to the northwest into the valley. That implies these beds are overturned, with a dip of $\sim 61^{\circ}SE$. This makes sense as the more easily eroded dolostones of the overlying Tomstown Formation are to the northwest in the valley and the underlying more resistant quartzites and phyllites of the Harpers Formation are to the southeast in the ridge crest.

This southeast dip is in contrast to the online state geologic map (Figure 1) which is based on Berg's (1978) compilation which is based on Freedman's (1967) map to the northeast and Fauth's (1968) map to the southwest, both of which show the Antietam dipping to the northwest. The faults in Figure 1 are from Becher and Root (1981), and

if the location and throw of the faults are correct, but the dip backwards, then the Antietam should be displaced to the south as indicated in the quarry, not the north. I also question the mapped geology in Figure 1 due to the disconnect between the outcrop pattern of the overlying carbonates (esp. the Waynesboro Fm.) which shows a fold immediately north of the quarry but which is absent in the underlying Chilhowee siliciclastics.

I think the upper bench penetrates through the Antietam Formation into the underlying Harpers Formation. This is supported lithologically by the mapping of Fauth (1968) who reported a finer-grained upper member of the Harpers Formation immediately below the Antietam. He termed it the Upper Harpers Member and described it as a green to greenish-gray, fine-grained quartzose graywacke, distinct from the overlying *Skolithos*-rich Antietam and the underlying *Skolithos*-rich Harper's Montalto Quartzite Member (Fauth, 1968). I picked this lithologic break in the upper bench of the quarry by the presence-absence of *Skolithos*. Walking up section (i.e., to the north toward the valley) along the western highwall of this bench, you do not start to see *Skolithos* until Stop 3.2.1. Walking down section (i.e., to the south toward the mountain) along the opposite eastern highwall, you do not see *Skolithos* after Stop 3.2.5. Stops 3.2.1 and 3.2.5 are roughly along strike, and I interpret this as the contact between the younger, *Skolithos*-rich, cleaner, better sorted, whiter, metasandstone of the Antietam to the north and the older, *Skolithos*-poor, muddier, more poorly sorted, darker (brownier/redder), metasandstone Harpers to the south.

For those of you with more paleontologic interests, at Stop 3.2.2 I have pulled out several samples of *Skolithos* tubes in the matrix and placed them on the berm in front of the highwall. Bedding planes are not well exposed on this bench; the best ones are at Stop 3.2.3. Do you see the *Skolithos* bottom end of the tubes (2-5 mm diameter) or the *Monocraterion* top end of the tubes (>5 mm diameter)? *Monocraterion* is a trumpet-like trace fossil (Figure 2B) (Key, 2014). The longest tube I found (i.e., 42 cm) was at Stop 3.2.4. Can you find one longer? At Stop 3.2.4 you will find the Antietam quite weathered so the tubes become free from their matrix.

For those of you with more structural geology interests, I recommend you visit Stops 3.2.7 and 3.2.8. In contrast to the bedding, the jointing (which is best seen at Stop 3.2.7) runs roughly north-south and is basically vertical (strike: ~N155°E; dip: ~84°E). At stop 3.2.8 look at a different joint surface and see the undulating minor folds whose hinges are oriented ~N44°E and plunging ~9°NE. They parallel the general strike of the beds and the regional fold axis. Look for the quartz-filled extension veins with tapered ends that are exposed on the same surface.










The deformation of these beds is reflected by the normally circular transverse cross-sectional shape of the *Skolithos* burrows being distorted into an ellipse (Key,

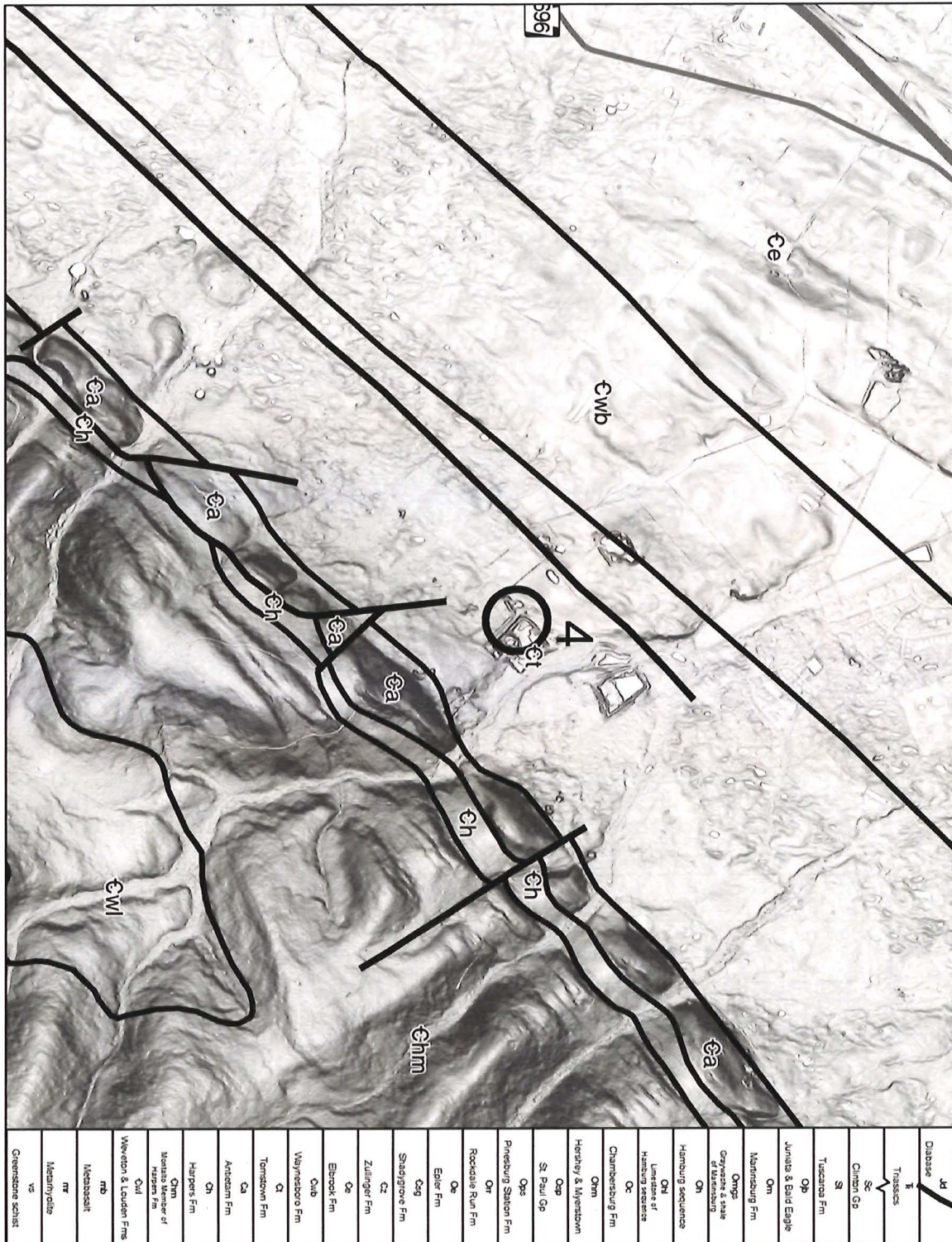
2014). I measured the long (L) and short (W) axes of 13 *Skolithos* tubes and calculated the L/W (i.e., Rf strain) ratio as 1.9. This is less than the 2.2-2.8 values that Potter et al. (1991) measured on pebbles in the Weverton Formation at Hammonds Rocks, but more than the 1.6 that Key and Sims (1991) calculated in the Antietam Formation exposed in the Mt. Holly Pennsy Supply quarry. Gourley and Key (1996) measured the same ratio in the underlying Montalto Member of the Harpers Formation at Pole Steeple and reported a ratio of 1.5. See if you can find any deformed *Skolithos* tubes, especially at Stop 3.2.4.

References

- Becher, A. E., and S. I. Root. 1981. Groundwater and Geology of the Cumberland Valley, Cumberland County, Pennsylvania. Pennsylvania Geological Survey, 4th ser., Water Resource Report 50, 95 p.
- Berg, T. M. 1978. Geologic map of the Walnut Bottom, PA Quadrangle. Pp. 597. In: T. M. Berg, and C. M. Dodge (eds.): Pennsylvania Geological Survey, 4th ser., Map 61, 1981.
- Cloos, E. 1971. Microtectonics along the western edge of the Blue Ridge, Maryland and Virginia. Johns Hopkins Press, Baltimore, 234 p.
- Dickinson, W. R., Beard, L. S., Brakenridge, G. R., Erjavec, J. J., Ferguson, R. C., Inman, K. F., Knepp, R. A., Lindberg, F. A., and Ryberg, P. T. 1983. Provenance of North American Phanerozoic sandstones in relation to tectonic setting. Geological Society of America Bulletin, 94 (2): 222-235.
- Fauth, J. L. 1968. Geology of the Caledonia Park Quadrangle Area, South Mountain, Pennsylvania: Pennsylvania Geological Survey, 4th ser., Atlas 129a, 133 p.
- Freedman, J. 1967. Geology of a portion of the Mount Holly Springs Quadrangle, Adams and Cumberland Counties, Pennsylvania. Pennsylvania Geological Survey, 4th ser., Progress Report 169, 66 p.
- Freedman, J. 1968. Bender's Quarry- Mt. Holly Springs, Pennsylvania: in The Geology of Mineral Deposits in South Central Pennsylvania: Guidebook, 33rd Annual Field conference of Pennsylvania Geologists, p. 28-37.
- Frey, R. W. and Pemberton, S. G. 1984. Trace fossils facies models. In: R.G. Walker (ed.), Facies Models. Geoscience Canada Reprints Series, pp. 189-207
- Gourley, J. R., and M. M. Key, Jr. 1996. Analysis of the *Skolithos* ichnofacies from the Cambrian Montalto Quartzite Member of the Harpers Formation in south central Pennsylvania. Pp. 152. In: J. E. Repetski (ed.). North American Paleontological Convention Abstracts of Papers. Paleontological Society, Special Publication, No. 8.

- Key, M. M., Jr. 1991. The Lower Cambrian Clastics of South Mountain, Pennsylvania. Pp. 21-27. In: W. D. Sevon and N. Potter, Jr. (eds.). Guidebook for the 56th Annual Field Conference of Pennsylvania Geologists. Field Conference of Pennsylvania Geologists. Harrisburg, PA.
- Key, M. M., Jr. 2014. *Skolithos* in the Lower Cambrian Antietam Formation at South Mountain, Pennsylvania. Pp. ??-??. In: D. Hoskins and N. Potter, Jr. (eds.). Guidebook for the 79th Annual Field Conference of Pennsylvania Geologists. Field Conference of Pennsylvania Geologists. Harrisburg, PA.
- Key, M. M., Jr. and S. J. Sims. 1991. Geology of the Pennsy Supply Quarry, Mt. Holly, Pennsylvania. Pp. 220-225. In: W. D. Sevon and N. Potter, Jr. (eds.). Guidebook for the 56th Annual Field Conference of Pennsylvania Geologists. Field Conference of Pennsylvania Geologists. Harrisburg, PA.
- Potter, N., Jr., H. Hansen, R. Ackermann, G. Dockter, S. Lev, L. Pezzoli, and T. Troy. 1991. Stop 8. Hammonds Rocks. Pp. 194-213. In: W. D. Sevon and N. Potter, Jr. (eds.). Guidebook for the 56th Annual Field Conference of Pennsylvania Geologists. Field Conference of Pennsylvania Geologists. Harrisburg, PA.
- Root, S. I. 1968. Geology and mineral resources of Southeastern Franklin County, Pennsylvania Geological Survey, 4th Ser., Atlas 119cd, 118 p.
- Smoot, J.P., and Southworth, S. 2014. Volcanic rift margin model for the rift-to-drift setting of the late Neoproterozoic-early Cambrian eastern margin of Laurentia: Chilhowee Group of the Appalachian Blue Ridge: Geological Society of America Bulletin, 126: 201-218.
- Stose, G. W. 1909. Description of the Mercersburg-Chambersburg district, Pennsylvania, U. S. Geol. Survey Atlas, Folio 170, 19 p.
- Tull, J. F., Allison, D. T., Whiting, S. E., and John, N. L. 2010. Southern Appalachian Laurentian margin initial drift-facies sequences: Implications for margin evolution, in Tollo, R. P., Bartholomew, M. J., Hibbard, J. P. , and Karabinos, P. M., eds., From Rodinia to Pangea: The Lithotectonic Record of the Appalachian Region: Geological Society of America Memoir 206, p. 935-956.

Mileage Interval	Cumulative Mileage	 = Stop Sign;  = Traffic Light; "T" = T Intersection; TR = Township Route; "Y" = Y intersection
0.0	32.6	Drive southwest (left on exiting quarry) on Sand Bank Road
0.8	33.4	 "T" Turn left onto Strohm Road; Note: in opposite cut bank gravel mantles deeply buried carbonates
0.1	33.5	At the "Y" Take first right onto South Mt. Estates Road (TR 317). Numerous karst depressions are visible with the next couple of miles.
1.5	35.0	Continue on S. Mountain Estates Road to  at High Road, (TR 317) name changes to Airport Road.
1.4	36.4	Continue on Airport Road, passing Southampton Township offices at Neil Road, to 2 nd entrance to Southampton Township Park (Beistle Park)
0.1	36.5	Turn right, continue to parking area near large pavilion DAY 1 LUNCH STOP, BEISTLE PARK, SOUTHAMPTON TOWNSHIP <div> <div> Exhibition of Pond Bank Core with Cretaceous Lignite (refer to p.23) optional visit to local caves </div>  </div>
0.1	36.6	Return to Airport Road, turn left
1.1	37.7	Retrace route on Airport Road to "Y" intersection; turn right onto Witmer Road
0.2	37.9	 Turn right onto Gilbert Road
1.1	39.0	 At the 3-way intersection of Cleversburg, Gilbert and Walnut Dale Roads turn right onto Cleversburg Road; Cleversburg Road turns sharp left and then sharp right in Cleversburg village.
1.0	40.0	 Cross Baltimore Road, bearing left and then crossing to continue on McCulloch Road
1.8	41.8	Cross Means Hollow Road; enter Franklin County. As you approach Mainsville the road name changes to Mainsville Road
0.6	42.4	 Turn left on Lindsay Lot Road in Mainsville village
0.8	43.2	Turn right and then immediate left onto un-named road at Quarry sign.
0.6	43.8	ARRIVE at Mainsville II quarry entrance – STOP 4



LIDAR image of Stop 4 – Valley Quarries, Inc. Mainsville II area, with geologic contacts overlain

STOP #4. VALLEY QUARRIES, INC., MAINSVILLE II

(Entrance requires signed liability waiver)

Stop Leader Frank Pazzaglia, Lehigh University



View of Mainsville II Quarry from entrance

Late Cenozoic sedimentology, stratigraphy, and pedogenesis of the Furnace Creek fan

The stop at Valley Quarries, Mainsville (39°59'35.6" N, 77°30'32.1"W) is designed to provide a venue to discuss the geomorphology, stratigraphy, and landscape evolution of South Mountain and the Cumberland Valley. The pits exposed here at Mainsville have long been visited and discussed given the excellent exposures and gracious access by the Valley Quarries principals. Extraction at this site first opened in 1989. The sand and gravel deposits found in portions of the site have been mined extensively since that time with the run of pit material shipped off-site and processed at one of the company's sand plants near Fayetteville, PA. Originally, the finished products included sand and crushed aggregates of various sizes and grades used mainly in construction trades, highway building, landscaping, ready mixed concrete, and precast concrete products. More recently, due to changes within the marketplace and shifting of sand production to different locations, the use of the remaining sand and gravel reserves at this site has been curtailed. Mining activity here is now limited to the removal of a smaller amounts of special clay for use in the manufacture of a ball diamond infield mix. Reclamation of

certain pit areas is also ongoing, as well as a portion of the site being used as a testing and proving ground for Volvo Construction Machinery.

Notable previous research at the site includes general geomorphology and stratigraphic descriptions (Sevon, 1991; Potter and Sevon, 2011; Sevon, 2013), detailed mapping, sedimentologic, and pedologic descriptions (Grote, 2006; Grote and Kite, 2006), and analysis of clastic dikes and karst-collapse features (Sevon, 1994). In general, these studies are part of a broader effort by geomorphologists in the mid-Atlantic region that has investigated similar geomorphology and late Cenozoic stratigraphy on the western flank of the Blue Ridge (Wittecar, 1985; Wittecar and Duffy, 2000; Eaton et al., 2003). Long recognized as a source of iron and manganese ore (Hack, 1965), limited, but intriguing geochronology establishes a framework for the great antiquity of some of these deposits and residuum in the modern landscape (Pierce, 1965; Bikerman et al., 1999).

The goal of the present study builds upon the above scholarship with the expressed goal of trying to understand the genesis of these deposits in the context of environmental change and long-term landscape evolution of the mid-Atlantic region. Specifically, the Valley Quarries exposures provide a window into several, deeply-weathered paleosols that speak to an unsteadiness in deposition, landscape stability, and pedogenesis. We are interested in better understanding the temporal and genetic context of that unsteadiness and how it influences our thinking of the late Cenozoic, mostly erosion history of the Appalachians.

Geomorphology of the western flank of South Mountain

The piedmont that forms the western flank of South Mountain has long been recognized to be a zone of deep weathering of the carbonate bedrock underlying the Cumberland Valley juxtaposed against the relatively resistant Antietam Fm ridge that underlies the western flank of South Mountain (Pierce, 1965; Becher and Root, 1981). Dissolution of the carbonates results in local subsidence and the production of accommodation space to trap sediment shed from South Mountain. As a result, and in contrast to most of the rest of the mid-Atlantic region, a rich record of erosion is preserved here in the form of large, thick, alluvial, colluvial, and debris-flow fans that otherwise are thin or absent in the rest of the erosion Appalachian landscape. A similar rich stratigraphic record of late Cenozoic deposits and erosional unroofing of the post-orogenic Appalachians is not encountered until one travels to the Coastal Plain.

Detailed maps and stratigraphy of the South Mountain piedmont can be obtained from several published and unpublished sources including Grote (2006), Grote and Kite (2006) and Merritts et al. (this guidebook). Here, our goal is to provide a basic, portable, geomorphic and lithostratigraphic framework that is mappable at a scale of 1:24,000. The large alluvial-colluvial fan that spills westward from South Mountain at this locality has been built by Furnace Run and Shirley Run that meet in the town of Mainsville so we refer to the fan as the Furnace Run fan. There are three main, and several minor geomorphic surfaces associated with this fan complex (Fig. 1). The main surfaces are denoted as Qf1, Qf2, and Qf3 and all three are underlain by distinct lithostratigraphic and pedostratigraphic units. Minor surfaces or treads cut into these units are denoted with the subscripts a, b, etc, such as Qf2a. The cross-section clearly shows the inset nature of the three main surfaces and their underlying deposits (Fig. 1b). Distal equivalents to these piedmont fans, not shown in Fig. 1, are known to be preserved further west in the Cumberland Valley. Active sinkholes and disrupted drainages are clear evidence of ongoing dissolution and subsidence beneath the piedmont fan cover.

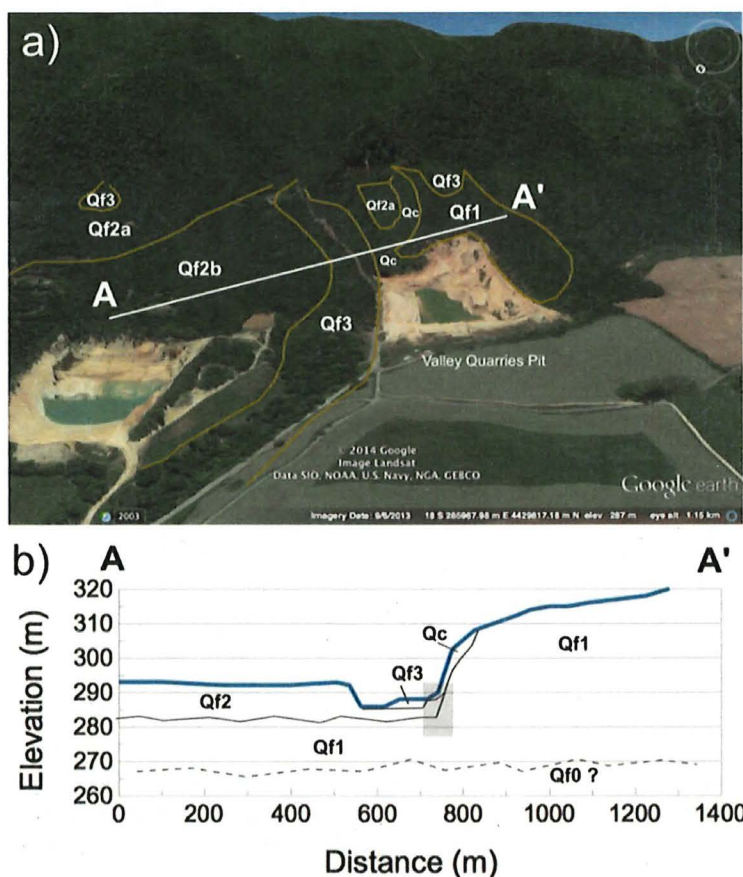


Figure 1. (a) Oblique view to the SSE of the western flank of South Mountain, including piedmont alluvial fans, showing approximate outlines of major geomorphic surfaces. These surfaces are interpreted to be part of a large fluvial-colluvial fan complex and are underlain by the lithostratigraphic units identified in (b) the cross section and Fig 2. The shaded box in (b) indicates the location of the stratigraphic column in Fig. 2. Qf1, Qf2, and Qf3 are described in the text, Qc = colluvium.

Base image from Google Earth

Fan lithostratigraphy

Fan surfaces Qf3, Qf2, and Qf1 are underlain by litho- and pedostratigraphically distinct deposits that are mappable at a scale of 1:24,000 (Fig. 1b and Fig. 2). In general, these three deposits crudely correlate to the LQa, LPc-a, and M-EP-a-c deposits of Grote and Kite (2006), respectively. These three units bury a thick, undivided subsurface deposit with no corresponding geomorphic surface, here denoted as Qf0 and in Grote and Kite (2006) as subsurface sand and gravel. The Qf0 deposit hosts the Pond Bank lignite (see Pazzaglia, this guidebook) and unconformably overlies tens of meters of residuum and saprolite formed from dissolution of the carbonate bedrock (Tomstown and Waynesboro fms).

Qf1 is characterized by red, orange, white, and yellow gravel, sand, silt, and clay. Gravel clasts are mostly saprolitized and there is significant clay coating sand grains and as matrix material (Fig. 2). There are several buried soils in the Qf1 unit, all of which show evidence of intense weathering. Depositional facies are dominated by poorly-sorted hyperconcentrated alluvial and debris flows with lesser examples of alluvial and colluvial facies. Bedding is indistinct and commonly distorted presumably by karst subsidence and clastic dike injection (Sevon, 1994). At 10s of meters thick, Qf1 is the thickest deposit underlying the Furnace Creek fan.

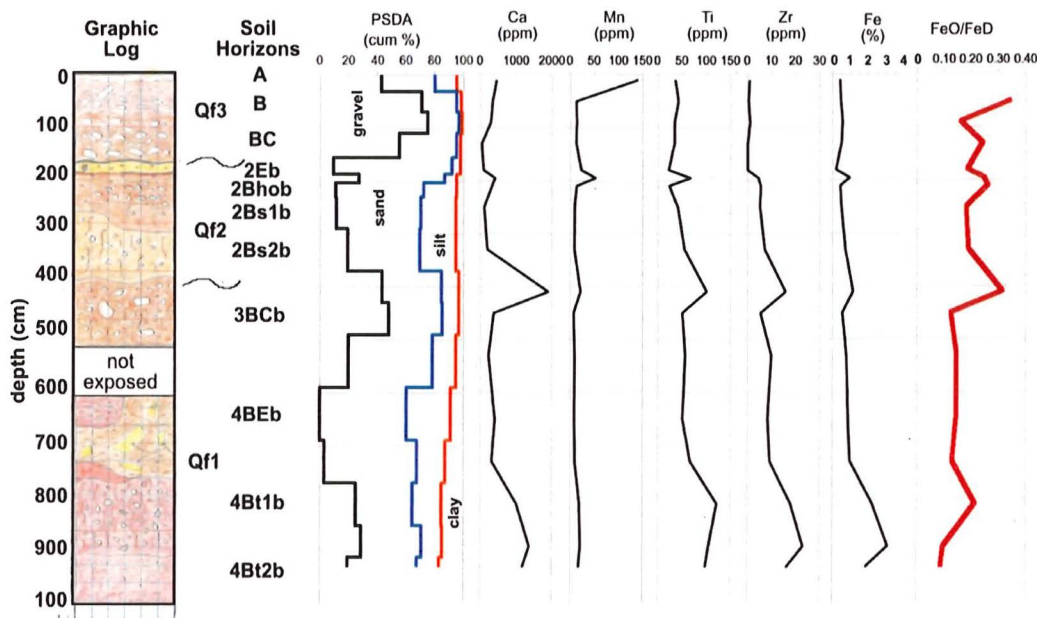


Figure 2. Summary plot of lithostratigraphic, soil stratigraphic, and soil weathering data for the north wall of the Valley Quarries pit. Particle size distribution analysis (PSDA) follows standard NRCS pipette procedures. All chemical data concentrations are reported with respect to the iron-dithionite leach fraction. Ca and Mn represent mobile elements whereas Ti and Zr represent elements traditionally held to be immobile and conserved in the weathering profile. The amorphous iron (FeO) to crystalline iron (FeD) ratio is expanded upon in Fig. 3

Qf2 is 1-10 m thick, white, yellow, and salmon-colored sand and gravel, also deeply weathered, but less so than Qf1. Qf2 contains more silt and less clay than Qf1 (Fig. 2), has more organized bedding, and is comparatively better sorted. The Qf2 facies are thought to be a mix of alluvial and hyperconcentrated flows with lesser amounts of debris flows and colluvium. One or more paleosols are also present in Qf2, one of which preserves a buried spodosol, characteristic of the modern soil forming environment altering similar parent material. Qf2 is less thick overall than Qf1 and underlies the fan lobe north of Furnace Creek. Qf2 is everywhere inset into Qf1.

Qf3 occurs in two landscape positions on the Furnace Creek fan (Fig. 1). Along Furnace Creek and Shirley Run, Qf3 is a brown, moderately well-sorted and stratified sandy gravel alluvial deposit that is inset into both Qf2 and Qf1 where it is stratigraphically younger, but topographically lower than the other fan units. The depositional facies is interpreted to be alluvial and hyperconcentrated alluvial stream deposits. Qf3 occupies a second landscape position as small alluvial-colluvial-debris flow fans sourced in the Antietam ridge, and deposited atop Qf1 or Qf2 at the heads of these older units. In this landscape position, Qf3 is both younger and topographically higher than Qf2 and Qf1. Qf3 is only gently modified by weathering and pedogenesis.

All depositional facies, the stark unconformities and soils bounding the three main lithostratigraphic packages, and overall geomorphology of the Furnace Creek fan are consistent with unsteady production of sediment in South Mountain watersheds and unsteady transport of that sediment to the piedmont over 10^3 - 10^5 yr time scales. Periglacial processes and repeated glacial-interglacial cycles have undoubtedly played a role in this unsteadiness (Sevon, 1991; Potter and Sevon, 2011; Sevon, 2013; Grote, 2006; Grote and Kite, 2006), but the precise links remain elusive. Investigation of the modern landscape using LiDAR and synoptic classification of the myriad of talus, colluvial, and related cold-climate deposits (Merritts et al., this guidebook) provide an excellent analogue model for the processes responsible for creating the lithostratigraphy described here.

Pedogenesis, weathering, and age model

The soils formed in the three main lithostratigraphic units form a basis for understanding when they were deposited and the prevailing environmental conditions that has driven their subsequent weathering (Figs. 2 and 3). Significant changes in the concentrations of traditionally-held mobile and immobile elements occur at litho- and pedostratigraphic boundaries (Fig. 2). These changes are probably the result of accumulations and depletions that occurred during pedogenesis and subsequently by groundwater and diagenesis.

We focus on the iron chemistry as a crude measure of deposit age by correlation to what is (poorly) known about soil ages in the mid-Atlantic region. In soil profiles, iron is known to occur as amorphous non-crystalline iron-oxy-hydroxides as well as crystalline minerals such as hematite (reviewed in McFadden and Weldon, 1985). As iron in soil parent materials weather, the amorphous phases are produced and early in the development of a soil, they dominate the iron chemistry. With the passage of time, these amorphous iron phases transform to crystalline hematite, goethite, jarosite, etc, that accumulate and ultimately dominate the iron chemistry of old soils. As a result, the amorphous to crystalline phase ratio initially starts out relatively high (0.3-0.5) but then decreases with time towards zero. The amorphous iron phase is extracted from a soil sample using an oxalate leach procedure and is called the oxalate iron fraction, FeO. The crystalline phase is extracted using a citric dithionite leach and is called the dithionite iron fraction, FeD. Insofar that we know the numeric ages of some soils and buried soils in the Appalachian landscape, the FeO/FeD ratio can be used as a crude tool in determining soil age and provides a means for correlation (Ciolkosz et al., 1993).

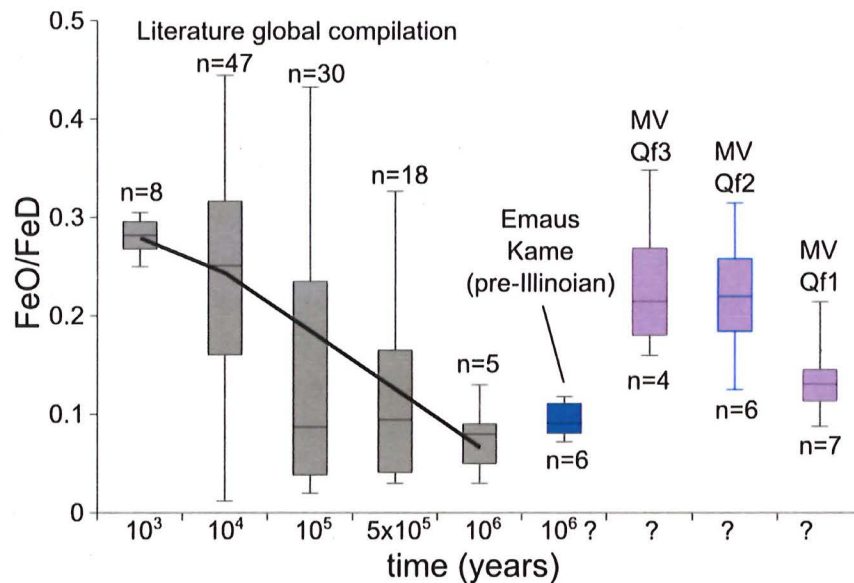


Figure 3. Plot of soil oxalate-extractable iron to dithionite-extractable iron ratio for soils assembled from the literature in comparison to the three main litho-pedostratigraphic units exposed in the Valley Quarries pit and the pre-Illinoian kame delta exposed at Emaus, PA. References used in the compilation of the global data are Ciolkosz et al., 1983; McFadden and Weldon, 1987; Layzell et al., 2012; Eppes et al., 2008.

The FeO/FeD data from Qf1, Qf2, and Qf3 are plotted with respect to an incomplete but representative global compilation of FeO/FeD data that is heavily weighted by Pennsylvania soil and paleosol data (Ciolkosz et al., 1993; Fig. 3). Also plotted are the FeO/FeD ratio from a soil developed in a pre-Illinoian kame delta exposed in Emaus, PA (Braun, 1996). The Emaus kame soil is an important one to use because if intact, it has

been in the landscape for > 788 ka (Braun, 1996), making it significantly older than most of the LGM and Illinoian soils described on well-preserved tills (Ciolkosz et al., 1993) but also significantly younger than the Tertiary Coastal Plain deposits that are known to be pre-glacial based on biostratigraphy (Pazzaglia et al., 1997). We note that the FeO/FeD ratios of Qf1, Qf2, and Qf3 are at least consistent with their relative stratigraphic age. The ratios suggest that Qf2 and Qf3 are Holocene to late and perhaps middle Pleistocene age deposits. In contrast, Qf1 is a middle, or even early Pleistocene deposit. Corresponding FeO/FeD ratios for Tertiary Coastal Plain gravels have not been compiled for this study, but remain a goal for our ongoing research.

REFERENCES

- Becher, A. E. and Root, S. I., 1981, Groundwater and geology of the Cumberland Valley, Cumberland County, Pennsylvania: Pennsylvania Geologic Survey, 4th ser., Water Resource Report 50, 95 p. (online at www.dcnr.state.pa/topogeo/pub/water/w050.aspx)
- Bikerman, M., Myers, T., Prout, A.A., and Smith, R.C., 1999. Testing the feasibility of KAR Dating of Pennsylvania cryptomelanes [potassium manganese oxides]: Journal of the Pennsylvania Academy of Science, v. 72, pp. 109-114.
- Braun, D., 1996, Surficial Geology of the Allentown East 7.5' quadrangle, Lehigh, Northampton, and Bucks Counties, Pennsylvania: Pennsylvania Geological Survey Open-File Report 96-43, 15 p.
- Ciolkosz, E. J., Waltman, W. J., and Thurman, N. C., 1993, Iron and Aluminum in Pennsylvania soils: Penn State University Agronomy Series 127, 33 p.
- Eaton, L. S., Morgan, B. A., Kochel, R. C., and Howard, A. D., 2003. Quaternary deposits and landscape evolution of the central Blue Ridge of Virginia: Geomorphology, v. 56, p. 139-154.
- Eppes, M. C., Bierma, R., Vinson, D., and Pazzaglia, F., 2008, A soil chronosequence study of the Reno valley, Italy: Insights into the relative role of climate verses anthropogenic forcing on hillslope processes during the mid-Holocene: Geoderma, 147, 97-107.
- Grote, T. and Kite, J. S., 2006, Surficial geology of the northwestern footslope of South Mountain, south-central Pennsylvania: USGS EDMAP program Open File Report 05HQAG0045, 34 p.
- Grote, T. D., 2006 Late Cenozoic Stratigraphy and Landscape Dynamics in the Unglaciaded Central Appalachians - a Case Study from the Northern Blue Ridge, South-Central Pennsylvania, USA (Ph.D. Dissertation): Morgantown, West Virginia University, 117 p., URL: <https://eidr.wvu.edu/eidr/documentdata.eIDR?documentid=4954>







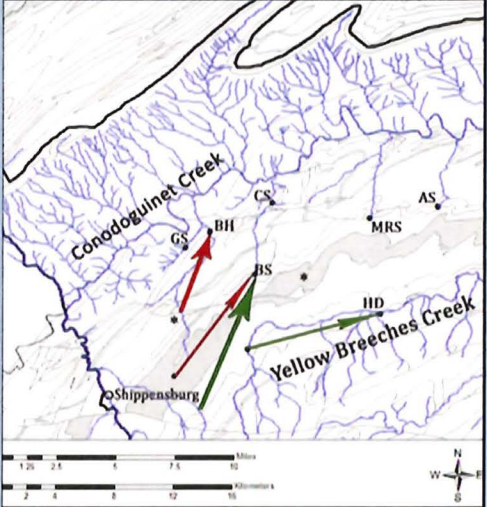
- Hack, J.T., 1965, Geomorphology of the Shenandoah Valley, Virginia and West Virginia and the origin of the residual ore deposits: U.S. Geological Survey Professional Paper 484, 84 p.
- Layzell, A. L., Eppes, M. C., and Lewis, R. Q., 2012, A soil chronosequence study on terraces of the Catawba River near Charlotte, NC: Insights into the long-term evolution of a major Atlantic Piedmont drainage basin: *Southeastern Geology*, 49, 13-24.
- McFadden, L. D. and Weldon, R. J., 1985, Rates and processes of soil development on Quaternary terraces in Cajon Pass, California: *Geological Society of America Bulletin*, 98, 280-293.
- Pazzaglia, F. J., Robinson, R., and Traverse, A., 1997, Palynology of the Bryn Mawr Formation (Miocene): Insights on the age and genesis of middle Atlantic margin fluvial deposits: *Sedimentary Geology*, v. 108, p. 19-44.
- Pierce, K. L., 1965, Geomorphic significance of a Cretaceous deposit in the Great Valley of southern Pennsylvania: US Geological Survey Professional Paper 525C, p. C152-C156.
- Potter, N., Jr. and Sevon, W. D., 2011, Geology and geomorphology of the South Mountain area, Cumberland and Franklin Counties, Pennsylvania: Harrisburg Area Geological Society, 20th Field Trip, 64 p. (Stop 6 is Mainsville.)
- Sevon, W. D., 1991, Stop 6. Mainsville quarry, Valley Quarries, Inc., in Sevon, W. D. and Potter, N. Jr., eds., *Geology in the South Mountain area, Pennsylvania: Field Conference of Pennsylvania Geologists, Annual Field Trip, 56th, Guidebook*, p. 176-188.
- Sevon, W. D., 1994, Solution below, injection within, and subsidence throughout alluvial-fan deposits, South Mountain, Pennsylvania: *Geological Society of America, Abstracts with Programs*, v. 26, no. 3, p. 72.
- Sevon, W. D., Day 2, Stop 3, Mainsville (p. 90-97), in Potter, N., Jr., Merritts, D., Walter, R., Clark, G. M., Pazzaglia, F., Price, J., and Sevon, W. D., 2013, *Geomorphology of the South Mountain Area, Cumberland and Franklin Counties, Pennsylvania: Southeast Friends of the Pleistocene, 2013 Field Trip, Guidebook*, 106 p.
- Whittecarr, G.R. and Duffy, D.F., 2000, Geomorphology and stratigraphy of Late Cenozoic alluvial fans, western Virginia, U.S.A.: *Southeastern Geology*, v. 39, p. 259-280.
- Whittecarr, G.R., 1985. Stratigraphy and soil development in upland alluvium and colluvium, North-central Virginia Piedmont: *Southeastern Geology*, v. 26, p. 117-129.




GREAT MOMENTS IN GEOLOGIC HISTORY

Part 1 - The Lower Cambrian



Yeah, it's a shame. Poor fella got caught up
in the latest housing bubble!

Mileage Interval	Cumulative Mileage	 = Stop Sign;  = Traffic Light; "T" = T Intersection; TR = Township Route; "Y" = Y intersection
0.0	43.8	Return northward toward Lindsay Lot Road; turn left on Lindsay Lot Rd
0.8	44.6	 Turn right on Mainsville Road
0.6	45.2	Cross Means Hollow Road; re-enter Cumberland County, road name changes to McCulloch Road
1.8	47.0	 Cross Baltimore Road; continue on Cleversburg Road
1.0	48.0	At 3-way intersection of Cleversburg, Gilbert and Walnut Dale Roads, turn left onto Gilbert Road
0.9	48.9	Turn left onto Witmer Road
0.3	49.2	 Turn left onto Airport Road
1.0	50.2	At 4-way intersection of Airport, Hershey and Neil Roads turn right onto Hershey Road; Southampton Township offices are to the right.
0.9	51.1	 Turn left onto Walnut Bottom Road; cross over I-81
0.2	51.3	Turn right onto Cramer Road (<i>immediately past the I-81 off-ramp</i>)
0.5	51.8	<p>Groundwater flowpaths in western Cumberland County, PA traced with fluorescent dyes since 2005. (Figure from <i>Pennsylvania Geology</i>, v.42 no. 3, Fall 2012)</p> <p>Cramer Road Dye Trace Site: (40°3'58.1"N, 77°28'22.9"W) The first modern dye trace in the Cumberland Valley occurred in 2005 when a fluorescent dye was injected at this site (butt end of green arrow shaft) into a failed storm water detention basin during a summer thunderstorm (Hurd et al. 2010). Review of regional water table maps suggest that groundwater in this region flows to the north toward the regional drain, the Conodoguinet Creek. Charcoal receptors were placed at eight springs to the north and east of the injection site that were considered</p> 

		<p>potential emergence points; two of the sites were at Big Spring (“East” and “West” springs). Collected over a two-week period at all eight sites water samples were analyzed on a spectrofluorophotometer. Evaluation of collected spring water samples revealed a spike in dye concentration 3.5 days after injection at Big Spring, 8.9 km to the north and east. A groundwater flow velocity of 2.5 km/day was based upon the linear distance and 3.5-day travel time. A second dye released into the upper Yellow Breeches Creek at Walnut Bottom was detected at Huntsdale Hatchery springs. This dye trace provided the first direct evidence of how the strike influenced groundwater flow in the Cumberland Valley karst aquifer, and in turn the anisotropic nature of flow here. Subsequent dye traces from other locations have followed much the same path.</p>
0.9	52.7	<p>Continue on Cramer Road to intersection with US Route 11.  Turn right on US 11</p>
0.4	53.1	<p>Just past the intersection of US 11 with Goodheart Road (to the left) is a lengthy outcrop of the Cambrian Zullinger Formation (Becher & Root, 1981). Here, and in additional outcrops along both sides of US 11 for the next mile, can be seen the formation’s characteristic dark-gray limestone lithology with laminae and crenulated siliceous seams as well as the region’s prominent strike parallel and perpendicular joint sets. Calcite veins fill many joints as well as occur in layer parallel fractures.</p>  <p>Cambrian Zullinger Formation exposed at mileage 53.7</p>
0.8	53.9	Turn left onto Foltz Road; = TR 4003
0.9	54.8	 Turn right onto PA Route 533
0.6	55.4	ARRIVE at plant entrance to Valley Quarries on left – STOP 5

112

STOP 5 – VALLEY QUARRIES, SHIPPENSBURG

(Entrance requires signed liability waiver)

*Stop Leaders – Economics – Valley Quarries staff
Geology – Donald Hoskins, PA Topo & Geologic Survey, Retired
Noel Potter, Dickinson College, Retired*



Entrance to Valley Quarries Shippensburg

Quarried here (40°5'53.5"N, 77°28'24.6"W) since 1936 the quarried rock includes the Ordovician Stonehenge and Rockdale Run Formations of ~450 million years. "Physical characteristics vary minimally between the formations as does the carbonate geochemistry which typically falls between 80 and 90%. The full range of typical crushed aggregate sizes and grades are produced here from pulverized limestone fines all the way to gabion stone and Rip-Rap. A large portion of the aggregate production is consumed internally to supply the company's concrete and hot mix asphalt (Blacktop) operations which in turn sell to individuals, private contractors, and state and municipal agencies as well as in-house construction and paving crews who rely on these value added products to complete their highway and paving projects throughout the region. Many miles of pavement on the nearby Interstate Route 81 and the PA Turnpike have been constructed with stone from the Shippensburg quarry." (*Randall Van Scyoc, Vice President, Valley Quarries, Inc.*)



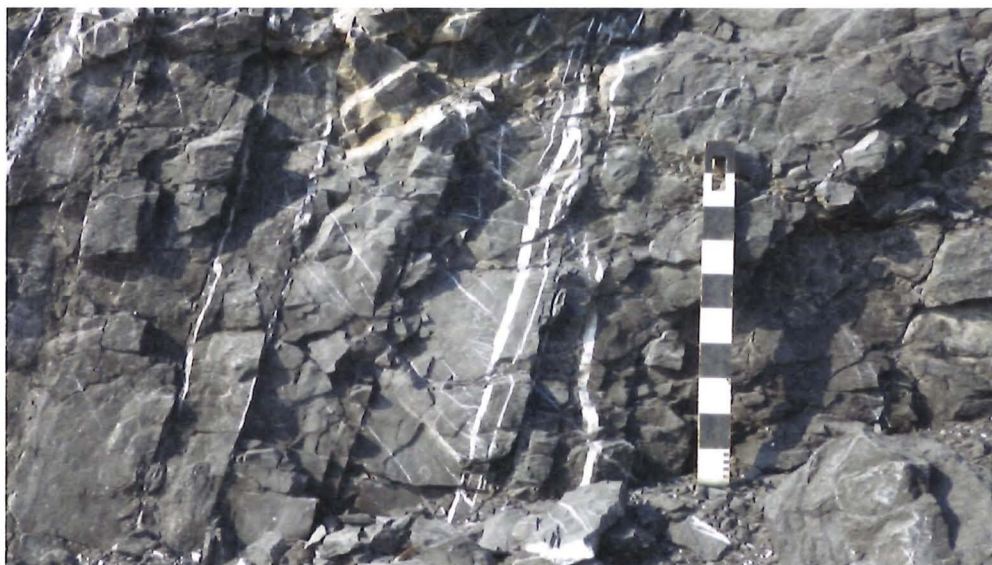
View to west of contact (left edge of buff zone) of the Stonehenge and Rockdale Run Formations in the Valley Quarries, Shippensburg.

The Stonehenge Formation (to the left of the light colored band in the photo above) is “light to medium gray, micrograined to micritic limestone containing zones and beds that are detrital to skeletal–detrital” (Root and Becher, 1981). Unfortunately, access to this part of the stratigraphic section is difficult without wading through water and very fine-grained mud that accumulates rapidly and remains stuck on footwear. The Stonehenge is not actively mined here because quarrying is focused to the north in the Rockdale Run Formation.



View of east wall showing repetitive light colored dolomitic zones characteristic of the Rockdale Run Formation

To the right of the light colored band, the result of deep weathering along a dolomitic zone, is the Rockdale Run Formation. These dolomite zones repeat cyclically to the right throughout the remainder of the exposed stratigraphic section. Described (Root and Becher, 1981) as “medium-bedded, finely laminated to homogenous, chert-bearing micritic limestone and stromatolitic limestone” at this site no chert or stromatolites were observed.



View of southwest wall of quarry exhibiting south dipping layers in the Rockdale Run Formation containing layer parallel calcite veins with shear direction denoted by *en echelon* calcite veins.

Structurally, all quarry rocks are positioned on the north limb of an overturned anticline whose axis is located ~0.6 miles south of the contact photo (refer to LiDAR/geologic map for view of local structure). All rocks in the quarry are overturned dipping steeply to the south from 70 to 80 degrees.



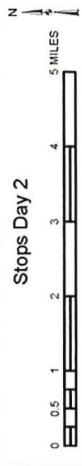
Finely laminated layering in the Rockdale Run Formation

Sedimentologic features such as ripple marks are rarely observed in the fresh rock exposures. In the deeply weathered portions of the Rockdale Run Formation on the uppermost level very thin and finely laminated siliceous layers protrude from weathered surfaces. Fresh rock surfaces exhibit the fine laminations characteristic of this formation.

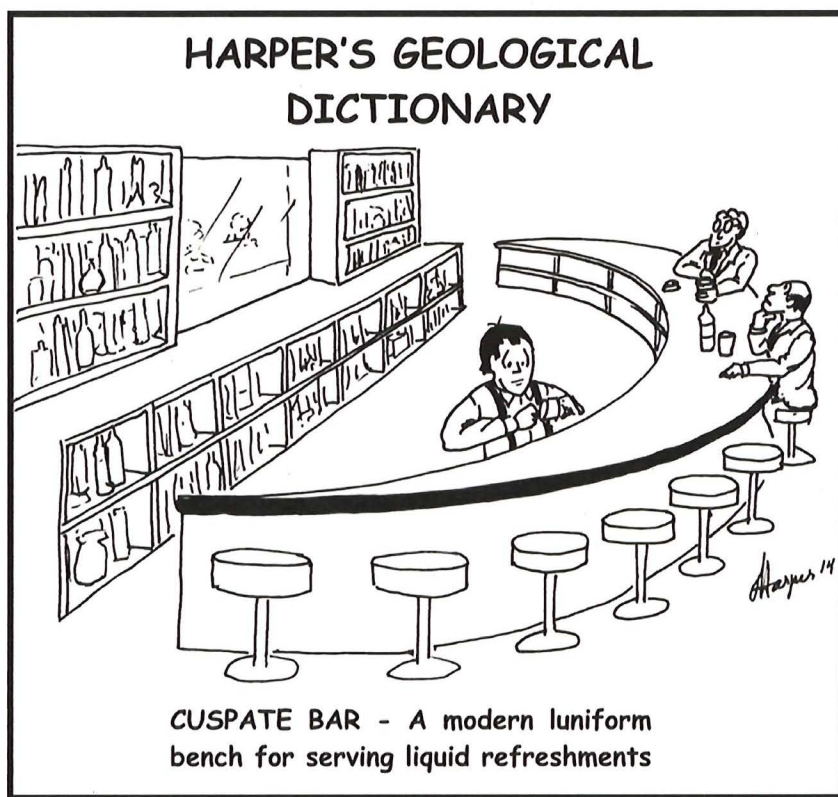







Calcite and Celestine are occasionally found in the Shippensburg quarry

Mileage Interval	Cumulative Mileage	 = Stop Sign;  = Traffic Light; "T" = T Intersection; TR = Township Route; "Y" = Y intersection
0.0	55.4	Return to PA Route 533 N
0.3	55.7	Turn right on Brown Road (TR 328)
1.0	56.7	 Turn left onto US Route 11 N
5.7	62.4	 PA 233 intersection; continue straight on US 11
10.3	72.7	 PA 465 intersection; continue straight on US 11
3.0	75.7	 PA 641 junction; continue on US 11
1.0	76.7	Turn right on S. Hanover Street
0.1	76.8	END of Day 1 tour at Comfort Suites, Carlisle, PA 



Day 2 Road Log. LiDAR image with Geologic Map showing Stops 6 – 10, Starting at Comfort Suites in Carlisle (HQ) & including Lunch Stop (L-D2)



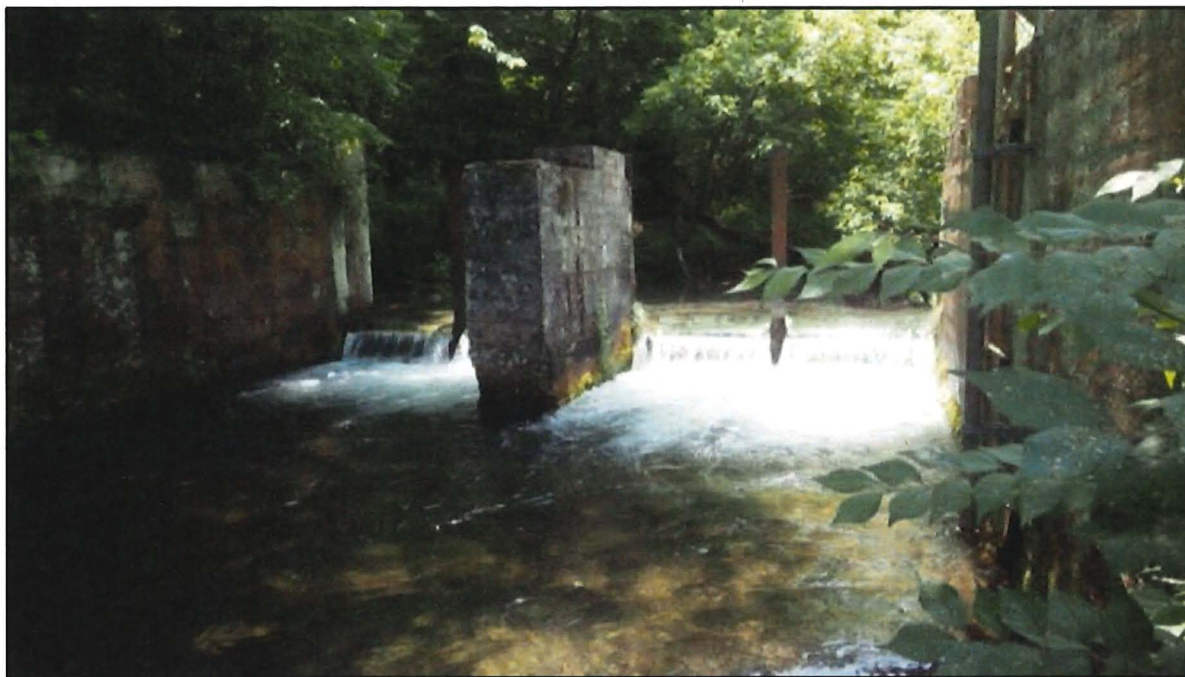
Interval Mileage	Cumulative Mileage	 = Stop Sign;  = Traffic Light; "T" = T Intersection; TR = Township Route; "Y" = Y intersection
0.0	0.0	Start at Carlisle Comfort Suites. Drive south on South Hanover Street passing several traffic lights toward I-81
0.7	0.7	Turn slight right to merge onto I-81 S
9.7	10.4	Take Exit 37 onto Pa Route 233 toward Newville; turn right at 
1.1	11.5	Turn left at  onto US Route 11 (Ritner Road)
3.9	15.4	Turn right onto Oakville Road (TR 386)
0.8	16.2	Turn right onto Springfield Road (TR 333)
1.2	17.4	Turn right on Horn Road (opposite to Willis Road)
0.2	17.6	View to right of pinnacle weathering of carbonates and sinkhole
 <div data-bbox="1117 1056 1416 1230" data-label="Text"> <p>View of sinkhole and associated 'pinnacle' weathering along Horn Road in the Shadygrove Formation.</p> </div> <div data-bbox="1117 1308 1393 1444" data-label="Text"> <p><i>Pinnacle weathering is prevalent in the Great Valley Province, but is rarely seen</i></p> </div>		
0.4	18.0	Turn left onto Big Spring Road (SR 3007). Unoccupied buildings along the route for the next 0.3 miles are of a former PA Fish Commission Hatchery whose operation closed due to pollution of Big Spring.
0.4	18.5	ARRIVE at parking area for off-loading to view Big Spring Run, the USGS gaging station & local geology – STOP 6



STOP # 6 – BIG SPRING

Stop Leaders

*Todd Hurd, Shippensburg University;
Noel Potter, Dickinson College, Retired*



USGS Gaging Station at former dam below Big Spring

Big Spring (40°7'42.6"N, 77°24'26.6"W) is considered one of the largest springs in Pennsylvania (Figure 1 – LiDAR). Big Spring actually consists of two springs spaced ~50 m from one another. The "West" spring is the main source of water, which joins with a smaller flow from the "East" spring to feed Big Spring Creek that flows northward in a broad, shallow, valley that appears to be a collapsed cave passage. In places, weathered travertine deposits are visible on rock outcrops near the main fish hatchery buildings, and cave passages and springs are known to lead laterally from this valley.

Big Spring occurs at or near the crest of an eastward plunging anticlinal fold in the Ordovician Stoufferstown Formation (Becher and Root, 1981). Outcrops can be examined on the west side of the road opposite the creek. These beds average about N60°E, 20°-77°NW indicating that they are on the NW flank of the anticline. Outcrops south of the springs on the east side of the road have gentler eastward dips indicating they are near the anticlinal fold hinge. Use caution in distinguishing often more prominent SE-dipping cleavage from bedding.

Prior to the 2005 dye trace the recharge area for Big Spring was thought to extend directly upgradient toward South Mountain. In a 1981 PGS report Becher and Root discuss the lack of needed size for a watershed toward South Mountain because of the location of Yellow Breeches Creek (Becher and Root, 1981). With limited discharge measurements and existing water table maps they concluded that flow was lost from the Yellow Breeches to sustain flow at Big Spring. The 2005 dye trace (and subsequent traces) have documented the importance of bedrock structure on creating an anisotropic groundwater flow along the NE trending strike in the valley, nearly perpendicular to the regional hydraulic gradient.

Big Spring Flow

Flow from Big Spring sustained a large State fish hatchery for decades before water quality issues dictated its closure. Although much of the infrastructure has been

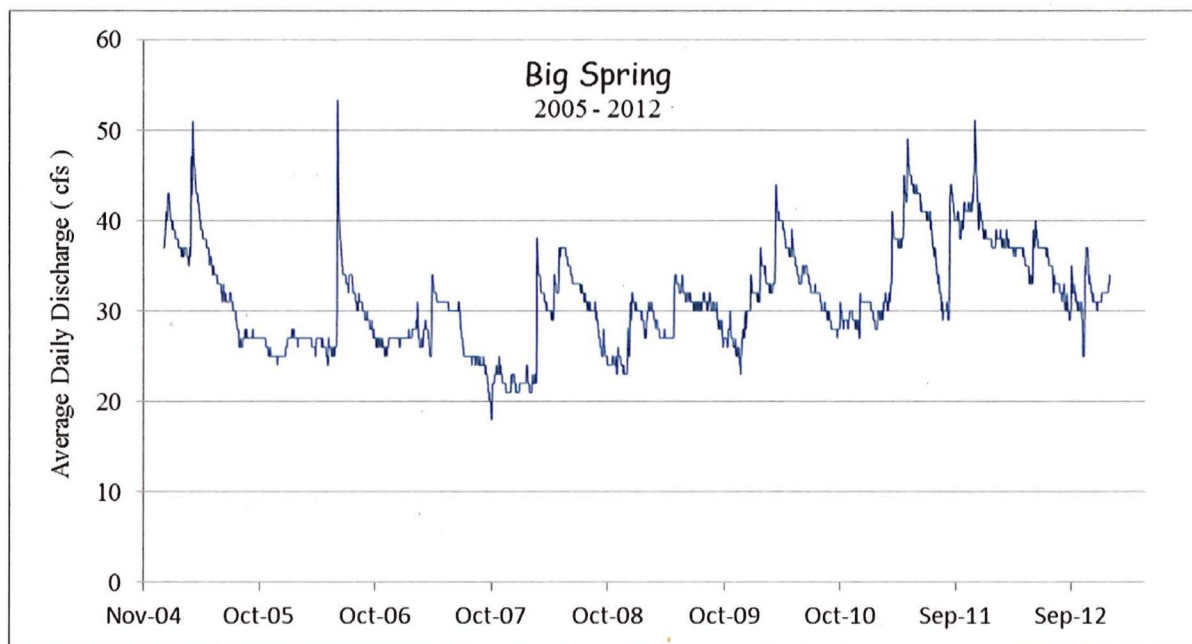


Figure 2. Average daily discharge measured 100m downstream of Big Spring on Big Spring Creek over an eight year period. All data from USGS.

removed, the pump house remains next to the main West Spring. In November 2004 the USGS began data collection at Big Spring as the direct result of a permit condition tied to the creation and operation of a limestone quarry located 2.5 km due east. The USGS measures discharge, temperature, and turbidity at a gage located approximately 100m downstream of the main spring head at the breastworks of an old mill below what is locally called "The Ditch." Average daily discharge collected over an eight year period shows a remarkably consistent flow, varying from a low of 18 cfs to a high of 52 cfs (Figure 2). The average daily flow is approximately 31 cfs.

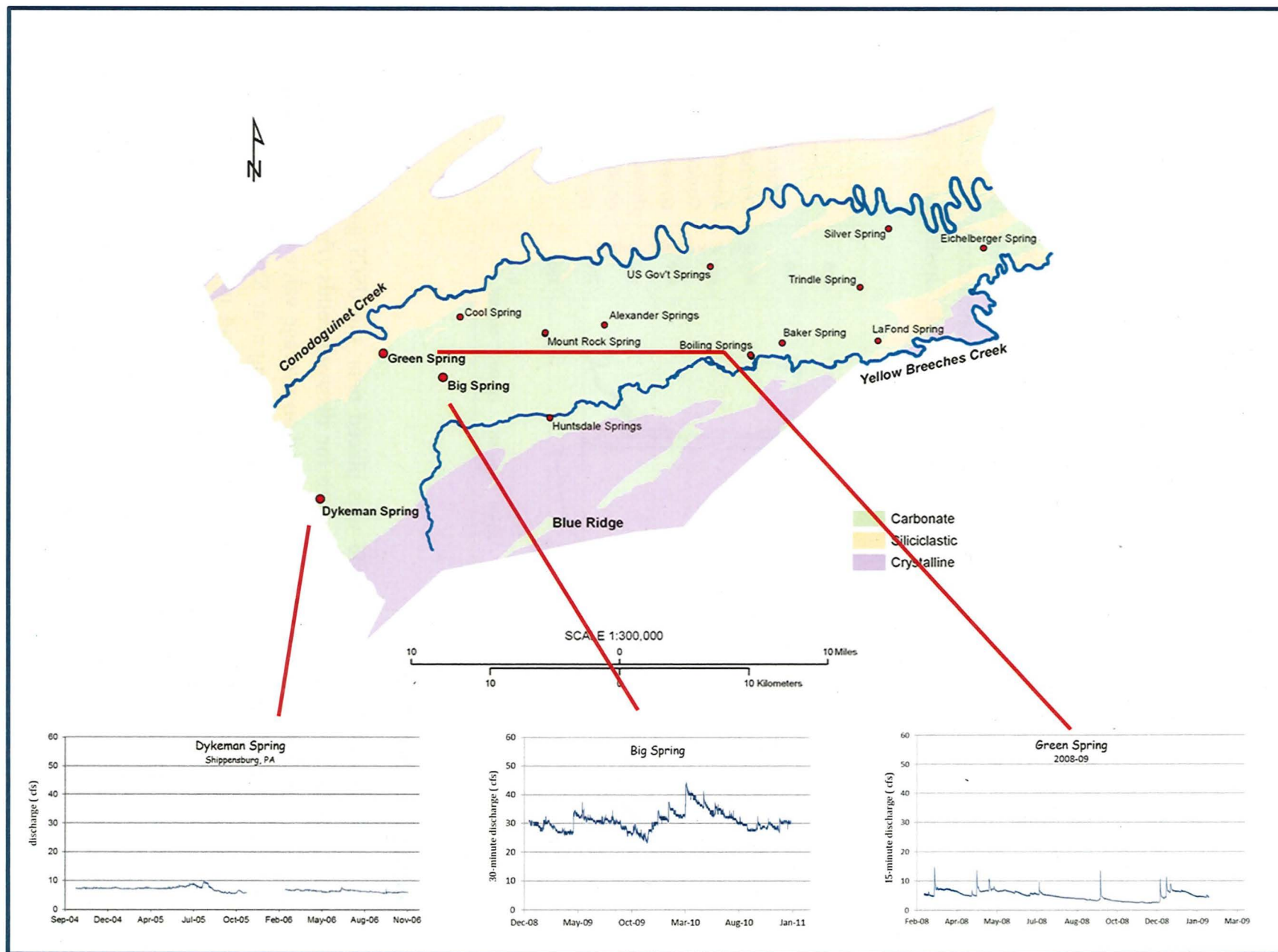


Figure 3. Comparison of 1-2 year hydrographs at Dykeman, Big, and Green Springs in Cumberland Co, Pennsylvania

Interestingly, the flow observed at Big Spring supports the developing model of a mantled karst in the Cumberland Valley where the colluvial apron extends from South Mountain toward the Valley axis, covering the carbonate sequence. In this model, Dykeman Spring, located in Shippensburg at the fringe of the colluvium has an extremely consistent flow; the high and low flow rainfall events are subdued by the porous colluvium. Big Spring, located further toward the Valley axis, exhibits greater fluctuation in flow due to the thinning of the colluvium and more rapid recharge through the karst. To further this example, flow from Green Spring is very flashy, revealing rapid response to rainfall events and a much smaller baseflow (*Figure 3*). Green Spring is a contact spring located north of Big Spring at the Martinsburg Shale - Chambersburg Limestone contact. Discharge and specific conductance collected at 15-minute intervals over a 12-month period revealed a flashy hydrograph response indicative of a conduit flow aquifer (*Figures 3 and 4*).

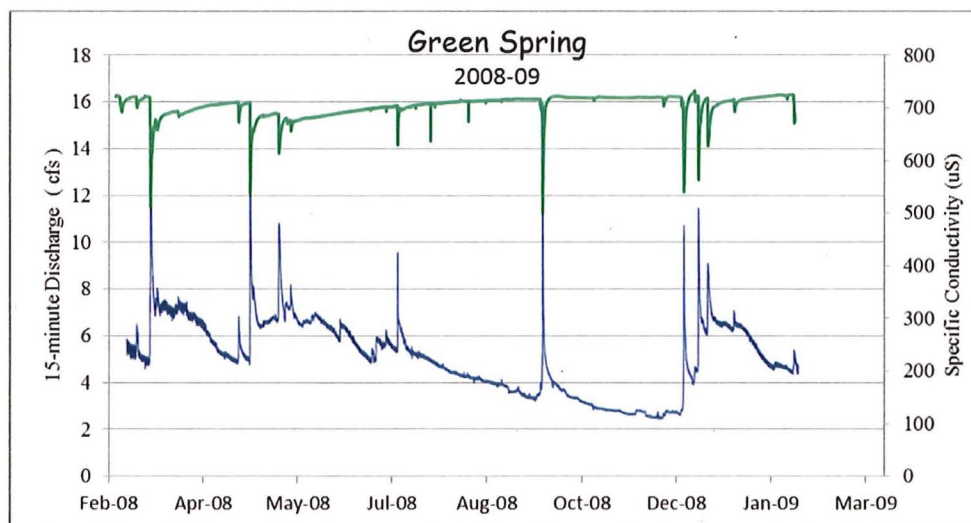


Figure 4.
Discharge and
Specific
Conductivity of
Green Spring
demonstrating
conduit flow
characteristics.

Big Spring Dissolved Load

In June 2012 an InSitu® Troll100 was placed near the USGS gaging station to measure specific conductivity as a surrogate for dissolved solids (*Figure 5*). Specific conductivity during the six month period showed an average value of 450 μS , roughly 100 units greater than that observed at Dykeman Spring near Shippensburg and 200 units less than Green Spring. Although the dissolved load in Green and Dykeman springs show variation with recharge events, their specific conductance remains fairly constant. Big Spring, however, reveals an oscillation of roughly 50 μS and a somewhat daily cycle. It is not clear why there is much more fluctuation in the conductivity data at Big Spring than at Dykeman Spring. We recently received approval from the PA Fish and Boat Commission to place a probe directly at the spring head.

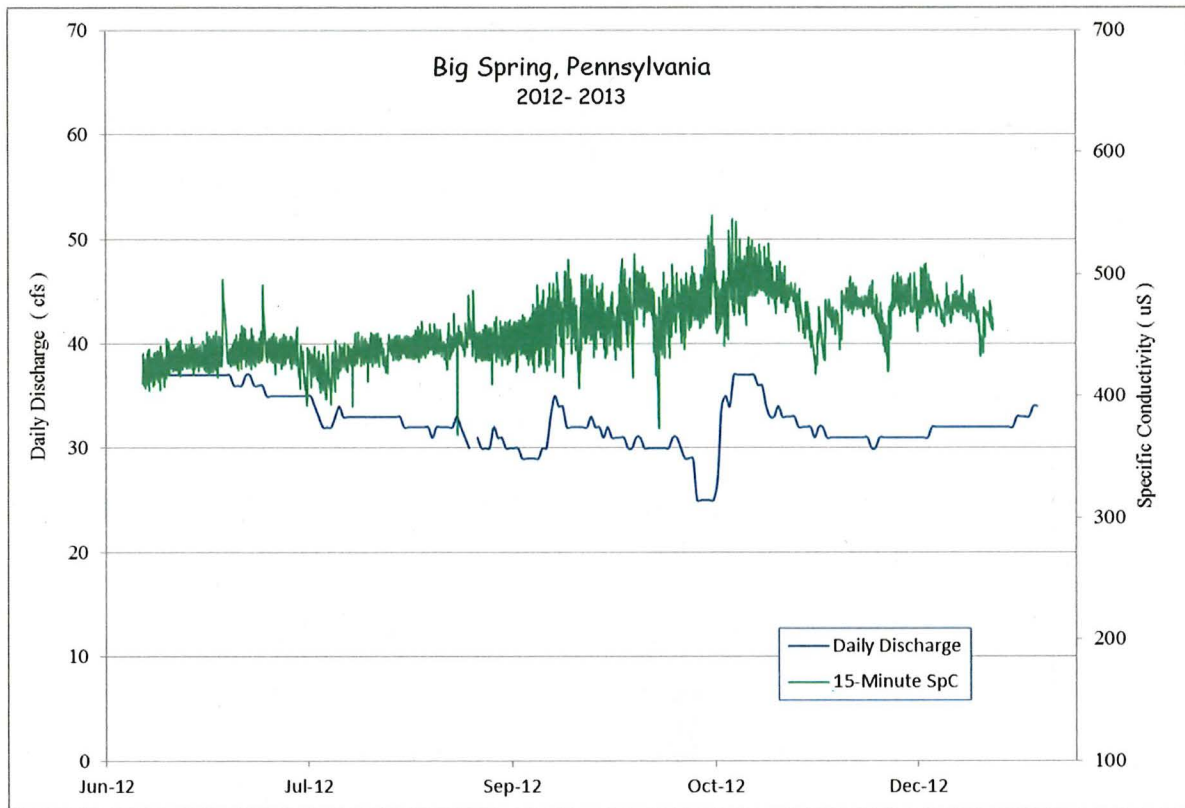









Figure 5.

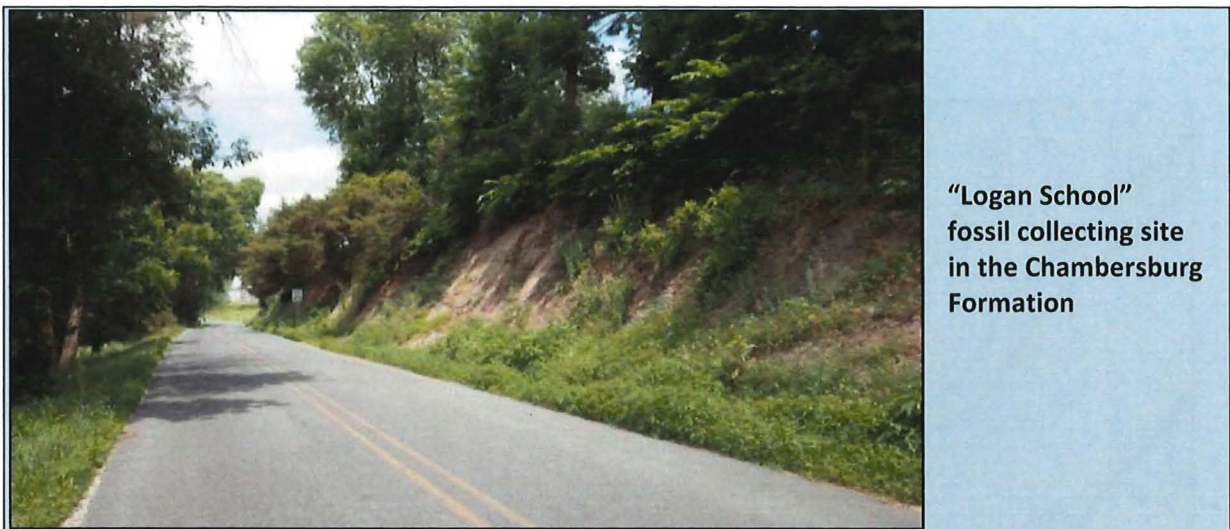
Specific Conductivity reported in microSeimens at 25° C and USGS-measured discharge at Big Spring over a six-month period in 2012.

It is not clear whether the fluctuation in SpC is instrument-related or a function of the aquifer.


References

- Becher, A. E. and Root, S. I., 1981, Groundwater and Geology of Cumberland Valley, Cumberland County, Pennsylvania: Pennsylvania Geological Survey, 4th Series, Water Resource Report W-50, 95 p.
- Hurd, T.M., A. Brookhart-Rebert, T.P. Feeney, M.H. Otz, and I. Otz,, 2010, Fast, regional conduit flow to an exceptional-value spring-fed creek: implications for source-water protection in mantled karst of south central Pennsylvania: Journal of Cave and Karst Studies, v. 72, no. 3, p. 129–136.

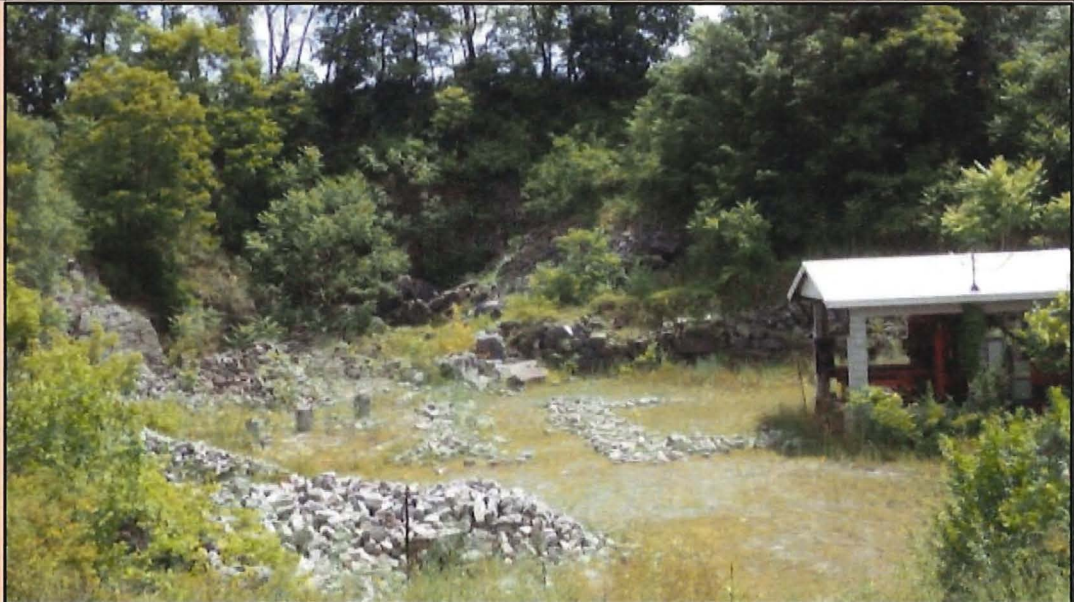
Interval Mileage	Cumulative Mileage	 = Stop Sign;  = Traffic Light; "T" = T Intersection; TR = Township Route; "Y" = Y intersection
0.0	18.5	Head north on Big Spring Road. Exposed rocks seen along the right side of the route are predominantly Ordovician Rockdale Run and St. Paul mapped units (<i>Becher & Root, 1981</i>). The flood plain and meandering course of Big Spring Creek along the route are the likely result of several former low-head dams, and their later removal, as well as the existing dam noted at mileage 22.4.
3.2	21.7	Enter Newville; continue slight right onto W Big Spring Avenue
0.2	21.9	 Cross Fairfield Street (PA Route 533); continue straight on W Big Spring Avenue
0.2	22.1	 Turn left onto S. High Street (PA Route 233)
0.1	22.2	Turn right at  onto Carlisle Road (PA Route 241)
0.2	22.4	Cross over Big Spring Creek; Note: <i>restored Laughlin Mill with dam and water wheel to the right</i>
1.1	23.5	Turn half left onto Creek Road; <i>if you continue on Route 241 past a cemetery on the right, you have gone too far.</i>
1.4	24.9	 continue straight past "T" with Crossroads School Road
1.0	25.9	 continue straight past Blosserville Road
1.9	27.8	Pass outcrop on right. This locality was described in the first edition of PA Geological Survey Report G40 "Fossil Collecting in Pennsylvania". The outcrop provides excellent examples of many genera found in the Chambersburg Formation. Later editions of G40 eliminated this locality. Known to collectors as the "Logan School" site, permission to collect here requires local owner agreement.



**“Logan School”
fossil collecting site
in the Chambersburg
Formation**

0.2	28.0	Pass restored Heishman’s Mill on left with low-head dam across the Conococheague Creek
0.1	28.1	 continue straight past “T” with Old Mill Road
0.8	28.9	Turn right onto Bears Road; note quarry entrance dead ahead
0.05	28.9+	ARRIVE at off-loading site for access to Dickinson College quarry

**STOP 7.
Dickinson
College
Quarry
with rock
trimming
facility**



128

STOP #7 – DICKINSON COLLEGE QUARRY

(Access to this quarry requires signed liability waiver)

Stop Leader – Noel Potter, Dickinson College, Retired



Dickinson College Quarry with rock trimming facility

The Dickinson College Quarry (40°12'48.9"N, 77°17'49.8"W) (Fig. 1) is one of only a few limestone dimension stone quarries still operating in Pennsylvania. It was originally the Morrison Quarry, operated by 3 generations of that family since the early 1900's. In the 1960's it was purchased by Caretti, Inc., a masonry contractor in Harrisburg. In the late 1980's it was acquired by Dickinson College, which has several buildings made of stone from here.



Figure 1. Dickinson College Quarry, looking South. Note gentle dip down to left and thin partings along which rocks weather and break.

The quarry has also furnished stone for a number of the original Pennsylvania Turnpike service area buildings, at least from Midway to King of Prussia, and for the old Carlisle Hospital, now turn down and some of the stone salvaged and lying on the quarry floor awaiting re-use. A short history of the quarry is in Pennsylvania Geology (Anonymous, 1986). The quarry was briefly visited during the 1982 Field Conference (Stephens, et al., 1982, p. 54-55).

The quarry is in the Ordovician Chambersburg Formation, the youngest and topmost of the thick sequence of Cambro-Ordovician carbonate units in the Cumberland Valley. This is the last unit before deposition of the Martinsburg shale, which is exposed just north of the quarry across Conodoguinet Creek.



Figure 2.
Dickinson College
Quarry, showing shaly
partings along which
rocks break, and a thin
calcite vein.
Pencil for scale.

The limestone is a dark gray micrite with beds 10-25 cm thick separated by thin 1-2 cm thick shaly beds (*Fig. 2*). There has been speculation over the years whether the shaly beds are episodic pulses of clay that were precursors to the overlying Martinsburg Formation. How long does it take for 10-25 cm of micritic limestone to be deposited? These clay pulses were clearly not very frequent events.

Bedding is oriented about $N15^{\circ}E, 20^{\circ}SE$, indicating that the quarry is near the hinge of a NE-plunging fold. Indeed Becher and Root (1981) have mapped the hinge of an anticline near here. Joints have a wide variety of orientations, but many trend about $N45^{\circ}W$ and are near vertical. Some joints are calcite filled, and some calcite occurs along bedding planes with slickensides trending about $N15^{\circ}W$ indicating flexural slip.

It is the thin shale partings along which the rock breaks to produce slabs that can be trimmed on the hydraulic guillotine into useable building blocks. The anonymous author (1986) of the Pennsylvania Geology article nicely summarizes the quarrying process and use of the stone:

“Quarrying is done mostly by hand, initial benches are started by jackhammer drilling 1.5 inch-diameter holes about 4 feet deep on centers ranging between 2.5 feet and 4 feet parallel to the quarry face. Coarse-grained black powder charges (typically 10 to 20 ozs. in the bottom of the holes) are used as a blasting agent to reduce discordant fracturing free workable blocks along bedding within benches. Conventional drilling and blasting has been unsuccessfully tried. Pry bars and muscle are standard working tools. The ring of a hammer against a sound rock and a trained ear constitute quality control.”

*Note from Noel: A few years ago the college hired a contractor to remove stone for a new building. The contractor used dynamite which produced many fractures in the stone and rendered it useless.

Slabs of stone are trimmed on the hydraulic guillotine—rectangular if the stone will be laid as ashlar (*Fig. 3*), and irregular if it will be laid as rubblework (*Fig. 4*). Fresh rock, when quarried is almost black; however after a few years of exposure to acidic rain the rocks turn to a mellow gray color.



Figure 3. Stone laid in random-coursed ashlar.



Figure 4. Stone laid in irregular rubblework pattern.

Paleontology at Dickinson College Quarry

Fossils are present at Dickinson College quarry, but access requires College permission. Used as a teaching site by Dickinson College faculty, they request that samples indicated as teaching samples not be removed or damaged.

Fossils occur in very large blocks and as small, weathered, hand samples. Large blocks, if sufficiently weathered, provide opportunities for photographs. Samples for collecting may be found as small, loose blocks in material against the southern portion of the quarry and in a vegetation covered pile on the flat area above and to the east of the quarried part of the site. Piles along the east wall are not quarry stone but are waste material from other sites.



From lower left to upper right, small branching bryozoan, Orthid brachiopod and colonial bryozoans. The orthid brachiopod is penny sized.

The most common fossils are bryozoans and crinoid columnals. More rarely, brachiopods, gastropods and trilobites occur. Use hand lenses to view delicate features.



**Branching bryozoans and
single and conjoined crinoid
columnals**

**Colonial branching bryozoans
require hand lens
to view zooecia**



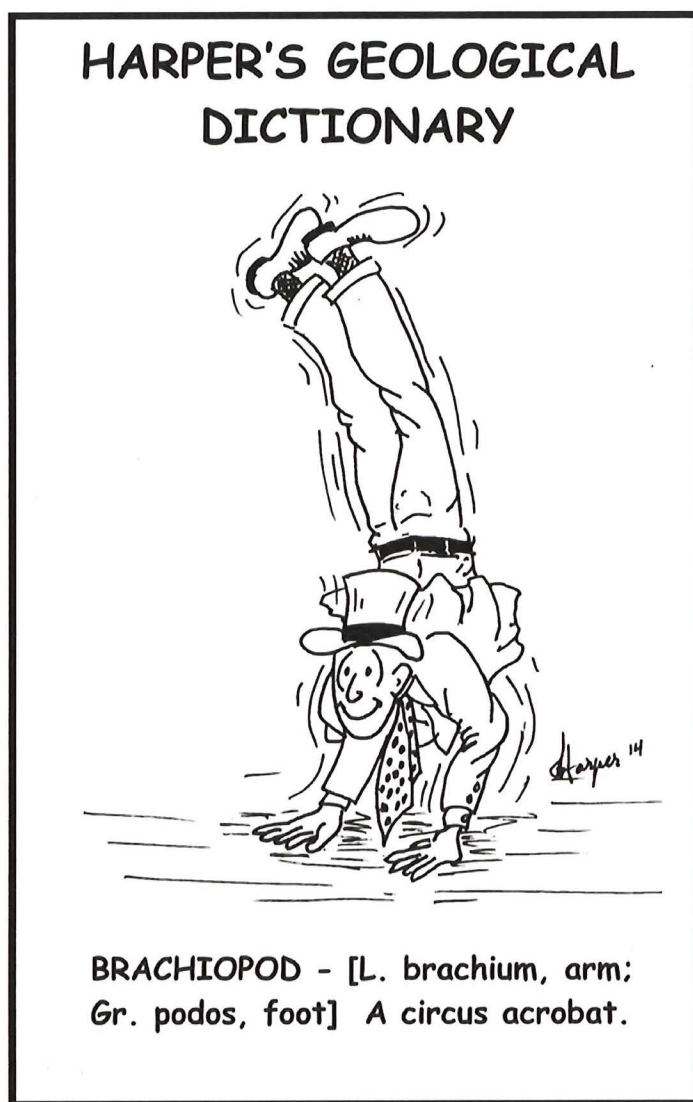
**Branching and fan shaped
bryozoans**










**Bryozoans imbedded
in large block show
internal features**



References

- Anonymous, 1986, Building Stones from Cumberland County: *Pennsylvania Geology*, v. 17, no. 1, p. 10-12.
- Becher, A. E. and Root, S. I., 1981, Groundwater and Geology of Cumberland Valley, Cumberland County, Pennsylvania: *Pennsylvania Geological Survey*, 4th Series, Water Resource Report W-50, 95 p.
- Stephens, G. C., Wright, T. O., and Platt, L. B., 1982, Geology of the Middle Ordovician Martinsburg Formation and Related Rocks in Pennsylvania: *Guidebook for the 47th Annual Field Conference of Pennsylvania Geologists*, 87 p



Interval Mileage	Cumulative Mileage	 = Stop Sign;  = Traffic Light; "T" = T Intersection; TR = Township Route; "Y" = Y intersection
0.0	28.9	Head south on Bears Road
0.6	29.5	Underpass under PA Turnpike
0.1	29.6	 Turn left onto PA Route 641 – Newville Road
2.7	32.3	Continue on PA 641 though Plainfield (on E. Main Street) to Meadowbrook Road; turn left before passing warehouse
0.6	32.9	Cross Conodoguinet Creek
0.1	33.0	 "T" Turn left on Meadowbrook Road (Dead-end Conodoguinet Avenue is to the right)
0.4	33.4	Exposures of the lowermost autochthonous Martinsburg shale on right in road bank. Although covered by vegetation, bedrock here dips steeply north with prominent south dipping cleavage. Mapping by Becher & Root, 1981 locates the contact with underlying Great Valley carbonates at this mileage.
0.5	33.9	Continue to "T" intersection with Creek Road  ; turn right on Meadowbrook Road. The outcrops for the last 0.5 mile are Martinsburg shales with prominent south dipping cleavage and less apparent open folds stratigraphically above a northeast plunging carbonate anticline located west of the Conodoguinet Creek paralleling the route.
		 <p>Anticline in the lowermost Martinsburg Formation shales between mileages 33.4-33.9</p>
0.1	34.0	Turn right on Willow Grove Road
0.6	34.6	 Cross McClures Gap Road; continue straight
1.0	35.6	 Turn right onto Easy Road
0.8	36.6	 Turn left onto Pa Route 74
0.2	36.8	Turn right on N. Middleton Road in community of Caprivi
0.3	37.1	Arrive at access road to N. L. Minich & Sons quarry; turn left
0.1	37.2	ARRIVE at off-loading site in the Minich quarry



LiDAR image of Stop 8 – Minich Quarry. Image with geologic contacts overlain shows area of autochthonous Martinsburg Formation (Om)

STOP #8 – AUTOCHTHONOUS MARTINSBURG FORMATION

(Access to this quarry requires signed liability waiver)

Stop Leader – Donald Hoskins, PA Topo & Geologic Survey, Retired



Entrance to N. L Minich & Sons, Inc. shale pit at Caprivi

Shales and greywacke sandstones underlie nearly half of Pennsylvania's Great Valley Province. Recognized as a separate lithologic unit in 1824 by William Darby, a surveyor and traveler, he then published a page-sized, hand-colored map of Pennsylvania delineating the shales and sandstones of the Great Valley as well as other units. For additional information on this map, see the brief chapter and reproduction of Darby's map in the full guidebook.

Named for the shale hills near Martinsburg, West Virginia, *(Keith, 1894)* the formational name was extended into and through Pennsylvania and south through Virginia into Tennessee. Generally poorly exposed and possessing rock types of little economic value not much attention has been paid to the Martinsburg west of the Susquehanna River. Two reports, Geology and Mineral Resources of Northeastern Franklin County, Pennsylvania *(Root, 1971)* and Groundwater and Geology of the Cumberland Valley, Cumberland County, Pennsylvania *(Becher and Root, 1981)* are the only ones describing and mapping the autochthonous Martinsburg in the area of the 2014 Field Conference. The Cumberland County report also describes and maps

allochthonous Martinsburg which includes rocks whose lithologies are markedly different from the rock types of the original type area.

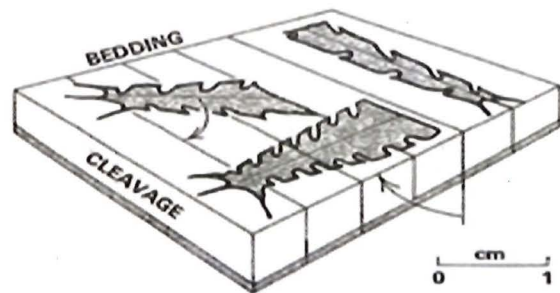
The Minich pit (40°14'50.6"N, 77°13'46.9"W) provides attendees an opportunity to examine autochthonous rock types of the classical "Martinsburg". Stop 9 will address the allochthonous rock types that extend west of the Susquehanna River.

The Minich pit extends in a northerly direction approximately 2500 feet that is nearly perpendicular to regional strike. Nearly 100% of the lithology is shale; only two thin greywacke sandstones occur in the pit as of this writing. The rocks are deeply weathered with relatively "fresh" rock seen only in the southern portion of the pit.

The shales are overturned and dip steeply south to vertical. Cleavage is pervasive in the rocks and also dips south producing excellent examples of pencil shale. Jointing is also pervasive with the J2 direction visible in unweathered rock. The J1 direction is seen in highwalls as nearly horizontal.

Fossils are present in this pit. Graptolites of at least three genera are present and date the Minich pit rocks as Middle Ordovician (*Robert Ganis, personal communication*). The collected specimens all have come from loose material at the base of the uppermost highwalls where they most easily appear on light colored chips. The chips have not been traced back to specific layers exposed in the highwalls. Stephens and Wright (1981) in their examination of the Martinsburg stratigraphy and paleontology west of the Susquehanna River identified these rocks as the "Lower Shale" unit and in the *Diplograptus multidens* Zone of Riva (1969). Although not observed to date in the Minich pit, Stephens and Wright report additional graptolite genera as well as several genera of shelled fauna to be present in the "Lower Shale" lithology.

Strain measurement of Martinsburg graptolites in the Great Valley from Carlisle southwest into Virginia establishes that pressure dissolution of calcite and silicate minerals removed half of the formation's original rock volume (Wright and Platt, 1982)

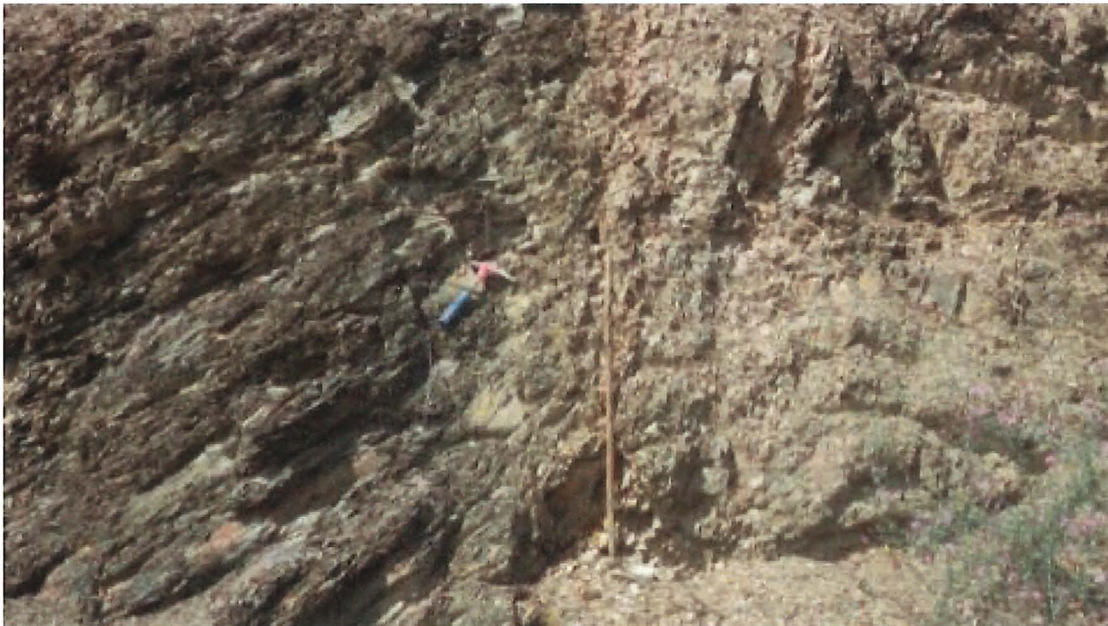


Relation of graptolites on bedding planes to shortening across cleavage.
Graptolites parallel to the trace of cleavage on the bedding are narrower than normal, and those perpendicular to the cleavage trace are shorter. Figure is from Wright and Platt (1982) Figure 2"

Specific features to be seen are described in following photographs:



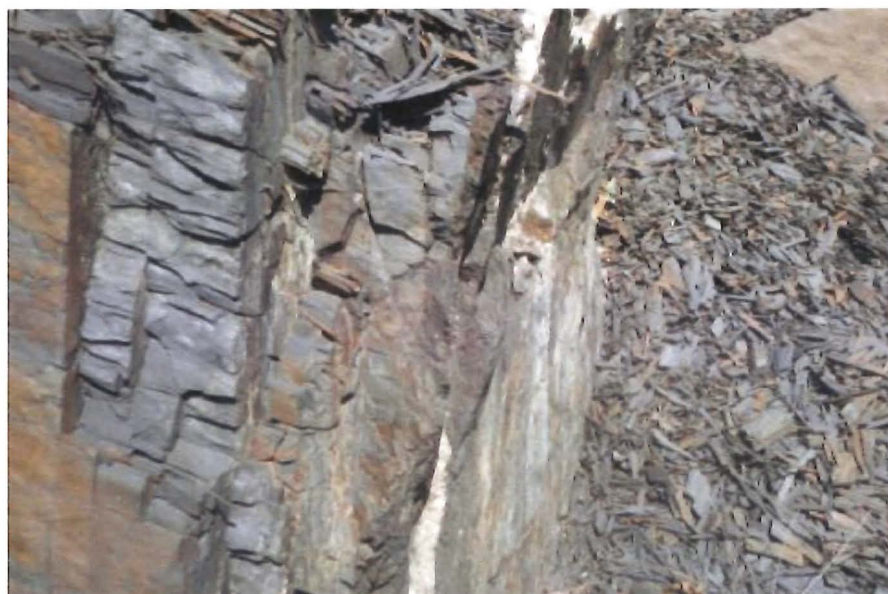
View of uppermost highwall at Minich pit. Graptolites occur in loose fragments in piles along the highwall base. Pick a pile, sit down, and using land lens look for tiny, very dark stripes on light shale chips.



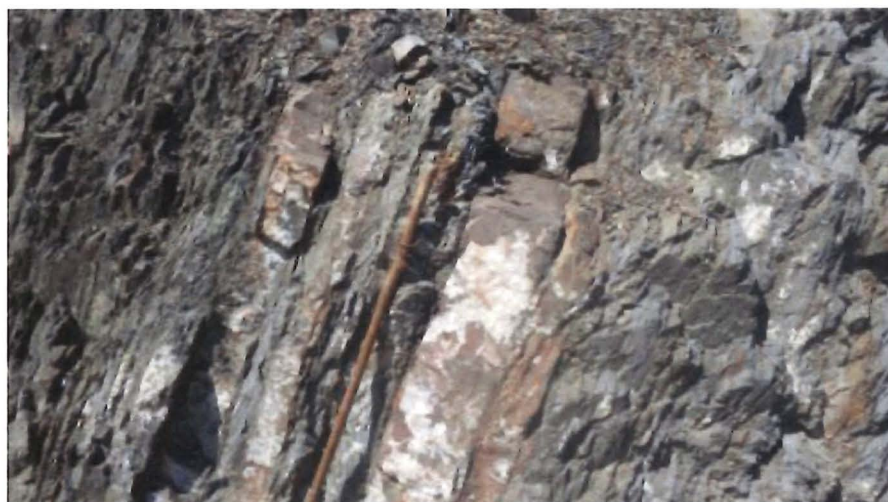
Intersection of vertical to steeply south dipping layering (paralleling the one meter long walking stick) with less steeply south dipping cleavage (paralleling the rock hammer handle)



Exposed rippled bedding plane with J2 joints present along left edge and to the right. Ripples imply flow direction toward viewer. One-meter stick provides scale

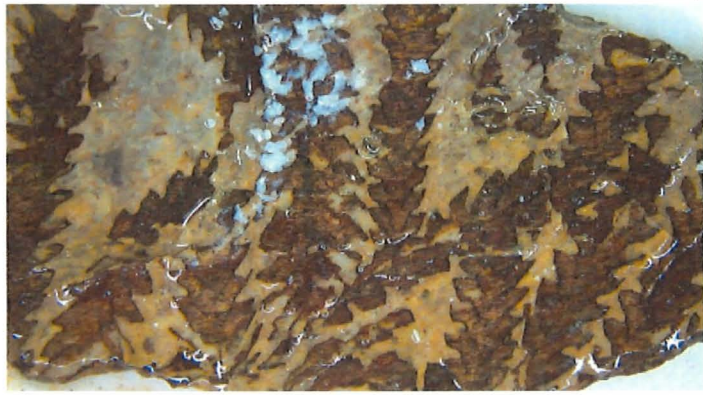


Left side of view shows nearly vertical brownish layer surface with intersecting south dipping cleavage plus J2 joints producing pile of pencil cleavage on right. In center is J2 joint filled with calcite vein.

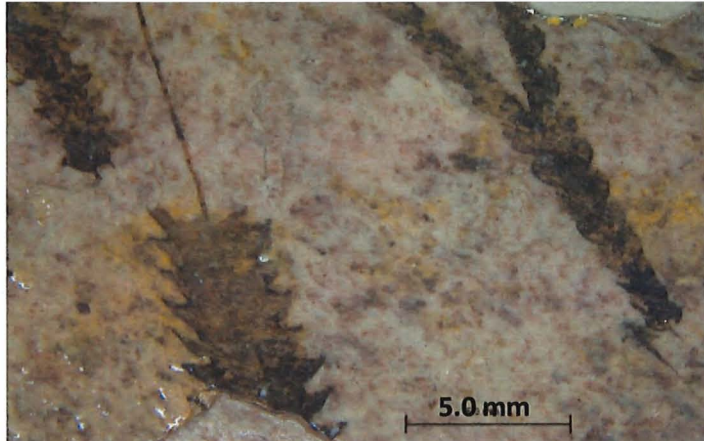


Overturned, south dipping greywacke sandstone and siltstone at Minich pit

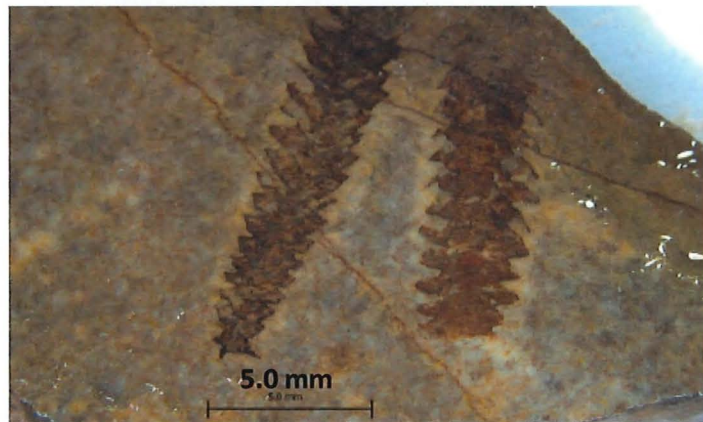
Group of genus
Amplexograptus
at Minich pit



Dicranograptus (right) and
Amplexograptus (lower left) at
Minich pit






Amplexograptus
at Minich pit



Dicranograptus at
Minich pit







Interval Mileage	Cumulative Mileage	 = Stop Sign;  = Traffic Light; "T" = T Intersection; TR = Township Route; "Y" = Y intersection
0.0	37.2	Return on access Road to N. Middleton Road; turn right toward Caprivi
0.3	37.5	 Turn left onto PA Route 74 S – Waggoners Gap Road
1.0	38.5	Turn left into North Middleton Park
0.1	38.6	Continue to lower level to pavilion area

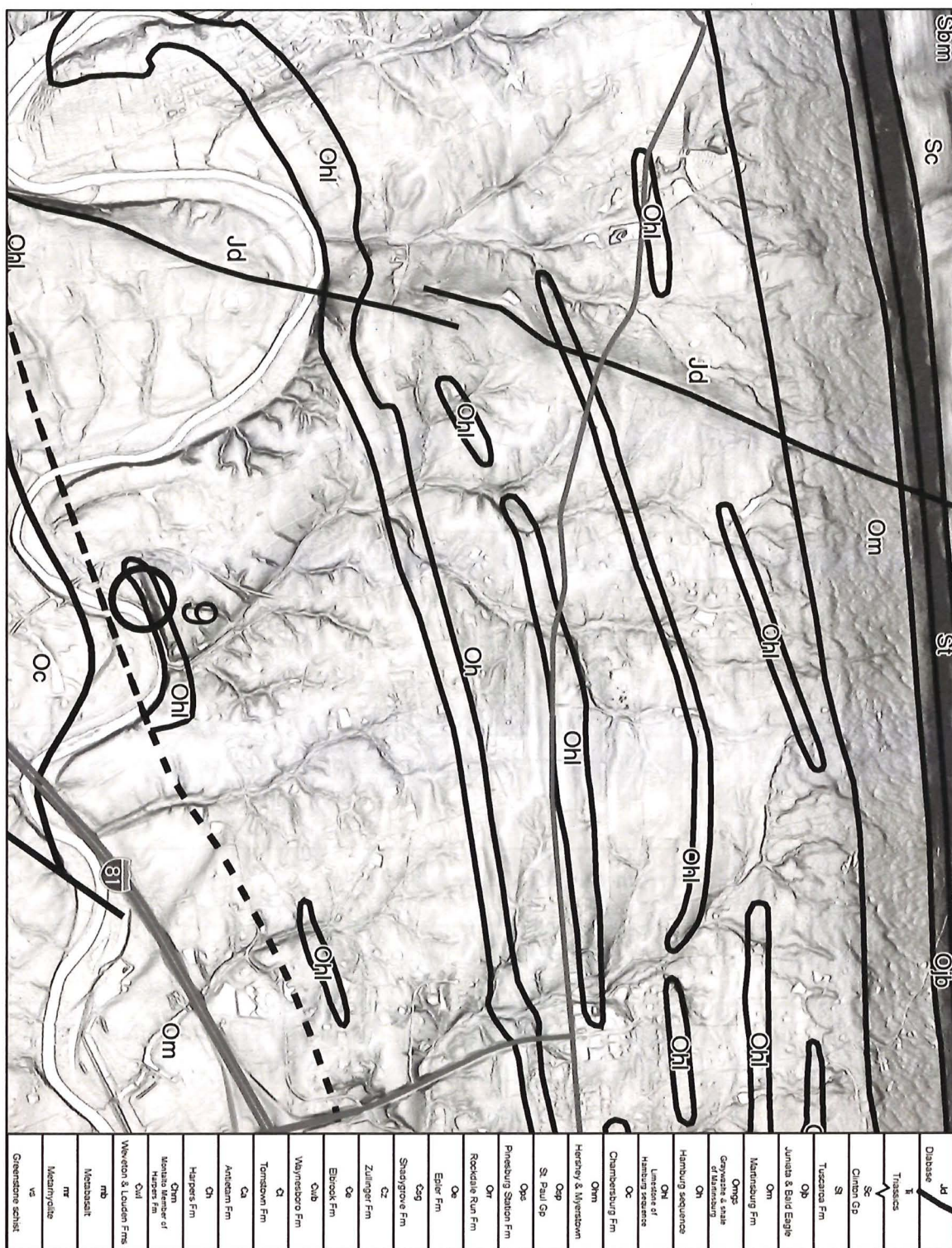
NORTH MIDDLETON TOWNSHIP PARK DAY 2 LUNCH STOP



**Aerial view of North Middleton Park
flooded because of 1972 Hurricane Agnes**
Lunch will be served in the pavilion denoted by the yellow arrow.

Photo by Noel Potter

Interval Mileage	Cumulative Mileage	 = Stop Sign;  = Traffic Light; "T" = T Intersection; TR = Township Route; "Y" = Y intersection
0.0	38.6	Return to entrance of N Middleton Park
0.1	38.7	Turn right onto PA Route 74 – Waggoners Gap Road
3.2	41.9	Turn right onto PA Route 944 E – Enola Road
5.2	47.1	 Intersection with PA Route 34; turn left to continue on PA Route 944 E and PA Route 34 (Spring Road) combined
0.3	47.5	Turn right onto Wertzville Road – PA Route 944 E, continue past two bends to next "T" intersection
3.2	50.7	 "T" turn right onto PA Route 944 E – Wertzville Road
1.2	51.9	Cross Deer Lane (<i>underlain by Triassic diabase dike</i>); continue on Wertzville Road
0.9	52.8	Turn right on Rich Valley Road
1.0	53.8	Turn left on Beechcliff Drive
0.4	54.2	"T" intersection; continue to the right on Beechcliff Drive
0.1	54.3	ARRIVE at off-loading site for Enola Allochthon – Stop 9



LiDAR image of Stop 9 – Enola Allochthon. Image with geologic contacts overlain shows allochthonous “Hamburg Klippe” (Oh) of Stose (1946). Shales and mudstones (Oh) interbed and encase the limestones (Ohl). Dashed line to the south and solid line to the north represent the divide between autochthonous Martinsburg Fm (Om) and allochthonous “Martinsburg”. Ganis and Blackmer (2010) propose new interpretations for these old terranes.

STOP #9 – ENOLA ALLOCHTHON

Stop Leader – Donald Hoskins, PA Topo. & Geologic Survey, Retired



**Isoclinal folds in discontinuous thin limestone layers of the Enola Allochthon
(Root & MacLachlan, 1978, GSA Bull., pp. 1515-28)**

The rocks of the autochthonous Martinsburg Formation seen at Stop 8 extend southwest along the Great Valley Section of the Appalachians Ridge and Valley Province into West Virginia and Virginia. Stop 9 (40°15'46.6"N, 77°4'30.5"W) represents allochthonous rocks markedly distinct in both lithology and geologic structure, yet possessing the same topographic expression long recognized as part of Pennsylvania's Great Valley. The geologic description of Stop 9 derives largely from Dyson (1967) and Root and MacLachlan (1978).

Exotic rock types have long been known to occur in a portion of the Great Valley Section that extends from northeast of Carlisle eastward to just beyond the county boundary between Berks and Lehigh counties. Stose (1946) recognized the allochthonous nature of these rocks and named them the "Hamburg Klippe." The allochthonous rocks include chert, limestones, red and green mudstones and volcanic rocks. Prior Field Conferences (2010, 1984, and 1982) examined these rocks mainly east of the Susquehanna River. The 2010 Field Conference Guidebook included a preliminary geologic map (Ganis and Blackmer, 2010) of the rocks of the northern part of the Great Valley in Dauphin and Lebanon Counties. Newly mapped Dauphin and Linglestown Formations in this map replace the "Hamburg Klippe"'s regional mapping and interpretations.

Root and MacLachlan (1978) identified and mapped terranes west of the Susquehanna as allochthons and wildflysch containing rocks that include reddish mudstones and gray limestones enclosed in greenish and greenish gray shales and mudstones as well as dark gray to black mudstones. These rocks are included in their "Enola Allochthon". Of limited lateral extent they extend from the Susquehanna River (Root, 1977) to Carlisle (Dyson, 1967) where they locally are conglomeratic and arenaceous. The limestones, generally less than 6 m thick, are composed of thin layers of platy weathering, dark-gray, micritic, argillaceous limestones. Some of the thicker layers contain oolites and large quantities of rounded, totally transparent, pure quartz. Thin to massive layers of black, limy shale, such as is present at this Stop, interbed or encase the limestones.



Isoclinally folded Enola Allochthon limestones at Beechcliff Drive at or near the site of Root and MacLachlan's (1978) Figure 7

Rocks of similar lithology exposed in relatively nearby areas east of the Susquehanna (Ganis and others, 2001) contain graptolites and conodonts dated as Lower to Middle Ordovician. They interpret that those sediments "were consolidated and incorporated as olistoliths in an olistostrome, possibly as a trench-fill complex during the Middle Ordovician." More recent explanations of the geologic history of these rocks that apply to Stop 9 rocks are in Ganis and Blackmer Stop 10 (2010) and Ganis and Blackmer (2010).

The exposures along Beechcliff Drive are replete with overgrowth and somewhat difficult to access. Hand samples abound at the foot of the steep sided outcrops. Stop 9 exhibits only the thin limestones and interbedded black to dark gray shales which have been extensively folded in small, tight chevron zones and crushed as broken clasts. At the far eastern end of the exposure are south dipping siltstones with prominent orthogonal jointing and cleavage. The strike of these rocks parallels that of layers seen in the bottom of the adjacent Conodoguinet Creek.



Hand sample
of tight
chevron style
folding at
Beechcliff
Drive

Hand sample of crushed
and rounded limestone
layers in clay matrix at
Beechcliff Drive.











Stretched and fragmented thin limestone layers at Beechcliff Drive.



South dipping layers at easternmost portion of Stop 9 on Beechcliff Drive

CAUTION: *this portion of the outcrop at Stop 9 is immediately adjacent to a blind traffic corner. The pavement extends within a few inches of the base of the outcrop. Traffic arriving from the right may not see you!*

Interval Mileage	Cumulative Mileage	 = Stop Sign;  = Traffic Light; “T” = T Intersection; TR = Township Route; “Y” = Y intersection
0.0	54.3	Drive west on Beechcliff Drive
0.3	54.6	 Turn right on Rich Valley Road
1.7	56.3	 Turn left on Pa Route 944 W – Wertzville Road
2.0	58.3	Turn left continuing on PA Route 944 W – Wertzville Road
1.5	59.8	At “Y” junction, bear left continuing on PA Route 944 W
1.7	61.5	At “T” junction, bear left continuing on PA Route 944 and PA Route 34S
0.3	61.8	Turn right , continuing on PA Route 944 W; Road name changes to Enola Road
5.3	67.1	 Turn right onto Pa Route 74 – Waggoners Gap Road
0.3	67.4	Blocks of Juniata and Tuscorora Formations present on both sides of route indicating local colluvium derived from Blue Mountain
0.3	67.7	On right is example of American culture
0.1	67.8	On left the soil in the cut bank behind North Mountain Inn was described by Edward Ciolkosz (Pennsylvania State University) published in Sevon (1989, p 40-42 and 2001, p. 83-86). Briefly, the soil in the colluvium at this site “is a composite with a weakly developed Wisconsinan upper profile and a much better developed truncated buried lower pre-Wisconsinan profile (at 325 cm).”
1.7	69.5	ARRIVE at off-loading site for Waggoner’s Gap – Stop 10 



LiDAR image of Stop 10 – Waggoners Gap area, with geologic contacts overlain

STOP #10 – WAGGONERS GAP

Stop Leaders: Donald Hoskins, PA Topo & Geologic Survey, Retired

Stratigraphy – Tuscarora & Juniata Outcrops

Dorothy Merritts, Franklin & Marshall College

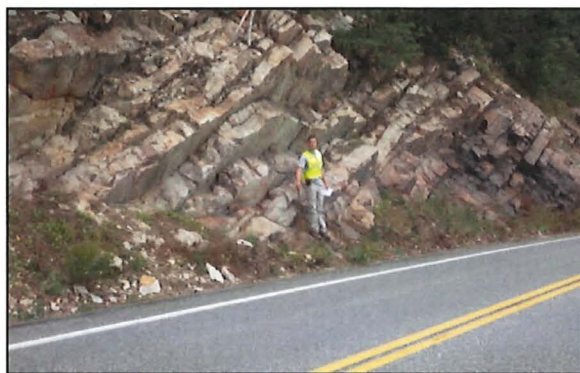
LIDAR Interpretation of Area's Colluvial Slopes

Noel Potter, Dickinson College, Retired

Geomorphology and Lesley's Structural Interpretation of the Great Valley



**The Great Valley Physiographic Province
from Waggoners Gap**



**Contact of the Silurian Tuscarora &
Ordovician Juniata Formations
at Waggoners Gap**

Last visited by the *Field Conference of Pennsylvania Geologists (FCOPG)* in 1982, we again chose this site (40°16'36.9"N, 77°16'36.7"W) for the opportunity to observe the geomorphology of the Great Valley, and to examine the stratigraphy and sedimentology of the Tuscarora and Juniata Formations. Tuscarora rocks support the crest of Blue Mountain and many of Pennsylvania's high ridges that dominate the geomorphology of the Appalachian Mountain Section of the Valley and Ridge Province. Exceptionally well exposed here is the underlying Juniata Formation, rarely seen on these ridges due to extensive colluvial cover.

The ridge and highway outcrops and the colluvial-covered slopes to the highway at Stop 10 are presently the property of, and managed by, the Audubon Society as the "Hawk Watch at Waggoners Gap". Please respect the property and signs as well as the Hawk Watch teams that you may encounter. Do not attempt to collect mineral specimens.

In May 1982, the *Society of Economic Paleontologists and Mineralogists – Eastern Section (SEPM-ES)* examined these rocks under the leadership of Edward Cotter, PhD, and Professor at Bucknell University. The October 1982 FCOPG Guidebook quoted much of Dr. Cotter's SEPM-ES text as the bulk of its Stop 4 description. With the permission of Dr. Cotter, his stop description and illustrations from the 1982 SEPM-ES

Guidebook (*pages 3 and 63–68*) are included as Appendix A to this road-log section of the 2014 FCOPG Guidebook.

Dr. Cotter's interpretations remain valid. In brief, deposited in braided river systems both the Juniata and overlying Tuscarora Formations were similar in origin. They differ partly in color and in their resistance to erosion. Additionally, here, and along Blue Mountain to the east, the basal 30 meters of Tuscarora represent a transgressive event producing a beach sequence along a retrograding coast. New full-color photographs are provided of features he figured.

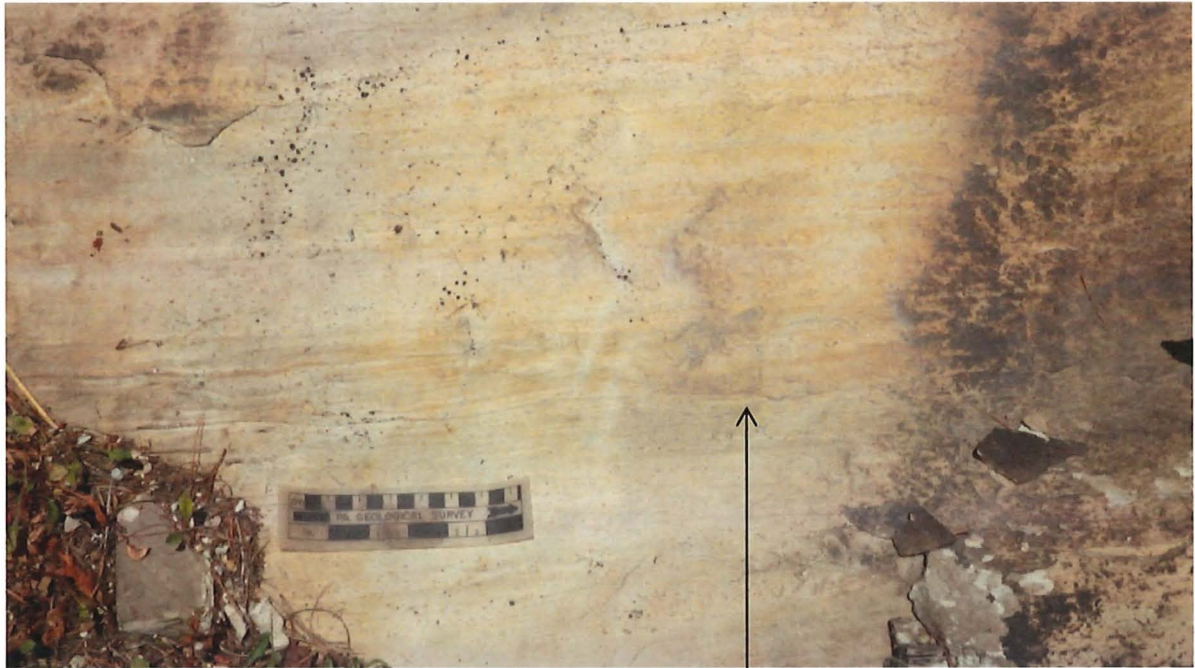
Since 1982 additional work, as well as the newly availability of LIDAR imagery, allow additional geological interpretations to be made of the exposed rocks and of the land surface here and nearby to this site.

Present as thin films on joint surfaces approximately 2 meters above the base of the Tuscarora's beach sand sequence are patches of supergene phosphates. Robert Smith (*personal communication*) states: "The main secondary (supergene) phosphate at Waggoners Gap is variscite. Specifically, it is the 'Lucin-type'.... Associated minerals at Waggoners Gap include pale green, chalky wavellite and trace green turquoise."

"The Mineralogy of Pennsylvania 1966-1975" (*Smith, 1982, p. 269-274*) provides a full description of these mineral occurrences at Waggoners Gap. The hardness of the rocks also mitigates collecting of specimens.



North dipping Tuscarora sandstone at the crest of Blue Mountain viewed from the Hawk Watch platform.



Stratification in the Tuscarora's basal horizontally laminated lithofacies (interpreted as beach origin) approximately 15 meters above formation base. This figure is \approx to Cotter's 1982 Figure 26 A.



Symmetrical ripples on layer base in upper right area of photo. This figure includes Cotter's 1982 Figure 26 B. Note that the larger scale ripples occur on the underside of layers in the lower left side of this photo, indicating two additional flow directions.



Basal lag gravel in the lowermost layer of the Tuscarora Formation's cross-laminated lithofacies.

This photo ~= Cotter's Figure 26 C



Trough cross-laminated Tuscarora sandstone with red shale clasts.

This photos ~= Cotter's Figure 26 D

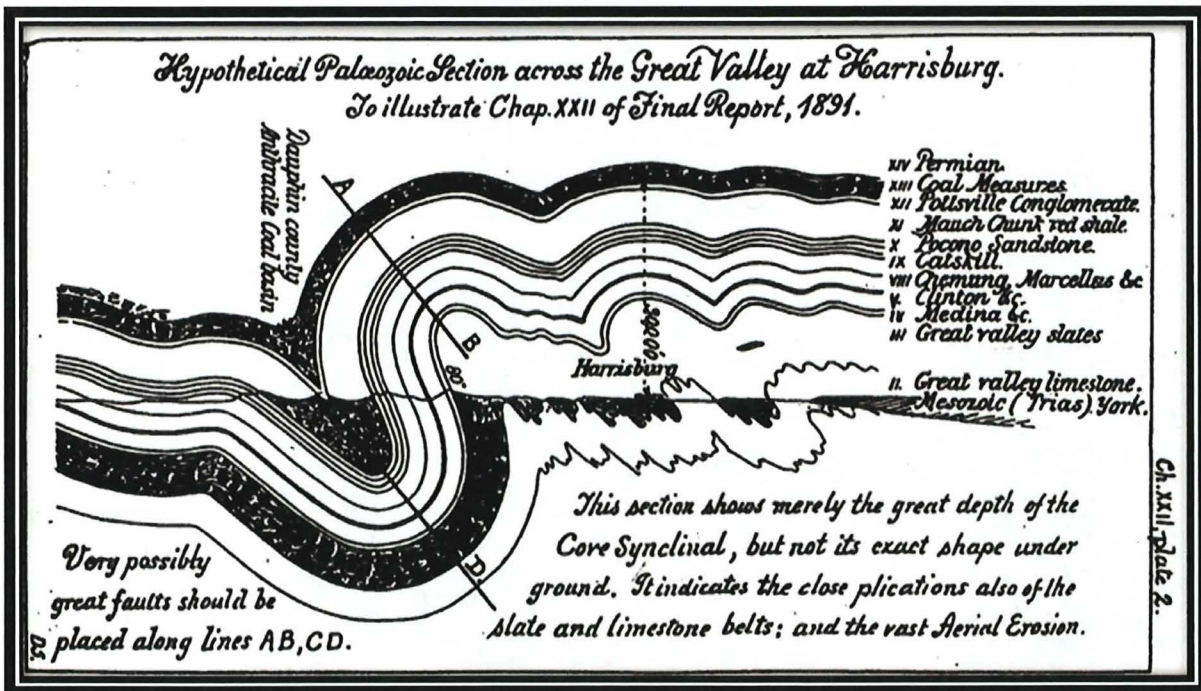


Contact of the Tuscarora and Juniata Formations at Waggoners Gap.

Interpreted as laminated beach deposits, the light colored layers of the Tuscarora exhibit neither cross layering (except in the lowermost two layers at the waist level of Shippensburg student Alex Suder) nor shale interlayers of the reddish Juniata Formation at the right side of the photo. Alex stands on the contact of the two formations.



Pennsylvania's Great Valley Section of the Ridge and Valley Province at Waggoners Gap



Cross section, looking East, across the Great Valley at Harrisburg, PA as envisioned by J. P. Lesley, 1892. This is a reasonable representation of the large amount of rock that has been eroded since the end of the Alleghanian orogeny 250 + 10 ma. This cross section constructed by a very astute geologist lacks only an indication of the very large thrust faults that carried material northwest over the Anthracite Basin. The nature of this thrusting was only understood during the latter part of the 20th century (from Sevon, 2001)

Interpretation of red shale clast origin and topography of red shale interlayers – an exercise in visualization

Reddish shale interlayers occur between many of the prominent sandstone layers that make up the bulk of the Juniata Formation exposures along the highway at Waggoners Gap. Weathering more rapidly than the sandstone layers, the shale layers are thin, recessed and difficult to examine. Originally deposited as reddish mud, they apparently became consolidated sufficiently to be eroded and be re-deposited as clasts that frequently occur within the cross-layered sandstones and, in a few examples, emphasize the cross layering. Similar red clay clasts occur in the lowermost cross-laminated layers of the Tuscarora above the beach sand facies. But, in this formation, the few shale interlayers observed are gray, not red. Where do these Tuscarora clasts originate?



Red mud clast included with gravel in cross-layered Juniata Formation sandstone at Waggoners Gap. Similar red clasts occur in Tuscarora layers.



Red mud clasts paralleling cross layering in Juniata Formation sandstone at Waggoners Gap

Additionally, clay interlayers developed topography of lumps, ripple marks, and miscellaneous surfaces that now reflect themselves as the mirrored topography seen on the underside of the overlying sandstone layers. The mud layers were also the likely site of burrowing biotic activity producing tubular features now exhibited mainly as raised features on the undersides of overlying sandstone layers.

**Burrow, likely
Arthropycus,
and cavities on
base of a Juniata
sandstone layer
at Waggoners
Gap**



Note the burrow stands in relief while the cavities are depressed into the lower surface of the sandstone layer. This vertical topography of the now absent clay layer may be deposits of burrower-ingested sediment. The depositional surface of the sandstone was relatively rugged. These surfaces are a common sight at Waggoners Gap. Some depressions on these surfaces retain the red clay of the now absent interlayer.

Are the burrows Arthropycus?

**Burrows on the
base of a
Tuscarora
Formation layer
at Waggoners
Gap**



Note that the burrows stand in relief on the layer base implying that the sand filled exposed or collapsed burrows in the underlying mud at the depositional surface. Most burrows do not retain fine details. Thus, identifying these to generic or specific detail is difficult without very close examination. At Waggoners Gap one small surface with the typical annulations of *Arthropycus alleghenyensis* occurs, allowing, by extrapolation, to identify all other burrows by this classic name.

Supergene phosphates at Waggoners Gap

(e-mail notes from Robert Smith, PA geological Survey, Retired)

"As far as I know, the first recorded recognition of phosphates at approximately this horizon was by Jack B. Epstein (1967 Subitzky volume part covering Shawangunk Formation). He found and described carbonate fluorapatite nodules. Many years later John H. Way and I found carbonate-fluorapatite nodules in Shawangunk/Tuscarora outcrop near Rockville on the east side of the Susquehanna, Blue Mountain, Dauphin County. These sedimentary nodules are very likely the "primary" source for the secondary (supergene) phosphates long known from Blue Mountain, Cumberland County."

"The main secondary (supergene) phosphate at Waggoners Gap is variscite. Specifically, it is the "Lucin-type. ... Associated minerals at Waggoners Gap include pale green, chalky wavellite and trace green turquoise. The same species have been verified in the Sterretts Gap area. The vast majority of the green and greenish minerals at both localities are variscite, not turquoise ..."



Variscite exposed as a film on joint surface of the "beach sand" facies of the Tuscarora Formation at Waggoners Gap



Supergene minerals are present at Waggoners Gap on the joint surface at Shippensburg student Alex Suter's eye height

Vertical biogenic structures at Waggoners Gap

Vertical biogenic structures occur in the Juniata Formation at Waggoners Gap. These structures occur in the layers immediately above a culvert, approximately midway in the Juniata Formation exposures.

Anne Kuebler's 1982 thesis at Bucknell University "*Trace Fossils in the Juniata Formation in Central Pennsylvania suggest Earliest Land Life in Late Ordovician Time*" describes and interprets biogenic structures that occur at Waggoners Gap in the Juniata layers as "essentially vertical, poorly defined, red clay-filled burrows" that she interprets as "evidence for earliest land life in Late Ordovician Time" (Kuebler, 1988 p.iv).

Red mud filled
vertical burrows in
the Juniata
Formation at
Waggoners Gap



Close up image of
vertical burrows in
gravelly sandstone
of the Juniata
Formation at
Waggoners Gap



APPENDIX A. WAGGONER'S GAP IN BLUE MOUNTAIN

(reprinted with author's permission from Cotter, Edward, "STOP 2. Waggoner's Gap in Blue Mountain", *SEPM-ES Guidebook*, May 1982, p.3; pp. 63 – 68.)

Horizontally laminated (beach) lithofacies overlying Juniata Formation and underlying eastern cross-laminated (braided fluvial) lithofacies

The Tuscarora Formation here forms the southeasternmost ridge in the Valley and Ridge geomorphic province, and this outcrop is the most proximal section of the formation we shall see on this trip. Toward the floor of the Great Valley below, the stratigraphic succession passes down through the Juniata and Martinsburg Formations and into Cambro-Ordovician carbonate units in the distance (Miller, 1961; Root, 1978).

This exposure demonstrates the relationship of the basal horizontally laminated lithofacies to the uppermost Juniata Formation upon which it rests. There is a small cove red interval at the top of the beach lithofacies, but in turn above the covered interval is a convincing example of the eastern cross-laminated (braided fluvial) lithofacies.

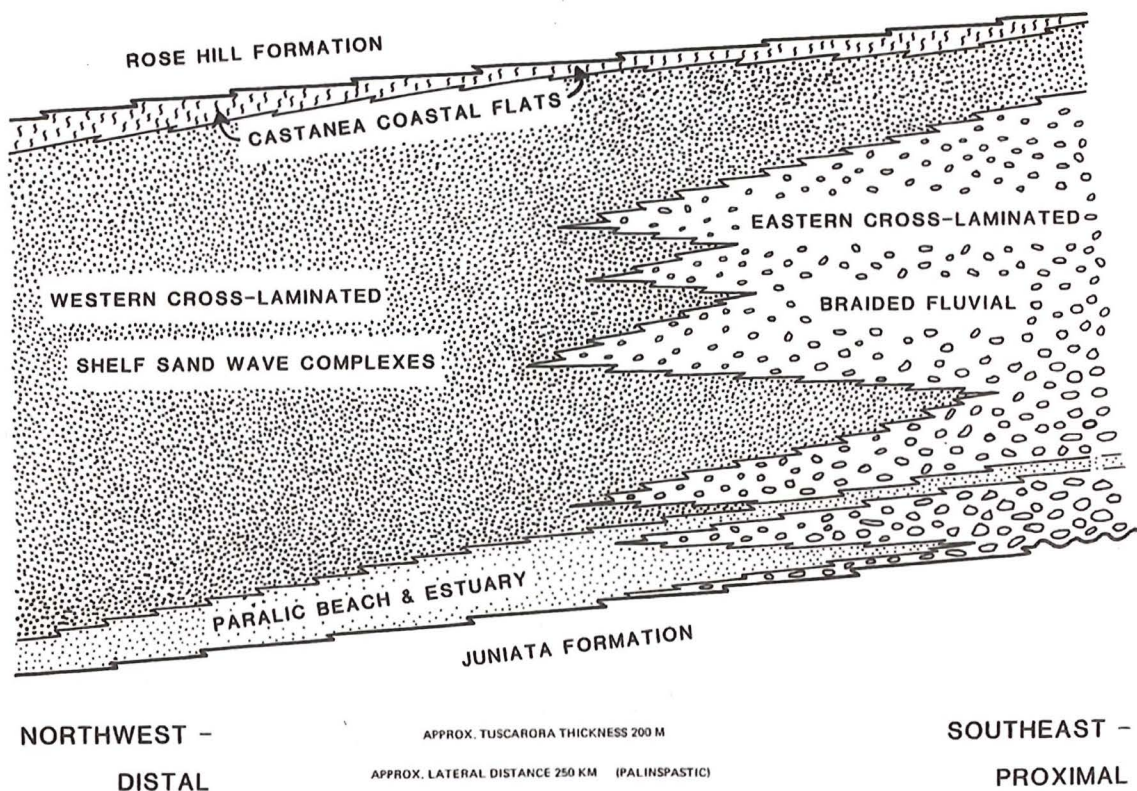


Figure 2. Generalized lithofacies profile in northwest – southeast transect of Tuscarora formation in central Pennsylvania outcrop belt.

Proximal locations, such as this and Stop 3, are significant in the context of reinterpretation of the Tuscarora. In the first place, the interpretation of beach origin for any part of the Tuscarora might be a contribution. But in addition, the demonstration of a lithofacies of beach origin at the base of the Tuscarora here at proximal localities shows that a significant transgressive event occurred as Tuscarora history began. The importance of this transgression will be reinforced at subsequent stops at which we view the base of the Tuscarora. This outcrop also demonstrates in a convincing way the role of depositional process in modifying the sandstone composition.

Blue Mountain, and the Tuscarora Formation that is its cause, can be traced eastward and northeastward to the Delaware Water Gap and on into New Jersey and New York. The basal horizontally laminated lithofacies has been traced for only part of that distance. Good exposures of the basal unit occur at Sterrett's Gap, at Susquehanna Gap (where it forms the Rockville Dam Member of Swartz, 1957; and Unit 22 of Dyson, 1967), and at Swatara Gap, about 40 km to the east. Outcrops east of there inadequately expose the base of the Tuscarora, but there are suggestions that the horizontally laminated lithofacies extends almost to the Schuylkill River, about 110 km east of this locality. Lateral correlation of the basal units of the Tuscarora is shown in Figure 12 and also on the composite lithofacies profile (*Fig. 2*).

Juniata Formation

The maroon-red Juniata consists of interbedded composite units of sandstone and subordinate thin darker shales. The sandstone is medium- to coarse-grained litharenite, with poor sorting and subangularity (*Fig. 25C*). Most of the sandstone is cross-stratified, with troughs more abundant than planar types. Gravel sizes occur at the bases of some beds, and shale intraclasts are present. There is a poorly developed cyclicity of fining- and thinning-upward sequences. Note that the bases of a number of sandstone beds contain biogenic structures, some of which are organized into forms that suggest *Arthropycus*.

These features indicate that deposition took place in braided river systems. This is not different from previous interpretations. What is important to note is the contrast with the features and origin of the basal 30 meters of the Tuscarora. However, in considering that striking contrast, do not overlook the similarity between features and origin of the uppermost Juniata and the features and origin of the eastern cross-laminated lithofacies above the covered interval over the beach lithofacies. These similarities include lithologic proportions sandstones composition and texture; interbedded shale and intraclasts of that shale; physical and biogenic structures, and cyclic vertical sequences.

I interpret this to mean that those uppermost Juniata river systems continued into Tuscarora time with the same magnitude and fluvial style. The only major change is in the color of the deposits. The basal transgressive event caused the deposition of a beach sequence along a retrograding coast, but there were times and places during which the river systems prograded out over the beach deposits. This is a pattern we shall examine at other stops (Stops 3, 6).

Basal Horizontally Laminated Lithofacies

In contrast with the units above and below, the basal 30 m of the Tuscarora here is all sandstone; there is no shale either interbedded or as intraclasts. Above a basal 2 m of coarser, poorly sorted sandstone, the unit is all fine to medium, well sorted, and has rounded grains (**Fig. 25B**). Grain size increases slightly at the top of the unit. All 30 m of this sandstone is quartz arenite; there are no lithic grains or chert.

The most common sedimentary structure is horizontal (even parallel) lamination. In thin section (**Fig. 25B**) this lamination is seen to consist of alternating laminae of coarser and finer grains. Some of the laminae show the reverse grading referred to as "beach lamination" by Clifton (1969). At about 15 m above the base, there is the broadly arching style of lamination known as antidune lamination on beach foreshores (Hayes and Kana, 1976) (**Fig. 26A**). Symmetrical ripples, although not photogenic, are present on exposed bedding planes (**Fig. 26B**). Other symmetrical ripples can be seen in cross section on the outcrop face (examine outcrop at about 14.5 m above base, near lower part of section illustrated in **Figure 26A**). Cross-laminated beds are not common in this unit, and the two-dimensional nature of the outcrop surface makes it difficult to interpret those that do occur. I think that some of the cross laminae are inclined to the east or southeast; one of these occurs about 16 m above the unit base (near the painted black 14 on outcrop). Do you agree?

When one compares the 30 m of horizontally laminated sandstone with the underlying upper Juniata Formation and the overlying eastern cross-laminated lithofacies, there are some important features missing from this unit. There is no shale, either interbedded or as intraclasts. The average grain size of the sandstone is smaller, and there are no very coarse sand or gravel particles. Lithic grains and chert are missing from the sandstone. Cross lamination is almost absent, and the few examples show possibly anomalous transport direction. There are no apparent patterns of grain sizes or sedimentary structures. And there are no biogenic structures, such as *Arthropycus*.

The characteristics of the basal horizontally laminated lithofacies consistently indicate that the environment of deposition was the lower foreshore and upper shoreface of a wave-dominated beach system.

Figure 25. Photomicrographs of sandstones at Waggoner's Gap; for each, the narrow dimension is



Figure 25A.
Upper Tuscarora unit; eastern
cross-laminated lithofacies above
covered zone

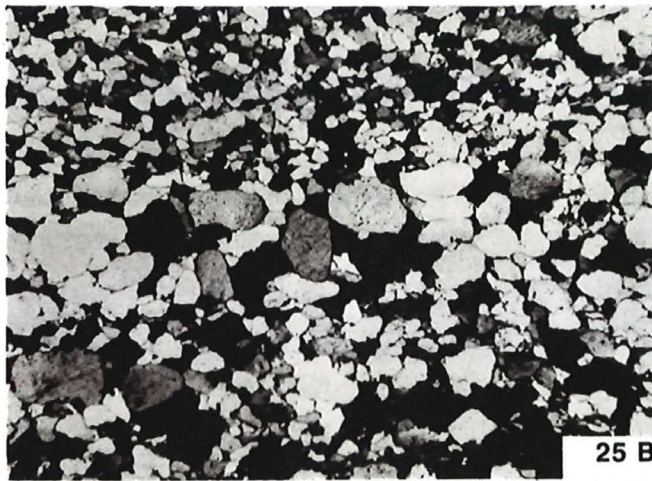


Figure 25B.
Basal horizontally laminated
lithofacies about 15 m above
Juniata contact. Shows inversely
graded laminae. Pure quartz
arenite.



Figure 25C.
Juniata Formation about 3 m below
contact with Tuscarora. Abundant
chert and some rock fragments.

3.7 mm

Eastern Cross-Laminated Lithofacies

Above the covered interval, the Tuscarora Formation has features that, but for color, are more like those of the uppermost Juniata than of the basal horizontally laminated lithofacies. Cross-laminated composite units of sandstone are interbedded with thin and lenticular beds of gray and greenish gray shale. The sandstone is medium to coarse grained, and contains granule and pebble lags at bed bases (**Fig. 26C**). Within the sandstone are shale intraclasts of the same composition as the thin shale interbeds. The sandstone is sublitharenitic, with fragments of sedimentary, metamorphic, and chert origins (**Fig. 25A**).

The most common sedimentary structure is trough cross lamination (**Fig. 26D**), generally ranging from 10 to 20 cm thick. Smaller scale current ripple lamination is uncommon, but present in finer-grained beds. The bases of a number of sandstone beds have preserved the biogenic structure *Arthropycus*.

As reviewed in earlier parts of this guidebook and at Stop 1, the characteristics of this lithofacies indicate deposition in braided fluvial systems. As stated earlier, the similarity between this unit and the uppermost Juniata suggests that the magnitude and style of the river system was approximately the same for each unit, and that the transgression of the wave-dominated beach coast was temporarily reversed.

The compositional contrast of the horizontally laminated lithofacies with this cross-laminated lithofacies also illustrates the role of depositional processes in determining sandstone composition. If the quartz arenitic composition of the basal Tuscarora were due to the introduction of a changed source material to the depositional site, one should expect that the cross-stratified sandstone above the horizontally laminated sandstone would also be quartz arenite. However, there is a distinct compositional contrast between these two units, with the upper fluvial unit returning to the sublitharenitic composition characteristic of the uppermost Juniata, and also characteristic of the fluvial Tuscarora seen at Millerstown (Stop 1). Instead, composition of the sandstone is related to depositional environment. Fluvial sandstones are sublitharenitic to litharenitic (whether Juniata or Tuscarora) and the beach sandstone derived from that fluvial sandstone is quartz arenite.

Figure 26. Features at Waggoner's Gap. Scale is 15.2 cm long.



Figure 26A. Antidune stratification at about 15 m above Juniata contact.



Figure 26B.

**Symmetrical ripples on
bed base; slightly
above A.**

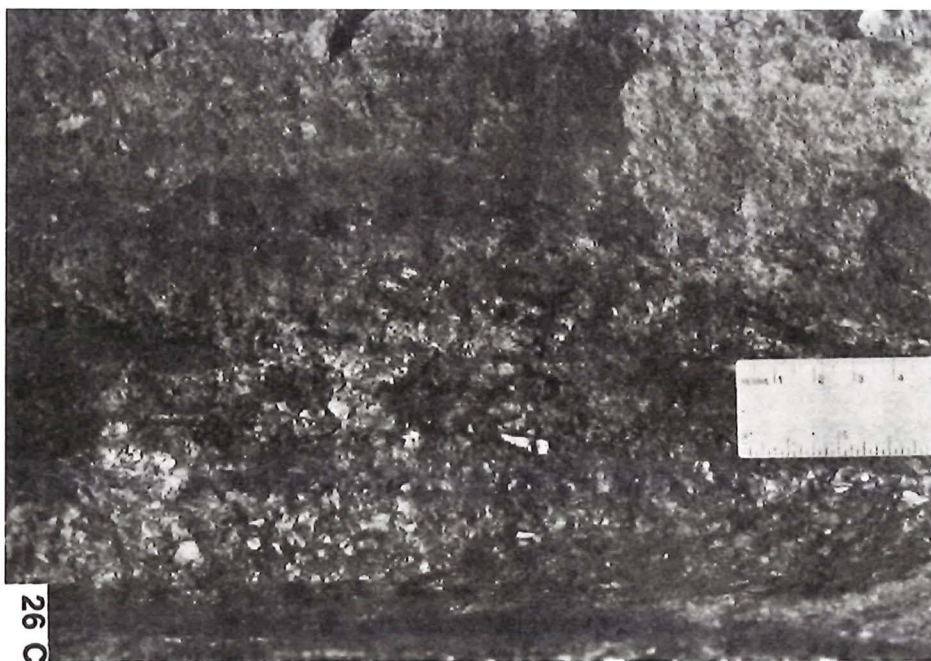


Figure 26C. Basal lag gravel overlying shale bed; upper unit of eastern cross-laminated lithofacies.



Figure 26D. Trough cross-laminated sandstone interbedded with shale; eastern cross-laminated unit above covered zone.

APPENDIX B.

Upper surface of a
colluvium block of
Tuscarora Formation
sandstone at
Waggoners Gap.






Depressed into the upper surface implies that the Arthropycus burrowers were excavating into the underlying sandstone layer as well as the mud interlayer and overlying layer

Arthropycus
burrows and
“pimpled” relief
features on the
base of Juniata
sandstone block at
Waggoners Gap.



Base of Juniata
sandstone layer at
Waggoners Gap
with reddish mud
lumps embedded
into sandstone
base.



Interval Mileage	Cumulative Mileage	 = Stop Sign;  = Traffic Light; "T" = T Intersection; TR = Township Route; "Y" = Y intersection
0.0	69.5	Drive south on PA Route 74
7.7	77.2	Turn right onto College Street in Carlisle
0.5	77.7	Turn left onto West High Street
0.4	78.1	Turn right onto South Hanover Street
0.1	78.2	ARRIVE at Comfort Suites. END of 2014 FCOPG Field trip  <div> Comfort Suites, Carlisle PA </div>

HYDROGEOLOGY OF BOILING SPRINGS, CUMBERLAND COUNTY, PENNSYLVANIA

Noel Potter, Jr., Department of Earth Sciences (retired), Dickinson College,
Carlisle, PA 17013 pottern@dickinson.edu



Figure 1. Boiling Springs “Children’s Lake,” looking south. Some springs occur near the rocks in the lower right corner.

Boiling Springs is a village about 6 miles SE of Carlisle in South Middleton Township, Cumberland County, PA. The springs are at and near the N end of Boiling Springs lake (Fig. 1) just SE and N of the junction of Forge Road (the main road from Carlisle) and PA 174. Park on Front St., W of the lake. Several springs bubble up (thus the name “boiling,” no hot water) in the NW corner of the lake (Fig. 2). The most prominent spring is just N of the Boiling Springs Tavern—walk N along Forge Road, and turn right on the sidewalk to the spring enclosed by a sidewalk and steel railing (Fig. 3). The local high school athletic teams are called “The Bubblers.” The PA Fish Commission now owns the lake, and fishing is reserved for children. A favorite pastime is to “feed the ducks”—take some stale bread.

Boiling Springs is actually a group of springs rather than a single one. General hydrogeology, summarized here, is from Becher and Root (1981, see also Becher, 1991). Average annual precipitation is about 42 inches (107 cm)/year, of which slightly more than half runs off and the rest returns to the atmosphere through evaporation and transpiration. Average discharge of the springs is about 16.5 million gallons/day.

This makes the springs the largest in Cumberland County, and seventh largest in Pennsylvania.



Figure 2. Springs emerging from between rocks in NW corner of Children's Lake.



Figure 3. Largest spring at Boiling Springs, behind (N of) Boiling Springs Tavern. Most water emerges from large hole in lower left of photo. This is the spring where Becher (1991) measured temperature and conductivity.

The springs are in the Cambrian Elbrook formation (Root, 1978), which is exposed near the springs in the NW corner of the lake and near the large spring behind the Tavern. The springs here occur at the junction of 2 branches of a Mesozoic diabase dike shaped like an inverted Y, with the open end facing south (Fig. 4). Both branches extend southward at least to the base of South Mountain, beneath colluvium on top of carbonates, and act as hydrologic dams underground funneling ground water toward the springs. Hawman (1977) used a magnetometer to map the subsurface extent of the eastern dike beneath colluvium all the way to the base of South Mountain (Fig. 5).

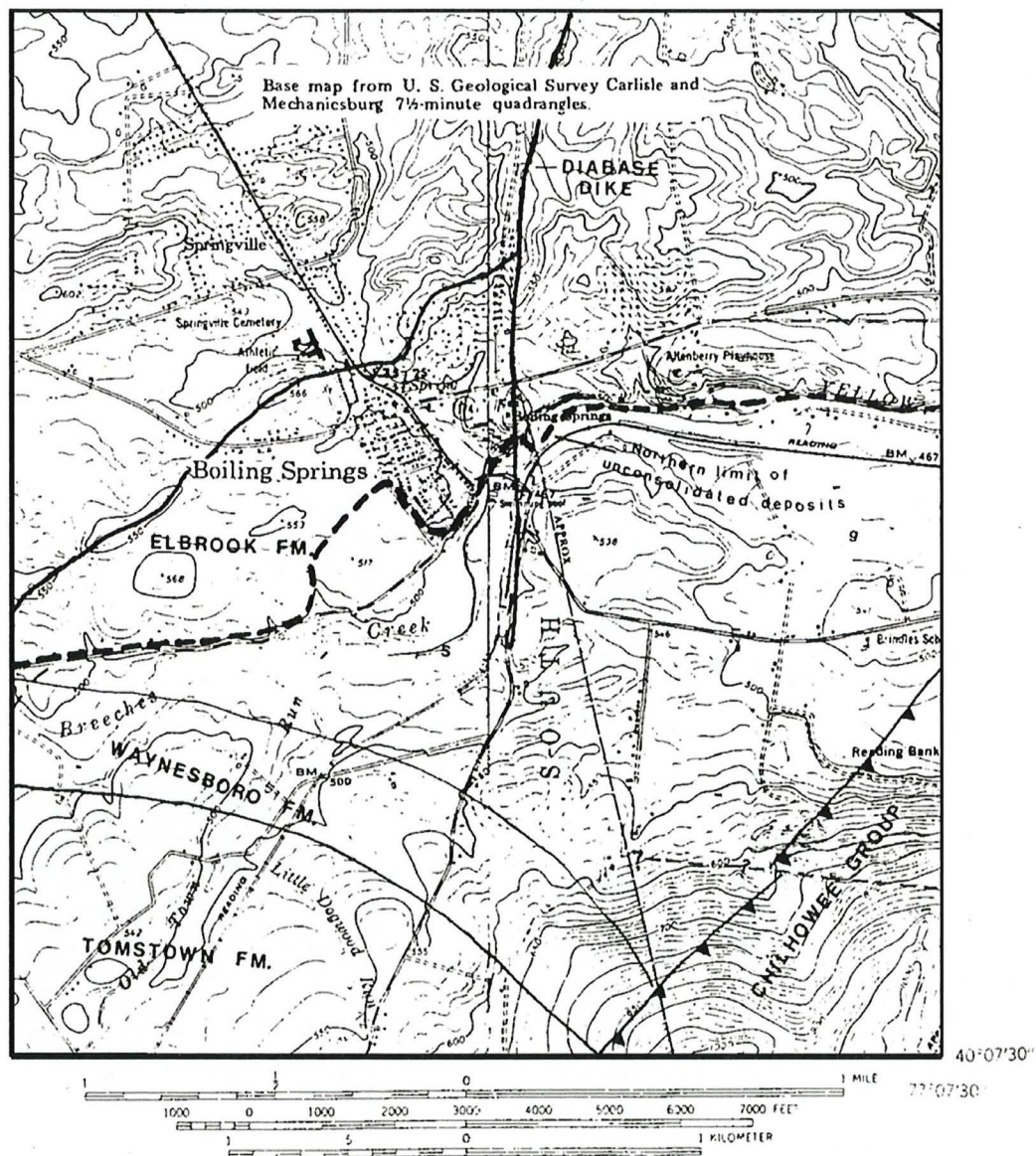


Figure 54. Map of Boiling Springs area

Figure 4. Note that springs occur at the confluence of the two branches of the diabase dike. (From Becher, 1991, p. 190). Heavy dashed line is the northern limit of colluvium/alluvium of quartzite from South Mountain over Tomstown dolomite and younger carbonates.

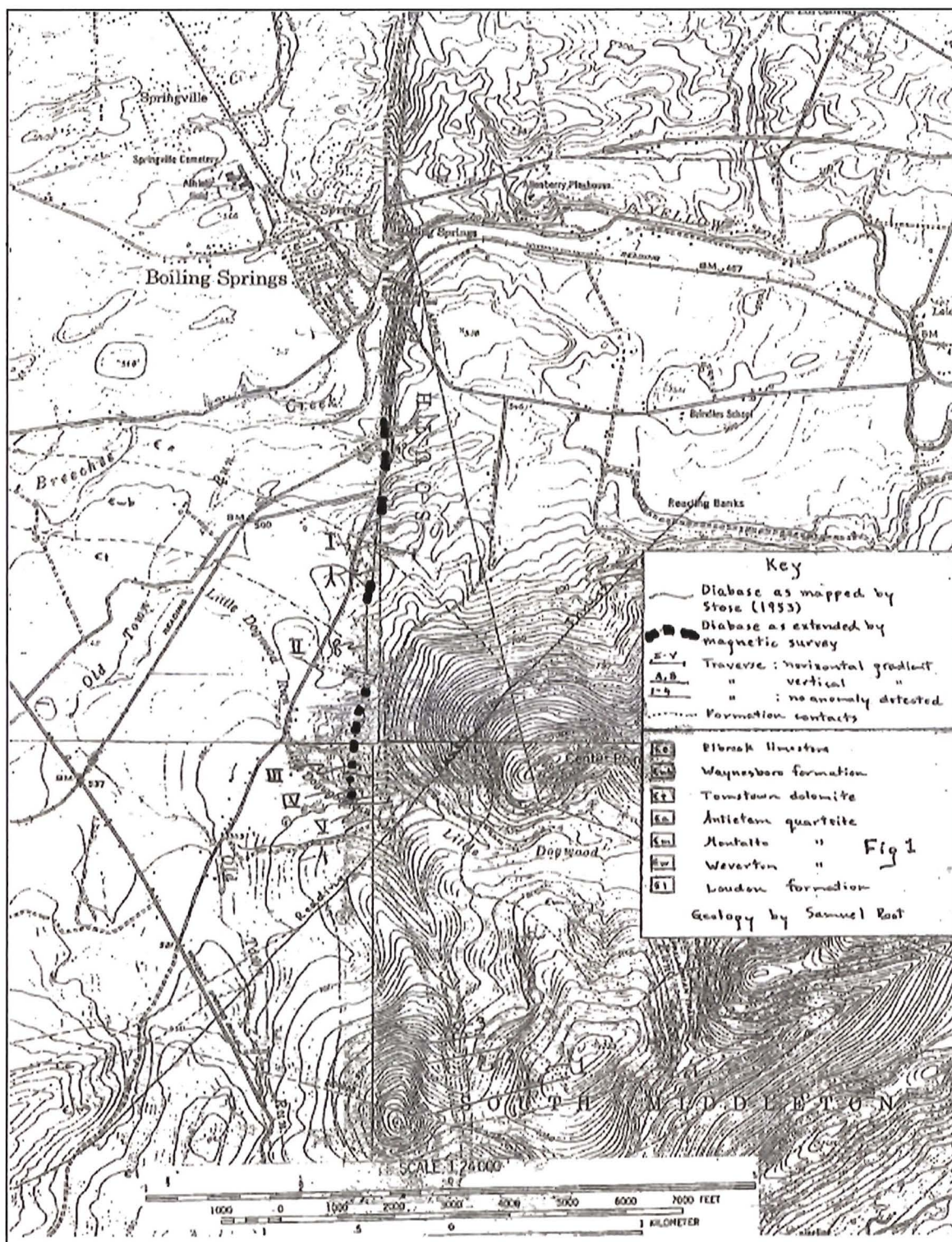


Figure 5. Map by Hawman (1977) showing extension of diabase dike (heavy dashed line) southward beneath colluvium/alluvium as determined with a magnetometer.

The diabase dike, which is about 50 ft wide, extends all the way across the Cumberland Valley, variously known as Stony Ridge or Ironstone Ridge, to the north and across Blue Mountain into Perry County (Figs. 6 and 7). Generally drainage in the middle of the Cumberland Valley is toward the east, and groundwater flows that way. Contours on the water table are in Becher and Root (1981, Plate 1). The water table on the west side of the diabase is about 50 feet higher than on the east side.



Figure 6. Ironstone Ridge looking N, defined by trees where it is too stony to farm. Nearest road crossing ridge is Lisburn Road. Note offset in ridge near upper left of photo.



Figure 7. Aerial view of Ironstone Ridge at PA Turnpike, looking N. Diabase dike is dark rock just to left of bridge. Lighter rock is limestone.

The thickness of the colluvium/alluvium at the northern base of South Mountain is not well known S of Boiling Springs. However at the site of the PPG Industries plate glass plant about 2.3 mi W of Boiling Springs pre-construction test borings in 1971 revealed thicknesses of 50-200 ft of colluvium over clay residuum from weathering of the underlying Tomstown dolomite from 0 to ~100 ft thick. One well went 230 ft and never penetrated bedrock. Several wells encountered cavities in the bedrock as much as 10 ft deep. It is clear, as described by Becher and Root (1981, p. 17-18) that water running off South Mountain is acidic and that it infiltrates the colluvium and dissolves the carbonates beneath, creating solution passages and residuum. Numerous shallow karst depressions on the surface of the colluvium attest to the solution of the underlying bedrock.

Becher (1991) determined a surface drainage area for the springs of about 3 mi², but the discharge of the springs requires a catchment area of about 20 mi², using mean annual precipitation and allowing for evapo-transpiration. It is clear that most of the water in the springs comes from the N flank of South Mountain and moves beneath the colluvium and Yellow Breeches Creek to emerge here. The basin behind the Tavern is 10-15 ft above Yellow Breeches Creek. Temperature of the spring water in the basin behind the Tavern averages about 12.9°C (near mean annual temperature) and fluctuates only 0.2°C annually, and lags air temperature changes by 4-6 months (Fig. 8-2). Furthermore, specific conductance (a measure of dissolved ions) of the spring water is about half that in nearby wells, but is like water in wells in the carbonate rock on the flank of South Mountain.

Root (1976) describes how shortly after new construction at the Boiling Springs High School, just NW of the springs, a corner of the building settled into a sinkhole that opened after a series of heavy rains. Other sinkhole problems have occurred near Boiling Springs since 1975.

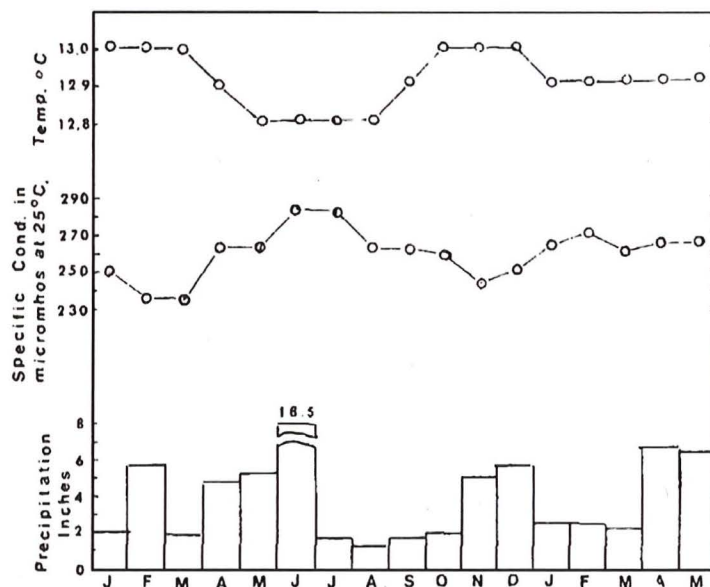


Figure 56. Monthly temperature and specific conductance of water from Boiling Springs and precipitation at Carlisle.

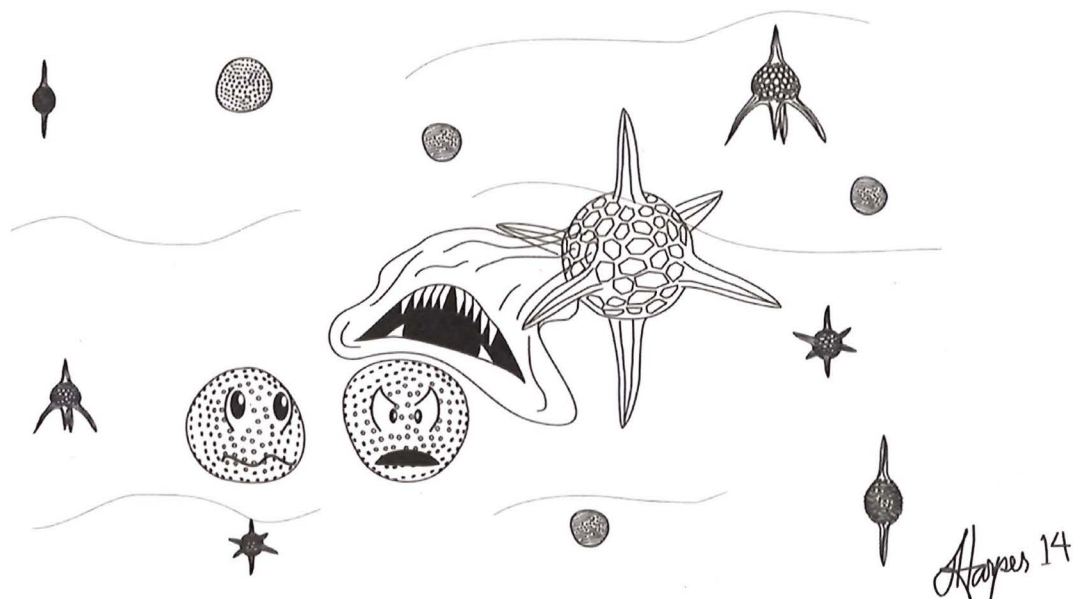
**Figure 8. Note that water temperatures lag air temperatures by 4-6 months.
(From: Becher, 1991, p. 191)**

References

- Becher, A. E. and Root, S. I., 1981, Groundwater and Geology of Cumberland Valley, Cumberland County, Pennsylvania: Pennsylvania Geological Survey, 4th Series, Water Resource Report W-50, 95 p.
- Becher, A. E., 1982, STOP 1. Hydrogeology and the source of Boiling Springs, Cumberland County, Pennsylvania: *in* Potter, N., Jr., *editor*, Geology in the South Mountain area, Pennsylvania: Guidebook, 1st Annual Field Trip of the Harrisburg Area Geological Society, p. 4-8.
- Becher, A. E., 1991, Stop 7, Hydrogeology and the Source of Boiling Springs, Cumberland County, Pennsylvania: *in* Sevon, W. D. and Potter, N., Jr., *eds.*, Geology in the South Mountain area, Pennsylvania: Guidebook for the 56th Annual Field Conference of Pennsylvania Geologists, p. 189-193.
- Hawman, R., 1977, Magnetometer Survey of a Diabase Dike South of Boiling Springs, PA: Dickinson College, Department of Geology, Independent Research Paper, 14 p. plus maps and profiles.
- Root, S. I., 1976, Engineering problems in areas of limestone springs: Pennsylvania Geology, April issue, p. 6-9.
- Root, S. I., 1978, Geology and Mineral Resources of the Carlisle and Mechanicsburg Quadrangles, Cumberland County, Pennsylvania: Pennsylvania Geological Survey, 4th Series, Atlas A 138ab.

GREAT MOMENTS IN GEOLOGIC HISTORY

Part 8 - The Middle Devonian



I don't mind them moving into the neighborhood, but I sure wouldn't want my sister to marry one.

GEOLOGY GUIDE TO THE YELLOW BREECHES CREEK FROM MESSIAH COLLEGE TO McCORMICK ROAD

Author – Rose-Anna Behr, P.G., Pennsylvania Geological Survey

Leader – Gary Kribbs, P.G., AEON Geoscience, Inc.

Introduction

The 2014 Field Conference of Pennsylvania Geologists preconference kayak trip explores the Yellow Breeches Creek from Messiah College to McCormick Road. This route is part of the Yellow Breeches Creek Water Trail with established launch and take-out areas (Cumberland County Planning Department, 2012). Launch permits are required from either the Department of Conservation and Natural Resources or the Pennsylvania Fish and Boat Commission. The water level is kayakable at 1.2' but there will be some scraping. At a level of 3.0', some of the outcrops may not be visible. The water level of the creek can be determined at the USGS stream gaging station near Camp Hill (USGS, 2014).

The Yellow Breeches Creek originates on South Mountain in Michaux State Forest (Susquehanna River Basin Commission, 2007). The stream descends the mountains and meanders 49 miles through the Cumberland Valley to the Susquehanna River. The watershed is 219 square miles and includes Adams, Cumberland, and York Counties (Figure 1). The creek is a world-renowned limestone stream, a High-Quality Cold Water Fishery, and a designated Scenic River.

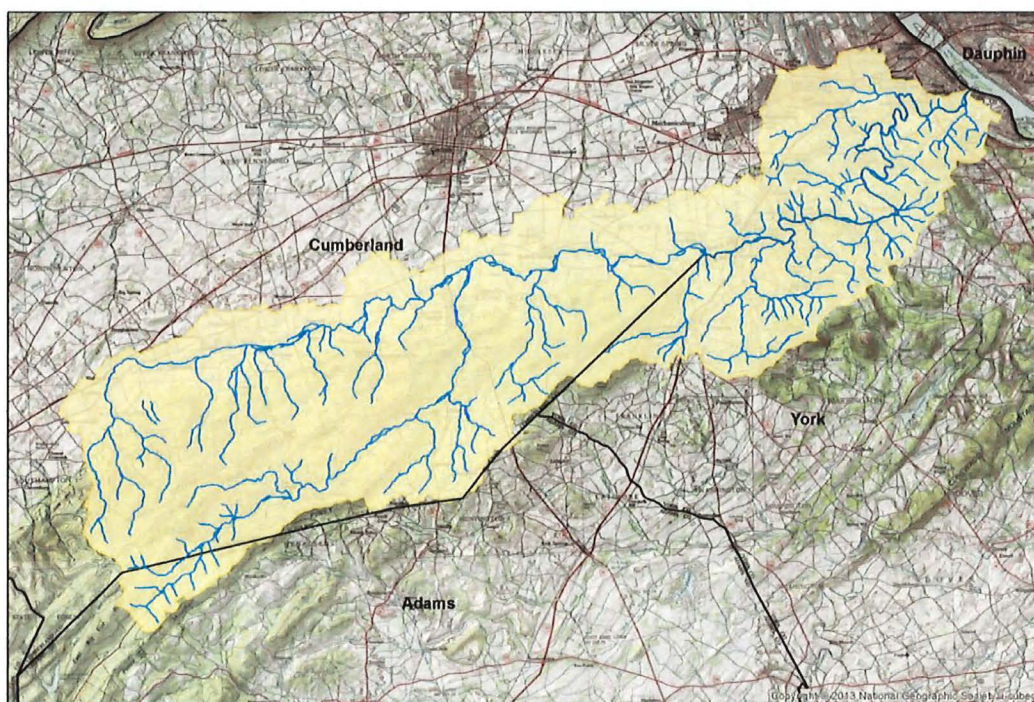


Figure 1. Yellow Breeches watershed covers parts of Adams, Cumberland & York Counties

The creek name has changed over time (Rowland, 2001). It is unknown if the Susquehannock tribe had a name for the river, but the Shawnee tribe – who moved in after the Susquehannock's demise knew the creek as Shawna Creek. For thirty years of their residency, the creek was also known as Callapus-Kinck, Callapus-Sink, Callapatschink, and Shawnee Creek. Callapatscink supposedly meant, “where the water turns back again” (Miller, 1909). The creek name as we know it today was first recorded in 1734 as “Yellow Britches” Creek with reference to an old-timer who washed his britches in the creek and turned it yellow (Rowland, 2001). A second theory is that it is a corruption of Yellow Beeches – from the abundant beech trees that grew on the banks. By 1736, it is mostly recorded as the Yellow Breeches Creek.

Setting

The Yellow Breeches Creek is famous for its trout fishing because it is largely a cold, limestone spring-fed stream. The stream meanders through two stratigraphic sequences of Cambro-Ordovician limestones and Ordovician shales before entering the Mesozoic rift basin and the setting for our trip. Downstream it exits the Mesozoic

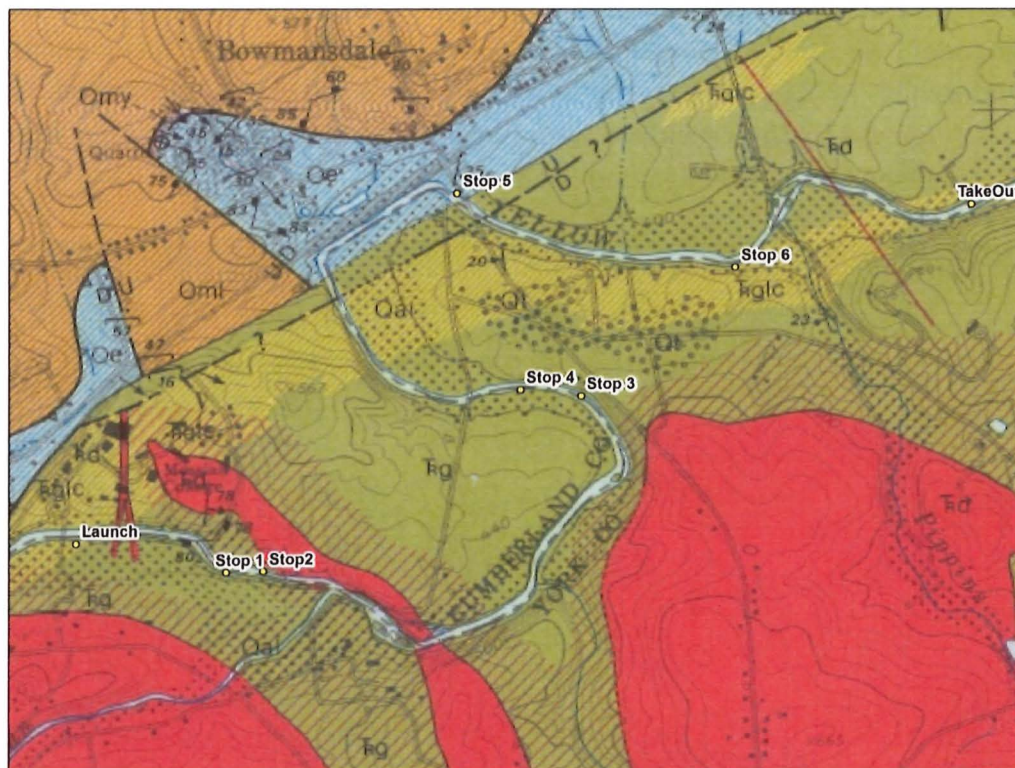


Figure 2. Geologic map of the river trip area (from Root, 1977)

basin and returns to the limestone and shale valley. Our trip will take us through Triassic sedimentary, intrusive, and metamorphosed rocks; and then out of the Triassic basin for one stop (Figure 2). The Cambro-Ordovician limestones and Ordovician

shales are grouped into two stratigraphic sequences: the Lebanon Valley sequence and the Cumberland Valley sequence. Though similar in age and lithology, the two have undergone disparate deformation events. The Lebanon Valley sequence was deformed into a series of nappes during the Ordovician Taconic orogeny. The Cumberland Valley sequence was folded into the gently plunging South Mountain anticlinorium during the Pennsylvanian-Permian-Alleghanian orogeny that was a part of the assembly of Pangea. Late-Alleghanian deformation emplaced the Lebanon Valley sequence on top of the Cumberland Valley sequence by the aptly named Yellow Breeches Thrust. During our paddle, we briefly exit the Triassic basin and visit one exposure of Lebanon Valley sequence Ordovician-age Epler Formation.

Sedimentation

Not long after Pangea was assembled, it began to tear apart. Several Triassic rift basins formed along the eastern seaboard as Africa began its departure (Glaeser, 1966). In Pennsylvania, Triassic rifting formed the Gettysburg-Newark Basin. The two are

separated by a narrow neck and an arbitrary line. Our kayak trip will follow the north edge of the Gettysburg Basin. As rifting developed, steep-normal faults formed at or near the northern boundary of the basin. The basin was an arid closed, non-marine depositional setting. Periods of drying resulted in mud cracks, raindrop impressions and formation of glauberite, a sodium chloride phosphate that results from evaporation in arid lakes (Stose and Jonas, 1939). Sediments shed from a granitic source to the south slowly filled the basin 15,000 feet deep (Figure 3). The lower half, the New Oxford Formation, is dominantly sandstone with some conglomerates. We will not see them on this trip. As rifting continued, sedimentation shifted to the north. These sediments formed the

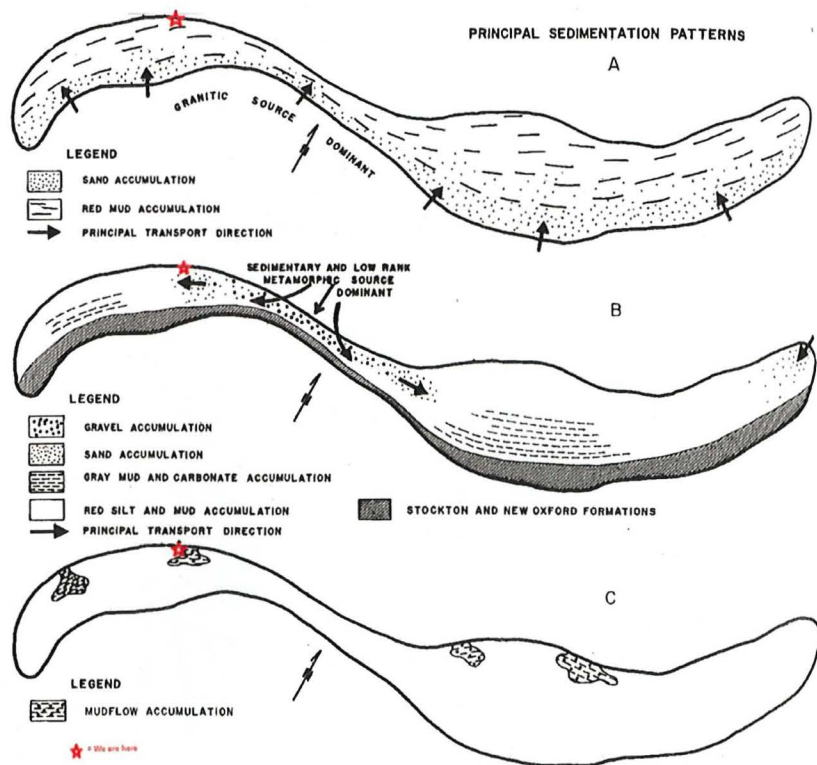


Figure 3. Basin- outline maps showing deposition of Triassic sediments. Our area marked with red star (from Glaeser, 1966)

basin 15,000 feet deep (Figure 3). The lower half, the New Oxford Formation, is dominantly sandstone with some conglomerates. We will not see them on this trip. As rifting continued, sedimentation shifted to the north. These sediments formed the

Gettysburg Formation. The Gettysburg Formation consists of continental red shales and medium to fine-grained sandstones with a few conglomerates. Impure limestones interbedded with red shales have also been reported (Stose and Jonas, 1939). In the area we will be visiting, the sediments actually on-lapped the edge of the basin. The northern basin-bounding fault is buried somewhere south of the Triassic-Ordovician rock contact (Figure 4).

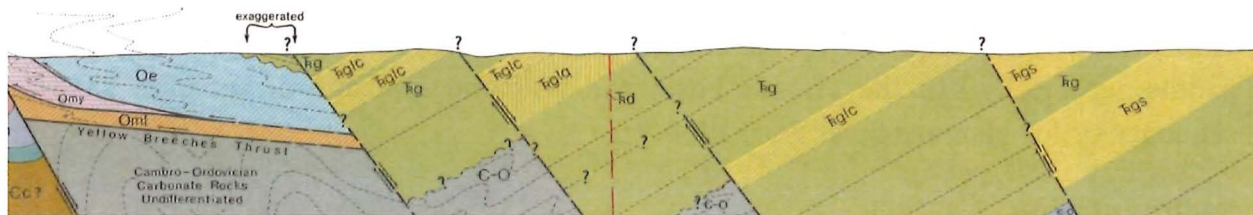


Figure 4. Cross section of Triassic basin showing dipping Triassic strata, normal faults, and sediments on lapping the edge of the basin (from Root, 1977)

The conglomerates are of interest and will be seen at more than one stop. They tend to be poorly sorted with a mud matrix. Clasts consist of limestone or quartzite, or limestone AND quartzite. Some clasts are fifteen inches across (Stose and Jonas,

1939). Angular limestone clasts are locally derived (Glaeser, 1966). Cobbles of Oriskany sandstone with large brachiopods have been reported, though it is a long way to any modern Oriskany outcrops. These conglomerates are interpreted to have been mudflows forming alluvial fans (fanglomerates) in the basin, likes is happening in the southwestern United States today (Glaeser, 1966; Root, 1977). The conglomerates have been stabbed, polished, and sold as Potomac or Calico marble.

Several kinds of fossils have been reported in the Triassic in York County (Figure 5). Plant fossils include thirty-one species of ferns, equisetum, cycads, ginkgoes, conifers, and ferns. Dinosaur footprints have been recorded next door in Adams County (Figure 6). In the New Oxford Formation, crocodile teeth and crustaceans have been found. To the east, reptile and fish fossils have been found in the Gettysburg Formation. Keep your eyes open, it would be great to find them along the Yellow Breeches Creek.



Figure 5. Plant fossils of the Gettysburg Formation collected and drawn by A. Wanner. A.) and B.) Conifer, C.) Ginkgo, D.) Fern, E.) Cycad. (Figure from Stose and Jonas, 1939).



Figure 6. Footprints of *Anchisauripus sillimani*, a carnivorous dinosaur, in Gettysburg Formation sandstone from Adams County. (Figure from Stose and Jonas, 1939)



Intrusion

As rifting continued, the continental crust grew thin, allowing hot magma to flow up the normal faults and bedding planes. The magma was quartz normative tholeiitic basalt, better known as diabase. It forms saucer-shaped sills and near-vertical dikes, taking advantage of joints and faults. The sills dip north-west, parallel to bedding. There are two types of diabase in York County, and ours is the York Haven type (Smith in Root, 1977). Titanium dioxide forms 1.1% of the chilled margins. The mafic minerals include olivine, augite, hypersthene, and pigeonite. The felsic minerals are mainly the plagioclase andesine. Labradorite, magnetite, apatite, and quartz are also reported (Stose and Jonas, 1939). The local term for the rock is ironstone. As you hammer on the outcrop at the diabase stop, you will understand why.

Several late-stage dikes were emplaced in the waning stages of the failed rifting. Stose and Jonas (1939) report one following a normal fault near the McCormick Road take out point. Root (1977) agreed with the dike placement, but did not agree it followed a fault.

Metamorphism

As the hot magma emplaced within the country rock, heat and hydrothermal fluids altered the host rock. Typically, the reds are bleached gray. Rocks are baked hard to hornfels and procelanite. The baked zone is typically a quarter- to half- a mile wide. Secondary minerals formed including epidote, specular hematite, zeolites, heulandite, and chlorite.

Four tenths of a mile upstream the launch point is the Grantham iron mines. High-grade magnetite ore was extracted from 1860 to 1890 (Stose and Jonas, 1939). The three mines are the Landis, or Fuller Mine, which cut two tunnels from the railroad, the Porter Mine, which was forty feet deep and went fourteen feet below the creek, and Shelley Mine, which cut through twenty feet of diabase to get to the ore. All extracted iron-ore from the limestone fanglomerates near the diabase. Spencer (1907) reports no ore could be found in the dumps. More famous and extensive than the Grantham mines are the Dillsburg mines located about four miles south. Both of these ores are referred to as Cornwall-type ores but were not mined as extensively as those of Cornwall, Pennsylvania.

Associated with the iron-ores and contact metamorphism are small yellow- green garnets. They are reported at the Grantham mines and a prospect pit on Stony Run (Stose and Jonas, 1939). Ten miles east of Grantham, a limestone fanglomerate whose clasts dissolved during metamorphism hosts beautiful, euhedral two centimeter-wide andradite garnets.

Geomorphology

Stose and Jonas (1939) mapped Eocene terrace deposits five hundred feet above the Susquehanna. Root finds these difficult to trace to the Yellow Breeches area (Root, 1977). The high terraces are not planar making them difficult to discern. Terrace deposits are several feet thick and locally up to ten feet thick (Root, 1977). Clasts are locally derived Triassic sandstone and conglomerates. Minor amounts of Paleozoic quartzitic sandstone are also noted. These have a red, sandy matrix. On the hilltop just east of Lisburn, Root (1977) mapped an extensive area of this terrace.

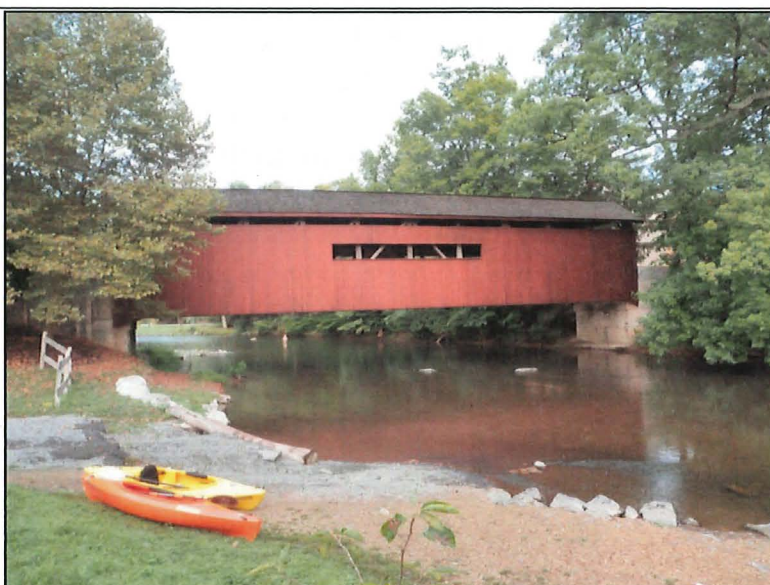
A lower terrace, forty to sixty feet above the creek of Quaternary age is also mapped (Stose and Jonas, 1939; Root, 1977). This deposit is a thin discontinuous

veneer, only a few feet thick along the Yellow Breeches (Root, 1977). Root has mapped this deposit west of Lisburn, and also south of our take out point along McCormick Road (Figure 2). This deposit is made of well-rounded siltstone, sandstone, and quartzite, with minor vein quartz pebbles in a poorly indurated reddish-brown silt-clay matrix (Root, 1977).



Alluvium exists along the modern stream. No effort has been made to map this carefully (Root, 1977). Along the creek bank, the author noted cobbles, gravel, and sand-size material of recent alluvial age.

YELLOW BREECHES: MESSIAH TO MCCORMICK RIVER LOG

**Figure 7. Bowmansdale
Covered Bridge on the
Messiah College campus
just upstream of launch point**
Photo by K. Hand



Mile	Description
0.0	Put in on the right bank of the Yellow Breeches Creek just downstream of the covered bridge at Messiah College in Grantham, PA. The college maintains this public launch and parking is permitted in the Starry Field Sports area lot. Stream elevation is 400 feet above sea level. (coordinates = 40.15513 -76.991)
	Bowmansdale Bridge (Figure 7) is a Burr truss bridge in 1867. It is a single span of 112 feet and is 15 feet wide. It was originally located in Bowmansdale (Figure 8) which we pass on our trip. In 1971, it was donated to the college and moved to its current location.

		<p>Figure 8. Covered bridge at Bowmansdale labeled in Stose and Jonas (1939) second printing</p>
0.14	Footbridge crosses creek.	
0.30	<p>STOP 1 RIVER RIGHT – As the river curves around to the left, a large cut bank with an outbuilding on top reveals a five-foot tall outcrop of Triassic rocks. About seventeen stratigraphic feet are exposed, as beds dip gently west. The rocks include slightly pink, coarse-grained sandstone with clay-rip up clasts and interbedded claystone and some blocky siltstone. A ten-foot thick bed of fanglomerate contains limestone, claystone, quartzite and chert clasts supporting each other in a clay matrix (Figure 9). This bed weathers easily into a lumpy, nodular, buff to pink, gray, and salmon-colored mess that at a glance looks alluvial. Limestone clasts in fanglomerates only occur on the north side of the Triassic basin, in very limited areas (Stose and Jonas, 1939). (40.15429 -76.9856)</p>	
		<p>Figure 9. Weathered fanglomerate with large clasts in a clay matrix. Clasts include limestone, claystone, quartzite and chert. Acid bottle for scale. <i>Photo by R. Behr</i></p>
0.36	Sewage treatment plant outflow is on river left. Thirty feet downstream, there is a small poorly exposed outcrop of interbedded sandstone and claystone with well-rounded to subrounded alluvial quartzite cobbles capping it.	
0.42	Cross into diabase around here.	
0.48	Gravel bar on left contains diabase cobbles with visible crystals. A small spring issues	
0.52	Stony Run enters river on right. Up this drainage were prospect pits for high-grade magnetite iron ore, which also found green andradite garnet (Stose and Jonas, 1939). Some old maps call this Fisher Run.	

0.55 STOP 2 RIVER LEFT – Do not get out! As you approach the bridge on the left side, in the deepest fastest moving water, you see a nice three-foot tall irregularly-jointed outcrop of diabase. This is a three-hundred foot wide part of the Gettysburg sill. The sill caps the hills to the south, and largely the river has cut down through it. The diabase is fine to medium-grained depending on cooling rates. Colors range from dark gray to black. The rock has a salt and pepper appearance caused by white plagioclase (especially andesine or labradorite) crystals and black pyroxene (especially augite), magnetite, and rare olivine (Stose and Jonas, 1939). From here to the end of the riffles, we will be in diabase or skirting the very edge of it. (40.15431 -76.9843)

Gilbert Road crosses on new bridge. This was the site of the historical Pratt Truss single-span bridge known as Gilbert Bridge or Halls Estate Bridge built in 1898 (figure 10)



Figure 10.
View of Gilbert Bridge with Stony Creek in foreground

*Photo from
Cultural Resources Geographic Information
System, 2008*

0.61	This riffle was the site of the Thomas J. Stephens woolen mill, originally a clover mill. There are three channels of the creek below this. The southern passage is usually open and affords a nice view of a lovely little French house.
0.75	End of the diabase.
0.97	Intermittent tributary on right. Private Hunting Lease sign.
1.05	River Left, nice exposure of alluvium. Large cobbles of former streambed show well rounded quartzites, Triassic rocks, and possibly reworked cobbles from the Triassic deposits. The stream bed is a staggered pavement of baked gray coarse-grained sandstone.
1.20	This riffle offers a bit of a challenge. Stay river right and shoot for the down-stream pointed V of calm water. If you bump bottom, just keep your balance and scoot on through. I suspect there was a mill here, but cannot determine which from the records.
1.26	Just past the large riffle is a large hillside exposure on the right bank. Massive beds eight feet thick expose medium gray homogeneous baked sandstone. There are also some beds of dark brick-colored claystone baked to almost slate consistency.

1.44

STOP 3 RIVER RIGHT – Just past the ledge drop on river right is a creekside outcrop with resistant conglomerate cap (Figure 11). Pebbles and cobbles are limestone, sandstone, quartz and angular claystone. Differential weathering of the cobbles and pebbles creates an artistic texture (Figure 12). A thin bed of claystone can be seen beneath the conglomerate. It weathers more easily causing a recess. Bedding dips 14 degrees west- southwest. (40.15893 -76.97279)

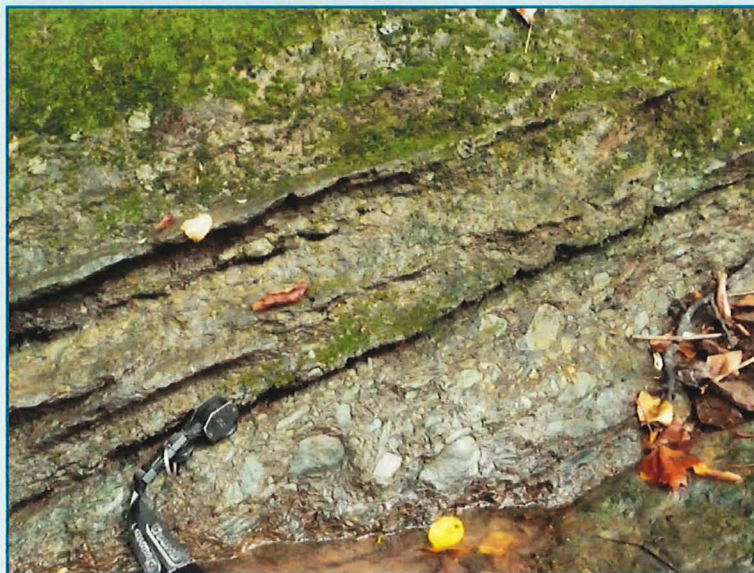


Figure 11.
Outcrop of Triassic conglomerate viewed from creek level.

Photo by K. Hand

Figure 12.
Close-up view of differential weathering on the cobbles and pebbles in the conglomerate. Hand lens for scale.

Photo by K. Hand



1.55

STOP 4 RIVER RIGHT – As you enter the mill pool for the former Bishop Mill, the right side of the creek reveals a cliff of Triassic fanglomerate. The red color of the rocks indicates it has not experienced metamorphism. Regular joints are spaced six to ten feet apart. One cobble is offset. Dissolution has occurred along one joint face (340/70), likely due to the calcareous nature of the matrix (Figure 13).
(40.15935 -76.975)

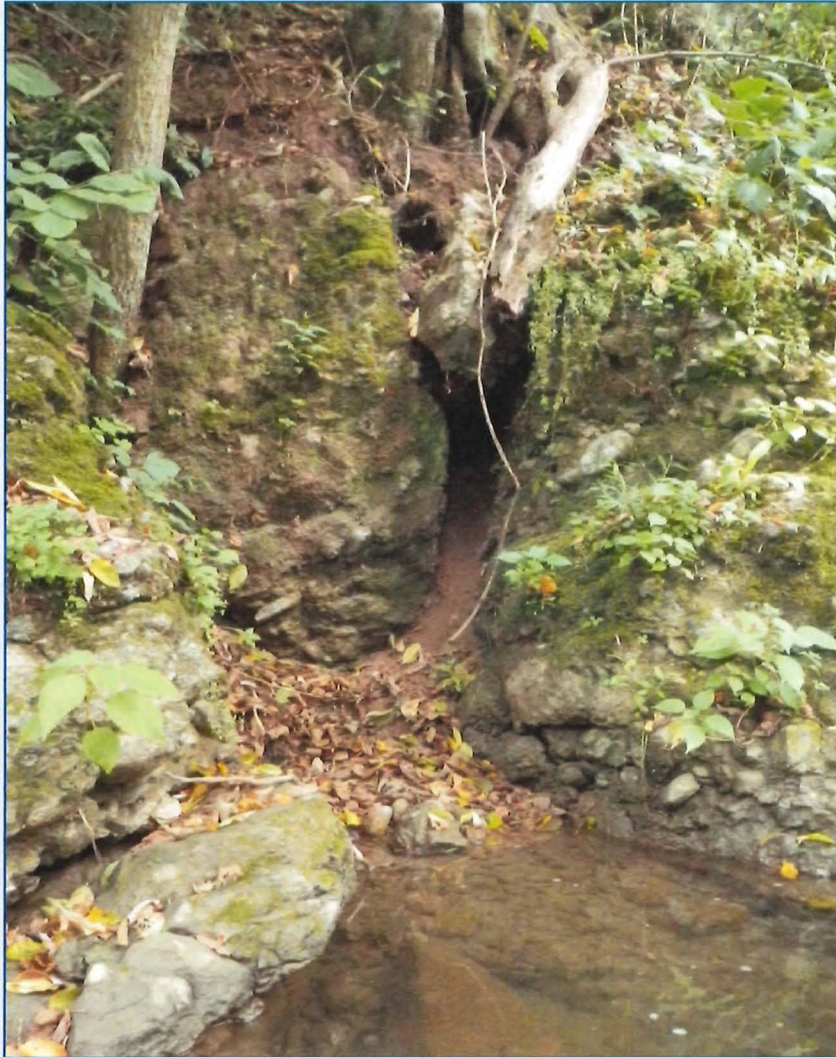



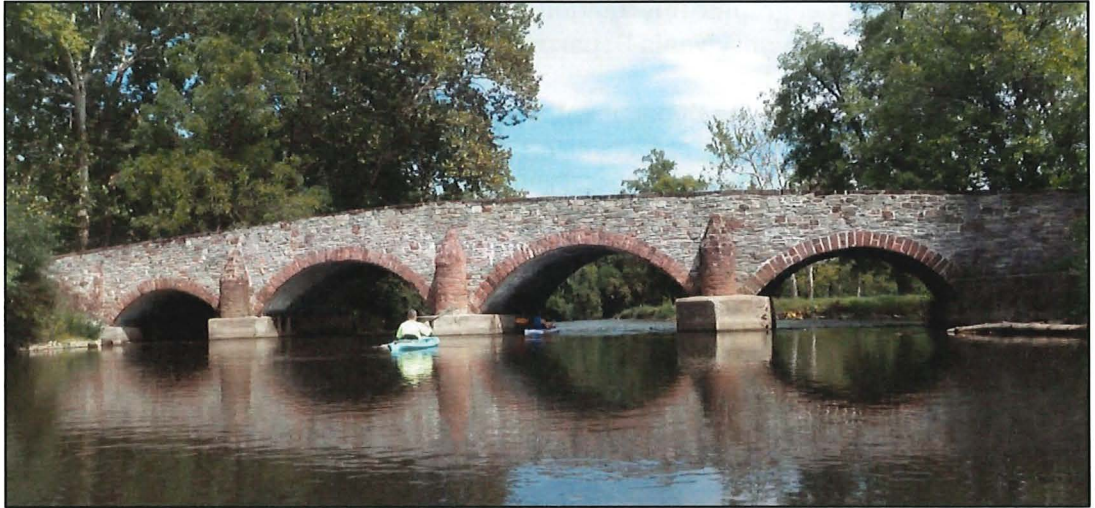
Figure 13.
Dissolution along
joint surfaces in
calcareous
fanglomerate in
Bishops Mill pool
Photo by K. Hand

1.63

Bishop Mill was located here. They milled many things, but only the carding machines are mentioned in Miller (1909). The milldam is breeched and the center has a fun chute.

1.65	<p>Bishop Road. Bishop Bridge was built in 1898, just two years before the Wrought Iron Bridge Company was bought out by the American Bridge Company (Figure 14). It is on the National Register of Historic Places (Historic Bridges, 2013). It was closed to traffic on June 30, 2014 (The Sentinel, 2014). Repairs will cost half a million dollars. Replacement would cost three million. Only two other bridges of this era remains on the Yellow Breeches. The Etters Bridge downstream near Green Lane Farms is also slated to close.</p>  <p>Figure 14. Bishop Bridge was built in 1898 Photo by K. Hand</p>
1.77	<p>A nice little eddy forms in the river at the beginning of a long outcrop of hard red well- jointed claystone. Some of the joints anastomose. Downstream are more fanglomerate beds forming large cliffs. As you float along this riffle, enjoy the huge exposure of the youngest Triassic rocks of the basin. You are crossing the basin-bounding fault!</p>
	Two mills and a distillery all operated between here and Bowmansdale.
2.05	Enter the Ordovician carbonates
2.08	River was straightened when the Philadelphia & Reading Railroad was built.
2.38	Old abutments from Bishop Road.

<p>2.40</p>	<p>STOP 5 RIVER LEFT – Just upstream of the bridge is a three-foot outcrop of limestone of the Epler Formation. This is our only stop outside the rift basin. Beds are finely laminated, medium gray to medium dark gray to medium bluish gray (Figure 15). They weather blue gray to dove gray with elephant skin texture. Joints are spaced every two to six inches. Dolomitized worm burrows, lenses of fossil fragments, dark gray to pink gray chert, and pink limestone are locally reported (Root, 1977). Typically, it is thought that the Triassic basin is bound on the northern edge by a normal fault. This is true overall, but in the area we are in, the sediments actually on-lap the Ordovician carbonates (Figure 4). The normal fault, or more likely a series of normal faults are further south. These Triassic sediments in the area near this bridge are the youngest in the entire basin! (40.1647 -76.9772)</p> <div data-bbox="440 730 1317 1390" data-label="Image"> </div> <p>Figure 15. Finely laminated limestone beds of the Ordovician Epler Formation indicate we have left the Triassic basin. Hammer head for scale.</p> <p style="text-align: right;"><i>Photo by R. Behr</i></p>
<p>2.42</p>	<p>North York Road Bridge, and return to the Triassic. Simpson Park on left.</p>
<p>2.75</p>	<p>Tributary enters on right.</p>

2.96	STOP 6 RIVER RIGHT – on the overgrown bank, you will see a low outcrop of brick red unbaked Triassic claystone with planar beds on top of brick red four- to six-inch thick sandstone beds. Red claystone beds are very weathering, forming chippy red clay-rich soil. A few stream-rounded cobbles are on top of the bank, indicating a former terrace. (40.16254 -76.9673)
3.07	<p>Bryson & Conklin Bridge named for two local families, was built in 1857. This four-arch bridge is on a private road (PHMC, figure 16). Scout your route carefully. Usually the second to the right arch is best, but beware of submerged jersey barrier at the downstream opening. Avoid tree debris at all costs!</p>  <p>Figure 16. Photo of Bryson & Conklin Bridge looking downstream. <i>Photo by Kristen Hand</i></p>
3.08	Pippins run enters on the right and an unnamed tributary enters on the left.
3.16	Approximate location of an oil mill (miller, 1909)
3.26	Extended outcrop on the left side of the creek reveals Triassic sediments, notably conglomerates. A thin diabase dike is mapped here somewhere. There are several dikes mapped in the county that post-date the main diabase emplacement. During the 1930's gravel was quarried out of the creek near here for local concrete and road fill (miller, 2004).
3.50	EXIT RIVER left onto McCormick road, river elevation is 376 feet above sea level. Look up towards the barn and note the milk house on the left side of the driveway. During Hurricane Agnes, the Yellow Breeches flooded to this elevation, only ten feet above current river level (P. J. Wash, personal communication, 2013). (40.1642 -76.9588)

Acknowledgments

The author wishes to acknowledge Kristen Hand who accompanied me on the kayak trip, took all the notes, and edited the guide. Her assistance has been invaluable. Thanks to Anne Muren and Robin Smith for being test subjects for the trip. Thanks to Gary Kribbs for graciously volunteering to lead the trip so the author can be setting up for the Field Conference itself. Finally, she wishes to thank Phil and Rebecca Walsh for telling me about Happy Yellow Breeches and for maintaining a beautiful landmark along the creek.

References

- Cultural Resources Geographic Information System, 2008,. Pennsylvania Historical and Museum Commission and Pennsylvania Department of Transportation. [<http://crgis.state.pa.us>] accessed 8/18/2014
- Cumberland County Planning Department, 2012, Yellow Breeches Creek Water Trail-Map & Guide, [<http://www.ccpa.net/DocumentCenter/Home/View/8814>] accessed 8/21/2014
- Glaeser, J. D., 1966. Provenance, dispersal, and depositional environments of Triassic sediments in the Newark-Gettysburg Basin, Pennsylvania Geological Survey, 4th ser., General Geology Report 43, 168 p.
- Historic Bridges, 2013, [<http://www.historicbridges.org/bridges/browser/?bridgebrowser=pennsylvania/bishoproad/#photosvideos>] accessed 8/22/2014
- Miller, J. R., 1909, Callapatscink- The Yellow Breeches Creek: reprinted from the Shippensburg News, 36 p.
- Miller, P. A., 2004, Happy Yellow Breeches: The Yellow Breeches Gazette, 82 p.
- Pennsylvania Covered Bridges, 2013, [<http://www.pacoveredbridges.com/cumberland-county/>] accessed 8/22/2014
- Root, S. I., 1977, Geology and Mineral Resources of the Harrisburg West Area, Cumberland and York Counties, Pennsylvania: Pennsylvania Geological Survey, 4th ser., Atlas 148ab, 106 p.
- Rowland, Bob, 2001, History of the Callapatschink [sic]/Yellow Breeches Creek: Yellow Breeches Watershed Association, [<http://www.cumberlandcd.com/~amcclain/ybwa/History.htm>] accessed 8/22/2014.
- The Sentinel, 6/27/2014, Bishop Bridge closed due to structural deficiencies, [http://cumberlink.com/news/local/communities/mechanicsburg/bishop-bridge-closed-due-to-structural-deficiencies/article_0bd0bbae-fe44-11e3-aac2-001a4bcf887a.html] accessed 8/22/2014
- Spencer, A. C., 1908, Magnetite deposits of the Cornwall type in Pennsylvania: United States Geological Survey, Bulletin 359, p. 71-98.
- Stose, G. W. and Jonas, A. I., 1939, Geology and Mineral Resources of York County, Pennsylvania: Pennsylvania Geological Survey, 4th ser., County Report no. 67, 199 p.
- Susquehanna River Basin Commission, 2007, Lower Susquehanna Subbasin Small Watershed Study: Yellow Breeches Creek: Publication 250, 20 p. [http://www.srbcc.net/pubinfo/techdocs/publication_250/techreport250.pdf] accessed 8/22/2014
- U.S.G.S. Gaging Station, http://waterdata.usgs.gov/pa/nwis/uv?site_no=01571500

STRUCTURAL COMPLEXITIES OF THE MARCELLUS FORMATION IN CENTRAL PENNSYLVANIA – A FIELD TRIP

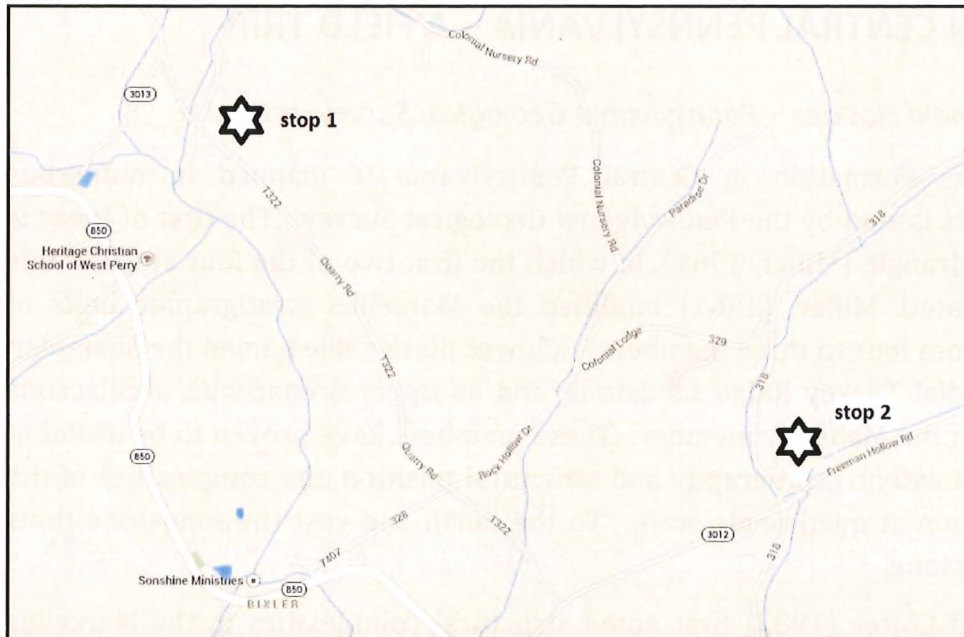
Donald Hoskins – Pennsylvania Geological Survey, retired

The Marcellus Formation in Central Pennsylvania is mapped in numerous quadrangle reports issued by the Pennsylvania Geological Survey. The first of these is the Loysville Quadrangle (Miller, 1961), in which the first two of the four stops of this field trip are located. Miller, (1961) modified the Marcellus stratigraphic units of Willard (1935) from four to three members – a lower black shale named the Shamokin black shale, a medial Turkey Ridge sandstone, and an upper arenaceous, argillaceous black shale named the Mahanoy member. These members have proven to be useful in mapping the areal extent, stratigraphy and structural position and complexities of the Marcellus Formation at quadrangle scale. To the north and east the sandstone thins and contains limestone.

Nickelsen and Cotter (1983) first noted structural complexities in the Marcellus Formation near Selinsgrove Junction, along the Susquehanna River. There, early Alleghanian thin and thick strain discontinuities, expressed as cleavage duplexes, are present in the lower and upper Marcellus shales.

Additional exposures of Marcellus shale strain discontinuities have been located, as additional mapping has progressed. The four localities described herein provide views of cleavage duplexes that now are more frequently observed as well as more intense deformation including chevron folds, folding of calcareous concretions and faulting of the medial Turkey Ridge Sandstone, a unit resistant to weathering, which underlies ridges, into complexes of cleavage duplexes and chevron folds.

STOP 1 Boose pit, Perry County



Location Map for
Stop 1 – Boose Pit
& Stop 2 – Pontius
Pit, Perry County



Horizontally
layered Marcellus
black shale with
multiple joint
sets, including the
J1 and J2
orthogonal sets

In the lower part of the pit are layered calcareous concretions that the joints apparently do not penetrate. Why? Other concretions are fractured with secondary calcite present.



Slickensides indicate that differential slippage occurred along the interfaces of the black shale and carbonate concretions. Secondary calcite is present in fractures.

Stop 2 Pontius Pit, Perry County

North dipping, undeformed, laminated calcareous concretions at Pontius Pit.

1 meter walking stick for scale.

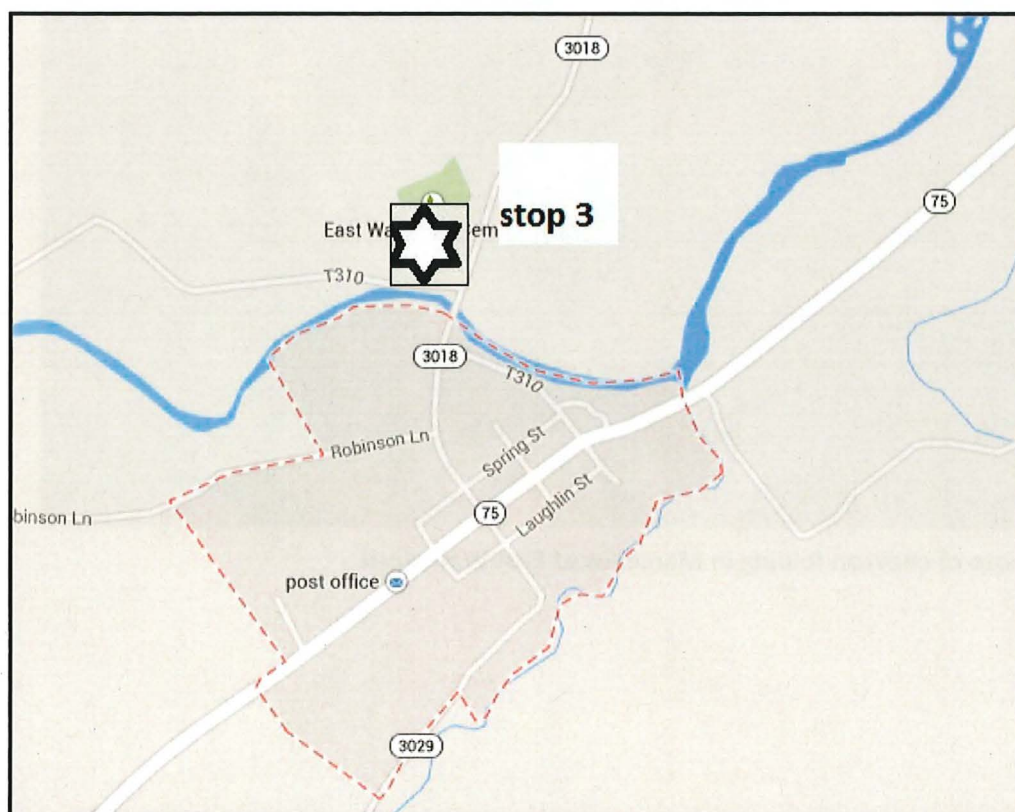


Deformed concretion at Pontius Pit from within zone of strain discontinuity.



Cleavage duplex
at Pontius Pit –
cleavage
direction
implies
movement
to the right

Stop 3 East Waterford, Juniata County



Location Map for
Stop 3 – East
Waterford,
Juniata County



Intense Chevron folding in Marcellus at East Waterford

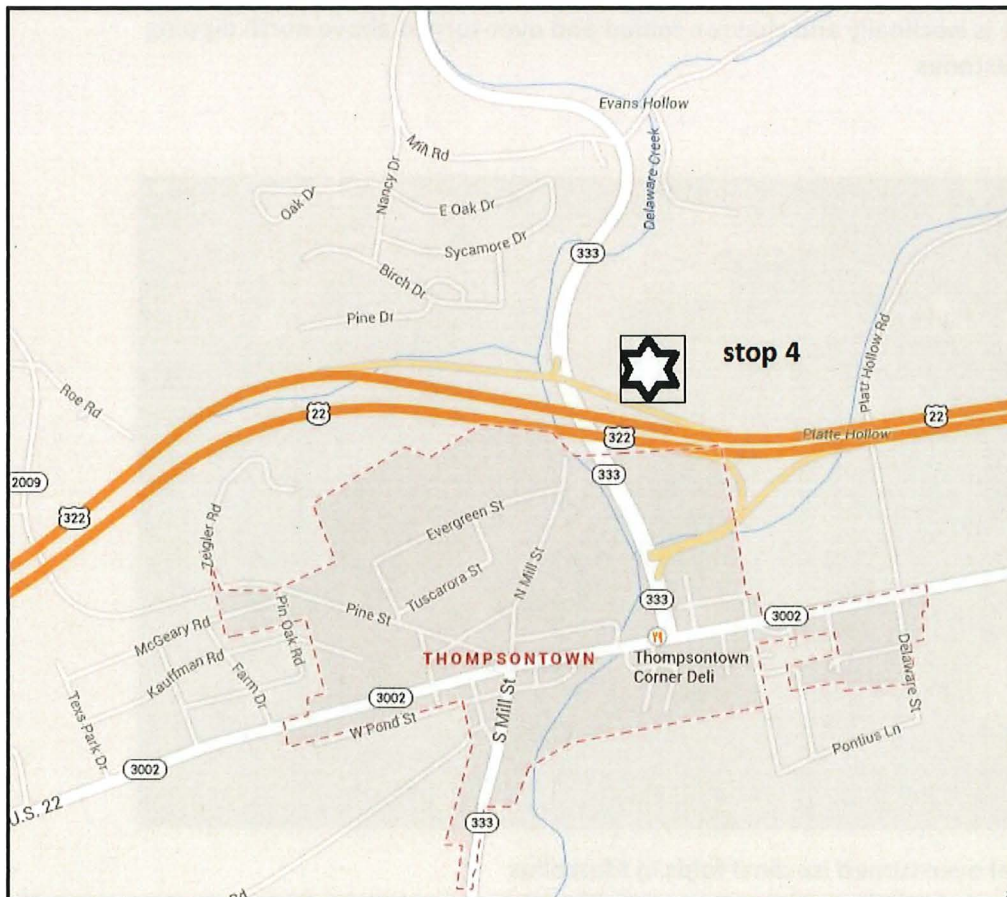


Close-up photo of chevron folding in Marcellus at East Waterford

**Onondaga
Formation
limestones
below Marcellus
shales at East
Waterford form
a buttress for
strain
discontinuity in
overlying shales**



Stop 4 Thompsontown, Juniata County



**Location Map for
Stop 4 –
Thompsontown,
Juniata County**



Marcellus here is Isoclinally and chevron folded and over-turned above north dipping Onondaga limestones



One of several over-turned isoclinal folds in Marcellus

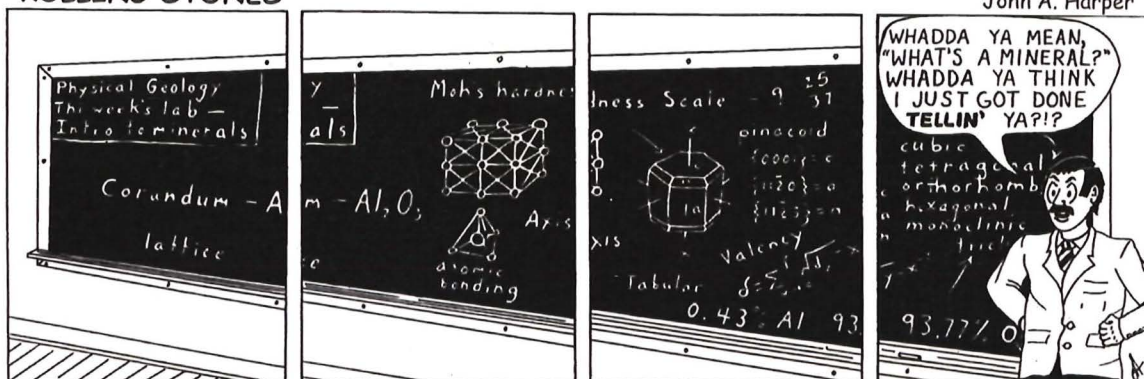


Photo is to the left of photo 1 and contains the overlying and overturned east dipping Turkey Ridge sandstone below fault with north dipping Marcellus above fault

References

- Miller, John T., 1961, *Geology and Mineral Resources of the Loysville Quadrangle, Pennsylvania* – Pennsylvania Geological Survey, 4th Series, Atlas 127.
- Nickelsen, Richard P. and E. Cotter, 1983, *Silurian depositional history and Alleghanian deformation in the Pennsylvania Valley and Ridge* – Guidebook for the 48th Annual Field Conference of Pennsylvania Geologists
- Willard, Bradford, 1935, *Hamilton Group in Pennsylvania* – Geological Society of America Bulletin, Vol. 46, p. 196-224.

ROLLING STONES



CONODOGUINET CAVE PRE-CONFERENCE FIELD TRIP

Katherine W. Schmid – Pennsylvania Geological Survey

Conodoguinet Cave has a very long history. People have been visiting this cave for centuries. Because of its cool air, the cave was very popular in times before air conditioning. Johann David Schöpf, a German geologist, included this cave on his geologic map of eastern North America in 1787 (Speece, 2013). Spencer Baird, a world famous paleontologist from Dickenson University, visited the cave in 1848 and classified the bones of 18 different animal species. Baird believed some of these bones to be from extinct species, but this was disproved when Gerrit S. Miller, curator of mammals division of the United States National Museum, re-examined the bones in 1940 (Speece, 2013). Ralph Stone of the Pennsylvania Geologic survey mapped the cave in 1930 (Stone, 1932). Bernie Smeltzer, who made very detailed maps of many Pennsylvania caves, mapped this cave in 1959 with the National Speleological Society (Figure 1). According to Tom Metzgar of the Mid-Atlantic Karst Conservancy, Cave Hill Park was the first cave park created in the Commonwealth of Pennsylvania. This park was created in 1963 to protect the land from further disturbance after the construction of the Pa Turnpike (Cavehill, 2013).

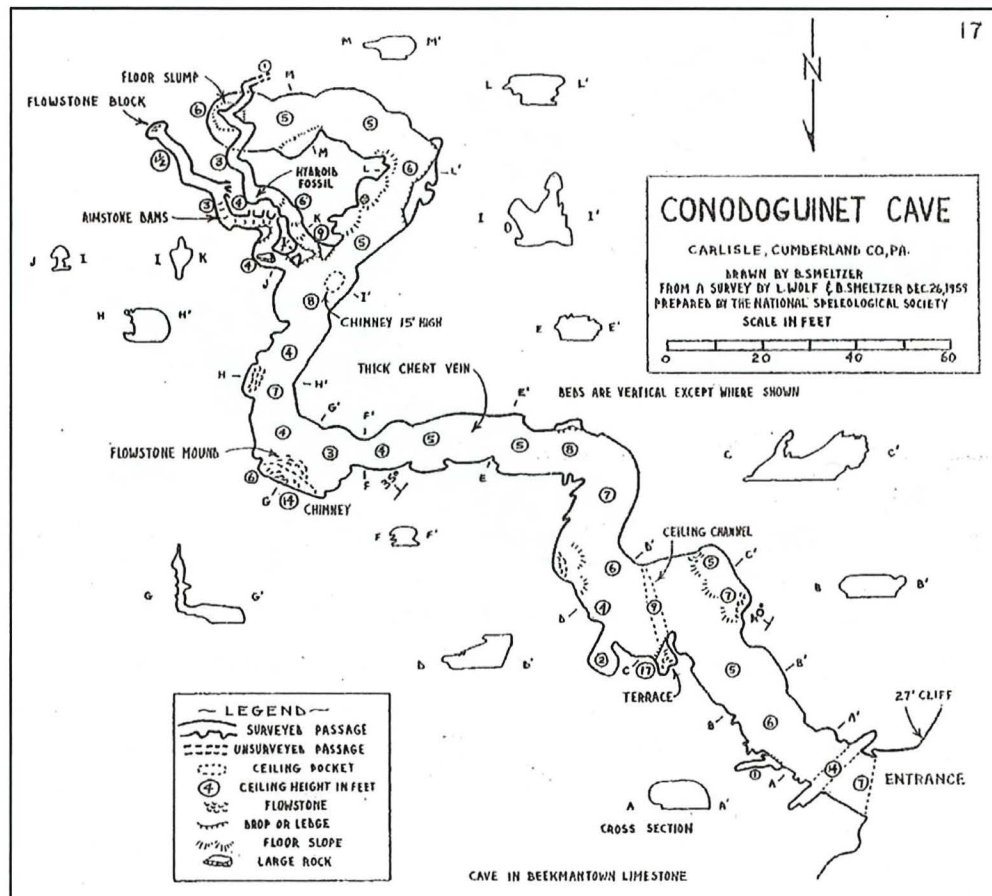


Figure 1. Map of Conodoguinet Cave (Smeltzer, 1959)

The cave developed in the Chambersburg Limestone in an area where the bedrock is folded and faulted (Miles and Whitfield, 2001 and Faill, 2011) (Figure 2). The Chambersburg Limestone is Middle Ordovician in age and is composed of dark gray, thin to medium-bedded nodular limestone and minor units of thin, evenly-bedded argillaceous limestone. This formation contains some thin bands of metabentonite (Lindsey, 2005). Stratigraphically below this is the Middle Ordovician St. Paul Group, composed of prominent beds of light gray, thick-bedded, high calcium micritic limestone and a medial zone of medium gray, granular black chert-bearing limestone, dolomite, and skeletal-detrital limestone (Lindsey, 2005). The limestone in this area is very steeply dipping $\sim 80^\circ$ (Figure 3), although there is some variation in the dip from local folding.

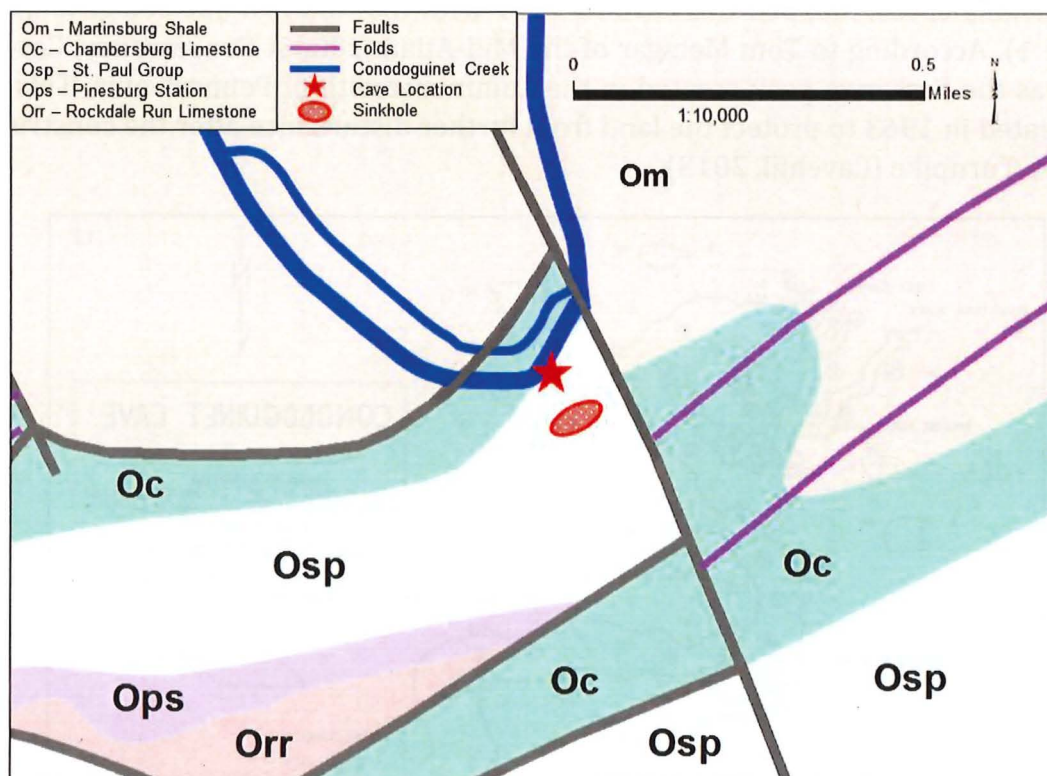


Figure 2 Map modified from Miles and Whitfield, 2001 and Faill, 2011

I do not see as much control from this geologic complexity on the cave's development as I have observed in other caves. The overall trend of the cave (azimuth $\sim 315^\circ$) is about 25° west of the trend of the nearest mapped fault (azimuth $\sim 340^\circ$). Interestingly, the cave has more bends in its passages than I have seen in other joint- or fault-controlled caves. Another mystery in the cave is that the main passage is nearly

horizontal despite the steeply dipping limestone. If you pay attention over the field conference, you may hear some reasons why this is the case.



Figure 3. Measuring strike and dip.

There are numerous small sinks in the large sinkhole above the cave. The large sinkhole is included on topographic maps created prior to turnpike construction. Some of the small sinks are recent features caused by the changes in drainage patterns from modern construction (Figure 4).

As we walk down the hill to the cave, we will pass several small springs that feed Conodoguinet Creek. Before the creek was dammed for the Carlisle Gas and Water Company in 1854, the water level was about eight feet below the cave's entrance (Speece, 2013). The cave has been gradually filling with mud as the creek floods into the cave.



Figure 4. Recent sink

Now, let's compare these surface features to what we see in the cave. There are numerous inlets for water inside the cave, including high domes (chimneys) and springs. The high domes probably lead to surface sinks that have existed since long before modern construction. The spring from the passage with the flowstone block (upper left corner of Figure 1) has been known to flow 1.5 to 2 hours after rain events. This passage is also home to rare amphipods (small crustaceans), so please watch your step here.

Despite being used heavily by people for centuries, the cave still has lots of speleothems including stalactites, flowstone, and rimstone dams. These formations are deposited as saturated water comes into contact with air that has a lower concentration of CO₂. Stalactites have the same morphology as an icicle. They begin as soda straws (a thin-walled, hollow formation) that form as calcite crystals form around the edges of saturated drops of water on the ceiling. This soda straw forms the central canal of the stalactite. Simultaneously, the outside layers form as crystals build perpendicularly to the walls of the soda straw as water flows down the outer surface of the speleothem (Hill and Forti, 1997). Flowstone is a sheet-like deposit that has a crystal orientation that builds up perpendicular to flow (Figure 5).

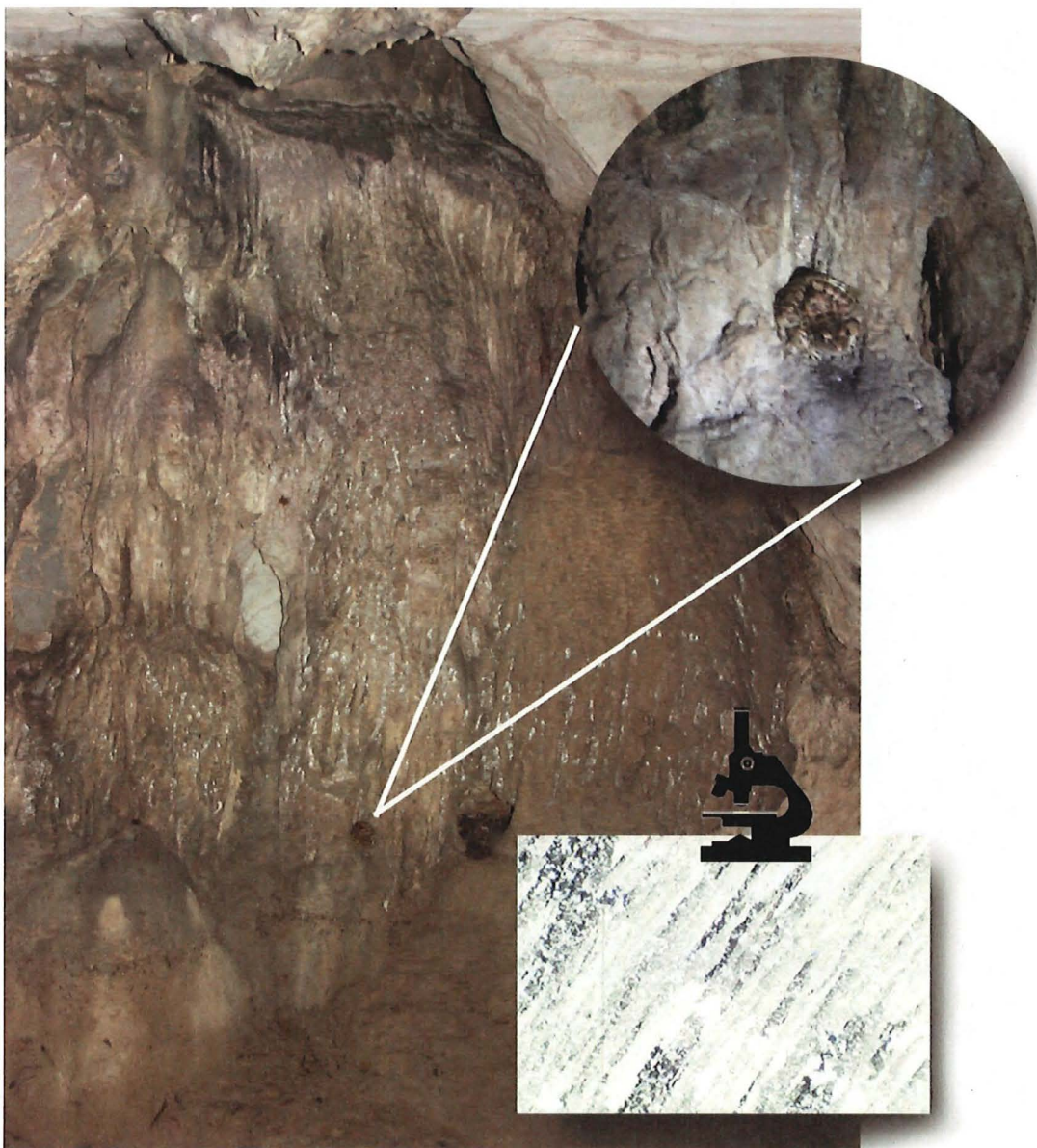


Figure 5. Frog sitting on flowstone. Upper insert is closeup of frog. Lower insert is speleothem thin section from Walden, 1999

Rimstone dams have a stair-step morphology. They build up as barriers perpendicular to flow that obstructs cave streams or pools. They form as crystallization occurs at the water/ice/rock interface and often grade into flowstone with gradient changes (Hill and Forti, 1997). Rimstone dams are shown in Figure 6.



Figure 6. Rimstone Dams

Look around and see what you can find in this cave. What fossils can you find here? Can you find any evidence of faulting or folding inside the cave? This Ordovician Limestone has very different fossils than the Mississippian and Pennsylvanian caves that I typically explore. Some of the fossils in this cave are shown in Figure 7. Note that a 'hydroid fossil' is mentioned on Bernie Smeltzer's map (Figure 8). Do you think this is truly a fossil? Looking at bedding planes will be useful when looking for folding or faulting (Figure 9). As a hint, I have included some pictures from a fault-controlled cave at the end of this article.



Figure 7a. Ammonite fossils



Figure 7b. Cephalopod Fossil



Figure 8 "Hydroid Fossil"



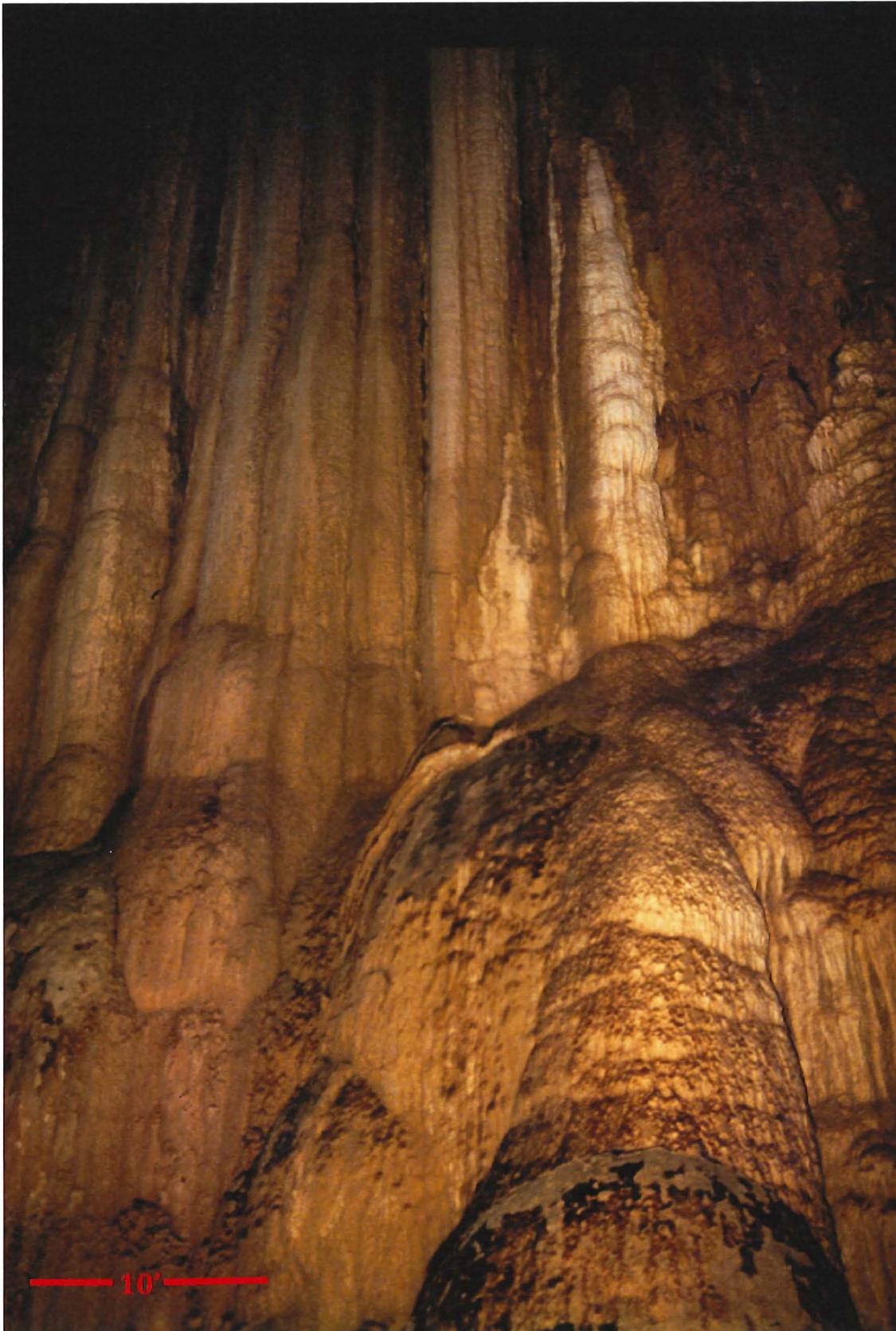
Figure 9. Looking at bedding planes is useful when looking for folding or faulting



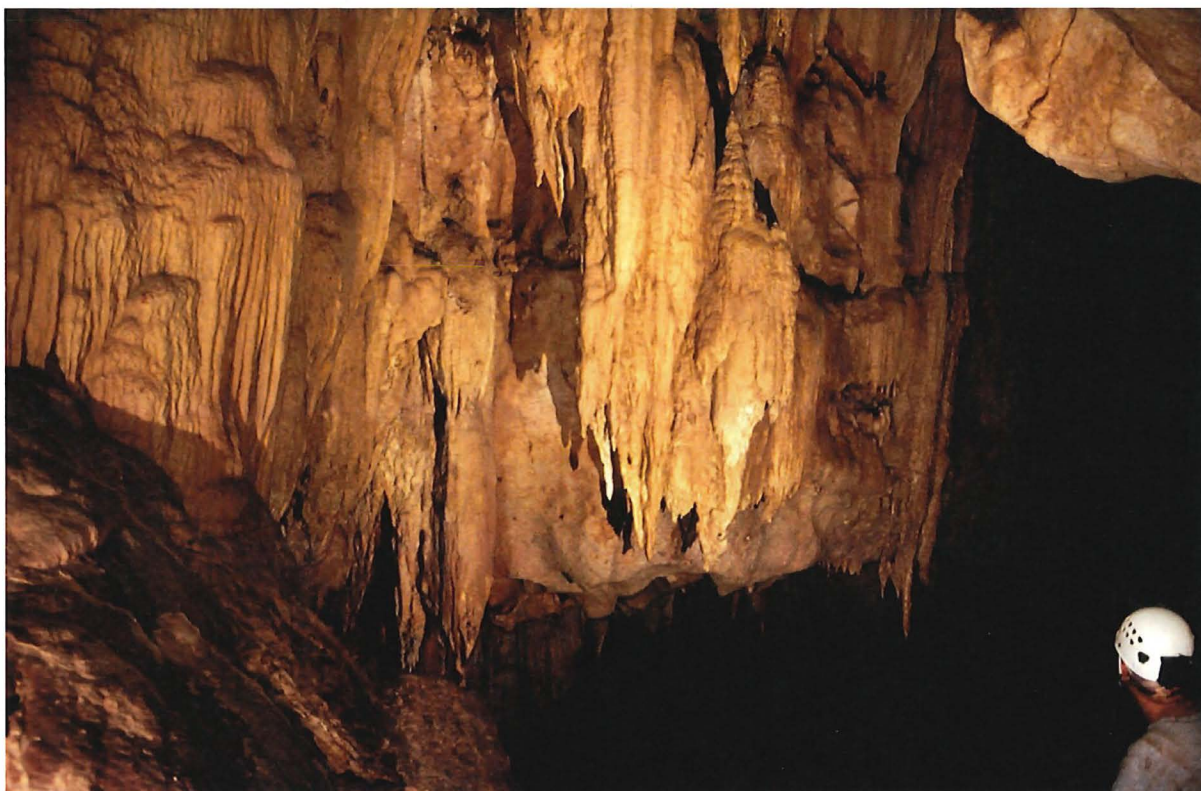
View along strike of bedrock above cave entrance



Barton Creek Cave is a fault-controlled cave in the Maya Mountains of Belize. The cave has few side passages and the main passage remains fairly uniform in size remaining close to 60 feet (18 meters) in width and 125 (38 meters) feet high. The main passage eventually comes into a large room with a large wall of flowstone. This wall must have formed as groundwater flowing along the fault line became supersaturated in calcite which was deposited when the water was exposed to air in the cave. Further in the cave, I saw more evidence of the thrust faulting that formed the mountains. In one section, I saw beautiful pink granite falling in from above the limestone.



Flowstone Wall, Barton Creek Cave

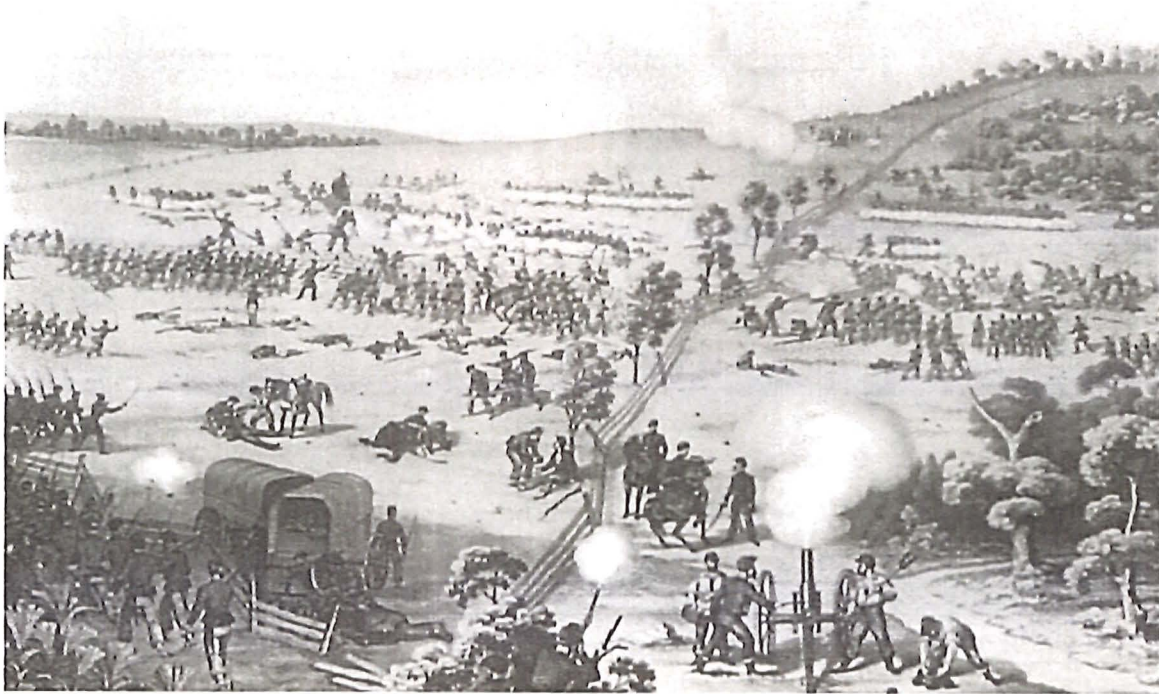


Base of flowstone wall.

References:

- Cavehill, 2013. <http://www.cavehillcarlisle.org/> accessed 2014.
- Faill, R. T., compiler, 2011, Folds of Pennsylvania—GIS data and map: Pennsylvania Geological Survey, 4th ser., Open-File Report OFGG 11–01.0, scale 1:500,000.
- Lindsey, Bruce D., 2005, Hydrogeology and Simulation of Source Areas of Water to Production Wells in a Colluvium-Mantled Carbonate-Bedrock Aquifer near Shippensburg, Cumberland, and Franklin Counties, Pennsylvania: U.S. Geological Survey Scientific Investigations Report 2005-5195, 49 p.
- Miles, C. E., and Whitfield, T. G., compilers, 2001, Bedrock geology of Pennsylvania: Pennsylvania Geological Survey, 4th ser., dataset, scale 1:250,000.
- Hill, Carol and Paolo Forti (1997) Cave minerals of the world. National Speleological Society, Huntsville, Alabama.
- Speece, Jack H., 2013. Conondoguinet Cave Cumberland County Pennsylvania, Speece Productions Spelean History series no. 11, Altoona Pa, 24 p.
- Stone, Ralph W., 1932. Pennsylvania Caves, Topographic and Geologic Survey Bulletin G3, Harrisburg Pa, 143 p.
- Walden, Katherine M., 1999. Strontium Isotopes of Redmond Creek Cave, Wayne County, Kentucky. Undergraduate thesis, Ohio State University.

SOUTH MOUNTAIN



Fox's Gap at the Battle of South Mountain, MD, Sunday, September 14, 1862. *Library of Congress*. (Wikipedia, Battle of South Mountain, accessed 10 September 2012).



Union
Maj. Gen. George B. McClellan
(1826-1885)

The
Army
Commanders
at
South
Mountain



Confederate
Gen. Robert E. Lee
(1807-1870)

MILITARY GEOLOGY OF THE BATTLE OF SOUTH MOUNTAIN (AND HISTORICAL GEOGRAPHY OF HARPERS FERRY)

John D. Inner, PaGS, retired

On 4-7 September 1862, Gen. Robert E. Lee and his Army of Northern Virginia crossed the Potomac River at fords near Leesburg, VA, to initiate the first Confederate invasion of the North, a complex troop movement that culminated in the battle of Antietam. The Confederates marched N to Frederick, MD, and then W across Catoctin and South Mountains toward the Great Valley, drawing Gen. George McClellan's Union Army of the Potomac out of positions around Washington, D.C. On 13 September, McClellan was handed the "Lost Order," a copy of Lee's dispatch to his generals dividing his forces into four scattered parts W of South Mountain. The stage was set for one of the great missed opportunities of the Civil War.¹

South Mountain is a narrow N-S ridge on the W side of the 7 mile wide Middletown Valley, the E side being formed by parallel Catoctin Mountain. These three topographic elements, along with Pleasant Valley and Elk Ridge to the W, constitute the Blue Ridge physiographic province in Maryland. The ridges mark the outcrop belts of resistant Lower Cambrian Chilhowee quartzites and phyllites; Neoproterozoic Catoctin metavolcanics and Mesoproterozoic gneisses underlie the valleys. Along most of its length, South Mountain is 1200 feet high, its narrow summit being formed by the Weverton quartzite. Turner's, Fox's, and Crampton's Gaps are prominent wind gaps where roads still pass over the mountain. The physiography and road network combined to confine the most severe fighting to these gaps.²

On the morning of 14 September, McClellan belatedly initiated engagement of the undermanned Confederate defenses on South Mountain, his right wing marching against Turner's and Fox's Gaps W of Middletown and his left wing against Crampton's Gap, 5 miles to the S. The Confederates stoutly resisted Union attacks up the steep, boulder-covered eastern slope of the mountain from behind stone walls and quartzite ledges. At nightfall, the Confederates had effectively lost control of the summit and gradually withdrew to a defensive line along Antietam Creek in the Great Valley to the W. Meanwhile, they had effectively invested Harpers Ferry, VA (now WV) from three sides and forced surrender of the Union garrison there. By the morning of 17 September, Lee had reassembled most of his army on the Antietam – McClellan had missed his chance to defeat his opponent "in detail."³

¹ Inners, Jon D., and Neubaum, John C., 2012. "Wind Gaps, Weverton Ledges, and Stone Walls: Military Geography and Geology of the Battle of South Mountain, Frederick and Washington Counties, Maryland – 14 September 1862." Northeastern Section – 47th Annual Meeting, (March 2012), Geological Society of America Abstracts with Programs, v.44 no. 2, p. 51

² Ibid.

³ Ibid.

Road Log for Battle of South Mountain Pre-Conference Field Trip

Int	Cum	Description
0.0	0.0	Parking lot in Rest Area on US 15S (Maryland Welcome Center).
0.1	0.1	Merge with US 15 South. To left is Day-1 Field Trip STOP 3 (Gettysburg Formation).
0.2	0.3	Emmitsburg exit (MD 140).
0.2	0.5	Cut through weathered red shale of Gettysburg Formation to left.
0.7	1.2	Cross Tom's Creek.
0.4	1.6	Mountain knob at the north end of Catoctin Mountain ahead to right is College Hill, underlain by Early Cambrian-age quartzite of the Weverton Formation. A sinistral northwest-southeast-trending transverse fault cutting the nose of College Hill here offsets the "Triassic" border fault several miles back into Pennsylvania. From here south to the Potomac River at Point of Rocks, MD, the border fault lies closely along the eastern base of Catoctin Mountain, juxtaposing the Gettysburg and New Oxford Formations against Cambrian-age Harpers phyllite for much of the distance down to Frederick.
1.1	2.7	To right is Mount St. Mary's University. Founded as Mount St. Mary's College and Seminary in 1808, it is the second oldest Catholic college in the United States (next to Georgetown) and has a student population of about 2100. Situated on the campus is the National Shrine Grotto of Lourdes in use since 1805.
2.1	4.8	Segment of Catoctin Mountain to right is Piney Hill, also underlain by Weverton quartzite.
0.7	5.5	Ahead to right is a splendid view of Catoctin Mountain. From its northern termination (see mile 1.6) to a point about five miles southwest of Thurmont, Catoctin Mountain is formed of two conspicuous parallel ridges, the eastern one formed mainly of Weverton quartzite and the western of Catoctin metabasalt. To the west, the next conspicuous ridge is South Mountain—here quite narrow, but broadening dramatically northward into the South Mountain of Pennsylvania.
0.7	6.2	To left is at exit ramp is cut through the Frederick Limestone and Harpers Phyllite? (Cambrian).
0.2	6.4	To right is gap cut through Catoctin Mountain by Owen's Creek.
0.7	6.9	Cross Owen's Creek.
0.2	7.1	Thurmont exit (MD 550).
0.5	7.6	Thurmont to left.
0.7	8.3	Cross Hunting Creek. Catoctin Mountain Park-Cunningham Falls State Park exit. The Hunting Creek gap though Catoctin Mountain is just to the west.
0.5	8.8	Catoctin Furnace Road-Thurmont exit.
2.2	11.0	Catoctin Furnace State Park-Manor exit.
0.3	11.3	Cross Little Hunting Creek.
0.1	11.4	Passing under Catoctin Furnace Historic Trail. To left old US 15 (now Catoctin Furnace Road) is Catoctin Furnace. Thomas Johnson, later first governor of Maryland constructed the first of eventually three furnaces in 1776. The second

Int	Cum	Description
		furnace, "Isabella," was added in 1858, and is the only one extant (Figures 8, 9). (The first furnace was probably located behind "Isabella.") Both of these furnaces were charcoal fueled, the ore coming from limonite deposits at the foot of Catoctin Mountain to the west. The first used waterpower from Little Hunting Creek to operate its bellows, while "Isabella" used steam power. A third furnace, "Deborah," was constructed somewhat later (probably just before or shortly after the start of the Civil War) and was fueled by anthracite. "Isabella" produced up to 3300 tons of pig iron annually. Production at Catoctin Furnace ceased in 1903, at which time "Deborah" was dismantled. The last local ore was mined in 1912.
1.9	13.3	Catoctin Mountain still prominent to right—and containing no conspicuous gaps for the next five or six miles.
6.6	19.9	Beckley's Gas-Liquor-Motel—a man can probably get all he needs here!
2.4	22.3	Exit 16—Motler Avenue (Frederick). Continue straight on US 15.
1.2	23.5	Exit 14—Rosemont Avenue. Continue straight ahead.
0.6	24.1	Bear right at exit to US 40W.
0.2	24.3	TRAFFIC LIGHT. Turn right on US 40W.
0.7	25.0	Get into left lane of US40W.
0.5	25.5	Bear left onto Alt. US 40W (old National Road).
1.5	27.0	Pass under I-70.
1.0	28.0	Braddock Heights at crest of Catoctin Mountain.
0.2	28.2	To left is the monument commemorating the passage of Gen. Edward Braddock and Lieut. Col. George Washington along this route in 1755 on the way west to the tragic battle of the Monongehela.
1.5	29.7	TRAFFIC LIGHT at Middletown Parkway. The broad, anticlinal Middletown Valley between Catoctin and South Mountains is underlain by Proterozoic metavolcanics and various metaigneous rocks.
1.2	30.9	Downtown Middletown.
1.0	31.9	Cross Catoctin Creek.
2.0	33.9	Historical Marker to left at the road intersection reads: RENO MONUMENT. Two miles to the southwest stands the monument to Major General Jesse L. Reno who was mortally wounded at the close of the fighting for Fox's Gap in the battle of South Mountain, September 14, 1862. Ahead is Turner's Gap on South Mountain.
1.1	35.0	Fox Gap Road to left.
1.0	36.0	Dahlgren Chapel to right.
0.1	36.1	Turner's Gap. Turn right on Washington Monument Road.
0.3	36.6	Crags of Catoctin metavolcanics to right (STOP 2).
0.4	37.0	STOP SIGN at intersection of Washington Monument Road and Zittlestown Road. Continue straight ahead and enter Washington Monument State Park (WMSP).
0.3	37.3	Parking lot at WMSP. Disembark. STOP 1. Washington Monument State Park. <i>Monument and scenic views, Weverton-quartzite boulder field (Pleistocene periglacial), Waysides.</i> Leave STOP 1, following park road back to park entrance.
0.5	37.8	STOP SIGN at park entrance. Continue straight ahead on Washington Monument Road.
0.4	38.2	High rock crags to left. Pull off onto right shoulder. Disembark. STOP 2. Catoctin metabasalt (Neoproterozoic). Leave STOP 2, continuing south.

Int	Cum	Description
0.2	38.4	Road cut in Catoclin Formation to left.
0.4	38.8	STOP SIGN. Turn left on Alt. US 40, then immediately right into parking lot. Disembark. STOP 3. Turner's Gap. <i>Weverton quartzite (Lower Cambrian) ledges, boulder fields and other periglacial effects, Mountain House, Dahlgren Chapel, Battle Waysides.</i> Leave STOP 3, turning right on Alt. US 40E.
1.1	39.9	Turn right on Fox Gap Road.
0.5	40.4	Grand view of Middletown Valley and Catoclin Mountain (in distance) to left.
0.5	40.9	STOP SIGN. Turn right on Reno Monument Road.
0.8	41.7	Fox's Gap. Turn left on Lamb's Knoll Road, then immediately right into parking area. Disembark. STOP 4. Fox's Gap. <i>Reno Monument, Weverton quartzite ledges (short walk to north), North Carolina Monument (short walk to south), Battle Waysides.</i> Leave STOP 4, turning left on Reno Monument Road.
1.3	43.0	Fine view of Pleasant Valley, with low hills at the end of "north-plunging" Elk Ridge in mid-distance. Fold mountains beyond the Great Valley on far horizon.
0.8	43.8	STOP SIGN. Turn left on MD 67, driving south through Pleasant Valley. Elk Ridge is to right, South Mountain to left. The valley is underlain by Proterozoic metaigneous rocks and is bounded on the east side (along South Mountain) by the east-dipping Short Hill thrust fault.
3.3	47.1	Road to Rohrsersville to right.
1.0	48.1	Crampton's Gap to left.
1.1	49.2	Turn left onto Gapland Road to Gathland State Park.
0.1	49.3	Historical Marker to right reads: CONFEDERATE RETREAT. Driven from Crampton's Gap on Sept. 14, 1862, by Gen. Franklin's Sixth Corps, elements of McLaw's Confederates formed across Pleasant Valley to bar Union advance on Maryland Heights and Harper's Ferry. Later these Confederates joined Lee about Sharpsburg. <i>Maryland Civil War Centennial Commission.</i> Just beyond marker to left the road cuts through Mesoproterozoic hornblende gneiss.
0.9	50.2	Crampton's Gap. Turn right into Gathland State Park.
0.1	50.3	Parking lot at Gathland State Park. Disembark. STOP 5. Crampton's Gap. <i>George Alfred Townsend, Gathland, War Correspondents' Arch, Battle Waysides.</i> Leave STOP 5, turning right on Gapland Road.
0.5	50.8	Battle Waysides to right (<i>Burkittsville: Henry Burkitt's Town, Chew's Ashby Artillery, and "Sealed with Their Lives"</i>) and old church and cemetery to left.
0.4	51.2	Intersection of Gapland Road and Mountain Church Road. Historical Marker to left details the Confederate order of battle in the defense of Crampton's Gap and then reads as follows: Upon the approach of the Sixth Corps Army of the Potomac, [Col. T. T.] Munford's Cavalry fell back through Jefferson and Burkittsville and prepared dispute the passage of South Mountain. Mahone's Brigade [Lt. Col. W. A. Parham, commanding] was marched over Crampton's Pass from Pleasant Valley and put in position behind the stone wall and rail fences running north from this point. The cavalry (dismounted) was disposed on either flank of Mahone's infantry. [Capt. R. P.] Chew's (Va.) Battery and two guns of Grime's Portsmouth (Va.) Battery were placed about half way up the mountain and five guns of Manly's (N.C.) Battery and Macon's (Va.) Battery were placed in Brownsville Pass [to the south]. About 3 P.M. Munford was attacked and for nearly three hours held position. Then

Int	Cum	Description
		his line began to yield. As it retired up the mountain, making several stands, it was reinforced by the 10 th Georgia of Semmes' Brigade and, when near the top, by Cobb's Brigade. But the entire line gave way and retreated in disorder into Pleasant Valley.
0.5	51.7	Burgittsville. Turn left into parking lot between impressive South Mountain Heritage Society (SMHS) headquarters (the former German Reformed Church) to left and St. Paul's Lutheran Church to right. Waysides in front of SMHS headquarters describe in heart-wrenching detail the former church's use as a hospital following the battle of South Mountain. The early scenes of the 1999 "classic" horror movie "The Blair Witch Project" was filmed in Burgittsville. The cemetery just to the north of the parking lot is readily identifiable. The weird and "scary" forest scenes were not shot on South Mountain, however, but far to the south in Seneca Creek State Park, Montgomery County.
0.1	51.8	Leave parking lot, turning right on East Main Street and continuing on Gapland Road over South Mountain.
1.1	52.9	Gapland State Park. Continue west on Gapland Road.
1.1	54.0	STOP SIGN. Turn left on MD 67 and proceed south through Pleasant Valley.
3.5	57.5	Weverton Road to left.
1.6	59.1	Bear right on US 340W.
1.2	60.3	Cross Potomac River. Harpers Ferry is directly upriver to the right between Maryland Heights to the north and Loudoun Heights to the south.
1.1	61.4	Enter West Virginia.
0.3	61.7	Beginning of long series of deep rock cuts in Lower Cambrian Weverton quartzite and Harpers phyllite to left.
0.8	62.5	Cross Shenandoah River.
0.9	63.4	Turn left at entrance to Harpers Ferry National Historical Park.
0.4	63.8	STOP SIGN at park entrance. Pay if necessary.
0.1	63.9	Enter parking lot. Disembark.
		STOP 6. Harpers Ferry National Historical Park. <i>Weverton quartzite and Harpers phyllite (Lower Cambrian) cliffs and ledges, Jefferson's Rock, Chesapeake and Ohio Canal, Shenandoah Canal, Civil War arsenal sites, John Brown's Raid (1859), battle of Harpers Ferry (1862), Waysides.</i> Leave STOP 6.
0.1	64.0	STOP SIGN. Turn right toward US 340.
0.1	64.1	TRAFFIC LIGHT. Turn right on US 340E.
0.9	65.0	Cross Shenandoah River.
1.4	66.4	Deep cuts in Cambrian quartzites and phyllites to right.
0.7	67.1	Cross Potomac River.
2.2	69.3	Enter Frederick County, MD.
2.2	71.5	Good views of Middletown Valley to north and south. South Mountain is to left.
7.0	78.5	Pass through Catocin Mountain.
0.8	79.5	Enter Frederick Valley. Mesozoic clastic rocks mainly underlie the west side of the valley, and Cambro-Ordovician carbonate rocks the east side.
0.6	79.9	Sugarloaf Mountain (to east of Frederick Valley) is visible off to right. (It appears several more times above the horizon in the next mile.) Sugarloaf Mountain is formed by the Sugarloaf Mountain quartzite (Lower Cambrian?), the probable stratigraphic equivalent of the Weverton quartzite.
4.0	83.9	Bear right to US 15N, following signs to Gettysburg.
0.3	84.2	Merge onto US 15N; then continue north past Fort Detrick (to left) and through Frederick.

Int	Cum	Description
25.1	109.3	Rest Area (Maryland Welcome Center) to left. End of Roadlog. Have a safe trip home!

ROADLOG to Alternate STOP 6 (Monocacy National Battlefield) from Burkittsville and back to Rest Area (Maryland Welcome Center on US 15S at Emmitsburg)

0.0	0.0	Leave parking lot at South Mountain Heritage Society/St. Paul's Lutheran Church, turning right on Gapland Road/E. Main Street, then take 1 st right on MD 17N/Burkittsville Road (after traveling 300 feet).
6.1	6.1	In Middletown, turn right on Alt-US 40E/E. Main Street/Old National Pike.
3.7	9.8	Turn right onto Alt-US 40E, then merge onto I-70E, via ramp to Washington/Baltimore.
4.9	14.7	Take Exit 54 for MD 85S for Buckeystown.
0.2	14.9	Turn right on MD 85S.
0.3	15.2	Turn left on MD 355S/Urbana Pike.
1.8	17.0	Turn left into entrance to Monocacy National Battlefield Visitors' Center (5210 Urbana Pike). Proceed to parking lot. Alternate STOP 6. Monocacy National Battlefield Visitors' Center. <i>Overview of battlefield topography and geology, the "Lost Order," Best Farm, Sugarloaf Mountain, Early, Gordon and Wallace, "On to Washington"!</i> Leave Alternate STOP 6, proceeding back to entrance and turning right on MD 355N/Urbana Pike.
1.5	18.5	Turn right onto MD 85/Buckeystown Pike (MD 85 is 0.4 mi past Grove Road). Stay to left.
0.4	18.9	Turn slight left on I-70W/US 40W ramp toward Hagerstown (0.2 mi past Francis Scott Key Drive). There is a double lane left turn here with a red- and green-arrow traffic signal. (Traffic is also merging from your left coming off I-70E.) Proceed down ramp for short distance and merge with I-70W/US 40W/Baltimore Pike.
0.9	19.8	Merge onto US 15N/Catactin Mountain Highway N via Exit 53B (first exit) toward Gettysburg.
26.0	45.8	Just past Emmitsburg, MD, watch for Rest Area on left. Turn left where Rest Area sign directs to access US 15 S, the. Turn again on US 15S.
0.3	46.1	Proceed on US 15S to entrance to Rest Area (Maryland Welcome Center.) End of field trip. Have a safe ride home!

SPONSORS

Anonymous	Paul Martino
Gary Ball	Jared Matteucci
Michael Bikerman	Daniel McMullen
William Bragonier	Edgar Meiser
Joseph Casey	Donald Monteverde
John Clarke	Sarah Newcomb
Neil Coleman	Walter Payne
Marco Droese	Frank Pazzaglia
Brian Dunst	Henry Prellwitz
Frank Fawcett	Katie Pressley
Thomas Fridirici	Robert Quick
Bob Ganis	Barbara Rudnick (<i>Bernice Pasquini</i>)
John Harper	Eric Schmidley
Gregory Herman	Steve Shank
Donald Hoskins	Jason Sheasley
Mark Ios	Sean Sherlock
Andy Jenkins	Mindi Snoparsky (<i>Bernice Pasquini</i>)
Thomas Keane	John Stefl
David Kistner	William Stephens
Gary Kribbs (<i>AEON Geoscience, Inc</i>)	Stephen Urbanik
Scott Laird	David Wilson
Michael Layton	Jay Winter
Walter Leis (<i>Tetrahedron/Memory of Steve Jakatt</i>)	
George Love	Joseph Young
Toni Markowski	Ed Zofchak
Jane Marshall	
Pennsylvania Council of Professional Geologists (<i>Veronica Reynolds</i>)	
Pittsburgh Geological Society	



Bey's Rock Shop
Roger Pollok Sculpture
and others



09.28.2013

Group photo of the 2013 Field Conference of Pennsylvania Geologists

SKOLITHOS IN THE LOWER CAMBRIAN ANTIETAM FORMATION AT SOUTH MOUNTAIN, PENNSYLVANIA

Marcus M. Key, Jr.,

Department of Earth Sciences, Dickinson College, Carlisle, PA 17013, key@dickinson.edu

The naming of *Skolithos*

Skolithos is one of the best known, globally distributed trace fossils, but it was first described from south central Pennsylvania. It was originally defined as an ichnogenus by Samuel Stehman Haldeman in 1840. He grew up in Bainbridge, PA, 15 km upstream from Chickies Rock where he studied *Skolithos*. In the middle of the Susquehanna River across from Bainbridge today is Haldeman Island which was named for him. Haldeman was a Dickinson College student from the class of 1831. After college he worked in his family sawmill and iron forge, but he was drawn to be a naturalist. He even corresponded with Charles Darwin. In 1836, Henry Darwin Rogers, a former professor of Haldeman's at Dickinson, asked him to take over the geology field operations in New Jersey that Rogers had to abandon on his being appointed the state geologist of Pennsylvania. Haldeman served in New Jersey for one year and, in 1837, came back to Pennsylvania to assist on the state survey here. It was then that he lived at the north end of Chickies Rock where he excavated a Native American archeological site and described *Skolithos* (Dickinson College Archives, 2005; Haldeman Mansion Preservation Society, 2011; Scharnberger et al., 2014). Soon after Haldeman's 1840 publication, there was confusion over the spelling of the genus. A GeoRef search on 6 May 2014 returned the following number of hits for the various spellings of *Skolithos* (999): *Scolithus* (38), *Skolithus* (6), and *Scolithos* (4). Based on the taxonomic nomenclatural principle of priority, the proper spelling is *Skolithos* (Häntzschel, 1975; Scharnberger et al., 2014) which is used here.

***Skolithos* morphology**

Skolithos is one of the simplest trace fossils. It normally consists of a single, vertical, long, thin, unbranched, straight cylinder, with or without a funnel top, that is perpendicular to bedding and never crosses adjacent tubes (Haldeman, 1840; Hallam and Swett, 1966; Alpert, 1974; Häntzschel, 1975; Schlirf and Uchman, 2005). Less commonly they are sub-cylindrical or prismatic when in contact, inclined to bedding, slightly curved, but these may simply be artifacts of tectonic deformation (see below). The burrow walls can be distinct/lined or indistinct/unlined, rough or smooth, and possibly annulated. *Skolithos* is so distinct that it has even furnished the name of a formal stratigraphic unit (i.e., *Skolithos* Sandstone of the Lower Cambrian of Sweden (Häntzschel, 1975)).

The tubes are typically filled with non-laminated, finer-grained sediment which are casts of the original burrow (Alpert, 1974; Goodwin and Anderson, 1974; Häntzschel, 1975; Schlirf and Uchman, 2005). The vertical continuity of the tubes as well as the textural and compositional differences between the cast and the surrounding matrix suggests there originally was a permanent mucous-cemented burrow (Goodwin and Anderson, 1974). They occasionally weather out so the tubes become free from their surrounding matrix (Howell, 1943). This has been attributed to slightly reduced sericite content in the sediment infilling relative to the rock matrix (Hallam and Swett, 1966). Wise (2010) attributed this at Chickies Rock to sericite micro-slickenlines “coating” the tubes in the plane of cleavage.

Funnel-topped (a.k.a., trumpet pipe) forms were originally assigned to a different ichnogenus, *Monocraterion* (Torell, 1870; Westergård, 1931). More recently as part of the single organism hypothesis, *Monocraterion* has been interpreted as simply the completely preserved top of the *Skolithos* tube (Howell, 1943; Hallam and Swett, 1966; Goodwin and Anderson, 1974; Barwis, 1985; Schlirf and Uchman, 2005). Environments with lower sedimentation rates and more frequent scour generally only preserve the bottom of the burrow (i.e., *Skolithos*), whereas environments with higher sedimentation rates and less frequent scour generally preserve the entire burrow (i.e., *Monocraterion*) (Hallam and Swett, 1966; Goodwin and Anderson, 1974; Bromley, 1990). Deep permanent vertical burrows dominate shallow water environments for two reasons. First, they protect the animal from desiccation and fluctuating water temperatures and salinities (Rhoads, 1967; Crimes, 1975). Second, they provide protection from erosion in environments with rapid shifts in the vertical position of the sediment-water interface (Seilacher, 1967). Deep, permanent, vertical burrows are characteristic of Seilacher's (1967) classic shallow water *Skolithos* ichnofacies. An ichnofacies is a sedimentary deposit defined by the preserved patterns (i.e., trace fossils) of the organisms that lived there (Miller, 2007).

Maximum *Skolithos* tube lengths are typically reported in the 1-2 m range (Alpert, 1974; Goodwin and Anderson, 1974; Schlirf and Uchman, 2005), but this is hard to measure to due erosional truncation of the tube tops. *Skolithos* tube diameters range from 1-30 mm (Alpert, 1974; Häntzschel, 1975; Schlirf and Uchman, 2005). The larger diameters reflect the apertural upper *Monocraterion* end of the tube. Most diameters in the local Cambrian quartzites are 2-6 mm (Goodwin and Anderson, 1974; Gourley and Key, 1996; Key, 2014).

What made the *Skolithos* trace fossil?

Polychaete annelids living today in shallow marine environments produce permanent mucous-lined dwellings that are *Monocraterion-Skolithos* shaped as the animal feeds on suspended food particles above or on the sediment-water interface (Schäfer, 1972).

Skolithos, like their modern analog polychaetes, are opportunistic colonizers following storm depopulation (Vossler and Pemberton, 1988). But this isn't the only possible candidate for the *Skolithos* trace maker. Hypotheses for the agent responsible for making the *Skolithos* trace were initially wide ranging, including plants, sponges, annelids, brachiopods, and phoronids (Häntzschel, 1975) or even inorganic (Högbom, 1915; Hofmann, 1971). Though most *Skolithos* are marine, some are terrestrial, and those have been attributed to insects, spiders, or plants (Schlirf and Uchman, 2005; Gregory et al., 2006; Netto, 2007). Marine forms are now thought to have been made by a burrowing, soft-bodied, worm-like polychaete annelid or phoronid lophophorate (Alpert, 1974; Pemberton and Frey, 1984; Barwis, 1985; Skoog et al., 1994; Schlirf and Uchman, 2005). Regardless of what made the *Skolithos* trace, it is important to keep in mind that trace fossil taxa are defined on their morphology, regardless of their origin (Häntzschel, 1975; Miller, 2007), so different trace-makers may produce identical structures when behaving similarly (Bromley, 1990). With a stratigraphic range spanning the Phanerozoic (see below), numerous different animals are undoubtedly responsible for making *Skolithos*, especially considering they form in both marine and terrestrial environments.

***Skolithos* geographic and stratigraphic range**

Skolithos is globally distributed (Alpert, 1974; Häntzschel, 1975; Behrensmeyer and Turner, 2013). Though *Skolithos* has a stratigraphic range from the Ediacaran to Recent, it is most common in the Paleozoic (Alpert, 1974; Häntzschel, 1975; Fillion and Pickerill, 1990; Droser, 1991; Ekdale and Lewis, 1991; Crimes, 1994; Behrensmeyer and Turner, 2013). As a result of its >600 Myr stratigraphic range, *Skolithos* is useless as a biostratigraphic index fossil. Regardless, the relative abundance of *Skolithos* can be used for lithostratigraphic correlation. They have been used for understanding the stratigraphy of and exploring for Cambro-Ordovician petroleum reservoirs in North Africa, the Middle East, and Australia (McIlroy and Garton, 2004).

Skolithos are especially common in Cambrian sedimentary rocks, even after correcting for relative geologic map area and period durations (Figure 1). During the Early Cambrian an abrupt increase in the diversity of bioturbators as well as the degree and depth of bioturbation occurred in conjunction with the rapid radiation of metazoans (McMenamin and Schulte-McMenamin, 1990; McIlroy and Logan, 1999). This has been termed the Cambrian Substrate Revolution (Bottjer et al., 2000). Major components of this ecological revolution include the first appearance of vertical burrows and the development of tiered endobenthic communities (McIlroy and Logan, 1999). This may have been associated with the extraordinarily large amounts of sand on Cambrian continental shelves due to the lack of land plants before the Ordovician that favored the development of extensive coastal subaerial dune fields and braided fluvial systems (MacNaughton et al., 1997; Desjardins et al., 2010).

Transgressive episodes in the Early Cambrian contributed to the flux of sediment from the coast to the shelf by flooding and ravinement of preexisting sandy coastal deposits

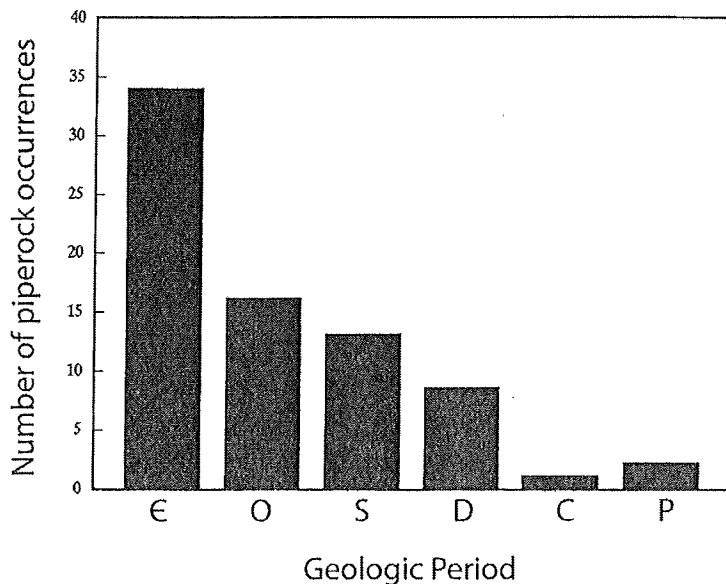


Figure 1. Distribution of piperock (see definition below) among Paleozoic periods normalized for differences in map area and period durations. € = Cambrian, O = Ordovician, S = Silurian, D = Devonian, C = Carboniferous, P = Permian. Modified from Droser (1991, fig. 5).

(Simpson and Eriksson, 1990; Desjardins et al., 2010). The post-Cambrian decrease in *Skolithos* has been attributed to a temporal decrease in nearshore sandstones as well as the Great Ordovician Biodiversification event. This event involved a radiation in the biodiversity of predators and an increase in competition for infaunal ecospace previously dominated by the *Skolithos* tracemakers (Bottjer et al., 2000; Droser, 1991; McIlroy and Garton, 2004; Webby et al., 2004; Desjardins et al., 2010) including the advent of “biological bulldozers” (Thayer, 1979).

In Pennsylvania, *Skolithos* has long been known from numerous Cambrian formations (Table 1). It has also been reported in the Silurian Tuscarora Formation (Cotter, 1982, 1983; Droser and Bottjer, 1989; Sanabria and Thompson, 1997) and the Devonian Catskill Formation (Bridge and Droser, 1985). Further south in Maryland and Virginia, it occurs in the Antietam (Howell, 1943; Simpson and Sundberg, 1987; Simpson and Eriksson, 1990; Simpson, 1991; Skoog et al., 1994) and Harpers (Brezinski, 2004). In the southern Appalachians, *Skolithos* is found in the Chilhowee’s Weisner and Wilson Ridge Formations, the latter correlative with the Antietam (Tull et al., 2010) as well as the Hampton (stratigraphic equivalent of the Harpers Formation) and Erwin (stratigraphic equivalent of the Antietam) Formations (Simpson and Sundberg, 1987; Simpson and Eriksson, 1990; Smoot and Southworth, 2014).

Table 1. Published reports of *Skolithos* trace fossils in Cambrian formations of Pennsylvania

Stratigraphic Formation	Reference(s)
Weverton	Smoot and Southworth, 2014
Chickies	Haldeman, 1840; Hunt, 1878; Stose and Jonas, 1939; Howell, 1943; Wise, 1960, 2010; Goodwin and Anderson, 1974; Kauffman, 1999; Scharnberger et al., 2014
Harpers	Stose, 1906, 1909; Freedman, 1967; Fauth, 1968; Root, 1968; Key, 1991; Gourley and Key, 1996
Antietam	Stose, 1906, 1909; Howell, 1945; Freedman, 1967, 1968; Fauth, 1968; Root, 1968; Key, 1991; Key and Sims, 1991; Sevon and Van Scyoc, 1991; Kauffman, 1999
Hardyston which is stratigraphically equivalent to the Antietam (Berg et al., 1983)	Leidy, 1882; Lyman, 1909; Howell, 1943, 1944; Aaron, 1969; Kauffman, 1999; Simpson et al., 2002
Setters which is stratigraphically equivalent to the Chilhowee Group (Berg et al., 1983)	Rand, 1900
Potsdam	Hunt, 1878; Bjerstedt and Erickson, 1989

Deformed *Skolithos*

Cylindrical *Skolithos* tubes have long been used to calculate strain (Wise, 1960, 2010; Brace, 1961; Sylvester and Christie, 1968; McLeish, 1971; Wilkinson et al., 1975; Allison, 1979). Deformation of *Skolithos* burrows has been noted in Cambrian quartzites locally (Key and Sims, 1991; Gourley and Key, 1996; Wise, 1960, 2010; Key, 2014). This is typically reflected by the normally circular transverse cross-sectional shape of the burrow being distorted into an ellipse (Häntzschel, 1975). Wise (2010) attributed this in the Blue Ridge anticlinorium to layer-parallel shortening that flattened the *Skolithos* tubes in the plane of cleavage resulting from the Appalachian orogenies, especially the Alleghanian. Key (2014) measured the long (L) and short (W) axes of *Skolithos* tubes from the Antietam

Formation near Shippensburg and calculated the L/W (i.e., Rf strain) ratio as 1.9. This is more than the 1.6 that Key and Sims (1991) measured in the Antietam Formation exposed in the Mt. Holly Pennsy Supply quarry as well as the 1.3 value reported by Kilby and Connors (2002) in the Antietam of Virginia. Gourley and Key (1996) measured the same ratio in the underlying Montalto Member of the Harpers Formation outcropping at Pole Steeple and reported a ratio of 1.5. *Skolithos* tubes can also refract into a sigmoid shape along with cleavage in response to flexural slip (Allison, 1979; Wise, 2010). This has been reported elsewhere in a Devonian *Skolithos*-bearing quartzite (Richter, 1920) and the Antietam Quartzite at Bender's quarry (Freedman, 1967, 1968), now Pennsy Supply's Mt. Holly quarry (Key and Sims, 1991).

***Skolithos* tube spacing**

Much research has been done on the spacing of *Skolithos* tubes as a paleoenvironmental indicator. This is because the preserved burrow density on a bedding plane is more closely related (i.e., inversely) to sedimentation rate than original animal density (Desjardins et al., 2010). *Skolithos* spacing is a function of both original animal density and contemporaneity of the burrows. The former is controlled by size of the animal's food-catching apparatus and the current velocity-regulated food density (Dodd and Stanton, 1981). The latter is controlled by the time available for colonization of the

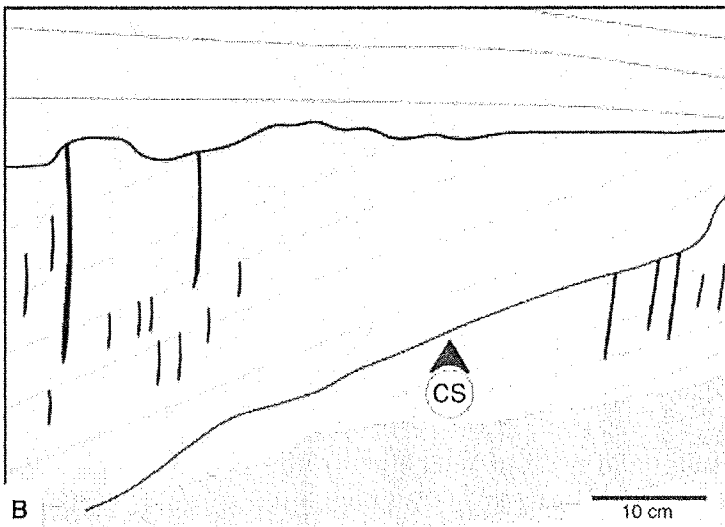


Figure 2. Schematic diagram showing the cross cutting relationships of erosional and *Skolithos* colonization surfaces (CS) indicates lack of contemporaneity of preserved tubes. Modified from Desjardins et al. (2010, fig. 6B).

substrate, sedimentation rate, and burrow depth. Because all burrows are equally preservable, contemporaneity is virtually impossible to determine in the rock record (Figure 2) (Frey and Seilacher, 1980). That is one reason why *Skolithos* densities are at least one order of magnitude greater in fossils than with extant organisms (Skoog et al., 1994). In addition to spacing, work has been done on random versus clustered packing of *Skolithos* (e.g., Skoog et al., 1994; Gourley and Key, 1996).

Skolithos ichnofabric indices

Droser and Bottjer (1989) developed a *Skolithos* ichnofabric index that ranges from 1 (*Skolithos* absent) to 5 (complete bioturbation of the original bedding by *Skolithos*) (Figure 3A). Sandstone with a higher density of *Skolithos* is called piperock. The term piperock was coined by Peach and Horne (1884) to describe the dense assemblage of *Skolithos* in the so-named Pipe Rock Member of the Lower Cambrian Eriboll Sandstone of Scotland (McIlroy and Garton, 2004; Netto, 2007). Piperock has an ichnofabric index of 3-5 (Droser and Bottjer, 1989; Droser, 1991). This can produce a type of biostratification in response to non-bioturbated strata alternating with piperock (Figure 3B).

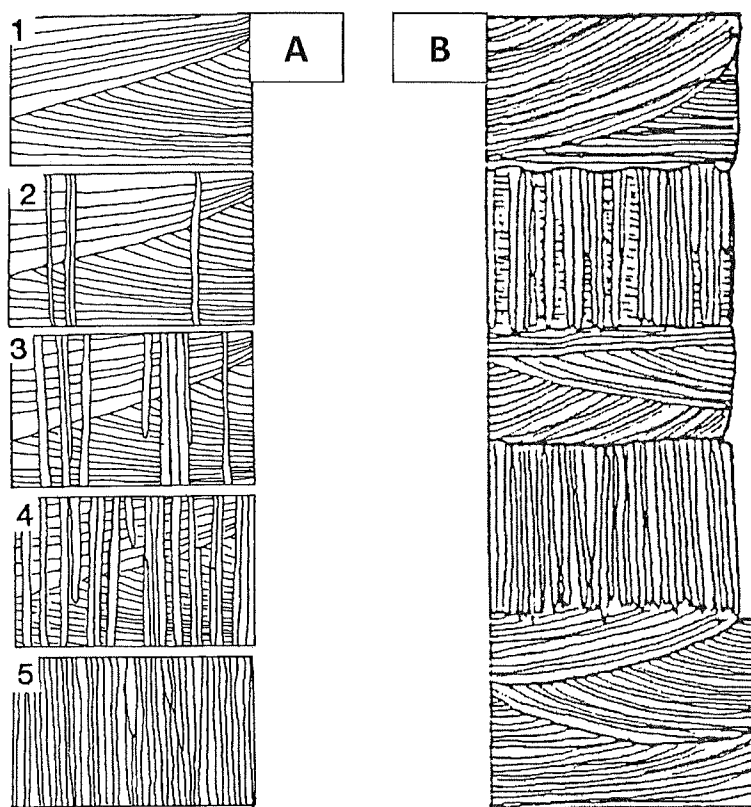


Figure 3. Schematic diagrams for (A) ichnofabric indices 1 through 5 for strata dominated by *Skolithos*. Modified from Droser and Bottjer (1989, fig. 1 left) and (B) biostratification resulting from a characteristic distribution of ichnofabric indices within strata with *Skolithos* as the dominant trace fossil. Modified from Droser and Bottjer (1989, fig. 4A).

Depositional environment of shallow marine *Skolithos*

Unlike conventional body fossils which are typically preserved in time averaged death assemblages which may be far from where the organism lived, trace fossils are preserved in situ as they cannot normally be transported without being destroyed (Häntzschel, 1975; Bromley, 1990; Miller, 2007). This is why they are effective tools for interpreting depositional environments. Though *Skolithos* also occurs in a variety of terrestrial (Netto, 2007), subtidal shelf (Vossler and Pemberton, 1988), and deep marine environments (Ekdale, 1977), here we focus on the more ubiquitous shallow marine *Skolithos*. Seilacher (1967) originally named his shallowest marine ichnofacies after *Skolithos* for the littoral environment with frequent sediment transport and little net deposition due to episodic erosion and deposition. Based on characteristics of the surrounding sediment and sedimentary structures, shallow marine *Skolithos* have been interpreted to form in a variety of high energy, mature, siliciclastic, nearshore environments including tidal flats, tidal channels, beach shorefaces, and offshore sand bars (Frey and Pemberton, 1985; Simpson and Eriksson, 1990; Droser, 1991; Skoog et al., 1994). *Skolithos* achieves its greatest density in conditions with more consistent, higher velocity, wave/tidal currents near the low tide line, whereas *Monocraterion* is most common where there are inconsistent, lower velocity, wave/tidal currents near the high tide line (Goodwin and Anderson, 1974). *Skolithos* densities are highest near the low tide line due the longer duration and more favorable submerged feeding conditions.

Acknowledgments

This manuscript would not have been possible without permission from Valley Quarries' Randy Van Scyoc (Vice President of Operations) and Dean Fogal (Superintendent of Mt. Cydonia Sand Plant III) to access their quarry to examine *Skolithos* in the Antietam Formation. Don Hoskins (PA Geological Survey) and Noel Potter (Dickinson College) helped with the field work. This manuscript was greatly improved by the helpful comments of Noel Potter.

References

- Aaron, J. M. 1969. Petrology and origin of the Hardyston Quartzite (Lower Cambrian) in eastern Pennsylvania and western New Jersey. Pp. 21-34. In: S. Subitzky (ed.). Geology of selected area in New Jersey and eastern Pennsylvania and guide book. Rutgers University Press, New Brunswick.
- Allison, I. 1979. Variations of strain and microstructure in folded Pipe Rock in the Moine Thrust Zone at Loch Eriboll and their bearing on the deformational history. Scott. J. Geol. 15, (4), 263-269.

- Alpert, S. P. 1974. Systematic review of the genus *Skolithos*. *Journal of Paleontology*, 48: 661-669.
- Alpert, S.P., 1975, Planolites and Skolithos from the Upper Precambrian-Lower Cambrian, White-Inyo Mountains, California: *Journal of Paleontology*, v. 49, p. 508-521.
- Barwis, J. H. 1985. Tubes of the modern polychaete *Diopatra cuprea* as current velocity indicators and as analogs for *Skolithos-Monocraterion*. Pp. 225 – 235, In: Biogenic structures: their use in interpreting depositional environments / edited by H. Allen Curran. SEPM Special Publication 35
- Berg, T.M., McNerney, M.K., Way, J.H., and MacLachlan, D.B. 1983. Stratigraphic correlation chart of Pennsylvania. Pennsylvania Geological Survey, General Geology Report 75.
- Behrensmeyer, A. K., and A. Turner. 2013. Taxonomic occurrences of *Olenellus* recorded in the Paleobiology Database. Fossilworks. <http://fossilworks.org>. search 23 June 2014.
- Bjerstedt, T.W. & Erickson, J.M. 1989: Trace fossils and bioturbation in peritidal facies of the Potsdam–Theresa formations (Cambrian–Ordovician), northwest Adirondacks. *Palaos* 4, 203–224.
- Bottjer, D.J., Hagadon, J.W. & Dornbos, S.Q. 2000: The Cambrian substrate revolution. *GSA Today* 10, 2–7.
- Brace, W. F. 1961. Mohr construction in the analysis of large geologic strain, *Geol. Soc. America, Bull.*, 72:1059-1080.
- Bridge, J. S., and M. L. Droser. 1985. Unusual marginal-marine lithofacies from the Upper Devonian Catskill clastic wedge. *Geological Society of America Special Paper* 201.
- Bromley, R. G. 1990. Trace fossils: biology and taphonomy. Unwin Hyman, 280 p.
- Cotter, E. 1982. Tuscarora Formation of Pennsylvania. Guidebook for the Society of Economic Paleontologists and Mineralogists, Eastern Section field trip. Lewisburg, PA. 105 p.
- Cotter, E. 1983. Shelf, paralic, and fluvial environments and eustatic sea-level fluctuations in the origin of the Tuscarora Formation (Lower Silurian) of central Pennsylvania. *Journal of Sedimentary Petrology*, 53 (1): 25-49.
- Crimes, T. P. 1975. The stratigraphical significance of trace fossils. Pp. 109-130. In: R. W. Frey (ed.). *The Study of Trace Fossils*. Springer-Verlag, New York.
- Crimes, T. P. 1994. The period of early evolutionary failure and the dawn of evolutionary success: the record of biotic changes across the Precambrian–Cambrian boundary, in Donovan, S.K., ed., *The Paleobiology of Trace Fossils*: Baltimore, The John Hopkins University Press, p. 105–133.
- Desjardins, P.R., Mángano, M.G., Buatois, L.A. and Pratt, B.R. 2010. *Skolithos* pipe rock and associated ichnofabrics from the southern Rocky Mountains, Canada:

- colonization trends and environmental controls in an early Cambrian sand-sheet complex. *Lethaia*, 43: 507–528.
- Dickinson College Archives. 2005. Samuel Stehman Haldeman (1812-1880). <http://archives.dickinson.edu/people/samuel-stehman-haldeman-1812-1880>. Accessed 23 June 2014.
- Dodd, J. R., and Stanton, R. J., Jr. 1981. *Paleoecology, Concepts and Applications*: New York, Wiley, 559 p.
- Droser, M.L., 1991, Ichnofabric of the Paleozoic *Skolithos* ichnofacies and the nature and distribution of *Skolithos* piperock: *Palaaios*, v. 6, p. 316-325.
- Droser, M.L., and Bottjer, D.J., 1989. Ichnofabric of sandstones deposited in high-energy nearshore environments: Measurement and utilization: *Palaaios*, v. 4, p. 598-604.
- Ekdale, A. A. 1977. Abyssal trace fossils in worldwide Deep Sea Drilling Project cores: in Crimes, T. P., and Harper, J. C., eds., *Trace Fossils 2: Geological Journal Special Issue No. 9*, Seel House Press, p. 163-182.
- Ekdale, A. A. & Lewis, D. W. 1991, Trace fossils and paleoenvironmental control of ichnofacies in a late Quaternary gravel and loess fan delta complex, New Zealand: *Palaeogeography, Palaeoclimatology, Palaeoecology*, v. 81, p. 253-279.
- Fauth, J. L. 1968. Geology of the Caledonia Park Quadrangle Area, South Mountain, Pennsylvania: Pennsylvania Geological Survey, 4th ser., Atlas 129a, 133 p.
- Fillion, D. and R. K. Pickerill. 1990. Ichnology of the Upper Cambrian? to Lower Ordovician Bell Island and Wabana groups of eastern Newfoundland, Canada. *Palaeontographica Canadiana*, 7: 1- 119.
- Frey, R. W., and Pemberton, S. G. 1985. Biogenic structures in outcrops and cores: I: Approaches to ichnology. *Bulletin of Canadian Petroleum Geologists*, 33:72-115.
- Frey, R. W. and Seilacher, A. 1980. Uniformity in marine invertebrate ichnology. *Lethaia*, 13: 183-207.
- Goodwin, P. W., and Anderson, E. J. 1974. Associated physical and biogenic structures in environmental subdivision of a Cambrian tidal sand body: *Journal of Geology*, v. 82, p. 779-794.
- Gourley, J. R., and M. M. Key, Jr. 1996. Analysis of the *Skolithos* ichnofacies from the Cambrian Montalto Quartzite Member of the Harpers Formation in south central Pennsylvania. Pp. 152. In: J. E. Repetski (ed.). *North American Paleontological Convention Abstracts of Papers*. Paleontological Society, Special Publication, No. 8.
- Haldeman, S. S. 1840. Supplement to number one of "A monograph of the *Limniades*, and other freshwater univalve shells of North America" containing new descriptions of apparently new animals in different classes, and the names and characters of the subgenera *Paludina* and *Anculosa*. Philadelphia. 3 p.

- Haldeman Mansion Preservation Society. 2011. Samuel Steman Haldeman.
<http://www.haldeman-mansion.org/samuelstemanhaldeman.htm>. Accessed 24 June 2014.
- Hallam, A., and Swett, K. 1966. Trace fossils from the Lower Cambrian Pipe Rock of the north-west Highlands. *Scottish Journal of Geology*, 2: 101-106.
- Häntzschel, W. 1975. Miscellanea: supplement 1: trace fossils and problematica. *Treatise on Invertebrate Paleontology, Part W. Geological Society of America, Boulder Colorado*, 269 p.
- Hofmann, H. J. 1971. Precambrian fossils, pseudofossils, and problematica in Canada. *Geol. Surv. Canada, Bull.* 189, 146 p.
- Högbom, A.G. 1915. Zur Deutung der Scolithus-Sandsteine und "Pipe Rocks". *Bull. geol. Instn. Univ. Upsala*, 13: 45-60.
- Howell, B. F. 1943. Burrows of *Skolithos* and *Planolites* in the Cambrian Hardyston Sandstone at Reading, Pennsylvania. *Bulletin of the Wagner Free Institute of Sciences of Philadelphia*. 3:1-33.
- Howell, B. F. 1944. A new *Skolithos* from the Cambrian Hardyston Formation of Pennsylvania. *Bulletin of the Wagner Free Institute of Sciences of Philadelphia*, 19 (4): 41-46.
- Howell, B. J. 1945. *Skolithos*, *Diplocraterion*, and *Sabellidites* in the Cambrian Antietam Sandstone of Maryland. *Bulletin of the Wagner Free Institute of Sciences of Philadelphia*, 20: 33-42.
- Hunt, T. S. 1878. Special report on the trap dykes and azoic rocks of southeastern Pennsylvania. Part 1. Historical introduction. *Second Geological Survey of Pennsylvania*, E: 1-253.
- Kauffman, M. E. 1999. Eocambrian, Cambrian, and transition to Ordovician. Pp. 58-73, In: *The geology of Pennsylvania*. Shultz, C. H. (ed.). Special Publication - Geological Survey of Pennsylvania, Harrisburg.
- Key, M. M., Jr. 1991. The Lower Cambrian Clastics of South Mountain, Pennsylvania. Pp. 21-27. In: W. D. Sevon and N. Potter, Jr. (eds.). *Guidebook for the 56th Annual Field Conference of Pennsylvania Geologists*. Field Conference of Pennsylvania Geologists. Harrisburg, PA.
- Key, M. M., Jr. 2014. *Skolithos* in the Lower Cambrian Antietam Formation at South Mountain, Pennsylvania. Pp. 13-26. In: D. Hoskins and N. Potter, Jr. (eds.). *Guidebook for the 79th Annual Field Conference of Pennsylvania Geologists*. Field Conference of Pennsylvania Geologists. Harrisburg, PA.
- Key, M. M., Jr. and S. J. Sims. 1991. Geology of the Pennsy Supply Quarry, Mt. Holly, Pennsylvania. Pp. 220-225. In: W. D. Sevon and N. Potter, Jr. (eds.). *Guidebook for the 56th Annual Field Conference of Pennsylvania Geologists*. Field Conference of Pennsylvania Geologists. Harrisburg, PA.

- Kilby, R. E., and C. D. Connors. 2002. Preliminary strain analysis of the Antietam Fm., southern Central Appalachians, Virginia. Geological Society of America, Abstracts with Programs 34 (6): 439.
- Leidy, J. 1882. Remarks on some rock specimens. Proceedings of the Academy of Natural Sciences of Philadelphia. 1882: 10-12.
- Lyman, B. S. 1909. *Scolithus linearis* burrows with the orifice complete. Proceedings of the Academy of Natural Sciences of Philadelphia. 1909: 296-297.
- MacNaughton, R.B., Dalrymple, R.W. & Narbonne, G.M. 1997: Early Cambrian braid-delta deposits, Mackenzie Mountains, north-western Canada. Sedimentology 44, 587-609.
- McIlroy, D. & Garton, M. 2004: A worm's eye view of the early Paleozoic sea floor. Geology Today 20, 224-230.
- McIlroy, D. & Logan, G. 1999: The impact of bioturbation on infaunal ecology and evolution during the Proterozoic-Cambrian transition. Palaios 14, 58-72.
- McLeish, A. J. 1971. Strain analysis of deformed pipe rock in the Moine Thrust Zone, northwest Scotland. Tectonophysics 12, 469-503.
- McMenamin, M.A.S., and Schulte-McMenamin, D.L., 1990. The Emergence of Animals: The Cambrian Breakthrough. Columbia University Press, New York, 217 p..
- Miller, W. C. 2007. Trace fossils: concepts, problems, prospects. Elsevier, 611 p.
- Netto, R. G. 2007. *Skolithos*-dominated piperock in nonmarine environments: An example from the Triassic Caturrita Formation, southern Brazil. Pp. 107-121, In: Sediment-Organism Interactions: Multifaceted Ichnology, Edited by R. G. Bromley, L. A. Buatois, G. Mángano, J. F. Genise, and R. N. Melchor. SEPM Special Publication No. 88.
- Peach, B.N., and Horne, J. 1884. Report on the geology of the north-west of Sutherland. Nature, 31: 31-34.
- Pemberton, S.G., and Frey, R.W., 1984, Quantitative methods in ichnology: Spatial distribution among populations. Lethaia, v. 17, p. 33-49.
- Rand, T. D. 1900. Notes of the geology of southeastern Pennsylvania. Proceedings of the Academy of Natural Sciences of Philadelphia. 1909: 160-338.
- Rhoads, D. C., 1967, Biogenic reworking of intertidal and subtidal sediments in Barnstable Harbor and Buzzards Bay, Massachusetts. Journal of Geology, 75: 461-476.
- Richter, R. 1920. Ein devonischern 'Pfeifenquarzit' verglichen mit der heutigen "Sandkoralle" (*Sabellaria*, Annelida). Senckenbergiana, 2: 215-235.
- Root, S. I. 1968. Geology and mineral resources of Southeastern Franklin County, Pennsylvania Geological Survey, 4th Ser., Atlas 119cd, 118 p.

- Sanabria, D. I., and A. M. Thompson. 1997. Stratigraphic relations of the Juniata-Tuscarora contact in central Pennsylvania. Pennsylvania Geological Survey, 4th Series, Open-Fire Report 97-01, Harrisburg. 30 p.
- Schäfer, W. 1972. Ecology and Palaeoecology of Marine Environments. University of Chicago Press, Chicago, Illinois, 568 p.
- Scharnberger, C., E. Simpson, J. Jones, and J. Smoot. 2014. Stratigraphy and structure of the Chilhowee Group in Lancaster and York Counties. Pp. 53-72. In: de Wet, A. P. (ed.). Field Trip Guide, Northeastern Section of the Geological Society of America, Lancaster.
- Schlirf, M., and Uchman, A. 2005, Revision of the ichnogenus *Sabellarifex* Richter, 1921 and its relationship to *Skolithos* Haldeman 1840 and *Polykladichnus* Fürsich, 1981: Journal of Systematic Palaeontology, v. 3, p. 115-131.
- Schwab, F. L., 1972, The Chilhowee Group and the late Precambrian-early Paleozoic sedimentary framework in the Central and Southern Appalachians, in Lessing, P., et al, eds., Appalachian Structures: Origin, Evolution, and Possible Potential for New Exploration Frontiers; A Seminar: Morgantown, West Virginia University and West Virginia Geological and Economic Survey, p. 59-101.
- Seilacher, A. 1967. Bathymetry of trace fossils. Marine Geology, 5: 413-428.
- Sevon, W. D., and R. L. Van Scyoc. 1991. Mount Cydonia Quarry, Valley Quarries, Inc. Pp. 168-176. In: W. D. Sevon and N. Potter, Jr. (eds.). Guidebook for the 56th Annual Field Conference of Pennsylvania Geologists. Field Conference of Pennsylvania Geologists. Harrisburg, PA.
- Simpson, E. L., 1991, An exhumed Lower Cambrian tidal flat: the Antietam Formation , central Virginia, U.S.A., Pp. 123-134. In: Smith, D.G., Reinson, G.E. Zaitlin, B.A., and Rahmani, R.A., Eds., Clastic Tidal Sedimentology: Canadian Society of Petroleum Geologists Memoir No. 16.
- Simpson, E.L., Dilliard, K.A., Rowell, B.F. & Higgins, D. 2002: The fluvial to marine transition within the post-rift Lower Cambrian Hardyston Formation, eastern Pennsylvania, USA. Sedimentary Geology 147, 127–142.
- Simpson, E.L., and Eriksson, K.A., 1990, Early Cambrian progradational and transgressive sedimentation patterns in Virginia: An example of the early history of a passive margin: Journal of Sedimentary Petrology, 60: 84-100.
- Simpson, E. L., and Sundberg, F. A. 1987. Early Cambrian age for synrift deposits of the Chilhowee Group of southwestern Virginia. Geology, 15 (2): 123-126.
- Skoog, S.Y., Venn, C., and Simpson, E.L., 1994, Distribution of *Diopatra cuprea* across modern tidal flats: Implications for the Skolithos: Palaios, v. 9, p. 188-201.
- Smoot, J.P., and Southworth, S. 2014. Volcanic rift margin model for the rift-to-drift setting of the late Neoproterozoic-early Cambrian eastern margin of Laurentia: Chilhowee Group of the Appalachian Blue Ridge: Geological Society of America Bulletin, v. 126, p. 201-218.

- Stose, G. W. 1906. The sedimentary rocks of South Mountain, Pennsylvania. *Journal of Geology*, 14: 201-220.
- Stose, G. W. 1909. Mercersburg-Chambersburg folio. U.S. Geological Survey Geologic Atlas, Folio No. 170, 19 p.
- Stose, G. W., and A. I. Jonas. 1939. Geology and mineral resources of York County, Pennsylvania. Pennsylvania Geological Survey, 4th Series, Bulletin C67.
- Sylvester, A. G., and J. M. Christie. 1968. The origin of crossed-girdle orientations of optic axes in deformed quartzites. *Journal of Geology* 76: 571-580.
- Thayer, C. W. 1979. Biological bulldozers and the evolution of marine benthic communities. *Science*, 203: 458-461.
- Torell, O. 1870. Petrificata suecana formationis Cambricae. *Lunds Universitets ars.* Volume 6, Avdel. 2, No. VIII: 1-14.
- Tull, J.F., Allison, D.T., Whiting, S.E., and John, N.L., 2010, Southern Appalachian Laurentian margin initial driftfacies sequences: Implications for margin evolution, in Tollo, R.P., Bartholomew, M.J., Hibbard, J.P. , and Karabinos, P.M., eds., *From Rodinia to Pangea: The Lithotectonic Record of the Appalachian Region: Geological Society of America Memoir* 206, p. 935-956.
- Vossler, S.M., and Pemberton, S.G., 1988, *Skolithos* in the Upper Cretaceous Cardium Formation: An ichnofossil example of opportunistic ecology: *Lethia*, v. 21, p. 351-362.
- Webby, B. D., F. Paris, M. L. Droser, I. G. Percival. 2004. The great Ordovician biodiversification event. Columbia University Press, 484 p.
- Westergård, A. H. 1931. *Diplocraterion*, *Monocraterion*, and *Scolithus* from the Lower Cambrian of Sweden. *Sveriges Geologiska Undersökning*. C372: 1-25.
- Wilkinson, P., Soper, N. J., Bell, A. M. 1975. *Skolithos* pipes as strain markers in mylonites. *Tectonophysics*, 28 (3): 143-157.
- Wise, D. U. 1960. Stop #8: Chickies Rock, in Wise, D. U and M. E. Kauffman, eds., *Some Tectonic and Structural Problems of the Appalachian Piedmont along the Susquehanna River*, 25th Annual Field Conference of Pennsylvania Geologists, Lancaster, PA, p. 68-75.
- Wise, D. U. 2010. Stop #5: Structural geology at Chickies Rock, in Wise, D. U and Gary M Fleege, eds., *Tectonics of the Pennsylvania Piedmont along the Susquehanna River*, 75th Annual Field Conference of Pennsylvania Geologists, Lancaster, PA, p. 49-57.